ANALYTICAL HEAT TRANSFER

Mihir Sen

Department of Aerospace and Mechanical Engineering
University of Notre Dame
Notre Dame, IN 46556

May 3, 2017

Preface

These are lecture notes for *AME60634: Intermediate Heat Transfer,* a second course on heat transfer for undergraduate seniors and beginning graduate students. At this stage the student can begin to apply knowledge of mathematics and computational methods to the problems of heat transfer. Thus, in addition to undergraduate heat transfer, students taking this course are expected to be familiar with vector algebra, linear algebra, ordinary differential equations, particle and rigid-body dynamics, thermodynamics, and integral and differential analysis in fluid mechanics. The use of computers is essential both for the purpose of computation as well as for display and visualization of results.

The main purpose of these notes is to develop the ability to mathematically model physical processes involving heat transfer. The models should have all the essential ingredients but ignore those that are not so. What is quantitatively lost in the approximations is gained by a qualitative understanding of the physical processes.

The student is encouraged to make extensive use of the literature listed in the bibliography. There are many examples inserted in the text to illustrate the modeling process. The students are also expected to attempt the problems at the end of each chapter to reinforce their learning.

At present these notes are in the process of being written, and I will be glad to receive comments and have mistakes brought to my attention.

Mihir Sen
Department of Aerospace and Mechanical Engineering
University of Notre Dame

Contents

Chapter 1

Introduction

It is assumed that the reader has had an introductory course in heat transfer of the level of [12, 14, 19, 20, 22, 24, 26, 34, 68, 80, 84, 93, 95, 113, 118, 119, 125, 130, 146, 164, 186, 193, 198, 218, 221, 222]. More advanced books are, for example, [216, 223]. A classic work is that of Jakob [100].

1.1 Mathematical background

1.1.1 Coordinate systems

The physical quantities discussed here will be scalars, vectors or tensors. Although other coordinate systems can be used, we will generally restrict ourselves to Cartesian, cylindrical, and spherical systems. A time-dependent scaler field is $u(\boldsymbol{x}, t)$. A vector field $\boldsymbol{V}(\boldsymbol{x}, t)$ can be written in these coordinates systems as

$$\begin{aligned} \boldsymbol{V} &= V_x \boldsymbol{i} + V_y \boldsymbol{j} + V_z \boldsymbol{k} && \text{Cartesian} \\ &= V_r \boldsymbol{e}_r + V_\theta \boldsymbol{e}_\theta + V_z \boldsymbol{e}_z && \text{cylindrical} \\ &= V_r \boldsymbol{e}_r + V_\theta \boldsymbol{e}_\theta + V_\phi \boldsymbol{e}_\phi && \text{spherical} \end{aligned}$$

We will also use $\boldsymbol{\nabla}$, called del or nabla, as shorthand to indicate the operations

$$\begin{aligned} \text{grad } u &= \boldsymbol{\nabla}\phi \\ \text{div } \boldsymbol{V} &= \boldsymbol{\nabla} \cdot \boldsymbol{V}, \\ \text{Laplacian } u &= \boldsymbol{\nabla} \cdot \boldsymbol{\nabla} u = \nabla^2 u = \Delta u \end{aligned}$$

where u and $\boldsymbol{V}$ are any scalar and vector fields, respectively. In general $\boldsymbol{\nabla}$ is not an operator, and can be only written explicitly in Cartesian form as

$$\boldsymbol{\nabla} = \frac{\partial}{\partial x}\boldsymbol{i} + \frac{\partial}{\partial y}\boldsymbol{j} + \frac{\partial}{\partial z}\boldsymbol{k},$$

so that

$$\begin{aligned}\text{grad } u &= \frac{\partial u}{\partial x}\boldsymbol{i} + \frac{\partial u}{\partial y}\boldsymbol{j} + \frac{\partial u}{\partial z}\boldsymbol{k},\\ \text{div } \boldsymbol{V} &= \frac{\partial V_x}{\partial x} + \frac{\partial V_y}{\partial y} + \frac{\partial V_z}{\partial z},\\ \text{Laplacian } u &= \frac{\partial^2 u}{\partial x^2} + \frac{\partial^2 u}{\partial y^2} + \frac{\partial^2 u}{\partial z^2}.\end{aligned}$$

In cylindrical coordinates (r, θ, z)

$$\begin{aligned}\text{grad } u &= \frac{\partial u}{\partial r}\boldsymbol{e}_r + \frac{1}{r}\frac{\partial u}{\partial \theta}\boldsymbol{e}_\theta + \frac{\partial u}{\partial z}\boldsymbol{e}_z,\\ \text{div } \boldsymbol{V} &= \frac{1}{r}\frac{\partial}{\partial r}(rV_r) + \frac{1}{r}\frac{\partial V_\theta}{\partial \theta} + \frac{\partial V_z}{\partial z},\\ \nabla^2 u &= \frac{1}{r}\frac{\partial}{\partial r}\left(r\frac{\partial u}{\partial r}\right) + \frac{1}{r^2}\frac{\partial^2 u}{\partial \theta^2} + \frac{\partial^2 u}{\partial z^2}\end{aligned}$$

and in spherical coordinates (r, θ, ϕ)

$$\begin{aligned}\text{grad } u &= \frac{\partial u}{\partial r}\boldsymbol{e}_r + \frac{1}{r}\frac{\partial u}{\partial \theta}\boldsymbol{e}_\theta + \frac{1}{r\sin\theta}\frac{\partial u}{\partial \phi}\boldsymbol{e}_\phi,\\ \text{div } \boldsymbol{V} &= \frac{1}{r^2}\frac{\partial}{\partial r}(r^2 V_r) + \frac{1}{r\sin\theta}\frac{\partial}{\partial \theta}(V_\theta \sin\theta) + \frac{1}{r\sin\theta}\frac{\partial V_z}{\partial z},\\ \nabla^2 u &= \frac{1}{r^2}\frac{\partial}{\partial r}\left(r^2\frac{\partial u}{\partial r}\right) + \frac{1}{r^2\sin\theta}\frac{\partial}{\partial \theta}\left(\sin\theta\frac{\partial u}{\partial \theta}\right) + \frac{1}{r^2\sin^2\theta}\frac{\partial^2 u}{\partial \phi^2}\end{aligned}$$

1.1.2 Polynomial approximations

If the function $y(x)$ is known, then a Taylor series can be used to generate a polynomial at any point. The expansion of $y(x)$ around $x = 0$ is

$$y(x) = y(0) + \left.\frac{\partial y}{\partial x}\right|_{x=0} x + \left.\tfrac{1}{2!}\frac{\partial^2 y}{\partial x^2}\right|_{x=0} x^2 + \left.\tfrac{1}{3!}\frac{\partial^3 y}{\partial x^3}\right|_{x=0} x^3 + \ldots \tag{1.1}$$

If, on the other hand, $y(x)$ is known only at discrete points, then approximations at other points can be generated by an interpolation. Thus, if $y(x_1)$ and $y(x_2)$ are known, then

$$y(x) = y(x_1) + \frac{x - x_1}{x_2 - x_1}\left(y(x_2) - y(x_1)\right)$$

is a linear interpolation. Higher-order polynomials can be determined if the values of $y(x)$ are known at more values of x. The Lagrange interpolation formula is

$$\begin{aligned}y(x) = {} & \frac{(x-x_1)(x-x_2)\cdots(x-x_n)}{(x_0-x_1)(x_0-x_2)\cdots(x_0-x_n)}y_0 + \frac{(x-x_0)(x-x_2)\cdots(x-x_n)}{(x_1-x_0)(x_1-x_2)\cdots(x_1-x_n)}y_1 + \\ & \ldots + \frac{(x-x_0)(x-x_1)\cdots(x-x_{n-1})}{(x_n-x_0)(x_n-x_1)\cdots(x_n-x_{n-1})}y_n\end{aligned}$$

1.1.3 Complex numbers

A complex number z may be written as

$$z = x + iy$$

where $i = \sqrt{-1}$, and x and y are real. The real and imaginary parts of z are

$$\begin{aligned} x &= \mathrm{Re}(z), \\ y &= \mathrm{Im}(z). \end{aligned}$$

z can also be written as

$$\begin{aligned} z &= A\angle\theta \\ &= Ae^{i\theta}, \\ &= A(\cos\theta + i\sin\theta), \end{aligned}$$

where $A = \sqrt{x^2 + y^2}$ and $\tan\theta = y/x$. $A = |z|$ is called the magnitude, modulus, or absolute value of z.

Euler's formula is

$$e^{i\theta} = \cos\theta + i\sin\theta,$$

from which

$$e^{-i\theta} = \cos\theta - i\sin\theta.$$

The trigonometric functions are obtained as

$$\begin{aligned} \cos\theta &= \frac{1}{2}(e^{i\theta} + e^{-i\theta}), \\ \sin\theta &= \frac{1}{2i}(e^{i\theta} - e^{-i\theta}) \end{aligned}$$

The hyperbolic functions are defined in parallel as

$$\begin{aligned} \cosh\theta &= \frac{1}{2}(e^{\theta} + e^{-\theta}), \\ &= \cos(i\theta), \\ \sinh\theta &= \frac{1}{2}(e^{\theta} - e^{-\theta}), \\ &= -i\sin(i\theta). \end{aligned}$$

Sometimes the real parts of complex numbers are used instead of a cosine, as in

$$\cos\theta = \mathrm{Re}(e^{i\theta}).$$

At other times a complex conjugate is added, like

$$\cos\theta = \frac{1}{2}(e^{i\theta} + *),$$

where $*$ (or cc) indicates the complex conjugate of the preceding term. In any case Re, $*$ or cc may be understood and not explicitly written.

1.1.4 Ordinary differential equations

The following are some of the procedures of solution used.

Direct integration

To solve

$$\frac{d}{dx}\left[k(x,y)\frac{dy}{dx}\right]=0,$$

we find the first integral to be

$$k(x,y)\frac{dy}{dx}=C_1.$$

Special cases:
(a) For $k(x,y)=k$, the equation can be integrated again to give

$$k\ y=C_1x+C_2.$$

(b) If $k(x,y)=k(x)$, we can write

$$\frac{dy}{dx}=\frac{C_1}{k(x)},$$

from which

$$y=C_1\int\frac{dx}{k(x)}+C_2.$$

A closed-form function or numerical values may be obtained for the integral on the right.
(c) For $k(x,y)=k(y)$, we integrate to get

$$\int k(y)\ dy=C_1\frac{x^2}{2}+C_2$$

Integrating factor

To solve the linear equation

$$\frac{dy}{dt}+P(t)\ y=Q(t), \tag{1.2}$$

multiply first by the integrating factor $e^{\int_a^t P(s)\ ds}=e^{F(t)-F(a)}$. Choose a such that $F(a)=0$. This gives

$$\frac{dy}{dt}\ e^{\int_a^t P(s)\ ds}+P(t)\ y\ e^{\int_a^t P(s)\ ds}=Q(t)\ e^{\int_a^t P(s)\ ds},$$
$$\frac{d}{dt}\left[y\ e^{\int_a^t P(s)\ ds}\right]=Q(t)\ e^{\int_a^t P(s)\ ds}.$$

Integrating

$$y\ e^{\int_a^t P(s)\ ds}=\int_{t_0}^{t}Q(r)\ e^{\int_a^r P(s)\ ds}\ dr+C,$$

so that

$$y = e^{-\int_a^t P(s)\ ds}\left[\int_{t_0}^{t} Q(r)\ e^{\int_a^r P(s)\ ds}\ dr + C\right].$$

Trial solutions

For

$$a\frac{d^2y}{dt^2} + b\frac{dy}{dt} + cy = 0,$$

assume that

$$y = e^{rt}$$

so that

$$\begin{aligned} ar^2e^{rt} + bre^{rt} + ce^{rt} &= 0, \\ ar^2 + br + c &= 0, \\ r_{1,2} &= \frac{1}{2a}\big[-b \pm \sqrt{b^2 - 4ac}\big] \end{aligned}$$

Since the equation is linear, the general solution is a linear combination

$$y = C_1e^{r_1t} + C_2e^{r_2t}.$$

Change variables

Change of reference: In

$$a\frac{d^2y}{dt^2} + b\frac{dy}{dt} + c(y - y_0) = 0,$$

let $\eta = y - y_0$ to give

$$a\frac{d^2\eta}{dt^2} + b\frac{d\eta}{dt} + c\eta = 0.$$

Similarity:

Periodic forcing

The forced first-order equation is

$$\frac{dy}{dt} + \lambda y = A\cos\omega t.$$

Let the solution be

$$y(t) = C_1\cos\omega t + C_2\sin\omega t.$$

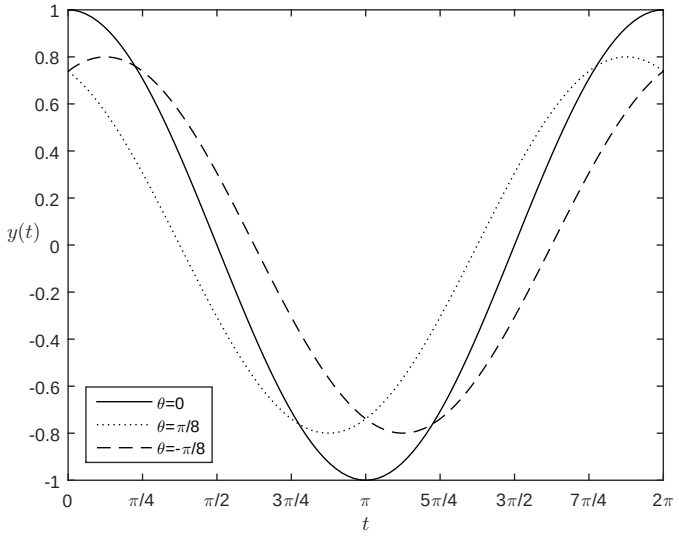

Figure 1.1: Sinusoids that lead $(\cdots)$ and lag $(-\ -)$ the reference (—). $\omega = 1$; amplitudes of the reference and the other two are 1, 0.8, and 0.8, respectively.

Substituting and comparing the coefficients of the $\sin \omega t$ and $\cos \omega t$ terms gives

$$\omega C_1 + \lambda C_2 = A,$$
$$\lambda C_1 - \omega C_2 = 0,$$

from which

$$C_1 = \frac{\omega A}{\omega^2 + \lambda^2},$$
$$C_2 = \frac{\lambda A}{\omega^2 + \lambda^2},$$

Thus

$$y(t) = \frac{\omega}{\omega^2 + \lambda^2} A \cos \omega t + \frac{\lambda}{\omega^2 + \lambda^2} A \sin \omega t. \tag{1.3}$$

With phasors

The solution, Eq. (1.3), can also be written as

$$\begin{aligned} y(t) &= B \cos(\omega t + \phi), \\ &= B(\cos \omega t \cos \phi - \sin \omega t \sin \phi), \end{aligned} \tag{1.4}$$

where ϕ is a phase angle ($\phi > 0$ is for $y(t)$ leading $\cos \omega t$, and $\phi < 0$ for lagging). Fig. 1.1 shows sinusoids that are leading and lagging a reference sinusoid. The right side of Eq. (1.4) is sometimes written as $B\angle\phi$ that provides the magnitude and phase information (but not the frequency).

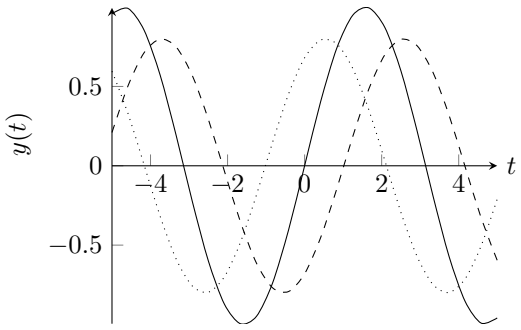

Figure 1.2: Sinusoids of same frequency that lead ($\cdots$) and lag ($-\ -$) the reference (—). Tikz code has to be corrected to replace Fig. 1.1.

Comparing coefficients

$$B\cos\phi = A\ \frac{\omega}{\omega^2+\lambda^2},$$
$$B\sin\phi = -A\ \frac{\lambda}{\omega^2+\lambda^2}.$$

from which

$$\tan\phi = -\frac{\lambda}{\omega},$$
$$B = \frac{A}{\omega^2+\lambda^2}.$$

For $\lambda > 0, \omega > 0$ we note that $\phi < 0$ meaning that the response lags the external forcing.

With complex numbers

For the equation

$$\frac{dy}{dt} + \lambda y = Ae^{i\omega t},$$

where A is real, let us write the solution as

$$y(t) = Be^{i\omega t},$$

where B is in general complex. Substituting in the equation and canceling $e^{i\omega t}$, we get

$$i\omega B + \lambda B = A,$$

from which

$$\begin{aligned} B &= A\ \frac{1}{\lambda+i\omega}, \\ &= A\ \frac{\lambda-i\omega}{\lambda^2+\omega^2} && \text{multiplying above and below by the conjugate,} \\ &= A\ \frac{\lambda}{\lambda^2+\omega^2} - iA\ \frac{\omega}{\lambda^2+\omega^2}. \end{aligned}$$

Writing $B = |B|e^{i(\omega t+\theta)}$, we can find the magnitude of the solution $|B|$ and the phase angle θ.

Delay equations

As an example consider the first-order linear

$$\frac{dy}{dt} = ky(t - t_d) \quad \text{with} \quad y = 1 \text{ for } -t_d \leq t < 0.$$

Notice that the initial condition is given in an interval rather than at a point.

If we take

$$y(t) = Ae^{rt},$$

we get the transcendental characteristic equation

$$r - ke^{-rt_d} = 0.$$

Of course when there is no delay, $t_d = 0$, $r = k$, and the initial condition is $y = 1$ for $t = 0$. The solution reduces to $y(t) = e^{kt}$.

In general, however, $t_d \neq 0$, and there may be multiple real, imaginary or complex roots of the equation which will determine the kind of solution obtained. For example, let us search for a sinusoidal solution

$$y(t) = A \sin \omega t.$$

Substituting into the equation, we have

$$\omega A \cos \omega t = kA\Big[\sin \omega t \cos \omega t_d - \cos \omega t \sin \omega t_d\Big].$$

Comparing the coefficients of $\cos \omega t$ and $\sin \omega t$, we get

$$\cos \omega t_d = 0,$$
$$k \sin \omega t_d = -\omega.$$

One possible solution for the first equation is $\omega t_d = \pi/2$, for which the second gives $k = -\omega$ or $kt_d = -\pi/2$. Thus values of k and t_d satisfying these conditions will give oscillatory solutions. Similarly, another possibility is $\omega t_d = 3\pi/2$, and $k\tau_d = 3\pi/2$.

Numerical solutions

To solve an equation of the form

$$\frac{dy}{dt} = f(t, y)$$

some of the following methods may be used. Start at a point (t_0, y_0) to calculate (t_1, y_1) and then (t_2, y_2), and so on, where $t_{i+1} - t_i = h > 0$.

Euler:

$$y_{n+1} = y_n + f(t_n, y_n)\ h$$

Modified Euler:

$$y'_{n+1} = y_n + f(t_n, y_n)\ h,$$
$$y_{n+1} = y_n + f(t_n, y'_{n+1})\ h$$

Fourth-order Runge-Kutta:

$$y_{n+1} = y_n + \frac{h}{6}(k_1 + 2k_2 + 2k_3 + k_4)$$

where

$$k_1 = f(t_n, y_n),$$
$$k_2 = f(t_n + \frac{h}{2}, y_n + \frac{h}{2}\ k_1),$$
$$k_3 = f(t_n + \frac{h}{2}, y_n + \frac{h}{2}\ k_2),$$
$$k_4 = f(t_n + h, y_n + h\ k_3).$$

1.1.5 Nonlinear equations

Bifurcations

Pitchfork, transcritical, saddle-node, Hopf

Linear stability

Consider a transcritical bifurcation example

$$\frac{dx}{dt} = -x\big[x - (r - r_0)\big],$$

where $x = x(t)$. This is the dynamical system and r is the bifurcation parameter.

Steps

- Find critical points (steady states, time-independent solutions, stationary solutions, equilibria). Take $d/dt = 0$ so that

  $$-\bar{x}\big[\bar{x} - (r - r_0)\big] = 0,$$

  where $\bar{}$ indicates a critical point. The two critical points are the solutions

  $$\bar{x} = 0; \quad \bar{x} = r - r_0.$$

- Apply a small perturbation to a critical point, i.e.

  $$x = \bar{x} + x',$$

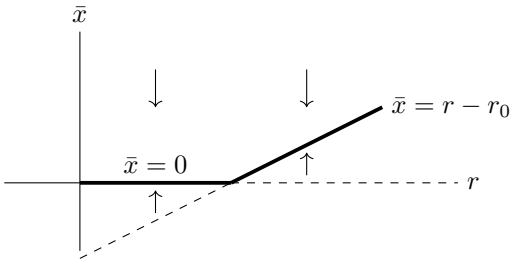

Figure 1.3: Diagram for transcritical bifurcation. Thick lines are stable and dashed lines are unstable.

where $x' = x'(t)$ is a coordinate around the critical point. Substituting in the dynamical system and linearizing

$$\begin{aligned}
\frac{d}{dt}(\bar{x} + x') &= -(\bar{x} + x')\big[(\bar{x} + x') - (r - r_0)\big], \\
\frac{dx'}{dt} &= -(\bar{x} + x')^2 + (\bar{x} + x')(r - r_0), \\
&= -\underbrace{\bar{x}\big[\bar{x} - (r - r_0)\big]}_{=0} - 2\bar{x}x' - \underbrace{(x')^2}_{\approx 0} + x'(r - r_0), \\
&= \big[-2\bar{x} + (r - r_0)\big]x'.
\end{aligned}$$

- Consider the stability of each critical point separately.

  (a) First $\bar{x} = 0$ for which

  $$\frac{dx'}{dt} = (r - r_0)x'.$$

  This is stable for $r < r_0$ and unstable for $r > r_0$.

  (b) Next $\bar{x} = r - r_0$, so that

  $$\begin{aligned}
  \frac{dx'}{dt} &= \big[-2(r - r_0) + (r - r_0)\big]x', \\
  &= -(r - r_0)x'.
  \end{aligned}$$

  This is unstable for $r < r_0$ and stable $r > r_0$.

  Fig. 1.3 shows the bifurcation diagram. The arrows indicate the path from different initial conditions.

Nonlinear stability

Lyapunov functions

Chaos

Lorenz equations

$$\begin{aligned}\frac{dx}{dt} &= \sigma(y-x),\\ \frac{dy}{dt} &= rx - y - xz,\\ \frac{dz}{dt} &= -bz + xy.\end{aligned}$$

1.1.6 Relaxation

Here are some examples.

Exponential: A solution will be presented followed by the differential equation of which it is a solution. For known C and real $\lambda > 0$ the solution is

$$y = Ce^{-\lambda t}$$

Differentiating

$$\begin{aligned}\frac{dy}{dt} &= -C\lambda e^{-\lambda t},\\ &= -\lambda y.\end{aligned}$$

This can be written as

$$\frac{dy}{dt} + \lambda y = 0.$$

This is a first-order linear equation. Note that λ has units of inverse time and that any value of C will satisfy the same differential equation.

If one wanted to work in the reverse direction and solve the differential equation, one will obtain $y = Ce^{-\lambda t}$ where C is arbitrary. To pin down the value of C, an initial condition will have to be provided. This can be, for instance, $y(t_1) = y_1$, from which $C = y_1 e^{\lambda t_1}$.

Stretched exponential function: Taking

$$\begin{aligned}y(t) &= Ce^{-t^\beta},\\ \frac{dy}{dt} &= Ce^{-t^\beta}\left(-\beta t^{\beta-1}\right)\\ &= y\left(-\beta t^{\beta-1}\right),\\ \frac{dy}{dt} &+ \beta t^{\beta-1} y = 0.\end{aligned}$$

Double exponential function:

Two decay constants: If λ_1 and λ_2 are two different real, positive numbers, then

$$y = C_1 e^{-\lambda_1 t} + C_2 e^{-\lambda_2 t}, \tag{1.5}$$

$$\frac{dy}{dt} = -C_1\lambda_1 e^{-\lambda_1 t} - C_2\lambda_2 e^{-\lambda_2 t}, \tag{1.6}$$

$$\frac{d^2y}{dt^2} = C_1\lambda_1^2 e^{-\lambda_1 t} + C_2\lambda_2^2 e^{-\lambda_2 t}. \tag{1.7}$$

Solving C_1 and C_2 from Eqs. (1.5) and (1.6) we get

$$C_1 = \frac{e^{\lambda_1 t}}{\lambda_2 - \lambda_1}\big(\lambda_2\ y + \frac{dy}{dt}\big),$$
$$C_2 = \frac{e^{\lambda_2 t}}{\lambda_1 - \lambda_2}\big(\lambda_1\ y + \frac{dy}{dt}\big).$$

Substituting these in Eq. (1.7) gives the second order differential equation

$$\begin{aligned}\frac{d^2y}{dt^2} &= \Big[\frac{e^{\lambda_1 t}}{\lambda_2 - \lambda_1}\big(\lambda_2\ y + \frac{dy}{dt}\big)\Big]\lambda_1^2 e^{-\lambda_1 t} + \Big[\frac{e^{\lambda_2 t}}{\lambda_1 - \lambda_2}\big(\lambda_1\ y + \frac{dy}{dt}\big)\Big]\lambda_2^2 e^{-\lambda_2 t},\\ &= \frac{\lambda_1^2\lambda_2 - \lambda_2^2\lambda_1}{\lambda_2 - \lambda_1}\ y + \frac{\lambda_1^2 - \lambda_2^2}{\lambda_2 - \lambda_1}\frac{dy}{dt},\\ &= -\lambda_1\lambda_2\ y - (\lambda_1 + \lambda_2)\ \frac{dy}{dt}.\end{aligned}$$

Alternatively

The two exponential complementary functions in the solution Eq. (1.5) come from the quadratic characteristic equation

$$(r + \lambda_1)(r + \lambda_2) = 0,$$

for which the differential equation is

$$(\frac{d}{dt} + \lambda_1)(\frac{d}{dt} + \lambda_2)\ y = 0,$$
$$\frac{d^2y}{dt^2} + (\lambda_1 + \lambda_2)\ \frac{dy}{dt} + \lambda_1\lambda_2\ y = 0.$$

Multiple decay constants: In a similar way, higher-order differential equations with different multiple decay constants

$$(\frac{d}{dt} + \lambda_1)(\frac{d}{dt} + \lambda_2)\cdots(\frac{d}{dt} + \lambda_n)\ y = 0,$$

can appear.

Logarithmic relaxation:

Nonlinear: Sometimes a solution is implicit. The solution of

$$\tau\frac{dy}{dt} + \alpha(y^3 - \bar{y}^3) = 0$$

is (?)

$$t + \frac{1}{3}\frac{\tau(y - \bar{y})}{\alpha\bar{y}^2} - \frac{1}{6}\frac{\tau\ln(y^2 + y\bar{y} + \bar{y}^2)}{\alpha\bar{y}^2} - \frac{1}{3}\tau\sqrt{3}\arctan\big[\frac{1}{3}\frac{(2y + \bar{y})\sqrt{3}}{\bar{y}}\big]\alpha^{-1}\bar{y}^{-2} + C_1 = 0$$

Another nonlinear: The solution for

$$\tau\frac{dy}{dt} + \alpha(y - \bar{y})^3 = 0$$

will be different from that given above.

Example 1.1

Find the lowest-order differential equation for $y(t)$ corresponding to

$$y = Ce^{-y^2 t}.$$

Differentiating

$$\begin{aligned}\frac{dy}{dt} &= Ce^{-y^2 t}(-2yt\frac{dy}{dt} - y^2),\\ &= y(-2yt\frac{dy}{dt} - y^2)\end{aligned}$$

from which

$$\left(1 + 2y^2 t\right)\frac{dy}{dt} + y^3 = 0.$$

1.1.7 Optimization

To curve-fit empirical data $(y_i, t_i), i = 1, \ldots, n$, one must minimize the error E, where

$$E^2 = \sum_i (y_i - y(t_i; a, b, \ldots))^2,$$

between the data and a chosen function $y(t; a, b, \ldots)$, where $a, b, \ldots$ are parameters in the function that have to be determined.

Fig. 1.4 shows an example of the shape of E with respect to two parameters a and b. The coordinate descent method is a simple way to find the values of a and b for which E is a minimum. This works by a search for a minimum by varying a and keeping b constant, followed by varying b and keeping a constant; the process is repeated until a local minimum is reached where any change in a or b will lead to a climb.

1.2 Thermodynamic basis

A system is an identifiable part of the universe that is being studied, and the rest are the surroundings. Energy can enter or leave a system in the form of heat or work. A closed system does not exchange mass with its surroundings, and an isolated system does not exchange energy either. There is thermal equilibrium between two systems if there is no heat flow between them. Both heat and work are taken to be positive if they enter the system and negative if they leave.

The laws of thermodynamics that are needed in heat transfer are the following.

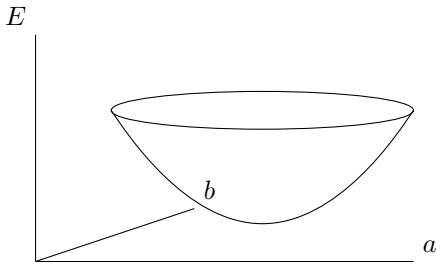

Figure 1.4: $E(a, b)$

Zeroth law: If two systems are each in thermal equilibrium with a third, they must also be in thermal equilibrium with each other. This enables temperature to be defined.

First law: The internal energy of a system increases by as much energy enters the system. This is the conservation of energy

$$dU = \delta Q + \delta W,$$

where dU is the differential change in internal energy, and δQ and δW are the small heat and work energies entering the system. This defines the internal energy.

The temperature is associated with the motion of molecules within a material, being directly related to the kinetic energy of the molecules, including vibrational and rotational motion. The change in internal energy of a body can be written in terms of a coefficient of specific heat as $\delta U = M\ c\ \delta T$. If we wanted to distinguish between the specific heat determined in a constant volume or constant pressure process, we would write c_v or c_p, respectively; for an incompressible substance they are both the same.

Second law: There are many equivalent statements and corollaries of this law. The one that is most relevant to heat transfer is that the change in entropy dS for a closed system receiving heat Q is

$$dS \geq \frac{\delta Q}{T},$$

where T its absolute temperature. The entropy of an isolated system can thus only increase. The equality holds for reversible processes and the inequality for irreversible. This law thus defines entropy.

1.2.1 Nonequilibrium thermodynamics

In general the driving potential (force or cause) $\Delta\phi$ and the resulting flow Q (flux or effect) are related in some way. Though the flow is more properly written $\dot{Q}$ indicating a rate, we will leave the dot as understood. Thus

$$Q = f(\Delta\phi)$$

Applying Eq. (1.1) to $\Delta\phi = 0$ around $\Delta\phi = 0$ gives

$$Q = f(0) + f'(0)(\Delta\phi) + \tfrac{1}{2!}f''(0)(\Delta\phi)^2 + \tfrac{1}{3!}f'''(0)(\Delta\phi)^3 + \dots$$

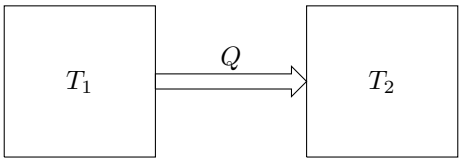

Figure 1.5: Two systems with heat transfer between them

Consider two systems, such as those in Fig. 1.5, that can exchange heat with each other but are isolated from their surroundings. From the zeroth law we know that the heat flow rate $Q = 0$ if the $\Delta\phi = T_1 - T_2 = 0$, so that $f(0) = 0$. Q may, however, be non-zero if $T_1 \neq T_2$. Keeping only one non-zero term in the expansion, we have

$$Q = C(T_1 - T_2), \tag{1.8}$$

where $C = f'(0)$ is a constant. This is a constitutive relation that can be taken to be empirical. Onsager's reciprocal relations relate the different kinds of driving potentials and their resulting flows.

Considering only the system on the left, and assuming that the heat exchange is reversible, its change in entropy is

$$\delta S_1 = -\frac{\delta Q}{T_1},$$

where δQ is the amount of heat transferred, and similarly that of the one in the right is

$$\delta S_2 = \frac{\delta Q}{T_2}.$$

We have taking into account the fact that heat is leaving one system and entering the other. The total entropy change of the combined system is

$$\begin{aligned}\delta S &= \delta S_1 + \delta S_2, \\ &= -\frac{\delta Q}{T_1} + \frac{\delta Q}{T_2}.\end{aligned}$$

Together the two systems are isolated from the surroundings, so the total entropy can only increase. Thus we must have $T_1 > T_2$, so that $C \geq 0$.

Onsager reciprocity

$$\boldsymbol{J}_\alpha = \sum_\beta L_{\alpha\beta} \boldsymbol{\nabla} f_\beta$$

where $L_{\alpha\beta}$ is the Onsager matrix of phenomenological coefficients.

1.2.2 Phase change

We will be dealing with solids, liquids and gases as well as the transformation of on to the other. Again, thermodynamics dictates the rules under which these changes are possible. For the moment, we will define the enthalpy of transformation, also called the latent heat, as the change in enthalpy that occurs when matter is transformed from one state to another.

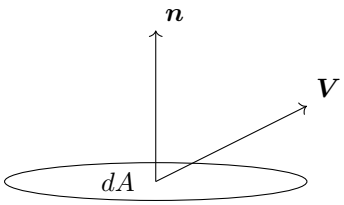

Figure 1.6: Advection by a flow with velocity $\boldsymbol{V}$ through an area $dA\ \boldsymbol{n}$

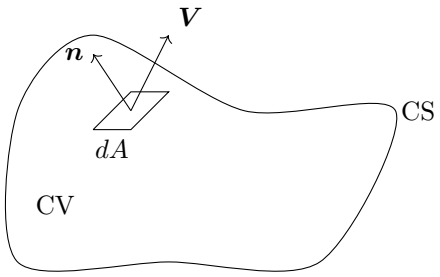

Figure 1.7: Control surface (CS) and control volume (CV) of arbitrary shape with an element of area dA on the surface.

1.3 Balance equations in integral form

The advective transport of a quantity X per unit mass (where X can be a scalar, vector or tensor) by the bodily motion of a fluid flow through an area $d\boldsymbol{A} = dA\ \boldsymbol{n}$ is shown in Fig. 1.6. Quantities are taken to be positive in the outward direction. The rate of transport of X through $d\boldsymbol{A}$ is $X\ \rho\ \boldsymbol{V} \cdot d\boldsymbol{A}$.

Consider an arbitrary control surface CS that encloses a control volume CV, as shown in Fig. 1.7. Balance of X gives

$$\frac{\partial}{\partial t} \int_{\mathcal{CV}} \rho\ X\ d\mathcal{V} + \int_{\mathcal{CS}} \rho\ X\ (\boldsymbol{V} \cdot d\boldsymbol{A}) = S,$$

where S is a source of X inside the volume.

Mass: For mass conservation, $X = 1$ and

$$\frac{\partial}{\partial t} \int_{\mathcal{CV}} \rho\ d\mathcal{V} + \int_{\mathcal{CS}} \rho\ (\boldsymbol{V} \cdot d\boldsymbol{A}) = 0.$$

Momentum: For Newton's second law, $X = \boldsymbol{V}$, so that

$$\frac{\partial}{\partial t} \int_{CV} \rho\ \boldsymbol{V}\ d\mathcal{V} + \int_{CS} \rho\ \boldsymbol{V}\ (\boldsymbol{V} \cdot d\boldsymbol{A}) = \boldsymbol{F}$$

Energy: The first law gives a quantitative relation between the heat and work input to a system. We will assume that there is no work transfer, as in Fig. 1.8. The simplest approach is to consider the entire system. In this case

$$\frac{\partial}{\partial t} \int_{CV} e\ \rho\ d\mathcal{V} + \int_{CS} e\ \rho\ (\boldsymbol{V} \cdot d\boldsymbol{A}) = Q + W + Q_g$$

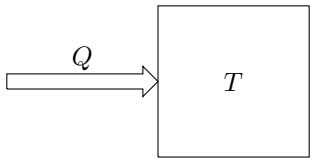

Figure 1.8: System with heat input

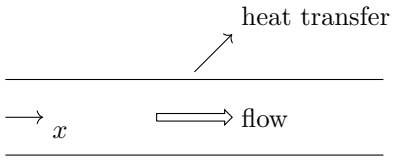

Figure 1.9: Pipe with phase change.

where

$$W = W_s + W_f + W_F,$$

and W_s = shaft work, W_f = flow work due to pressure, and W_F = work done by external force. Q and W are the rates of heat and work transfer into the system, respectively; Q_g is the rate of generation of heat. It is possible to put $e = u + p/\rho + V^2/2 + gz$ in the second integral on the left and $W = W_s$ on the right. This balance equation will be useful in many instances where only an overall knowledge of the internal energy of the system is required. However, in other instances detailed knowledge of the variation of the temperature is beneficial and differential equations inside the system are needed.

Example 1.2

A saturated liquid enters a heated pipe, Fig. 1.9, and leaves as a liquid-vapor mixture. How much energy has been transferred to the fluid from the pipe?

Assumptions:

Variables: Q = heat transfer rate to liquid, $\dot{m}$ = mass flow rate, h_2 and h_1 are the specific enthalpies at the outlet and inlet, respectively.

The heat transfer rate is

$$Q = \dot{m}(h_2 - h_1),$$

Of course, being a phase change process, the temperature difference is not proportional to the enthalpy change. From thermodynamics, $h_1 = h_f$ and $h_2 = (1 - x)h_f + xh_g$ where subscripts f and g refer to the saturated liquid and vapor states, respectively, and x is the quality factor (ratio by weight of gas to liquid).

1.4 Modeling

1.4.1 Theory and empiricism

We will use relations that we take to be either absolutely true or empirically (phenomenologically) based. Examples of the former are the laws of thermodynamics and Newton's laws. The fact that

these laws are ultimately verified experimentally is not of concern to engineers in most situations; they can assumed to be tested and true. Among the empirical relations are the analysis of frictional force using a friction coefficient and heat transfer with a convective heat transfer coefficient. Although these concepts cannot be thoroughly justified theoretically, they are none the less useful in practice. A related idea, useful in mathematical modeling, is that of constitutive relations. These are equations that related two or more quantities of interest in the process that have been found to work in practice. Often the constitutive is a linear relationship between two variables. Another class of empirical information is that related to material properties which are the result of experiments. Among these are densities, specific heats, and viscosities, which are sometimes taken to be constants.

In science, the ultimate arbiter of correctness of a theory is a comparison with experiments. Engineering, however, does not have the luxury of waiting until complete theories are developed and experimentally verified, so an empirical short cut is often used. These short cuts may be at different stages of the complete analysis; the process itself may be empirically modeled or the properties used in a detailed analysis may experimentally obtained. In any case there are always experiments behind the theory.

1.4.2 Relation to other perspectives

There are at least three purposes to the study of models.

Mathematical modeling: To obtain a model that can be solved analytically, numerically, or by a combination of both.

Physical understanding: To understand what is happening without the need for a solution.

Actual behavior: To predict behavior before making experimental runs.

1.5 Nondimensionalization

Making equations nondimensional is commonly practiced to compact the understanding of solutions obtained either experimentally or numerically. Thus if there are a total of n independent and dependent variables, it may be possible to combine them in some manner to have m variables, where $m < n$. Thus it is only necessary to determine a smaller number of dependent variables, after which the definitions of these variables may be used to get calculate the original variables.

Example 1.3

Nondimensionalize the forced vibration equation

$$m\frac{d^2x}{dt^2} + c\frac{dx}{dt} + kx = f\ \cos\omega t \text{ with } x = x_0, dx/dt = 0 \text{ at } t = 0,$$

where m, c, k, f, ω, x_0 are parameters that are provided.

Let $x^* = x/x_c,\ t^* = t/t_c$, where the subscript c indicates characteristic and the asterisks dimensionless quantities respectively, so that

$$\frac{mx_c}{t_c^2}\frac{d^2x^*}{dt^{*2}} + \frac{cx_c}{t_c}\frac{dx^*}{dt^*} + kx_cx^* = f\ \cos(\omega\ t_ct^*) \text{ with } x_cx^* = x_0, (x_c/t_c)\ dx^*/dt^* = 0 \text{ at } t_ct^* = 0.$$

Dividing by mx_c/t_c^2

$$\frac{d^2x}{dt^2} + C\frac{dx}{dt} + Kx^* = f^*\ \cos\omega^*t^* \text{ with } x^* = x_0/x_c,\ dx^*/dt^* = 0 \text{ at } t^* = 0,$$

where $C = ct_c/m,\ K = kt_c^2/m,\ f^* = ft_c^2/mx_c,\ \omega^* = \omega t_c$.

We still need to choose t_c and x_c. For example, if we choose $t_c = \sqrt{m/k}$ and $x_c = x_0$, the equation becomes

$$\frac{d^2x^*}{dt^{*2}} + C\frac{dx^*}{dt^*} + 1 = f^*\ \cos\omega^* t^* \text{ with } x^*(0) = 1,\ dx^*/dt^* = 0 \text{ at } t^* = 0.$$

Alternatively, we could choose $\omega t_c = 1$, and $ft_c^2/mx_c = 1$.

1.6 Problem analysis procedure

Though each problem is unique, there are some overall guiding principles that can be laid down. The following are some of the steps that may be considered. The *Example* in Section 7.5.1 on page 138 uses many of these steps, though most of the other examples are compressed with the extra steps being understood.

- Draw a schematic of layout to help clarify the problem in your own mind. See first if the answer sought makes physical sense.
- Identify physical processes. Consult and study appropriate literature both on the generalities of the processes as well as the specific problem at hand. Consult others but make up your own mind.
- Write appropriate equations of balance (integral or differential). Derive, or re-derive, each one as far as possible or practical.
- Simplify as needed to enable solution without removing essentials.
- Solve symbolically. There may be more than one way to do it. Use a symbolic algebra program if needed. Refresh or sharpen your analytical tools if necessary. Check solutions by substitutions.
- Solve numerically as a last resort if need be.
- Check that the solution makes physical sense; think of the consequences of varying parameters and for limiting cases.
- Check equations and solutions for dimensional consistence.
- Graph result.
- Improve results by including other previously disregarded factors, and obtaining numerical solutions.

Bibliography

C. Borgnakke and R.E. Sonntag, *Fundamentals of Thermodynamics,* 8th Ed., Wiley, 2012.

T. Erneux, *Applied Delay Differential Equations,* Springer, 2009.

M.J. Moran, H.N. Shapiro, D.D. Boettner and M.B. Bailey, *Fundamentals of Engineering Thermodynamics,* 7th Edition, 7th Ed., Wiley, 2010.

J.M. Powers and M. Sen, *Mathematical Methods in Engineering,* Cambridge University Press, 2015.

Problems

1. Choose a quadratic $y(x)$, and then take three values of x and find their corresponding y's. From the three (x, y) pairs, find the quadratic.

Chapter 2

Mechanisms of heat transfer

This chapter is brief summary of an introductory course on heat transfer.

2.1 Conduction

[31, 69, 71, 81, 106, 144, 145, 157]

We will now take up conduction in a stationary continuum. Consider the conduction heat flux $q(x)$ through a thick plate such as the one shown in Fig. 2.1. The coordinate through the plate is x, and the temperature field is assumed to vary only in that direction, i.e. $T = T(x)$. Two elements in the plate a distance dx apart are at temperatures T and $T + dT$, respectively. From Eq. (1.8), q will be zero if the temperature is uniform. So, q should depend on the first and higher derivatives of the temperature. Thus

$$q(x) = f(\frac{\partial T}{\partial x}, \frac{\partial^2 T}{\partial x^2}, \frac{\partial^3 T}{\partial x^3}, \ldots)$$

Taking only the linear term of a Taylor series expansion in the different arguments, we can write

$$q = k_1 \frac{\partial T}{\partial x} + k_2 \frac{\partial^2 T}{\partial x^2} + k_3 \frac{\partial^3 T}{\partial x^3}, \ldots$$

where the k's are constants. Taking only the first term

$$q = -k \left. \frac{\partial T}{\partial x} \right|_x .$$

The negative sign is introduced to make k, called the coefficient of thermal conductivity, positive since from Eq. (1.8) heat flows down a temperature gradient. This is Fourier's law of conduction.

For three-dimensional anisotropic conduction we can write

$$q_i = -\sum_j k_{ij} \frac{\partial T}{\partial x_j}$$

where q_i is the heat flux vector in the i-direction, T is the temperature field, and $\partial T/\partial x_j$ its partial derivative in the j-direction. k_{ij} is the coefficient of thermal conductivity; from Eq. (1.8) it is positive. Actually, being a matrix, it is positive definite. For an isotropic material

$$\boldsymbol{q} = -k \, \boldsymbol{\nabla} T$$

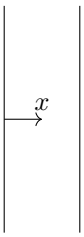

Figure 2.1: 1D conduction through a plate

where $\boldsymbol{q}$ is the heat flux vector, $T(\boldsymbol{x})$ is the temperature field, and $k(T)$ is the coefficient of thermal conductivity.

2.1.1 Fourier's law

$$
\begin{aligned}
q_x &= -k\,\frac{\partial T}{\partial x} && \text{one-dimensional Cartesian,}\\
q_r &= -k\,\frac{\partial T}{\partial r} && \text{radial cylindrical,}\\
q_r &= -k\,\frac{\partial T}{\partial r} && \text{radial spherical,}\\
\boldsymbol{q} &= -k\,\boldsymbol{\nabla} T && \text{vector form.}
\end{aligned}
$$

2.1.2 Heat equation

Substituting Fourier's law, Eqs. (2.1), into the various forms of the energy balance equation in Chapter 1, we get

$$
\begin{aligned}
\rho c\frac{\partial T}{\partial t} &= \frac{\partial}{\partial x}\left(k\,\frac{\partial T}{\partial x}\right) && \text{one-dimensional Cartesian,}\\
\rho c\frac{\partial T}{\partial t} &= \frac{1}{r}\,\frac{\partial}{\partial r}\left(k\,r\frac{\partial T}{\partial r}\right) && \text{radial cylindrical,}\\
\rho c\frac{\partial T}{\partial t} &= \frac{1}{r^2}\,\frac{\partial}{\partial r}\left(k\,r^2\frac{\partial T}{\partial r}\right) && \text{radial spherical,}\\
\rho c\frac{\partial T}{\partial t} &= \boldsymbol{\nabla}\cdot\left(k\,\boldsymbol{\nabla} T\right) && \text{vector form.}
\end{aligned}
$$

For constant k and with heat generation, we can write

$$\frac{\partial T}{\partial t} = \alpha\nabla^2 T + Q_g$$

where $\alpha = k/\rho c$ is the thermal diffusivity.

2.2 Convection

[11, 21, 27, 70, 101, 104, 105, 108, 111, 141].

Figure 2.2: Process of convection.

Fig. 2.2 shows the process of convection from a wall to a flow that is at a different temperature. First there is conduction from the wall to the fluid and then the heat is carried by the bodily motion of the fluid. The latter is called advection.

2.2.1 Governing equations

For incompressible flow with constant properties, the energy equation is

$$\rho c \left(\frac{\partial T}{\partial t} + \boldsymbol{V} \cdot \boldsymbol{\nabla} T \right) = k \, \nabla^2 T + \Phi$$

where $\Phi = \boldsymbol{\tau} \colon \boldsymbol{\nabla} \boldsymbol{V}$ is the viscous dissipation. The hydrodynamic equations decouple from the thermal equation. For natural convection, however, there is coupling since $\boldsymbol{f} = -\rho g (T - T_{\text{ref}}) \boldsymbol{k}$. There is also coupling for compressible flow or for temperature-dependent viscosity.

For constant properties and turbulent flow, we can take $\boldsymbol{V} = \bar{\boldsymbol{V}} + \boldsymbol{V}'$, where the bar indicates a time average, from which the time average of the momentum equation for a Newtonian fluid becomes

$$\rho \left(\frac{\partial \bar{\boldsymbol{V}}}{\partial t} + \bar{\boldsymbol{V}} \cdot \boldsymbol{\nabla} \bar{\boldsymbol{V}} \right) = -\boldsymbol{\nabla} p + \mu \nabla^2 \boldsymbol{V} + \boldsymbol{\nabla} \cdot \boldsymbol{\tau}^R + \boldsymbol{f},$$

where $\tau_{ij}^R = -\rho \, \overline{V_i' \, V_j'}$ is the Reynolds stress. This is generally a priori unknown, leading to the closure problem in turbulent flow. Usually a turbulence model is assumed for this.

2.2.2 Heat transfer coefficient

Based on Eq. (1.8), Newton's law of cooling can be proposed: The convective heat flux from a body q is proportional the heat transfer area and the difference in temperature between the body and the surrounding fluid. Thus, we can write

$$Q = hA(T_s - T_\infty), \tag{2.2}$$

where A is the surface area of the body, T_s is its temperature, T_∞ is that of the fluid, and h is the coefficient of thermal convection between them.

Example 2.1

What is the steady state temperature of a resistor through which a current is flowing?

Assume: (a) Only convection heat transfer to air. (b) Resistor at uniform temperature. (c) No heat conduction through electrical wires. (d) Joule heating in resistor. (e) Convection governed by Newton's law of cooling.

Figure 2.3: *Example 1.*

Variables: Q_g = rate of heat generation, i = electrical current, R = resistance, Q_{conv} = rate of heat lost by convection, h = convection heat transfer between resistor and surrounding air, A = heat transfer area of resistor, T_R = temperature of resistor, T_∞ = temperature of surrounding air. (d) Joule heating in wire.

The heat generation and heat loss are

$$Q_g = i^2 R,$$
$$Q_{\text{conv}} = h\ A\ (T_R - T_\infty),$$

respectively. At steady state, $Q_g = Q_{\text{conv}}$, so that

$$i^2 R = h\ A\ (T_R - T_\infty),$$
$$T_R = T_\infty + \frac{i^2 R}{h\ A}.$$

Example 2.2

A 1 mm diameter, 20 mm long nichrome wire of resistivity 10^{-6} Ω·m carries a current of 0.5 A. What is the surface temperature of the wire if it is placed (a) in a transverse flow of 20 °C air at 1 m/s, or (b) horizontally in quiescent air at 20 °C?

Variables: i = electrical current; R = electrical resistance; T_s = surface temperature of wire; Q = heat generated in wire; σ = resistivity; L = length of wire; A = cross sectional area of wire.

$$R = \frac{\sigma L}{A},$$
$$Q = i^2 R, \quad \text{Joule heating}$$
$$= hA_s(T_s - T_\infty).$$

Thus

$$T_s = \frac{Q}{hA_s} + T_\infty,$$
$$= \frac{i^2 \sigma L}{hA_s A} + T_\infty,$$

2.2.3 Correlations

Common nondimensional groups are shown in Table 2.1. For forced convection, correlations are of the form of *Nu*, *St* or j as a function of (*Re*, *Pr*). For natural convection the independent groups are (*Ra*, *Pr*) or (*Gr*, *Pr*).

Fouling

Bulk temperature

Table 2.1: Common nondimensional groups used in heat transfer

Biot number	$Bi = \dfrac{hL}{k_s}$	Fourier number	$Fo = \dfrac{\alpha t}{L^2}$
Reynolds number	$Re = \dfrac{VL}{\nu}$	Peclet number	$Pe = \dfrac{VL}{\alpha}$
Grashof number	$Gr = \dfrac{g\beta\Delta T L^3}{\nu^2}$	Rayleigh number	$Ra = Gr\ Pr$
Prandtl number	$Pr = \dfrac{\nu}{\alpha}$	Nusselt number	$Nu = \dfrac{hL}{k}$
Stanton number	$St = \dfrac{Re}{Pr\ Re}$	Colburn j-factor	$j = St\ Pr^{2/3}$
Friction factor	$f = \dfrac{2\tau_w}{\rho U^2}$		

Forced convection

Natural convection

2.2.4 Phase change convection

[29, 42, 208]

Pool boiling

Boiling curve. See Fig. 2.4.

- Heat flux for nucleate boiling

$$q = \mu_l h_{fg} \left[\frac{g(\rho_l - \rho_v)}{\sigma} \right]^{1/2} \left(\frac{c_{p,l}\ \Delta T_e}{C_{s,f}\ h_{fg}\ Pr_l^n} \right)^3 \quad \text{Rohsenow}$$

- Critical heat flux

$$q_{max} = C h_{fg} \rho_v \left[\frac{\sigma g(\rho_l - \rho_v)}{\rho_v^2} \right]^{1/4} \quad \text{Zuber}$$

- Minimum heat flux

$$q_{min} = C h_{fg} \rho_v \left[\frac{g\sigma(\rho_l - \rho_v)}{(\rho_l + \rho_v)^2} \right]^{1/4} \quad \text{Zuber}$$

- Film boiling

$$h_{eq} = h^{4/3} + h_r h_{eq}^{1/3}$$

where h is the convective and h_r the radiative heat transfer coefficient.

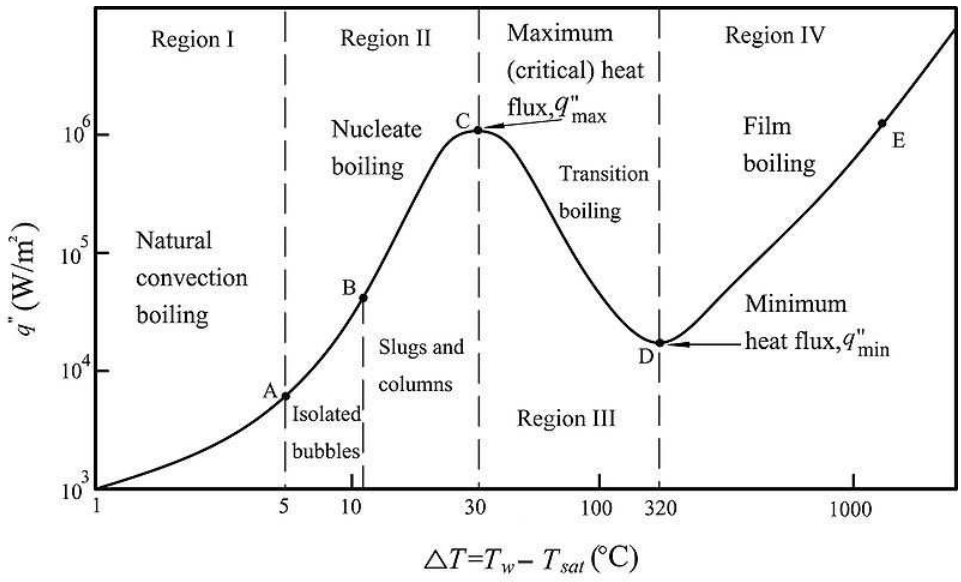

Figure 2.4: Boiling curve

- Film boiling on a sphere

$$Nu = C\left[\frac{g(\rho_l - \rho_v)h'_{fg}D^3}{\nu_v k_v (T_s - T_{sat}}\right]^{1/4}$$

- Condensation
  Nusselt's solution for falling film
- Homogeneous nucleation
- Flow boiling

$$\begin{aligned}\frac{q_{max}}{\rho_v h_{fg} V} &= \frac{1}{\pi}\left[1 + \left(\frac{4}{We_D}\right)^{1/3}\right] && \text{low velocity}\\ &= \frac{(\rho_l/\rho_v)^{3/4}}{169\ \pi} + \frac{\rho_l/\rho_v}{19.2\ \pi\ We_D^{1/3}} && \text{high velocity}\end{aligned}$$

  where $We_D = \rho_v V^2 D/\sigma$.
- Two-phase flow

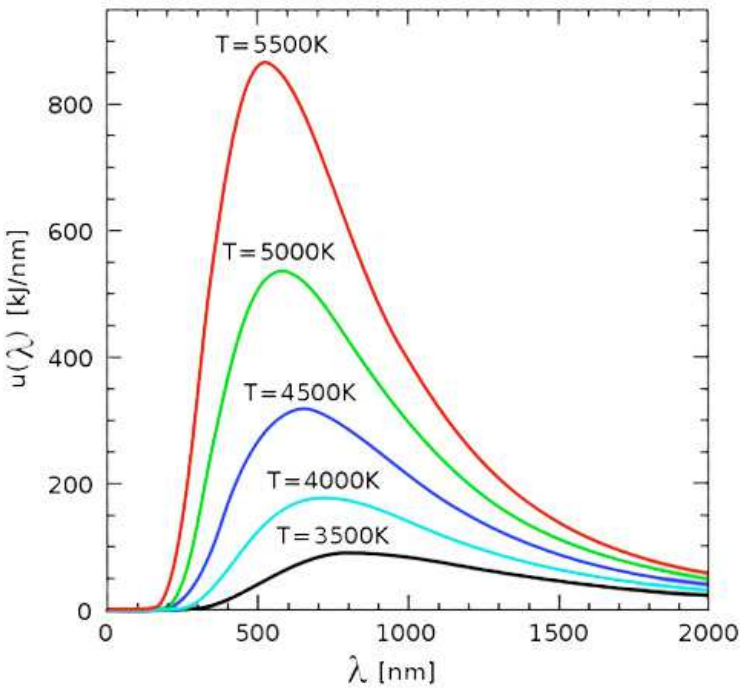

Figure 2.5: Planck distribution

2.3 Radiation

[25, 59, 135, 220]

Emission can be from a surface or volumetric. Monochromatic radiation is at a single wavelength. The spectral intensity of emission is the radiant energy leaving per unit time, unit area, unit wavelength, and unit solid angle. The emissive power E is the emission of an entire hemisphere. Irradiation G is the radiant energy coming in, while the radiosity J is the energy leaving including the emission plus the reflection.

2.3.1 Blackbody

Planck's distribution [155] See Fig. 2.5.

$$E_\lambda = \frac{C_1\ \lambda^{-5}}{e^{C_2/\lambda T} - 1}$$

Wien's law: Putting $dE_\lambda/d\lambda = 0$, the maximum is seen to be at $\lambda = \lambda_m$, where

$$\lambda_m T = C_3$$

and $C_3 = 2897.8\ \mu$m K.

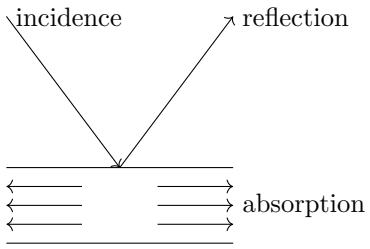

Figure 2.6: Absorption, transmission and reflection

Stefan-Boltzmann's law: The total radiation emitted is

$$\begin{aligned} E_b &= \int_0^\infty E_\lambda \, d\lambda \\ &= \sigma T^4 \end{aligned}$$

where $\sigma = 5.670 \times 10^{-8}$ W/m^{2}K^4.

2.3.2 Real surfaces

Reflection: The direction distribution of radiation from a surface may be either specular (i.e. mirror-like with angles of incidence and reflection equal) or diffuse (i.e. equal in all directions).

Translucent media: See Fig. 2.6. The absorptivity α_λ, the reflectivity ρ_λ, and transmissivity τ_λ are all functions of the wavelength λ. Also

$$\alpha_\lambda + \rho_\lambda + \tau_\lambda = 1$$

Integrating over all wavelengths

$$\alpha + \rho + \tau = 1$$

Emissivity: The emissivity is defined as

$$\epsilon_\lambda = \frac{E_\lambda(\lambda, T)}{E_{b\lambda}(\lambda, T)}$$

where the numerator is the actual energy emitted and the denominator is that that would have been emitted by a blackbody at the same temperature. For the overall energy, we have a similar definition

$$\epsilon = \frac{E(T)}{E_b(T)}$$

so that the emission is

$$E = \epsilon \sigma T^4$$

For a gray body ϵ_λ is independent of λ.

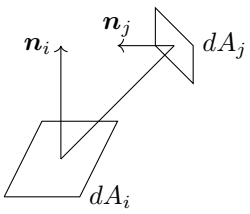

Figure 2.7: Two elemental areas dA_i and dA_j with unit normals $\boldsymbol{n}_i$ and $\boldsymbol{n}_j$ respectively.

Kirchhoff's law: $\alpha_\lambda = \epsilon_\lambda$ and $\alpha = \epsilon$.

Gray surface: ϵ_λ and $\alpha = \epsilon$ are independent of λ.

Net heat rate: For a surface i

$$\begin{aligned} Q_i &= A_i(J_i - G_i) \\ &= A_i(E_i - \alpha_i\ G_i). \end{aligned}$$

Surface radiative resistance: In

$$Q_i = \frac{E_{bi} - J_i}{(1-\epsilon_i)/\epsilon_i A_i} \tag{2.3}$$

the driving potential is $E_{bi} - J_i$ and the surface resistance is $(1-\epsilon_i)/\epsilon_i A_i$ due to its not being black.

2.3.3 Radiation between surfaces

View factor: See Fig. 2.7. Assume that emission and reflection are diffuse. F_{ij} is the fraction of the radiation leaving surface i that falls on surface j. It can be calculated from

$$F_{ij} = \frac{1}{A_i} \int_{A_i} \int_{A_j} \frac{1}{\pi R^2}\ \cos\theta_i\ \cos\theta_j\ dA_i\ dA_j$$

Reciprocity: $A_i\ F_{ij} = A_j\ F_{ji}$

2.3.4 Enclosures

Summation rule:

$$\sum_{j=1}^{N} F_{ij} = 1.$$

Exchange between surfaces: The radiative heat transfer from surface i to j is

$$Q_{ij} = \frac{J_i - J_j}{(A_i F_{ij})^{-1}} = \frac{J_i - J_j}{(A_j F_{ji})^{-1}}. \tag{2.4}$$

Large blackbody enclosure: For a small body 1 radiating to a large blackbody enclosure 2, the net radiation emitted by 1 is

$$\begin{aligned} Q &= \sigma F_{12} A_1 T_1^4 - F_{21} A_2 T_2^4, \\ &= \sigma A_1 (T_1^4 - T_2^4) \qquad \text{by reciprocity} \end{aligned} \tag{2.5}$$

where $F_{12} \approx 1$.

Radiation shield: If between two plates 1 and 2, a third plate 3 is introduced then

$$Q_{12} = \frac{A_1 \sigma (T_1^4 - T_2^4)}{\epsilon_1^{-1} + \epsilon_2^{-1} + (1 - \epsilon_{3,a})\epsilon_{3,a}^{-1} + (1 - \epsilon_{3,b})\epsilon_{3,b}^{-1}}$$

where $\epsilon_{3,a}$ and $\epsilon_{3,b}$ are the emissivities of the two sides of 3 facing 1 and 2 respectively. This is less than the the value without the shield, which is

$$Q_{12} = \frac{A \sigma (T_1^4 - T_2^4)}{\epsilon_1^{-1} + \epsilon_2^{-1} - 1}$$

Resistance network: Consider the example of n gray surfaces forming an enclosure. Fig. 2.8 shows an example with $n = 3$. The temperatures of the surfaces T_i, are known as well as their emissivities ϵ_i, areas A_i, and the view factors between them F_{ij}. Then the voltages and resistances are

$$\begin{aligned} E_{bi} &= \sigma T_i^4, && \text{driving blackbody potential} \\ R_i &= \frac{1 - \epsilon_i}{\epsilon_i A_i}, && \text{surface radiative resistance} \\ R_{ij} &= (A_i F_{ij})^{-1} = (A_j F_{ji})^{-1} && \text{view factor resistance} \end{aligned}$$

The circuit equations for the nodes and the branches can be written. For example, the sum of the currents flowing into node i must be zero, so that

$$\frac{\sigma T_i^4 - J_i}{(1 - \epsilon_i)/\epsilon_i A_i} + \sum_{j \neq i} \frac{J_j - J_i}{(A_j F_{ji})^{-1}} = 0.$$

These are n equations in the unknowns J_i, $i = 1, 2, 3, \ldots, n$ which can be solved for J_i. Using J_i, the branch currents Q_i can be determined from Eq. (2.3), and Q_{ij} from Eq. (2.4). The currents are equivalent to the heat rates.

2.4 Steady state electrical analog

In an electrical analog, $\Delta T \sim$ voltage difference and $Q \sim$ current. In analogy with Ohm's law, the thermal resistance is defined as

$$R = \frac{\Delta T}{Q}. \tag{2.6}$$

Thus Table 2.2 shows thermal resistances of different types. An example of a composite wall with convection and conduction and its resistance circuit is in Figs. 2.9 and 2.10.

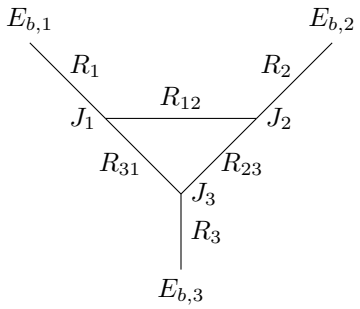

Figure 2.8: Enclosure of three gray surfaces

Table 2.2: Thermal resistances

Mode		*thermal resistance*
Conduction		
	Cartesian	$\frac{L}{k\ A}$
	cylindrical	$\frac{\ln(r_2/r_1)}{2\pi\ L\ k}$
	spherical	$\frac{(1/r_1)-(1/r_2)}{2\pi k}$
Convection		$\frac{1}{h\ A}$
Radiation		$\frac{1}{h_r\ A}$

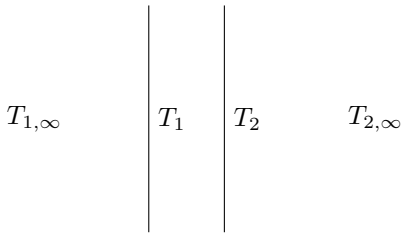

Figure 2.9: Composite wall with convection and conduction.

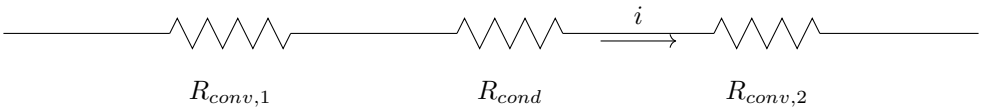

Figure 2.10: Electrical analog of Fig. 2.9.

Contact resistance: This is R_c defined as

$$R_c = \frac{\Delta T}{Q}$$

where ΔT is the temperature difference across two surfaces in contact, and Q is the heat rate through them.

Radiative thermal resistance approximation: For a surface at T_s and the surroundings at T_∞, the blackbody radiation heat exchange from Eq. (2.5) is

$$Q = A\ \sigma(T_s^4 - T_\infty^4).$$

Since

$$\begin{aligned} T_s^4 - T_\infty^4 &= \big(T_s^2 + T_\infty^2\big)\ \big(T_s^2 - T_\infty^2\big), \\ &= \big(T_s^2 + T_\infty^2\big)\ \big(T_s + T_\infty\big)\ \big(T_s - T_\infty\big) \end{aligned}$$

we have

$$Q = A\ \sigma\big(T_s^2 + T_\infty^2\big)\ \big(T_s + T_\infty\big)\ \big(T_s - T_\infty\big).$$

Comparing with Eqs. (2.2) and (2.6) we can write the radiative heat transfer coefficient and thermal resistance as

$$h_r = \sigma\ \big(T_s^2 + T_\infty^2\big)\ \big(T_s + T_\infty\big), \tag{2.7}$$

$$R_r = \frac{1}{h_r\ A}, \tag{2.8}$$

respectively. Even though h_r is a function of the temperature T_s, for small enough differences $T_s - T_\infty$ it can be taken to be a constant. In fact, it can be shown that

$$h_r = 4\sigma T_\infty^3\big(1 + \tfrac{3}{2}\delta + \delta^2 + \tfrac{1}{4}\delta^3\big),$$

where $\delta = (T_s - T_\infty)/T_\infty$. Just to be clear, the use of Eq. (2.7) with Eq. (2.2) is exact in the steady state when T_s and T_∞ are not changing with time, but is approximate otherwise.

Thermal resistances in series: For several thermal resistance in series, as in a composite wall, for each one we have

$$\Delta T_i = Q\ R_i.$$

Also, since $\Delta T = \sum_i \Delta T_i$, we have for a composite wall

$$\Delta T = Q\ R_{eq},$$

where the equivalent thermal resistance is

$$R_{eq} = \sum_i R_i.$$

Thermal resistances in parallel: For this configuration

$$\frac{1}{R_{eq}} = \sum_i \frac{1}{R_i}.$$

Overall heat transfer coefficient: This is defined as U where

$$Q = U\ A\ \Delta T.$$

From this

$$\frac{1}{U\ A} = \sum_i R_i \quad \text{series},$$

$$U\ A = \sum_i \frac{1}{R_i} \quad \text{parallel}.$$

Bibliography

M. Becker, *Heat Transfer, A Modern Approach,*, Plenum, 1986.

L.R. Glicksman and J.H. Lienhard V, *Modeling and Approximation in Heat Transfer,* Cambridge University Press, 2016.

J.P. Holman, *Heat Transfer,* 7th Ed., McGraw-Hill, 1990.

F.P. Incropera and D.P. Dewitt, *Fundamentals of Heat and Mass Transfer,* 5th Ed., John Wiley, 2002.

M.F. Modest, *Radiative Heat Transfer,* Academic Press, 2003.

R.H.S. Winterton, *Heat Transfer,*, Oxford, 1997.

K.-F.V. Wong, *Intermediate Heat Transfer,* Marcel Dekker, 2003.

Problems

1. For a perimeter corresponding to a fin slope that is not small, derive Eq. 6.1.
2. The two sides of a plane wall are at temperatures T_1 and T_2. The thermal conductivity varies with temperature in the form $k(T) = k_0 + \alpha(T - T_1)$. Find the temperature distribution within the wall.
3. Consider a cylindrical pin fin of diameter D and length L. The base is at temperature T_b and the tip at T_∞; the ambient temperature is also T_∞. Find the steady-state temperature distribution in the fin, its effectiveness, and its efficiency. Assume that there is only convection but no radiation.
4. Show that the efficiency of the triangular fin shown in Fig. E.32 is

   $$\eta_f = \frac{1}{mL}\frac{I_1(2mL)}{I_0(2mL)},$$

   where $m = (2h/kt)^{1/2}$, and I_0 and I_1 are the zeroth- and first-order Bessel functions of the first kind.
5. A constant-area fin between surfaces at temperatures T_1 and T_2 is shown in Fig. E.33. If the external temperature, $T_\infty(x)$, is a function of the coordinate x, find the general steady-state solution of the fin temperature $T(x)$ in terms of a Green's function.

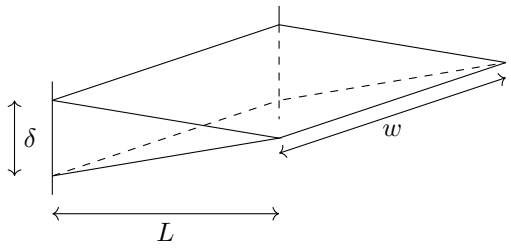

Figure 2.11: Triangular fin.

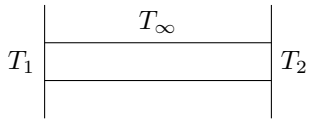

Figure 2.12: Constant-area fin.

6. Using a lumped parameter approximation for a vertical flat plate undergoing laminar, natural convection, show that the temperature of the plate, $T(t)$, is governed by

$$\frac{dT}{dt} + \alpha(T - T_\infty)^{5/4} = 0$$

Find $T(t)$ if $T(0) = T_0$.

7. Show that the governing equation in Problem 3 *with* radiation can be written as

$$\frac{d^2T}{dx^2} - m^2(T - T_\infty) - \epsilon(T^4 - T_\infty^4) = 0.$$

Find a two-term perturbation solution for $T(x)$ if $\epsilon \ll 1$ and $L \to \infty$.

8. The fin in Problem 3 has a *non-uniform* diameter of the form

$$D = D_0 + \epsilon x.$$

Determine the equations to be solved for a two-term perturbation solution for $T(x)$ if $\epsilon \ll 1$.

9. Determine computationally the view factor between two rectangular surfaces (each of size $L \times 2L$) at 90° with a common edge of length $2L$. Compare with the analytical result.

10. Calculate the view factor again but with a sphere (diameter $L/2$, center at a distance of $L/2$ from each rectangle, and centered along the length of the rectangles) as an obstacle between the two rectangles; see Fig. 2.13.

11. (From Incropera and DeWitt) Consider a diffuse, gray, four-surface enclosure shaped in the form of a tetrahedron (made of four equilateral triangles). The temperatures and emissivities of three sides are

$$T_1 = 700\text{K}, \quad \epsilon_1 = 0.7$$
$$T_2 = 500\text{K}, \quad \epsilon_2 = 0.5$$
$$T_3 = 300\text{K}, \quad \epsilon_3 = 0.3$$

The fourth side is well insulated and can be treated as a reradiating surface. Determine its temperature.

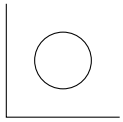

Figure 2.13: Two rectangular surfaces with sphere.

Chapter 3

Lumped systems (zero-dimensional)

Steady and unsteady states

3.1 Balance equations

We assume that all properties are uniform inside the system.

Momentum:

$$\frac{d^2\boldsymbol{V}}{dt^2} = \boldsymbol{F}$$

Energy:

$$\frac{dU}{dt} = Q$$

where Q is the heat rate coming in from the surroundings. Using the specific heat

$$Mc\frac{dT}{dt} = Q$$

3.2 Validity of lumped approximation

3.2.1 Conduction

According to this the temperature inside a body $T_s(t)$ is assumed to be uniform, though it may be unsteady. For example, consider a solid with a boundary with a fluid as shown in Fig. 3.1. Since the mass of a surface is zero, there is no accumulation of energy possible there and the heat coming in by conduction should equal that going out by convection. Since the fluid velocity is zero at the surface, the heat transfer into the fluid there is by conduction also. The temperature gradients on the two sides of the interface are in inverse ratio of the thermal conductivities of the solid and fluid. As an example, the ratio of the thermal conductivities of steel and water is about 28 so that the solid to liquid temperature gradients on either side of the interface are $1 : 28$. The temperature is continuous across the interface but the temperature gradient is not.

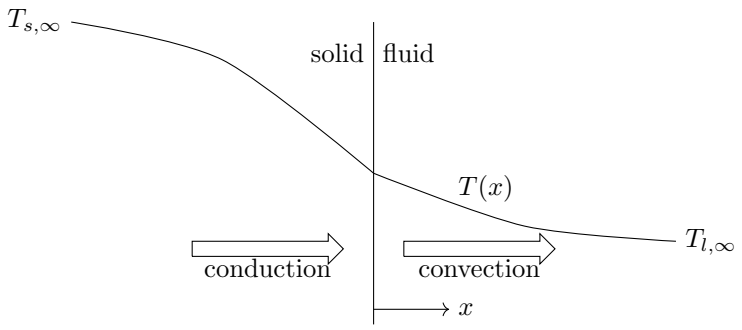

Figure 3.1: Solid fluid interface

We may, however, use a convection heat transfer coefficient approximation on the fluid side. Then, at the $x = 0$ interface

$$-k_s \frac{\partial T}{\partial x}\bigg|_{x=0^-} = h(T - T_{f,\infty})\bigg|_{x=0^+}.$$

If $T_{s,\infty}$ and $T_{f,\infty}$ are the temperatures far from the interface on the solid and fluid sides, respectively, then we can nondimensionalize and normalize the temperatures in the solid and fluid as

$$T^* = \frac{T - T_{f,\infty}}{T_{s,\infty} - T_{f,\infty}}.$$

In addition we need a characteristic length scale on the solid side; let that be L_c. Then $x^* = x/L_c$ in the solid, and the interface condition becomes

$$\begin{aligned} -\frac{k_s}{L_c}\,(T_{s,\infty} - T_{f,\infty})\frac{\partial T^*}{\partial x^*} &= hT^*(T_{s,\infty} - T_{f,\infty}), \\ -\frac{\partial T^*}{\partial x^*} &= \frac{hL_c}{k_s}\,T^*, \\ &= Bi\,T^*, \end{aligned}$$

where the Biot number is $Bi = hL_c/k_s$. Thus $\partial T_s^*/\partial x^* \to 0$ as $Bi \to 0$; a small Bi implies a small temperature gradient in the solid. In practice $Bi \lessapprox 0.1$ is considered to be small enough. The Biot number is the ratio of the conductive thermal resistance in the solid to the convective thermal resistance in the fluid.

3.2.2 Convection

The temperature of the fluid in an enclosed chamber can be considered to be uniform if it is well mixed by a fan or other medium.

3.3 Relaxation

This is the return of a system to a time-independent state after being perturbed from it. Shown in Fig. 3.2 are two traces, one for rising and the other for falling relaxation. In either case the quantity

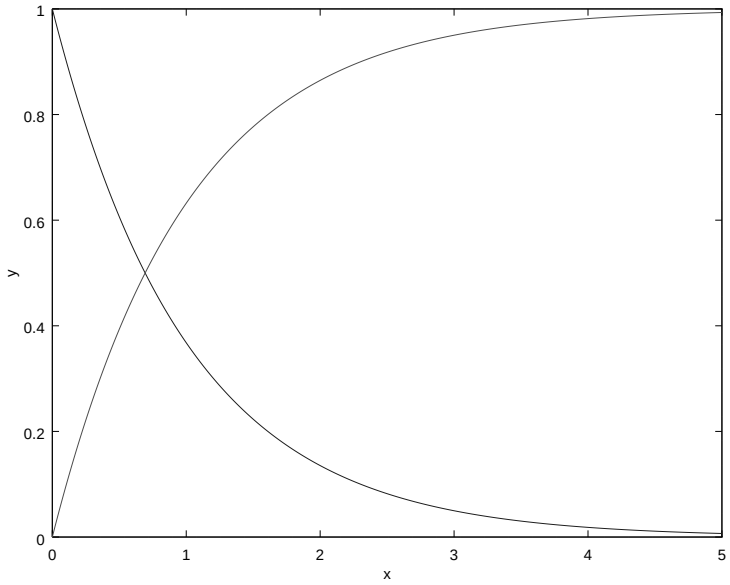

Figure 3.2: Two typical relaxation responses

asymptotes in a non-oscillatory manner to a final value. The time constants τ of both falling and rising traces are defined by

$$\tau = \int_0^\infty \frac{T(t) - T(\infty)}{T(0) - T(\infty)}\, dt. \tag{3.1}$$

The reciprocal of τ is the decay constant $\lambda = 1/\tau$.

Example 3.1

A body at temperature T, such as that shown in Fig. 3.3, is placed in an environment of different temperature, T_∞, and is convectively cooled. Find the time constant.

Assume: Newton's law of cooling. Variables: $T(t)$ = temperature of body, t = time; T_∞ = ambient temperature; m = mass of body; c = specific heat of body; h = convective heat transfer coefficient; A = convection surface area.

The governing equation is

$$mc\frac{dT}{dt} + hA(T - T_\infty) = 0 \quad \text{with} \quad T(0) = T_0. \tag{3.2}$$

We nondimensionalize using

$$T^* = \frac{T - T_\infty}{T_0 - T_\infty}; \quad t^* = \frac{hAt}{mc}. \tag{3.3}$$

The nondimensional form of the governing equation (3.2) is

$$\frac{dT^*}{dt^*} + T^* = 0 \quad \text{with} \quad T^*(0) = 1,$$

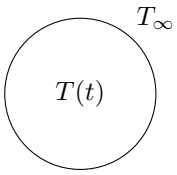

Figure 3.3: Body undergoing convective cooling.

the solution to which is

$$T^* = e^{-t^*}. \tag{3.4}$$

This corresponds to the falling trace in Fig. 3.2. Since $T^*(t^*)$ goes from $T^*(0) = 1$ to $T^*(\infty) = 0$, from Eq. (3.1) the nondimensional time constant is

$$\tau^* = \int_0^\infty \frac{T^*(t) - T^*(\infty)}{T^*(0) - T^*(\infty)}\ dt^*, \tag{3.5}$$

$$= \int_0^\infty e^{-t^*}\ dt^*, \tag{3.6}$$

$$= 1. \tag{3.7}$$

The nondimensional time constant τ^* is unity, and so the dimensional time constant is $\tau = mc/hA$.

3.3.1 Unsteady electrical analog

The voltage across each one of the following electrical components in Fig. 3.4 is

$$\begin{aligned} V_R &= iR && \text{resistance } R, \\ V_C &= \frac{1}{C}\int i(t)\ dt, && \text{capacitance } C, \\ V_L &= L\frac{d^2 i}{dt^2}, && \text{inductance } L. \end{aligned}$$

The total voltage $V(t)$ applied across the circuit must be equal to the voltage drops across each one of the components. Thus

$$iR + \frac{1}{C}\int i(t)\ dt = V,$$

from which, by differentiation

$$\begin{aligned} R\frac{di}{dt} + \frac{1}{C}i &= \frac{dV}{dt}, \\ \frac{di}{dt} + \frac{1}{RC}i &= \frac{1}{R}\ \frac{dV}{dt}. \end{aligned} \tag{3.8}$$

Eqs. (**??**) and (3.8) are analogs of each other, with i, RC and $\frac{1}{R}\ \frac{dV}{dt}$ corresponding to T, τ, and Q.

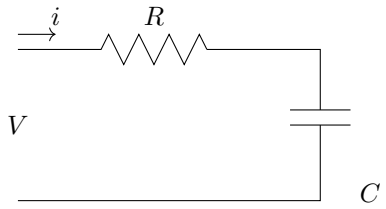

Figure 3.4: Electrical analog of Fig. 3.3.

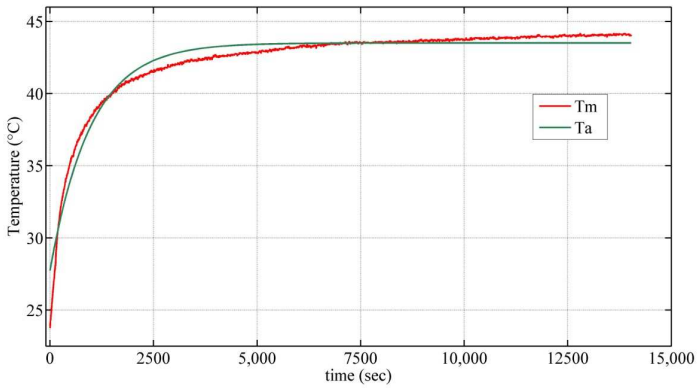

Figure 3.5: Temperature measurement compared to exponential.

3.3.2 Experiment

The measured temperature change in a room is shown in Fig. 3.5 along with a best-fit exponential[1]. It is seen at some parts that the exponential does not completely fit the data.

3.3.3 Time scales

Consider a lumped body with external temperature oscillation as is

$$\frac{dT}{dt} + \lambda T = A\cos\omega t.$$

The two time scales are the cooling time scale $\tau_1 = 1/\lambda$ and the external forcing time scale $\tau_2 = 1/\omega$. Though this linear problem can be solved to be

$$T = Ce^{-\lambda t} + B\cos(\omega t + \phi),$$

approximations can be made in the following two ways.

(a) $\tau_1 \ll \tau_2$: The body temperature changes much faster than the outside temperature, so the latter may be approximated to be a constant. Thus

$$T = Ce^{-\lambda t} + \frac{A}{\lambda}\cos\omega t.$$

(b) $\tau_1 \gg \tau_2$: The response of the body is much slower than the outside temperature oscillations. Neglecting λ gives us the solution

$$T = \frac{A}{\omega}\sin\omega t.$$

3.4 Further lumped-parameter approximations

3.4.1 Two-fluid thermal problem

Consider a wall with fluid on both sides as shown in Fig. 3.6. The fluid temperatures are $T_{\infty,1}$ and $T_{\infty,2}$ and the temperatures on either side of the wall are $T_{w,1}$ and $T_{w,2}$. The initial temperature in the wall is $T(x,0) = f(x)$.

In the steady state, we have

$$h_1(T_{\infty,1} - T_{w,1}) = k_s\frac{T_{w,1} - T_{w,2}}{L} = h_2(T_{w,2} - T_{\infty,2})$$

from which

$$\frac{h_1 L}{k_s}\frac{T_{\infty,1} - T_{w,1}}{T_{\infty,1} - T_{\infty,2}} = \frac{T_{w,1} - T_{w,2}}{T_{\infty,1} - T_{\infty,2}} = \frac{h_2 L}{k_s}\frac{T_{w,2} - T_{\infty,2}}{T_{\infty,1} - T_{\infty,2}}$$

[1] Chávez & Sen (2014).

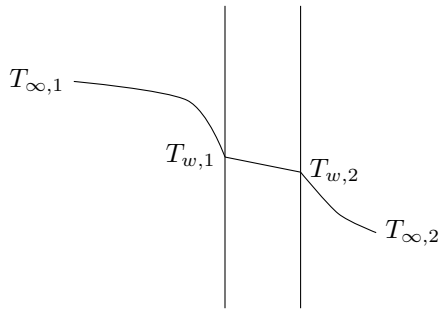

Figure 3.6: Wall with fluids on either side.

Thus we have

$$\frac{T_{w,1}-T_{w,2}}{T_{\infty,1}-T_{\infty,2}} \ll \frac{T_{\infty,1}-T_{w,1}}{T_{\infty,1}-T_{\infty,2}} \quad \text{if} \quad \frac{h_1 L}{k_s} \ll 1$$
$$\frac{T_{w,1}-T_{w,2}}{T_{\infty,1}-T_{\infty,2}} \ll \frac{T_{w,2}-T_{\infty,2}}{T_{\infty,1}-T_{\infty,2}} \quad \text{if} \quad \frac{h_2 L}{k_s} \ll 1.$$

For $Bi \ll 1$ at both interfaces, the temperature variation in the wall is much smaller than those in the two fluids. Using the lumped approximation, the governing equation is

$$Mc\frac{dT}{dt} + h_1 A_1 (T - T_{\infty,1}) + h_2 A_2 (T - T_{\infty,2}) = 0$$

where $T(0) = T_i$. If $T_{\infty,1}$ and $T_{\infty,2}$ are constants, we can nondimensionalize the equation using the parameters for one of them, fluid 1 for instance. Thus we have

$$T^* = \frac{T - T_{\infty,1}}{T_i - T_{\infty,1}}; \quad t^* = \frac{h_1 A_1 t}{Mc}$$

from which

$$\frac{dT^*}{dt^*} + T^* + \alpha(T^* + \beta) = 0$$

with $T^*(0) = 1$, where

$$\alpha = \frac{h_2 A_2}{h_1 A_1}$$
$$\beta = \frac{T_{\infty,1} - T_{\infty,2}}{T_i - T_{\infty,1}}$$

The equation can be written as

$$\frac{dT^*}{dt^*} + (1+\alpha)T^* = -\alpha\beta$$

with the solution

$$T^* = Ce^{-(1+\alpha)t^*} - \frac{\alpha\beta}{1+\alpha}$$

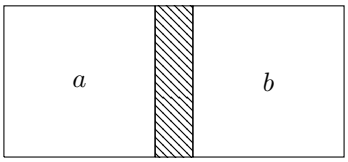

Figure 3.7: Two bodies in thermal contact.

The condition $T^*(0) = 1$ gives $C = 1 + \alpha\beta/(1+\alpha)$, from which

$$T^* = \left(1 + \frac{\alpha\beta}{1+\alpha}\right) e^{-(1+\alpha)t^*} - \frac{\alpha\beta}{1+\alpha}$$

For $\alpha = 0$, the solution reduces to the single-fluid case, Eq. (3.4). Otherwise the time constant of the general system is

$$\tau = \frac{Mc}{h_1 A_1 + h_2 A_2}$$

3.4.2 Two-body thermal problem

Convective

Suppose now that there are two bodies at temperatures T_1 and T_2 in thermal contact with each other and exchanging heat with a single fluid at temperature T_∞ as shown in Fig. 3.7.

The mathematical model of the thermal process is

$$M_1 c_1 \frac{dT_1}{dt} + \frac{k_s A_c}{L}(T_1 - T_2) + hA(T_1 - T_\infty) = Q_1$$
$$M_2 c_2 \frac{dT_2}{dt} + \frac{k_s A_c}{L}(T_2 - T_1) + hA(T_2 - T_\infty) = Q_2$$

Radiative

Fig. 3.8 shows two bodies, 1 and 2, generating heat and interacting with each other through a solid bar s. Taking into account conduction in the bar as well as radiation between the two bodies and the bar, energy balance gives

$$M_1 c_1 \frac{dT_1}{dt} + \frac{k_s A_c}{L}(T_1 - T_2) + A_1\sigma F_{1s}(T_1^4 - T_s^4) + A_1\sigma F_{12}(T_1^4 - T_2^4) = Q_1$$
$$M_2 c_2 \frac{dT_2}{dt} + \frac{k_s A_c}{L}(T_2 - T_1) + +A_1 F_{2s}(T_2^4 - T_s^4) + A_2\sigma F_{21}(T_2^4 - T_1^4) = Q_2$$

3.4.3 Variable heat transfer coefficient

If the h is slightly temperature-dependent, then we have

$$\frac{dT^*}{dt^*} + (1 + \epsilon T^*)T^* = 0, \tag{3.9}$$

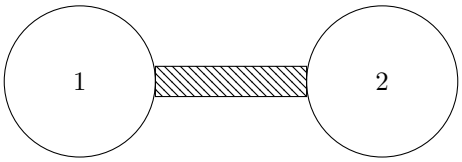

Figure 3.8: Bodies with radiation and conduction interaction.

for $\epsilon \ll 1$, which can be solved by the method of perturbations. We assume that

$$T^*(t^*) = T_0^*(t^*) + \epsilon T_1^*(t^*) + \epsilon^2 T_2^*(t^*) + \dots. \tag{3.10}$$

To order ϵ^0, we have

$$\begin{aligned} \frac{dT_0^*}{dt^*} + T_0^* &= 0, \\ T_0^*(0) &= 1. \end{aligned}$$

which has the solution

$$T_0^* = e^{-t^*}.$$

To the next order ϵ^1, we get

$$\begin{aligned} \frac{dT_1^*}{dt^*} + T_1^* &= -T_0^{*2}, \\ &= -e^{-2t^*}, \\ T_1^*(0) &= 0, \end{aligned}$$

the solution to which is

$$T_1^* = -e^{-t^*} + e^{-2t^*}.$$

Taking the expansion to order ϵ^2

$$\begin{aligned} \frac{dT_2^*}{dt^*} + T_2^* &= -2T_0^* T_1^* \\ &= -2e^{-2t^*} - 2e^{-3t^*}, \\ T_2^*(0) &= 1, \end{aligned}$$

with the solution

$$T_2^* = e^{-t^*} - 2e^{-2t^*} + e^{-3t^*}.$$

And so on. Combining, we get

$$T^* = e^{-t^*} - \epsilon(e^{-t^*} - e^{-2t^*}) + \epsilon^2(e^{-t^*} - 2e^{-2t^*} + e^{-3t^*}) + \dots$$

Alternatively

We can find an exact solution to equation (3.9). Separating variables, we get

$$\frac{dT^*}{(1+\epsilon T^*)T^*} = dt^*.$$

Integrating

$$\ln \frac{T^*}{\epsilon T^* + 1} = -t^* + C.$$

The condition $T^*(0) = 1$ gives $C = -\ln(1+\epsilon)$, so that

$$\ln \frac{T^*(1+\epsilon)}{1+\epsilon T^*} = -t^*.$$

This can be rearranged to give

$$T^* = \frac{e^{-t^*}}{1+\epsilon(1-e^{-t^*})}.$$

A Taylor-series expansion of the exact solution gives

$$\begin{aligned} T^* &= e^{-t^*}\left[1+\epsilon(1-e^{-t^*}\right]^{-1}, \\ &= e^{-t^*}\left[1-\epsilon(1-e^{-t^*}) + \epsilon^2(1-e^{-t^*})^2 + \ldots\right], \\ &= e^{-t^*} - \epsilon(e^{-t^*} - e^{-2t^*}) + \epsilon^2(e^{-t^*} - 2e^{-2t^*} + e^{-3t^*}) + \ldots \end{aligned}$$

Radiative cooling

If the heat loss is due to radiation, we can write

$$Mc\frac{dT}{dt} + \sigma A(T^4 - T_\infty^4) = 0 \quad \text{with} \quad T(0) = T_0.$$

Nondimensionalizing using

$$T^* = \frac{T - T_\infty}{T_0 - T_\infty}; \quad t^* = \frac{\sigma A(T_i - T_\infty)^3 t}{Mc}$$

and introducing the parameter

$$\beta = \frac{T_\infty}{T_i - T_\infty} \tag{3.11}$$

we get

$$\frac{d\phi}{dt^*} + \phi^4 = \beta^4$$

where

$$\phi = T^* + \beta$$

Writing the equation as

$$\frac{d\phi}{\phi^4 - \beta^4} = -dt^*$$

the integral is

$$\frac{1}{4\beta^3} \ln\left(\frac{\phi - \beta}{\phi + \beta}\right) - \frac{1}{2\beta^3} \tan^{-1}\left(\frac{\phi}{\beta}\right) = -t^* + C$$

Using the initial condition $T^*(0) = 1$, we get (?)

$$t^* = \frac{1}{2\beta^3}\left[\frac{1}{2} \ln \frac{(\beta + T^*)(\beta - 1)}{(\beta - T^*)(\beta + 1)} + \tan^{-1} \frac{T^* - 1}{\beta + (T^*/\beta)}\right]$$

Convective with weak radiation

The governing equation is

$$Mc\frac{dT}{dt} + hA(T - T_\infty) + \sigma A(T^4 - T_\infty^4) = 0$$

with $T(0) = T_i$. Using the variables defined by Eqs. (3.3), we get

$$\frac{dT^*}{dt^*} + T^* + \epsilon\left[(T^* + \beta^4)^4 - \beta^4\right] = 0 \tag{3.12}$$

where β is defined in Eq. (3.11), and

$$\epsilon = \frac{\sigma(T_i - T_\infty)^3}{h}$$

If radiative effects are small compared to the convective (e.g., for $T_i - T_\infty = 100$ K and $h = 10$ W/m^{2}K we get $\epsilon = 5.67 \times 10^{-3}$), we can take $\epsilon \ll 1$. Substituting the perturbation series, Eq. (3.10), in Eq. (3.12), we get

$$\frac{d}{dt^*}\left(T_0^* + \epsilon T_1^* + \epsilon^2 T_2^* + \ldots\right) + \left(T_0^* + \epsilon T_1^* + \epsilon^2 T_2^* + \ldots\right) + \epsilon\big[\left(T_0^* + \epsilon T_1^* + \epsilon^2 T_2^* + \ldots\right)^4$$
$$+4\beta\left(T_0^* + \epsilon T_1^* + \epsilon^2 T_2^* + \ldots\right)^3 + 6\beta^2\left(T_0^* + \epsilon T_1^* + \epsilon^2 T_2^* + \ldots\right)^2 4\beta^3\left(T_0^* + \epsilon T_1^* + \epsilon^2 T_2^* + \ldots\right)\big] = 0$$

In this case

$$\frac{dT^*}{dt^*} + (T^* - T_0^*) + \epsilon(T^{*4} - T_s^{*4}) = 0$$
$$T^*(0) = 1$$

As a special case, of we take $\beta = 0$, i.e. $T_\infty = 0$, we get

$$\frac{dT^*}{dt^*} + T^* + \epsilon T^{*4} = 0$$

which has an exact solution

$$t^* = \frac{1}{3} \ln \frac{1 + \epsilon T^{*3}}{(1 + \epsilon)T^{*3}}$$

3.4.4 Power-law cooling

Assume: (a) Constant properties. (b) Power law heat transfer.

Energy balance gives

$$Mc\frac{dT}{dt} + hA(T - T_\infty) = 0, \quad \text{with} \quad T(0) = T_0.$$

Nondimensionalizing using Eq. (3.3), we get

$$\frac{dT^*}{dt^*} + \frac{hA}{Mc}T^* = 0, \tag{3.13}$$

where

$$T^* = T - T_\infty.$$

From the definitions

$$Nu = \frac{hL}{k},$$
$$Ra = \frac{g\beta L^3}{\nu\alpha}T^*,$$

and using the correlation

$$Nu = C_1 Ra^n,$$

we have

$$\begin{aligned} h &= \frac{k}{L}Nu, \\ &= \frac{C_1 k}{L}Ra^n, \\ &= \frac{C_1 k}{L}\left(\frac{g\beta L^3}{\nu\alpha}\right)^n T^{*n}. \end{aligned}$$

Thus Eq. (3.13) becomes

$$\frac{dT^*}{dt^*} + C_2 T^{*n+1} = 0,$$

where

$$C_2 = \frac{C_1 kA}{McL}\left(\frac{g\beta L^3}{\nu\alpha}\right)^n,$$

so that

$$T^{*^{-n-1}}\, dT^* = -C_2\, dt^*.$$

For $n = 0$, Nu and h are constant. Upon integration

$$\begin{aligned} \ln T^* &= -C_2 t + \ln a, \\ T^* &= ae^{-C_2 t^*} \end{aligned}$$

With $T(0) = T_0$,

$$a = T_0 - T_\infty,$$

so that

$$\frac{T - T_\infty}{T_0 - T_\infty} = e^{-C_2 t}.$$

This can be written as

$$T^* = e^{-t^*}, \tag{3.14}$$

where

$$T^* = \frac{T - T_\infty}{T_0 - T_\infty}, \tag{3.15a}$$

$$t^* = C_2 t. \tag{3.15b}$$

However, for $n \neq 0$, integration gives

$$\begin{aligned} -\frac{1}{n}\, T^{*-n} &= -C_2 t^* - a, \\ T^{*^{-n}} &= n\left(C_5 t^* + a\right), \\ T^* &= n^{-1/n}\left(C_2 t^* + a\right)^{-1/n}. \end{aligned}$$

so that

$$T = T_\infty + n^{-1/n}\left(C_2 t + a\right)^{-1/n}.$$

From the initial condition

$$\begin{aligned} T_0 &= T_\infty + (na)^{-1/n}, \\ a &= \frac{1}{n}(T_0 - T_\infty)^{-n}, \end{aligned}$$

so that

$$T = T_\infty + n^{-1/n}\left[C_2 t + \frac{1}{n}(T_0 - T_\infty)^{-n}\right]^{-1/n}.$$

This can be written as

$$\begin{aligned} T^* &= n^{-1/n}\left(t^* + \frac{1}{n}\right)^{-1/n}, \\ &= \left(nt^* + n\right)^{-1/n}, \end{aligned} \tag{3.16}$$

where

$$T^* = \frac{T - T_\infty}{T_0 - T_\infty}, \quad \text{and} \quad t^* = C_2 (T_0 - T_\infty)^n t. \tag{3.17}$$

As $n \to 0$, the independent and dependent variables, Eq. (3.17), tend to Eq. (3.15) and, since

$$\lim_{n \to 0} \left(nt^* + 1\right)^{-1/n} = e^{-t^*},$$

the solution Eq. (3.16) tends to Eq. (3.14). Fig. 3.9 shows that, in spite of their different forms, Eqs. (3.16) and (3.14) give very similar numerical results for small positive and negatives values of n.

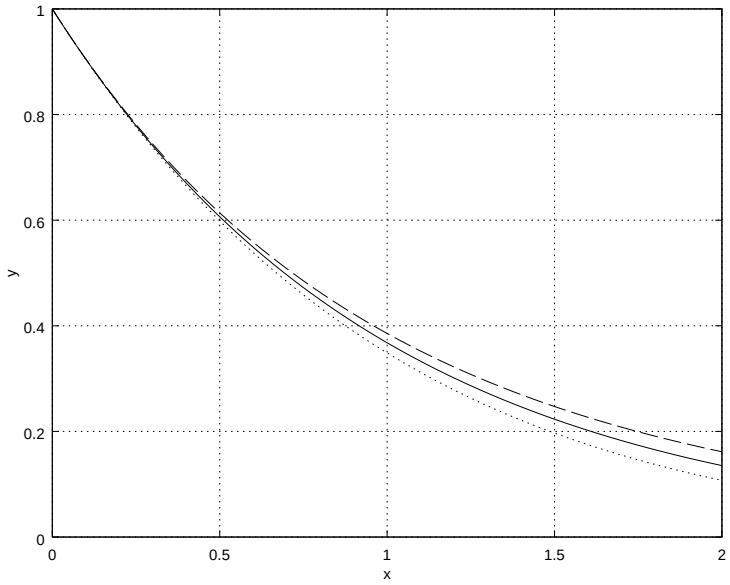

Figure 3.9: Continuous line is Eq. (3.14); dashed and dotted lines are Eq. (3.16) with $n = 0.1$ and -0.1, respectively.

3.4.5 Time-dependent T_∞

Let

$$Mc\frac{dT}{dt} + hA\big(T - T_\infty(t)\big) = 0 \quad \text{with} \quad T(0) = T_i.$$

This is a special case of Eq. (1.2).

Ramp

Let

$$T_\infty = T_{\infty,0} + at$$

Defining the nondimensional temperature as

$$T^* = \frac{T - T_{\infty,0}}{T_i - T_{\infty,0}} \tag{3.18}$$

and time as in Eq. (3.3), we get

$$\frac{dT^*}{dt^*} + T^* = At^* \tag{3.19}$$

where

$$A = \frac{aMc}{hA(T_i - T_{\infty,0})}$$

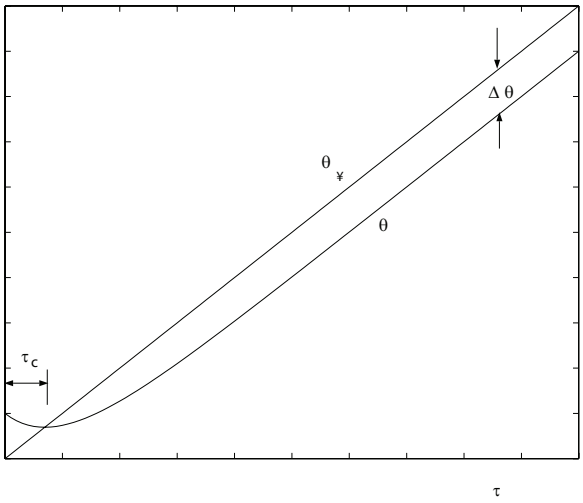

Figure 3.10: Response to ramp ambient temperature.

The nondimensional ambient temperature is

$$T^*_\infty = \frac{aMc}{hA(T_i - T_{\infty,0})} t^*$$

The solution to Eq. (3.19) is

$$T^* = Ce^{-t^*} + At^* - A$$

The condition $T^*(0) = 1$ gives $C = 1 + A$, so that

$$T^* = (1 + A)e^{-t^*} + A(t^* - 1)$$

The time shown in Fig. 3.10 at crossover is

$$\tau_c = \ln \frac{1 + A}{A}$$

and the offset is

$$\Delta T^* = A$$

as $t^* \to \infty$.

Oscillatory

Let

$$T_\infty = \bar{T}_\infty + \Delta T \sin \omega t$$

where $T(0) = T_i$. Defining

$$T^* = \frac{T - \bar{T}_\infty}{T_i - \bar{T}_\infty}$$

and using Eq. (3.3), the nondimensional equation is

$$\frac{dT^*}{dt^*} + T^* = \Delta T^* \sin \omega^* t^*$$

where

$$\Delta T^* = \frac{\Delta T}{T_i - \bar{T}_\infty}$$
$$\omega^* = \frac{\omega M c}{hA}$$

The solution is

$$T^* = Ce^{-t^*} + \frac{\Delta T^*}{(1+\omega^{*2})\cos\phi} \sin(\omega^* t^* - \phi)$$

where

$$\phi = \tan^{-1} \omega^*$$

From the condition $T^*(0) = 1$, we get $C = 1 + \Delta\omega^*/(1+\omega^{*2})$, so that

$$T^* = \left(1 + \Delta T^* \frac{\omega^*}{1+\omega^{*2}}\right) e^{-t^*} + \frac{\Delta T^*}{(1+\omega^{*2})\cos\phi} \sin(\omega^* t^* - \phi)$$

Example 3.2

Using a lumped approximation, determine the long time behavior of the temperature of a body convectively exposed to an oscillatory temperature.

Assume: Newton's law of cooling.

Variables: $T(t)$ = temperature of body, t = time; T_∞ = ambient temperature; $\bar{T}_\infty$ = external mean temperature; ΔT = amplitude of external temperature oscillation; ω = frequency of external temperature oscillation; m = mass of body; c = specific heat of body; h = constant convective heat transfer coefficient; A = convection surface area.

The governing equation is

$$mc\frac{dT}{dt} + hA\big[T - T_\infty(t)\big] = 0,$$

with $T_\infty = \bar{T}_\infty + \Delta T \cos\omega t$. Thus

$$\frac{dT}{dt} + \frac{hA}{mc}T = \frac{hA}{mc}\big(\bar{T}_\infty + \Delta T \cos\omega t\big),$$

which can then be solved.

3.5 Regenerative HX

A regenerator is schematically shown in Fig. 3.11.

$$Mc\frac{dT}{dt} + \dot{m}c(T_{in} - T_{out}) = 0$$

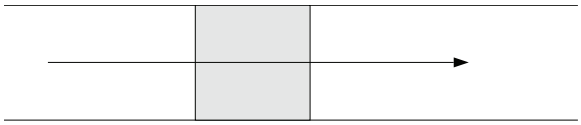

Figure 3.11: Schematic of regenerator.

3.6 Heating

$$\underbrace{Mc\frac{dT}{dt}}_{\text{I}} + \underbrace{hA(T-T_\infty)}_{\text{II}} = \underbrace{G(t)}_{\text{III}}, \quad T = T_0 \text{ at } t = 0,$$

where the terms and their units are

I = rate of accumulation of internal energy,	[(kg) (J/kg·K) (K/s) = W],
II = rate of heat loss to surroundings,	[(W/m^2) (m^2) (K) = W],
III = rate of heating,	[W].

Writing

$$T^* = \frac{T - T_\infty}{T_0 - T_\infty},$$
$$t^* = \frac{t}{\tau}, \quad \tau = \frac{Mc}{hA},$$

we have

$$\frac{Mc(T_0 - T_\infty)}{Mc/hA}\frac{dT^*}{dt^*} + hA(T_0 - T_\infty)T^* = G.$$

Dividing by $hA(T_0 - T_\infty)$, we get the nondimensional equation

$$\frac{dT^*}{dt^*} + T^* = \Gamma,$$

where

$$\Gamma(t^*) = \frac{Mc}{hA(T_0 - T_\infty)}\, G.$$

The solution of the homogeneous equation is

$$T_h^* = a\ e^{-t^*}.$$

3.6.1 Constant heating

If $G = G_0$, i.e. $\Gamma = \Gamma_0$, is constant, then the particular solution is

$$T_p^* = \Gamma_0.$$

The complete solution is

$$\begin{aligned} T^* &= T_h^* + T_p^*, \\ &= a\ e^{-t^*} + \Gamma_0. \end{aligned}$$

From the initial condition $T^*(0) = 1$, we get

$$a = 1 - \Gamma_0,$$

so that

$$T^* = (1 - \Gamma_0)\ e^{-t^*} + \Gamma_0.$$

For t^* or $t \to \infty$, $T^* = \Gamma_0$ and $T = T_\infty + \frac{McG_0}{hA}$.

3.6.2 Periodic heating

Let

$$\Gamma(t^*) = \Gamma_0 + \Gamma_1 \cos \omega^* t^*.$$

where the nondimensional and dimensional frequencies, ω^* and ω respectively, are related by $\omega^* t^* = \omega t$.

Assume the particular solution to be

$$T_p^* = C_1 + C_2 \sin \omega^* t^* + C_3 \cos \omega^* t^*.$$

Substituting in the equation, we get

$$(\omega^* C_2 \cos \omega^* t - \omega^* C_3 \sin \omega^* t^*) + (C_1 + C_2 \sin \omega^* t^* + C_3 \cos \omega^* t^*) = \Gamma_0 + \Gamma_1 \cos \omega^* t.$$

Comparing coefficients

$$\begin{aligned} C_1 &= \Gamma_0, \\ \omega^* C_2 + C_3 &= \Gamma_1, \\ -\omega^* C_3 + C_2 &= 0. \end{aligned}$$

The constants are

$$\begin{aligned} C_1 &= \Gamma_0, \\ C_2 &= \frac{\omega^* \Gamma_1}{1 + \omega^{*2}}, \\ C_3 &= \frac{\Gamma_1}{1 + \omega^{*2}}, \end{aligned}$$

so that the complete solution is

$$T^*(t^*) = a\ e^{-t^*} + \Gamma_0 + \frac{\omega^* \Gamma_1}{1 + \omega^{*2}} \sin \omega^* t^* + \frac{\Gamma_1}{1 + \omega^{*2}} \cos \omega^* t^*.$$

For long time, $t^* \to \infty$, only the particular solution is left.

We can write

$$\begin{aligned}\frac{\omega^*\Gamma_1}{1+\omega^{*2}}\sin\omega^*t^* + \frac{\Gamma_1}{1+\omega^{*2}}\cos\omega^*t^* &= A\cos(\omega^*t^*+\phi),\\ &= A\cos\omega^*t^*\ \cos\phi - \sin\omega^*t^*\ \sin\phi,\end{aligned}$$

and compare terms to get

$$\begin{aligned}A\sin\phi &= -\frac{\omega^*\Gamma_1}{1+\omega^{*2}},\\ A\cos\phi &= \frac{\Gamma_1}{1+\omega^{*2}}.\end{aligned}$$

so that

$$\begin{aligned}\tan\phi &= -\omega^*,\\ A &= \Gamma_1.\end{aligned}$$

Alternatively

$$\Gamma(t^*) = \Gamma_0 + \Gamma_1 e^{i\omega^*t^*}.$$

Assuming

$$T_p^* = C_1 + C_2 e^{i\omega^*t^*}.$$

then

$$\begin{aligned}C_1 &= \Gamma_0,\\ C_2 &= \frac{\Gamma_1}{1+i\omega^*},\end{aligned}$$

so that

$$\begin{aligned}T_p^* &= \Gamma_0 + \frac{\Gamma_1}{1+i\omega^*}e^{i\omega^*t^*},\\ &= \Gamma_0 + \Gamma_1\frac{1-i\omega^*}{1+\omega^{*2}}e^{i\omega^*t^*},\\ &= \Gamma_0 + \Gamma_1 e^{i(\omega^*t^*+\phi)}.\end{aligned}$$

The complex number $a+ib$ can be represented in polar form as $(a^2+b^2)^{1/2}\angle\tan^{-1}(b/a)$ so that

$$\begin{aligned}\Gamma &= \Gamma_0 + \Gamma_1\angle(\omega^*t^*),\\ T_p^* &= \Gamma_0 + \Gamma_1\angle(\omega^*t^*+\phi).\end{aligned}$$

3.6.3 Delayed effect of heating

$$\frac{dT^*}{dt^*} + T^* = \Gamma(t^*-\tau_d).$$

3.7 Nonlinear systems

We will look at the long time behavior and stability of nonlinear systems. The general form of the equation for heat loss from a body with internal heat generation is

$$\frac{dT^*}{dt^*} + f(T^*) = a \quad \text{with} \quad T^*(0) = 1. \tag{3.20}$$

Let

$$f(\bar{T}^*) = a,$$

where the bar indicates a steady state for which dT^*/dt is zero. Then we would like to show that $T^* \to \bar{T}^*$ as $t^* \to \infty$. Writing

$$T^* = \bar{T}^* + T^{*'},$$

where $T^{*'}$ is the deviation from the steady state, we have

$$\frac{dT^{*'}}{dt^*} + f(\bar{T}^* + T^{*'}) = a. \tag{3.21}$$

3.7.1 Separable

For $a = 0$ the equation is separable. Thus

$$\frac{dT^*}{dt^*} + f(T^*) = 0,$$

from which

$$\frac{dT^*}{f(T^*)} = -dt^*.$$

Integrating

$$\int \frac{dT^*}{f(T^*)} = -t^* + C.$$

3.7.2 Linearized analysis

If we assume that $T^{*'}$ is small, then a Taylor series expansion around $\bar{T}^*$ gives

$$f(\bar{T}^* + T^{*'}) = f\Big|_{\bar{T}^*} + T^{*'} \frac{df}{dT^*}\Big|_{\bar{T}^*} + \dots$$

from which

$$\frac{dT^{*'}}{dt^*} + bT^{*'} \approx 0,$$

where $b = df/dT^*$ at $T^* = \bar{T}^*$. This is a linearized approximation of the nonlinear equation Eq. (3.20). The solution is

$$T^{*'} = Ce^{-bt^*}$$

so that $T^{*'} \to 0$ as $t \to \infty$ if $b > 0$.

3.7.3 Nonlinear analysis

Multiplying Eq. (3.21) by $T^{*'}$, we get

$$\frac{1}{2}\frac{d}{dt^*}(T^{*'})^2 = -T^{*'}\left[f(\bar{T}^* + T^{*'}) - f(\bar{T}^*)\right]$$

Thus

$$\frac{d}{dt^*}(T^{*'})^2 \leq 0$$

if $T^{*'}$ and $[f(\bar{T}^* + T^{*'}) - f(\bar{T}^*)]$ are both of the same sign or zero, i.e., if $f(T^*)$ is monotonically increasing[2]. Thus $T^{*'} \to 0$ as $t^* \to \infty$.

Because this works on the square of the variable $T^{*'}$, this is known as the energy method.

Example 3.3

Show, without solving, that the solution of

$$(\frac{d}{dt^*} + \lambda_1)(\frac{d}{dt^*} + \lambda_2)T^* = 0$$

tends to zero as $t^* \to \infty$ if λ_1 and λ_2 are real and positive.

The equation is

$$\frac{d^2T^*}{dt^{*2}} + (\lambda_1 + \lambda_2)\frac{dT^*}{dt^*} + \lambda_1\lambda_2 T^* = 0,$$

which is the same as the system

$$\frac{dT^*}{dt^*} = S^*,$$
$$\frac{dS^*}{dt^*} = -(\lambda_1 + \lambda_2)S^* - \lambda_1\lambda_2\ T^*.$$

Multiplying the first by $\lambda_1\lambda_2\ T^*$, the second by S^*, and adding we get

$$\frac{1}{2}\frac{d}{dt^*}(\lambda_1\lambda_2\ T^{*2} + S^{*2}) = -(\lambda_1 + \lambda_2)\ S^{*2}.$$

Thus the non-negative quantity $\lambda_1\lambda_2\ T^{*2} + S^{*2}$ will always decrease for increasing t^* since the right side is non-positive. Thus both $T^* \to 0$ and $S^* \to 0$ as $t^* \to 0$.

3.7.4 Radiation in enclosures

Consider a closed enclosure with N walls radiating to each other and with a central heater H. The walls have no other heat loss and have different masses and specific heats. The governing equations are

$$M_i c_i \frac{dT_i}{dt} + \sigma\sum_{j=1}^{N} A_i F_{ij}(T_i^4 - T_j^4) + \sigma A_i F_{iH}(T_i^4 - T_H^4) = 0$$

[2] A real function $f(x)$ monotonically increases if $f(x) - f(y) \geq 0$ for $x \geq y$

where the view factor F_{ij} is the fraction of radiation leaving surface i that falls on j. The steady state is

$$\bar{T}_i = T_H \quad (i = 1, \ldots, N)$$

Linear stability is determined by a small perturbation of the type

$$T_i = T_H + T_i'$$

from which

$$M_i c_i \frac{dT_i'}{dt} + 4\sigma T_H^3 \sum_{j=1}^{N} A_i F_{ij}(T_i' - T_j') + 4\sigma T_H^3 A_i F_{iH} T_i' = 0$$

This can be written as

$$\boldsymbol{M}\frac{d\boldsymbol{T}'}{dt} = -4\sigma T_H^3 \boldsymbol{A}\boldsymbol{T}'$$

3.8 Chemical reaction

We consider the a convectively cooled chemical reactor generating heat. The energy balance for the reactor is

$$\underbrace{mc\frac{dT}{dt}}_{\text{accumulation}} = \underbrace{Ce^{-E_a/RT}}_{\text{generation}} - \underbrace{hA(T - T_\infty)}_{\text{convection}},$$

where the generation of heat is calculated by the Arrhenius reaction rate $ce^{-E_a/RT}$; C is a pre-exponential factor that is specific to the chemical reaction, E_a is the activation energy, T is the absolute temperature, and R is the universal gas constant.

Nondimensionalizing using

$$t^* = \frac{CR}{mcE_a}t; \quad T^* = \frac{RT}{E_a},$$

we have

$$\begin{aligned}\frac{dT^*}{dt^*} &= e^{-1/T^*} - \beta T^* + \alpha, \\ &= f(T^*),\end{aligned}$$

where

$$\alpha = \frac{hAT_\infty}{C}; \quad \beta = \frac{hAE_a}{CR}.$$

The heat generation and heat loss terms, e^{-1/T^*} and $\beta T^* - \alpha$ respectively, are schematically shown in Fig. 3.12 for different values of β. The intersection between the two is the steady solution. These are solutions of

$$f(\bar{T}^*) = 0,$$

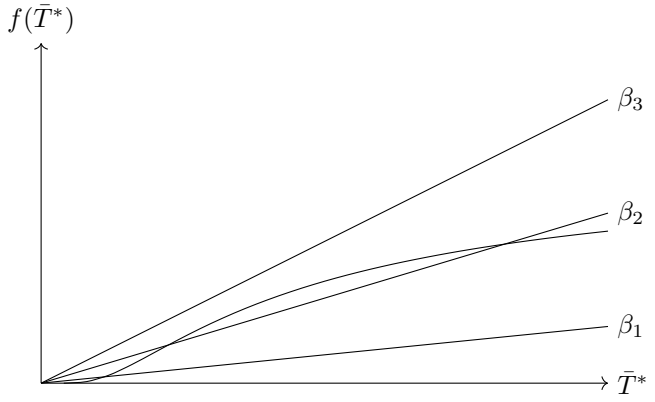

Figure 3.12: Heat generation and convection terms for $\beta = \beta_1$, β_2 and β_3.

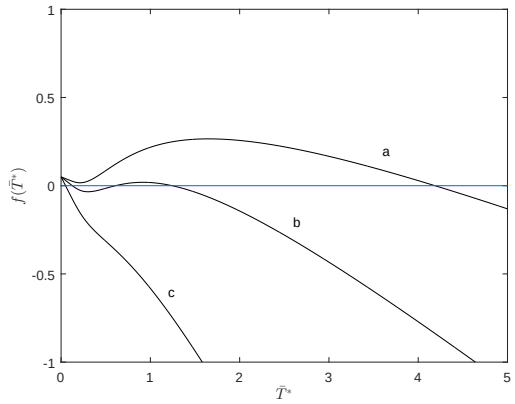

Figure 3.13: $f(\bar{T})$ with $\alpha = 0.05$; a, b and c correspond to $\beta = 0.2$, 0.4 and 1 respectively.

where $f(\bar{T}^*)$ is shown in Fig. 3.13 .

There are three possibilities: (a) One (an upper) solution exists for $\beta < \beta_{c,1}$; (b) Three (an upper, an intermediate, and a lower) solutions exist for $\beta_{c,1} < \beta < \beta_{c,2}$; (c) One (a lower) solution exists for $\beta > \beta_{c,2}$. The critical values $\beta_{c,1}$ and $\beta_{c,2}$ depend on α.

Fig. 3.14 is the bifurcation diagram.

To find the linear stability of the steady solution(s), we write

$$T = \bar{T} + T',$$

so that

$$\frac{dT'}{dt} = ST', \tag{3.22}$$

where $S = f'(\bar{T})$. The steady states with the slopes $S < 0$ are stable. Thus when they exist, the lower solution is stable, the intermediate is unstable, and the upper is also stable.

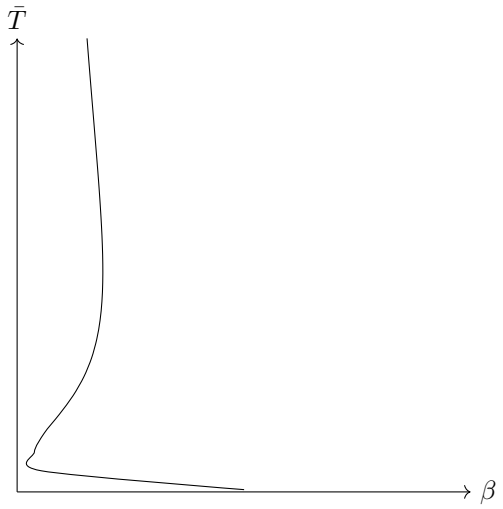

Figure 3.14: Bifurcation diagram for $\alpha =?$.

3.9 Multibody systems

3.9.1 Higher-order constant coefficient

Consider

$$(\frac{d}{dt^*} + \lambda_1)(\frac{d}{dt^*} + \lambda_2) \dots (\frac{d}{dt^*} + \lambda_n)T^* = 0.$$

This is equivalent to the system of equations

$$\begin{aligned}
(\frac{d}{dt^*} + \lambda_n)\ T^* &= T^*_{n-1}, \\
(\frac{d}{dt^*} + \lambda_{n-1})\ T^*_{n-1} &= T^*_{n-2}, \\
(\frac{d}{dt^*} + \lambda_{n-2})\ T^*_{n-2} &= T^*_{n-3}, \\
&\vdots \\
(\frac{d}{dt^*} + \lambda_2)\ T^*_2 &= T^*_1, \\
(\frac{d}{dt^*} + \lambda_1)\ T^*_1 &= 0.
\end{aligned}$$

The solution is

$$T^* = C_1 e^{-\lambda_1 t^*} + C_2 e^{-\lambda_2 t^*} + \ldots + C_n e^{-\lambda_n t^*}.$$

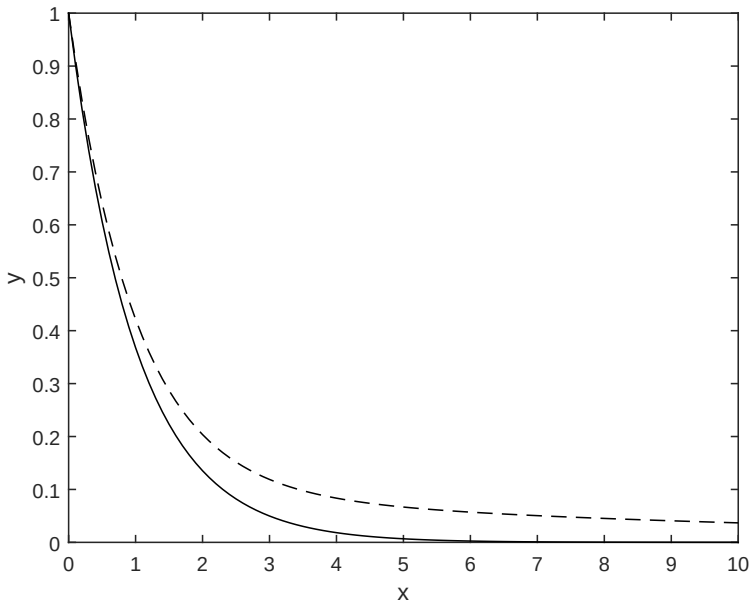

Figure 3.15: Multiple time constants; Eq. (3.23a) is continuous line, Eq. (3.23b) is dashed line.

Example 3.4

Let

$$y_1 = e^{-\lambda_1 t}, \tag{3.23a}$$

$$y_2 = ae^{-\lambda_1 t} + +(1-a)e^{-\lambda_2 t}. \tag{3.23b}$$

where $\lambda_1 = 1,\ \lambda_2 = 0.1,\ a = 0.9$.

Example 3.5

Let $C_i = C/2^{i-1}$, $\lambda_i = \lambda/2^{i-1}$ for $i = 1, 2, \ldots, n$ and $T^*(0) = 1$, then

$$T^* = Ce^{-t^*} + \frac{C}{2}e^{-t^*/2} + \ldots + \frac{C}{2^{n-1}}e^{-t^*/2^{n-1}}.$$

From the initial condition

$$1 = C + \frac{C}{2} + \ldots + \frac{C}{2^{n-1}},$$

$$= 2C\left(1 - 2^{-n}\right) \quad \text{since} \quad \sum_{i=1}^{n} r^{i-1} = \frac{(1-r^n)}{1-r}.$$

Thus

$$C = \frac{1}{2\left(1-2^{-n}\right)}.$$

Alternative formulation

$$\left(\tau_n \frac{d^n}{dt^n} + \tau_{n-1}\frac{d^{n-1}}{dt^{n-1}} + \ldots + \tau_1 \frac{d}{dt} + \tau_0\right) T^* = 0$$

gives

$$\begin{pmatrix} \frac{d}{dt}+\lambda_1 & -1 & & & \\ & \frac{d}{dt}+\lambda_2 & -1 & & \\ & & \ddots & & \\ & & & \frac{d}{dt}+\lambda_{n-1} & -1 \\ & & & & \frac{d}{dt}+\lambda_n \end{pmatrix} \begin{pmatrix} T_1^* \\ T_2^* \\ \vdots \\ T_{n-1}^* \\ T_n^* \end{pmatrix} = \begin{pmatrix} 0 \\ 0 \\ \vdots \\ 0 \\ 0 \end{pmatrix}$$

Example 3.6

See Fig. 3.16 for a large number of boxes, each within another. The equations are

$$\begin{aligned} \frac{dT_1}{dt} + \frac{1}{t_1}(T_1 - T_2) + \frac{1}{t_\infty}(T_1 - T_\infty) &= Q, \\ \frac{dT_2}{dt} + \frac{1}{t_1}(T_2 - T_1) + \frac{1}{t_2}(T_2 - T_3) &= 0, \\ \frac{dT_3}{dt} + \frac{1}{t_2}(T_3 - T_2) + \frac{1}{t_3}(T_3 - T_4) &= 0, \\ &\vdots \\ \frac{dT_{n-1}}{dt} + \frac{1}{t_{n-2}}(T_{n-1} - T_{n-2}) + \frac{1}{t_{n-1}}(T_{n-1} - T_n) &= 0, \\ \frac{dT_n}{dt} + \frac{1}{t_{n-1}}(T_n - T_{n-1}) &= 0. \end{aligned}$$

The characteristic equation of the homogeneous equation is

$$\begin{vmatrix} \lambda_1 & -1 & & & \\ & r+\lambda_2 & -1 & & \\ & & \ddots & & \\ & & & r+\lambda_{n-1} & -1 \\ & & & & r+\lambda_n \end{vmatrix} = 0.$$

Determine the n values of $r = \lambda_i$ and get the solution

$$T^* = C_1 e^{-\lambda_1 t^*} + C_2 e^{-\lambda_2 t^*} + \ldots + C_n e^{-\lambda_n t^*}.$$

Compare this to the PDE

$$\frac{\partial T}{\partial t} = \frac{1}{r^2}\frac{\partial}{\partial r}\left(k(r) r^2 \frac{\partial T}{\partial r}\right)$$

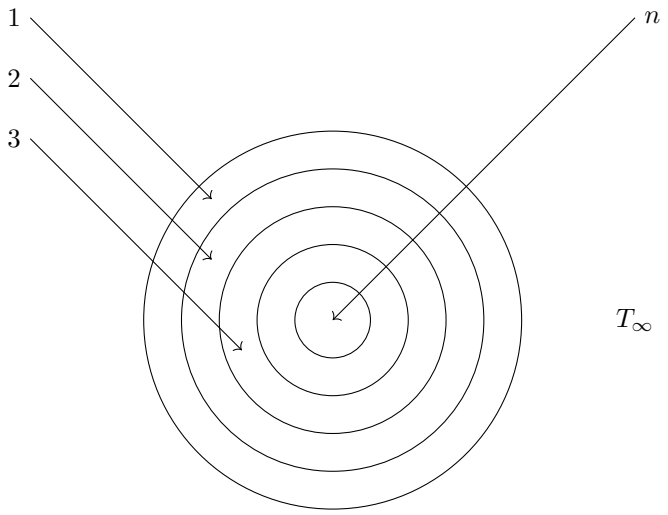

Figure 3.16: Boxes.

Bibliography

Problems

1. Show that the temperature distribution in a sphere subject to convective cooling tends to become uniform as $Bi \to 0$.
2. Check one of the perturbation solutions against a numerical solution.
3. Plot all real $\bar{T}^*(\beta, \epsilon)$ surfaces for the convection with radiation problem, and comment on the existence of solutions.
4. Complete the problem of radiation in an enclosure (linear stability, numerical solutions).
5. Lumped system with convective-radiative cooling and nonzero T_0^* and T_∞.
6. Find the steady-state temperatures for the two-body problem and explore the stability of the system for constant ambient temperature.
7. Consider the change in temperature of a lumped system with convective heat transfer where the ambient temperature, $T_\infty(t)$, varies with time in the form shown in Fig. 3.17. Find (a) the long-time solution of the system temperature, $T(t)$, and (b) the amplitude of oscillation of the system temperature, $T(t)$, for a small period δt.
8. Two bodies at temperatures $T_1(t)$ and $T_2(t)$, respectively, are in thermal contact with each other and with the environment. Show that the temperatures are governed by

$$M_1 c_1 \frac{dT_1}{dt} + C(T_1 - T_2) + C_{1,\infty}(T_1 - T_\infty) = Q_1$$
$$M_2 c_2 \frac{dT_2}{dt} + C(T_2 - T_1) + C_{2,\infty}(T_2 - T_\infty) = Q_2$$

where M_i is the mass, c_i is the specific heat, the Cs are thermal conductances, and Q_i is internal heat generation. Derive the equations above and explain the parameters. Find the steady-state temperatures and explore the stability of the system for constant T_∞.

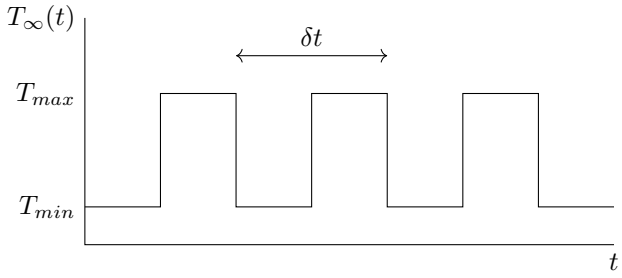

Figure 3.17: Ambient temperature variation.

Chapter 4

Thermal control

4.1 Introduction

There are many kinds of thermal systems in common industrial, transportation and domestic use that need to be controlled in some manner, and there are many ways in which that can be done. One can give the example of heat exchangers [89, 121], environmental control in buildings [73, 75, 86, 122, 161, 229], satellites [107, 181, 194, 232], thermal packaging of electronic components [158, 195], manufacturing [55], rapid thermal processing of computer chips [88, 167, 210], and many others. If precise control is not required, or if the process is very slow, control may simply be *manual*; otherwise some sort of mechanical or electrical feedback system has to be put in place for it to be *automatic*.

Most thermal systems are generally *complex* involving diverse physical processes. These include natural and forced convection, radiation, complex geometries, property variation with temperature, nonlinearities and bifurcations, hydrodynamic instability, turbulence, multi-phase flows, or chemical reaction. It is common to have large uncertainties in the values of heat transfer coefficients, approximations due to using lumped parameters instead of distributed temperature fields, or material properties that may not be accurately known. In this context, a complex system can be defined as one that is made up of sub-systems, each one of which can be analyzed and computed, but when put together presents such a massive computational problem so as to be practically intractable. For this reason large, commonly used engineering systems are hard to model exactly from first principles, and even when this is possible the dynamic responses of the models are impossible to determine computationally in real time. Most often some degree of approximation has to be made to the mathematical model. Approximate correlations from empirical data are also heavily used in practice. The two major reasons for which control systems are needed to enable a thermal system to function as desired are the approximations used during design and the existence of unpredictable external and internal disturbances which were not taken into account.

There are many aspects of thermal control that will not be treated in this brief review. The most important of these are hardware considerations; all kinds of sensors and actuators [60, 197] developed for measurement and actuation are used in the control of thermal systems. Many controllers are also computer based, and the use of microprocessors [91, 189] and PCs in machines, devices and plants is commonplace. Flow control, which is closely related to and is often an integral part of thermal control, has its own extensive literature [67]. Discrete-time (as opposed to continuous-time) systems will not be described. The present paper will, however, concentrate only on the basic principles relating to the theory of control as applied to thermal problems, but even then it will be impossible to go into any depth within the space available. This is only an introduction, and

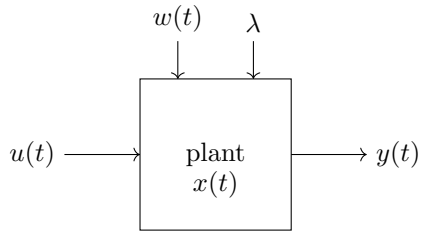

Figure 4.1: Schematic of a system without controller.

the interested reader should look at the literature that is cited for further details. There are good texts and monographs available on the basics of control theory [123, 140, 152, 166], process control [28, 78, 98, 160], nonlinear control [96], infinite-dimensional systems [39, 94], and mathematics of control [9, 188] that can be consulted. These are all topics that include and are included within thermal control.

4.2 Systems

Some basic ideas of systems will be defined here even though, because of the generality involved, it is hard to be specific at this stage.

4.2.1 Systems without control

The dynamic behavior of any thermal system (often called the open-loop system or *plant* to distinguish it from the system with controller described below), schematically shown in Fig. 4.1, may be mathematically represented as

$$\mathcal{L}_s(x, u, w, \lambda) = 0, \tag{4.1}$$

where $\mathcal{L}_s$ is a system operator, t is time, $x(t)$ is the state of the system, $u(t)$ is its input, $w(t)$ is some external or internal disturbance, and λ is a parameter that defines the system. Each one of these quantities belongs to a suitable set or vector space and there are a large number of possibilities. For example $\mathcal{L}_s$ may be an algebraic, integral, ordinary or partial differential operator, while x may be a finite-dimensional vector or a function. $u(t)$ is usually a low-dimensional vector.

In general, the output of the system $y(t)$ is different from its state $x(t)$. For example, x may be a spatial temperature distribution, while y are the readings of one or more temperature measurement devices at a finite number of locations. The relation between the two may be written as

$$\mathcal{L}_o(y, x, u, w, \lambda) = 0, \tag{4.2}$$

where $\mathcal{L}_o$ is the output operator.

The system is *single-input single-output* (SISO) if both u and y are scalars. A system is said to be *controllable* if it can be taken from one specific state to another within a prescribed time with the help of a suitable input. It is *output* controllable if the same can be done to the output. It is important to point out that output controllability does not imply system controllability. In fact, in practice for many thermal systems the former is all that is required; it has been reported that most industrial plants are controlled quite satisfactorily though they are not system controllable [165]. All possible values of the output constitute the *reachable* set. A system is said to be *observable* if its

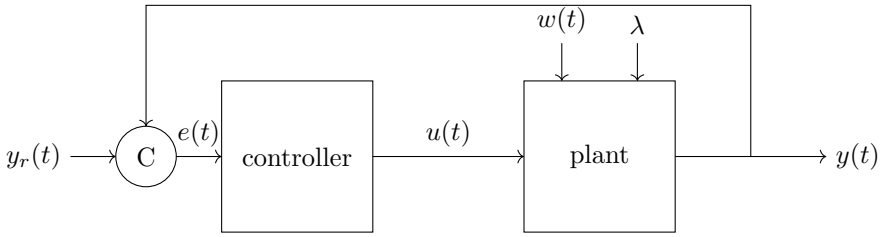

Figure 4.2: Schematic of a system with comparator C and controller.

state x can be uniquely determined from the input u and output y alone. The *stability* of a system is a property that leads to a bounded output if the input is also bounded.

4.2.2 Systems with control

The objective of control is to have a given output $y = y_r(t)$, where the *reference* or *set* value y_r is prescribed. The problem is called *regulation* if y_r is a constant, and *tracking* if it is function of time.

In *open-loop* control the input is selected to give the desired output without using any information from the output side; that is one would have to determine $u(t)$ such that $y = y_r(t)$ using the mathematical model of the system alone. This is a *passive* method of control that is used in many thermal systems. It will work if the behavior of the system is exactly predictable, if precise output control is not required, or if the output of the system is not very sensitive to the input. If the changes desired in the output are very slow then manual control can be carried out, and that is also frequently done. A self-controlling approach that is sometimes useful is to design the system in such a way that any disturbance will bring the output back to the desired value; the output in effect is then insensitive to changes in input or disturbances.

Open-loop control is not usually effective for many systems. For thermal systems contributing factors are the uncertainties in the mathematical model of the plant and the presence of unpredictable disturbances. Internal disturbances may be noise in the measuring or actuating devices or a change in surface heat transfer characteristics due to fouling, while external ones may be a change in the environmental temperature. For these cases *closed-loop* control is an appropriate alternative. This is done using *feedback* from the output, as measured by a *sensor*, to the input side of the system, as shown in Fig. 4.2; the figure actually shows unit feedback. There is a comparator which determines the error signal $e(t) = e(y_r, y)$, which is usually taken to be

$$e = y_r - y. \tag{4.3}$$

The key role is played by the *controller* which puts out a signal that is used to move an *actuator* in the plant.

Sensors that are commonly used are temperature-measuring devices such as thermocouples, resistance thermometers or thermistors. The actuator can be a fan or a pump if the flow rate is to be changed, or a heater if the heating rate is the appropriate variable. The controller itself is either entirely mechanical if the system is not very complex, or is a digital processor with appropriate software. In any case, it receives the error in the output $e(t)$ and puts out an appropriate control input $u(t)$ that leads to the desired operation of the plant.

The control process can be written as

$$\mathcal{L}_c(u, e, \lambda) = 0, \tag{4.4}$$

where $\mathcal{L}_c$ is a control operator. The controller designer has to propose a suitable $\mathcal{L}_c$, and then Eqs. (E.9)–(4.4) form a set of equations in the unknowns $x(t)$, $y(t)$ and $u(t)$. Choice of a control strategy defines $\mathcal{L}_o$ and many different methodologies are used in thermal systems. It is common to use *on-off* (or bang-bang, relay, etc.) control. This is usually used in heating or cooling systems in which the heat coming in or going out is reduced to zero when a predetermined temperature is reached and set at a constant value at another temperature. Another method is Proportional-Integral-Derivative (PID) control [225] in which

$$u = K_p e(t) + K_i \int_0^t e(s)\ ds + K_d \frac{de}{dt}. \tag{4.5}$$

4.3 Linear systems theory

The term *classical* control is often used to refer to theory derived on the basis of Laplace transforms. Since this is exclusively for linear systems, we will be using the so-called *modern* control or *state-space* analysis which is based on dynamical systems, mainly because it can be extended to nonlinear systems. Where they overlap, the issue is only one of preference since the results are identical. Control theory can be developed for different linear operators, and some of these are outlined below.

4.3.1 Ordinary differential equations

Much is known about a linear differential system in which Eqs. (E.9) and (4.2) take the form

$$\frac{dx}{dt} = Ax + Bu, \tag{4.6}$$

$$y = Cx + Du, \tag{4.7}$$

where $x \in \mathbb{R}^n$, $u \in \mathbb{R}^m$, $y \in \mathbb{R}^p$, $A \in \mathbb{R}^{n\times n}$, $B \in \mathbb{R}^{n\times m}$, $C \in \mathbb{R}^{p\times n}$, $D \in \mathbb{R}^{p\times m}$. x, u and y are vectors of different lengths and A, B, C, and D are matrices of suitable sizes. Though A, B, C, and D can be functions of time in general, here they will be treated as constants.

The solution of Eq. (4.6) is

$$x(t) = e^{A(t-t_0)}x(t_0) + \int_{t_0}^t e^{A(t-s)}Bu(s)\ ds. \tag{4.8}$$

where the exponential matrix is defined as

$$e^{At} = I + At + \frac{1}{2!}A^2t^2 + \frac{1}{3!}A^3t^3 + \ldots,$$

with I being the identity matrix. From Eq. (4.7), we get

$$y(t) = C\left[e^{At}x(t_0) + \int_{t_0}^t e^{A(t-s)}\ Bu(s)\ ds\right] + Du. \tag{4.9}$$

Eqs. (4.8) and (4.9) define the state $x(t)$ and output $y(t)$ if the input $u(t)$ is given.

It can be shown that for the system governed by Eq. (4.6), a $u(t)$ can be found to take $x(t)$ from $x(t_0)$ at $t = t_0$ to $x(t_f) = 0$ at $t = t_f$ if and only if the matrix

$$M = \left[B \vdots AB \vdots A^2B \vdots \ldots \vdots A^{n-1}B\right] \in \mathbb{R}^{n\times nm} \tag{4.10}$$

is of rank n. The system is then controllable. For a linear system, controllability from one state to another implies that the system can be taken from *any* state to any other. It must be emphasized that the $u(t)$ that does this is not unique.

Similarly, it can be shown that the output $y(t)$ is controllable if and only if

$$N = \left[D \vdots CB \vdots CAB \vdots CA^2B \vdots \ \ldots \ \vdots CA^{n-1}B \right] \in \mathbb{R}^{p \times (n+1)m}$$

is of rank p. Also, the state $x(t)$ is observable if and only if the matrix

$$P = \left[C \vdots CA \vdots CA^2 \ \ldots \ \vdots CA^{n-1} \right]^T \in \mathbb{R}^{pn \times n}$$

is of rank n.

4.3.2 Algebraic-differential equations

This is a system of equations of the form

$$E\frac{dx}{dt} = A\ x + B\ u, \tag{4.11}$$

where the matrix $E \in \mathbb{R}^{n \times n}$ is singular [120]. This is equivalent to a set of equations, some of which are ordinary differential and the rest are algebraic. As a result of this, Eq. (4.11) cannot be converted into (4.6) by substitution. The index of the system is the least number of differentiations of the algebraic equations that is needed to get the form of Eq. (4.6). The system may not be completely controllable since some of the components of x are algebraically related, but it may have restricted or R-controllability [45].

4.4 Nonlinear aspects

The following are a few of the issues that arise in the treatment of nonlinear thermal control problems.

4.4.1 Models

There are no general mathematical models for thermal systems, but one that can be used is a generalization of Eq. (4.6) such as

$$\frac{dx}{dt} = f(x, u). \tag{4.12}$$

where $f : \mathbb{R}^n \times \mathbb{R}^m \mapsto \mathbb{R}^n$. If one is interested in local behavior about an equilibrium state $x = x_0$, $u = 0$, this can be linearized in that neighborhood to give

$$\begin{aligned} \frac{dx}{dt} &= \left.\frac{\partial f}{\partial x}\right|_0 x' + \left.\frac{\partial f}{\partial u}\right|_0 u' \\ &= Ax' + Bu', \end{aligned} \tag{4.13}$$

where $x = x_0 + x'$ and $u = u'$. The Jacobian matrices $(\partial f/\partial x)_0$ and $(\partial f/\partial u)_0$, are evaluated at the equilibrium point. Eq. (4.13) has the same form as Eq. (4.6).

4.4.2 Controllability and reachability

General theorems for the controllability of nonlinear systems are not available at this point in time. Results obtained from the linearized equations generally do not hold for the nonlinear equations. The reason is that in the nonlinear case one can take a path in state space that travels far from the equilibrium point and then returns close to it. Thus regions of state space that are unreachable with the linearized equations may actually be reachable. In a thermal convection loop it is possible to go from one branch of a bifurcation solution to another in this fashion [1].

4.4.3 Bounded variables

In practice, due to hardware constraints it is common to have the physical variables confined to certain ranges, so that variables such as x and u in Eqs. (E.9) and (4.2), being temperatures, heat rates, flow rates and the like, are bounded. If this happens, even systems locally governed by Eqs. (4.6) and (4.7) are now nonlinear since the sum of solutions may fall outside the range in which x exists and thus may not be a valid solution. On the other hand, for a controllable system in which only u is bounded in a neighborhood of zero, x can reach any point in $\mathbb{R}^n$ if the eigenvalues of A have zero or positive real parts, and the origin is reachable if the eigenvalues of A have zero or negative real parts [188].

4.4.4 Relay and hysteresis

A relay is an element of a system that has an input-output relationship that is not smooth; it may be discontinuous or not possess first or higher-order derivatives. This may be accompanied by hysteresis where the relationship also depends on whether the input is increasing or decreasing. Valves are typical elements in flow systems that have this kind of behavior.

4.5 System identification

To be able to design appropriate control systems, one needs to have some idea of the dynamic behavior of the thermal system that is being controlled. Mathematical models of these systems can be obtained in two entirely different ways: from first principles using known physical laws, and empirically from the analysis of experimental information (though combinations of the two paths are not only possible but common). The latter is the process of *system identification*, by which a complex system is reduced to mathematical form using experimental data [78, 129, 137]. There are many different ways in which this can be done, the most common being the fitting of parameters to proposed models [149]. In this method, a form of $\mathcal{L}_s$ is assumed with unknown parameter values. Through optimization routines the values of the unknowns are chosen to obtain the best fit of the results of the model with experimental information. Apart from the linear Eq. (4.6), other models that are used include the following.

- There are many forms based on Eq. (4.12), one of which is the closed-affine model

$$\frac{dx}{dt} = F_1(x) + F_2(x)u$$

  The bilinear equation for which $F_1(x) = Ax$ and $F_2(x) = Nx + b$ is a special case of this.

- Volterra models, like

$$y(t) = y_0(t) + \sum_{i=1}^{\infty} \int_{-\infty}^{\infty} \dots \int_{-\infty}^{\infty} k_i(t; t_1, t_2, t_3, \dots, t_i) u(t_1) \dots u(t_i)\ dt_1 \dots dt_i$$

  for a SISO system, are also used.

- Functional [74], difference [23] or delay [58] equations such as

$$\frac{dx}{dt} = A\ x(t-s) + B\ u$$

  also appear in the modeling of thermal systems.

- Fractional-order derivatives, of which there are several different possible definitions [10, 17, 142, 143, 156] can be used in differential models. As an example, the Riemann-Liouville definition of the nth derivative of $f(t)$ is

$${}_a\mathcal{D}_t^n f(t) = \frac{1}{\Gamma(m-n+1)}\ \frac{d^{m+1}}{dt^{m+1}}\ \int_a^t (t-s)^{m-n} f(s)\ ds,$$

  where a and n are real numbers and m is the largest integer smaller than n.

4.6 Lumped temperature

4.6.1 Mathematical model

Consider a body that is cooled from its surface by convection to the environment with a constant ambient temperature T_∞. It also has an internal heat source $Q(t)$ to compensate for this heat loss, and the control objective is to maintain the temperature of the body at a given level by manipulating the heat source. The Biot number for the body is $Bi = hL/k$, where h is the convective heat transfer coefficient, L is a characteristics length dimension of the body, and k is its thermal conductivity. If $Bi < 0.1$, the body can be considered to have a uniform temperature $T(t)$. Under this lumped approximation the energy balance is given by

$$Mc\frac{dT}{dt} + hA_s(T - T_\infty) = Q(t), \tag{4.14}$$

where M is the mass of the body, c is its specific heat, and A_s is the surface area for convection.

Using Mc/hA_s and $hA_s(T_i - T_\infty)$ as the characteristic time and heat rate, this equation becomes

$$\frac{dT^*}{dt^*} + T^* = Q(t^*) \tag{4.15}$$

Here $T^* = (T - T_\infty)/(T_i - T_\infty)$ where $T(0) = T_i$ so that $T^*(0) = 1$. The other variables are now non-dimensional. With $x = T^*$, $u = Q$, $n = m = 1$ in Eq. (4.6), we find from Eq. (4.10) that rank(M)=1, so the system is controllable.

Open-loop operation to maintain a given non-dimensional temperature T_r^* is easily calculated. Choosing $Q = T_r^*$, it can be shown from the solution of Eq. (4.15), that is

$$T^*(t^*) = (1 - T_r^*)e^{-t^*} + T_r^*,$$

that $T^* \to T_r^*$ as $t^* \to \infty$. In practice, to do this the dimensional parameters hA_s and T_∞ must be exactly known. Since this is usually not the case some form of feedback control is required.

4.6.2 On-off control

In this simple form of control the heat rate in Eq. (4.14) has only two values; it is is either $Q = Q_0$ or $Q = 0$, depending on whether the heater is on or off, respectively. With the system in its *on* mode, $T \to T_{max} = T_\infty + Q_0/hA_s$ as $t \to \infty$, and in its *off* mode, $T \to T_{min} = T_\infty$. Taking the non-dimensional temperature to be

$$T^* = \frac{T - T_{min}}{T_{max} - T_{min}}$$

the governing equation is

$$\frac{dT^*}{dt^*} + T^* = \begin{cases} 1 & \text{on} \\ 0 & \text{off} \end{cases}, \tag{4.16}$$

the solution for which is

$$T^* = \begin{cases} 1 + C_1 e^{-t^*} & \text{on} \\ C_2 e^{-t^*} & \text{off} \end{cases}. \tag{4.17}$$

We will assume that the heat source comes on when temperature falls below a value T_L, and goes off when it is rises above T_U. These lower and upper bounds are non-dimensionally

$$T_L^* = \frac{T_L - T_{min}}{T_{max} - T_{min}},$$
$$T_U^* = \frac{T_U - T_{min}}{T_{max} - T_{min}}.$$

The result of applying this form of control is an oscillatory temperature that looks like that in Fig. 4.3, the period and amplitude of which can be chosen using suitable parameters. It can be shown that the on and off time periods are

$$t_{on}^* = \ln \frac{1 - T_L^*}{1 - T_U^*}, \tag{4.18}$$

$$t_{off}^* = \ln \frac{T_U^*}{T_L^*}, \tag{4.19}$$

respectively. The total period of the oscillation is then

$$t_p^* = \ln \frac{T_U^*(1 - T_L^*)}{T_L^*(1 - T_U^*)}.$$

If we make a small dead-band assumption, we can write

$$T_L^* = T_r^* - \delta,$$
$$T_U^* = T_r^* + \delta,$$

where $\delta \ll 1$. A Taylor-series expansion gives

$$t_p^* = 2\ \delta \left(\frac{1}{T_r^*} + \frac{1}{1 - T_r^*} \right) + \ldots$$

The period is thus proportional to the width of the dead band. The frequency of the oscillation increases as its amplitude decreases.

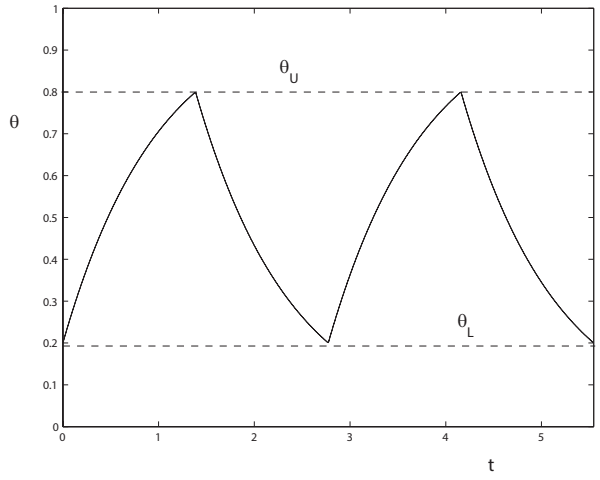

Figure 4.3: Lumped approximation with on-off control.

4.6.3 PID control

The error $e = T_r^* - T^*$ and control input $u = Q$ can be used in Eq. (4.5), so that the derivative of Eq. (4.15) gives

$$(K_d + 1)\frac{d^2T^*}{dt^{*2}} + (K_p + 1)\frac{dT^*}{dt^*} + K_i T^* = K_i T_r^*,$$

with the initial conditions

$$\begin{aligned} T^* &= T_0^* \quad \text{at} \quad t^* = 0, \\ \frac{dT^*}{dt^*} &= -\frac{K_p + 1}{K_d + 1} T_0^* + \frac{K_p T_r^*}{K_d + 1} \quad \text{at} \quad t^* = 0. \end{aligned}$$

The response of the closed-loop system can be obtained as a solution. The steady-state for $K_i \neq 0$ is given by $T^* = T_r^*$. It can be appreciated that different choices of the controller constants K_p, K_i and K_d will give overdamped or underdamped oscillatory or unstable behavior of the system. Fig. 4.4 shows two examples of closed-loop behavior with different parameter values.

4.7 One-dimensional flow temperature

Consider the control of temperature at a given point in the loop by modification of the heating. Both known heat flux and known wall temperatures may be looked at. In terms of control algorithms, one may use PID or on-off control.

4.8 Crossflow HX

A cross-flow heat exchanger model, schematically shown in Fig. E.34, has been studied using finite differences [4–6]. Water is the in-tube and air the over-tube fluid in the heat exchanger. This

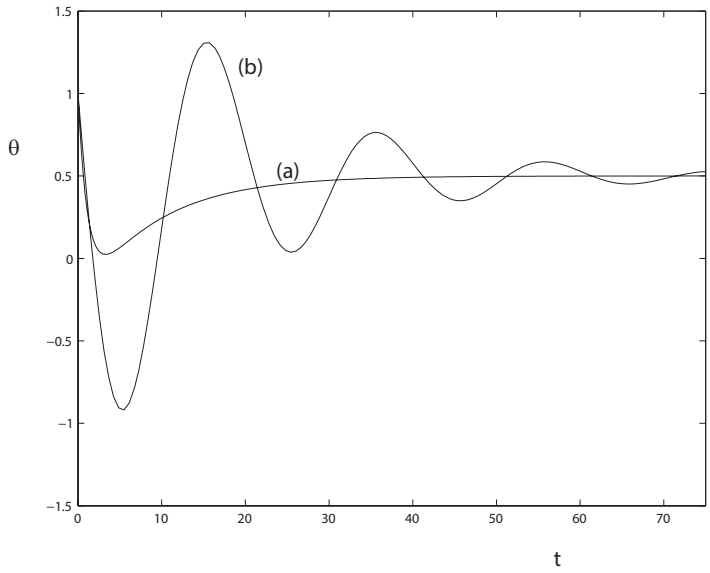

Figure 4.4: Lumped approximation with PID control; $K_i = K_d = -0.1$, $T_r^* = 0.5$, (a) $K_p = -0.1$, (b) $K_p = -0.9$.

example includes all the conductive, advective and convective effects discussed before. The governing equations on the outside of the tube, in the water, and in the wall of the tube are

$$\frac{\dot{m}_a}{L} c_a (T_{in}^a - T_{out}^a) = h_o 2\pi r_o (T_a - T_t), \tag{4.20}$$

$$\rho_w c_w \pi r_i^2 \frac{\partial T_w}{\partial t} + \dot{m}_w c_w \frac{\partial T_w}{\partial \xi} = h_i 2\pi r_i (T_t - T_w), \tag{4.21}$$

$$\rho_t c_t \pi (r_o^2 - r_i^2) \frac{\partial T_t}{\partial t} = k_t \pi (r_o^2 - r_i^2) \frac{\partial^2 T_t}{\partial \xi^2} + 2\pi r_o h_o (T_a - T_t) - 2\pi r_i h_i (T_t - T_w), \tag{4.22}$$

respectively. L is the length of the tube; $\dot{m}_a(t)$ and $\dot{m}_w(t)$ are the mass flow rates of air and water; T_{in}^a and $T_{out}^a(t)$ are the inlet and outlet air temperatures; $T_a(t)$ is the air temperature surrounding the tube; $T_t(\xi, t)$ and $T_w(\xi, t)$ are the tube-wall and water temperatures; h_i and h_o the heat transfer coefficients in the inner and outer surfaces of the tube; r_i and r_o are the inner and outer radii of the tube; c_a, c_w and c_t are the specific heats of the air, water and tube material; ρ_w and ρ_t are the water and tube material densities; and k_t is the thermal conductivity of the tube material. In addition, the air temperature is assumed to be $T_a = (T_{in}^a + T_{out}^a)/2$. The boundary and initial conditions are $T_t(0,t) = T_w(0,t) = T_{in}^w$, $T_t(L,t) = T_w(L.t)$, and $T_t(\xi, 0) = T_w(\xi, 0)$. Suitable numerical values were assumed for the computations.

The inlet temperatures T_{in}^a and T_{in}^w, and the flow rates $\dot{m}_a$ and $\dot{m}_w$ can all be used as control inputs to obtain a desired outlet temperature, T_{out}^a or T_{out}^w. The flow rates present a special difficulty; they appear in nonlinear form in Eqs. (4.20) and (4.21), and the outlet temperature is bounded. Fig. 4.6 shows the steady-state range of values of T_{out}^w that can be achieved on varying $\dot{m}_w$; temperatures outside this range cannot be obtained. It is also seen that the outlet water temperature is hard to control for large water flow rates. As an example of control dynamics, Fig. 4.7 shows the results of applying PI control on $\dot{m}_w$ to obtain a given reference temperature $T_{out}^w = 23°$C.

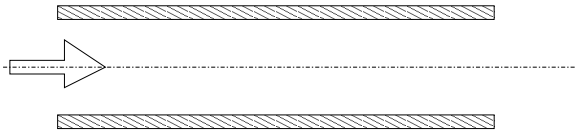

Figure 4.5: Schematic of single-tube cross-flow heat exchanger.

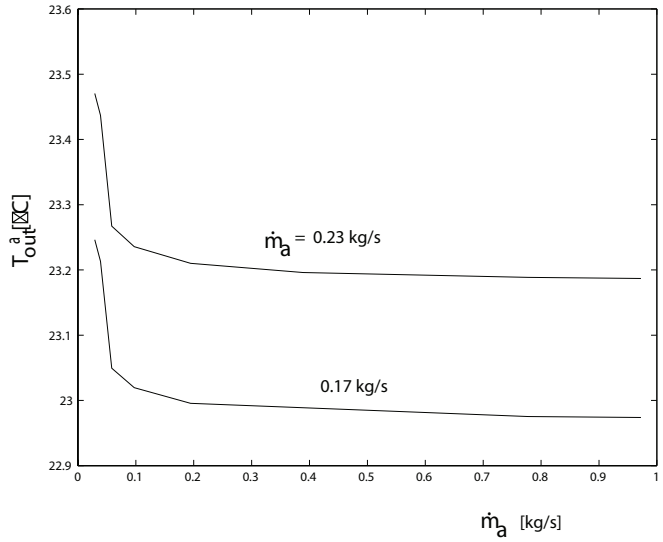

Figure 4.6: The relation between T^a_{out} and $\dot{m}_w$ for different $\dot{m}_a$ [4].

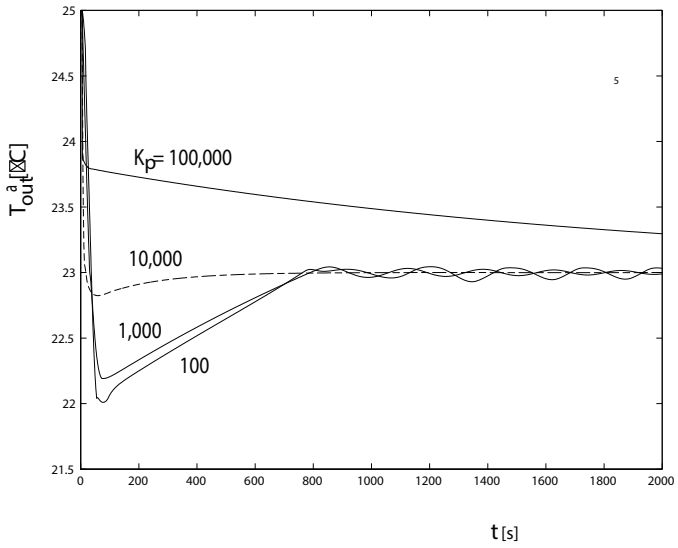

Figure 4.7: Behavior of T^a_{out} as a function of time for $K_i = 50$ and different K_p [4].

4.8.1 Control with heat transfer coefficient

4.8.2 Multiple room temperatures

Let there be n interconnected rooms. The wall temperature of room i is T_i^w and the air temperature is T_i^a. The heat balance equation for this room is

$$M_i^a c^w \frac{dT_i^w}{dt} = h_i A_i (T_i^a - T_i^w) + U_i A_i^e (T^e - T_i^w) \tag{4.23}$$

$$M_i^a c^a \frac{dT_i^a}{dt} = h_i A_i (T_i^w - T_i^a) + \frac{1}{2} c^a \sum_j (m_{ji}^a + |m_{ji}^a|) T_j^a - \frac{1}{2} c^a \sum_j (m_{ij}^a + |m_{ij}^a|) T_i^a + q_i \tag{4.24}$$

where T^e is the exterior temperature, m_{ij} is the mass flow rate of air from room i to room j. By definition $m_{ij} = -m_{ji}$. Since m_{ii} has no meaning and can be arbitrarily taken to be zero, m_{ij} is an anti-symmetric matrix. Also, from mass conservation for a single room, we know that

$$\sum_j m_{ji}^a = 0$$

Analysis

The unknowns in equations (4.23) and (4.24) are the $2n$ temperatures T_i^w and T_i^a.
(i) Steady state with $U = 0$
(a) The equality

$$\sum_i \sum_j (m_{ji}^a + |m_{ji}^a|) T_j^a - \sum_i \sum_j (m_{ij}^a + |m_{ij}^a|) T_i^a = 0$$

can be shown by interchanging i and j in the second term. Using this result, the sum of equations (4.23) and (4.24) for all rooms gives

$$\sum_i q_i = 0$$

which is a necessary condition for a steady state.
(b) Because the sum of equations (4.23) and (4.24) for all rooms gives an identity, the set of equations is not linearly independent. Thus the steady solution is not unique unless one of the room temperatures is known.

Control

The various proportional control schemes possible are:

- Control of individual room heating

$$q_i = -K_i (T_i^a - T_i^{set})$$

- Control of mass flow rates

$$m_{ji}^a = f_{ij} (T_j^a, T_i^a, T_i^{set})$$

Similar on-off control schemes can also be proposed.

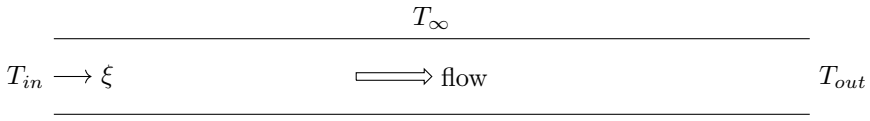

Figure 4.8: Schematic of duct of length L.

4.8.3 Two rooms

Consider two interconnected rooms 1 and 2 with mass flow m from 1 to 2. Also there is leakage of air into room 1 from the exterior at rate m, and leakage out of room 2 to the exterior at the same rate. The energy balances for the two rooms give

$$M_1 c^a \frac{dT_1}{dt} = U_1 A_1 (T^e - T_1) + \frac{1}{2}(m + |m|)(T^e - T_1) - \frac{1}{2}(m - |m|)(T_2 - T_1) + q_1 \tag{4.25}$$

$$M_2 c^a \frac{dT_2}{dt} = U_2 A_2 (T^e - T_2) - \frac{1}{2}(m - |m|)(T^e - T_2) + \frac{1}{2}(m + |m|)(T_1 - T_2) + q_2 \tag{4.26}$$

The overall mass balance can be given by the sum of the two equations to give

$$M_1 c^a \frac{dT_1}{dt} + M_2 c^a \frac{dT_2}{dt} = U_1 A_1 (T^e - T_1) + U_2 A_2 (T^e - T_2) + |m| T^e + \frac{1}{2}(m - |m|)T_1 - \frac{1}{2}(m + |m|)T_2 + q_1 + q_2$$

One example of a control problem would be to change m to keep the temperatures of the two rooms equal. Delay can be introduced by writing $T_2 = T_2(t - \tau)$ and $T_1 = T_1(t - \tau)$ in the second to last terms of equations (4.25) and (4.26), respectively, where τ is the time taken for the fluid to get from one room to the other.

4.8.4 Long duct

The diffusion problem of the previous section does not have advection. Transport of fluids in ducts introduces a delay between the instant the particles of fluid go into the duct and when they come out, which creates a difficulty for outlet temperature control. The literature includes applications to hot-water systems [43, 136] and buildings [8, 168]; transport [207] and heater [40, 41] delay and the effect of the length of a duct on delay [47] have also been looked at.

A long duct of constant cross section, schematically shown in Fig. 7.1 where the flow is driven by a variable-speed pump, illustrates the basic issues [4, 7]. The fluid inlet temperature T_{in} is kept constant, and there is heat loss to the constant ambient temperature T_∞ through the surface of the duct.

With a one-dimensional approximation, energy conservation gives

$$\frac{\partial T}{\partial t} + v \frac{\partial T}{\partial \xi} + \frac{4h}{\rho c D}(T - T_\infty) = 0, \tag{4.27}$$

with the boundary condition $T(0, t) = T_{in}$, where $T(\xi, t)$ is the fluid temperature, t is time, ξ is the distance along the duct measured from the entrance, $v(t)$ is the flow velocity, h is the coefficient of heat transfer to the exterior, ρ is the fluid density, c is its specific heat, and D is the hydraulic diameter of the duct. The flow velocity is taken to be always positive, so that the $\xi = 0$ end is

always the inlet and $\xi = L$ the outlet, where L is the length of the duct. The temperature of the fluid coming out of the duct is $T_{out}(t)$.

Using the characteristic quantities of L for length, $\rho cD/4h$ for time, and $hL/\rho cD$ for velocity, the non-dimensional version of Eq. (4.27) is

$$\frac{\partial \theta}{\partial t} + v\frac{\partial \theta}{\partial \xi} + \theta = 0, \tag{4.28}$$

where $\theta = (T - T_\infty)/(T_{in} - T_\infty)$, with $\theta(0,t) = 1$. The other variables are now non-dimensional. Knowing $v(t)$, this can be solved to give

$$\theta(\xi, t) = e^{-t}\ f\left(\xi - \int_0^t v(s)\ ds\right), \tag{4.29}$$

where the initial startup interval in which the fluid within the duct is flushed out has been ignored; f is an arbitrary function. Applying the boundary condition at $\xi = 0$ gives

$$1 = e^{-t}\ f\left(-\int_0^t v(s)\ ds\right). \tag{4.30}$$

The temperature at the outlet of the duct, *i.e.* at $\xi = 1$, is

$$\theta_{out}(t) = e^{-t}\ f\left(1 - \int_0^t v(s).\ ds\right) \tag{4.31}$$

Eqs. (4.30) and (4.31) must be simultaneously solved to get the outlet temperature $\theta_{out}(t)$ in terms of the flow velocity v.

The problem is non-linear if the outlet temperature $T_{out}(t)$ is used to control the flow velocity $v(t)$. The delay between the velocity change and its effect on the outlet temperature can often lead instability, as it does in other applications [16, 72, 77, 183]. Fig. 4.9 shows a typical result using PID control in which the system is unstable. Shown are the outlet temperature, flow velocity and residence time of the fluid in the duct, all of which ultimately achieve constant amplitude oscillations.

Bibliography

M.A. Henson and D.E. Seborg, *Nonlinear Process Control,* Prentice Hall, 1997.

O.L.R. Jacobs, *Introduction to Control Theory,* Oxford, 1993.

Problems

1. Two bodies at temperatures $T_1(t)$ and $T_2(t)$, respectively, are in thermal contact with each other and with the environment. The temperatures are governed by

$$M_1 c_1 \frac{dT_1}{dt} + h_c A_c (T_1 - T_2) + hA(T_1 - T_\infty(t)) = Q(t)$$
$$M_2 c_2 \frac{dT_2}{dt} + h_c A_c (T_2 - T_1) + hA(T_2 - T_\infty(t)) = 0,$$

   where $Q(t)$ is internal heat generation that can be controlled. Take T_∞ = constant. Show results for (a) PID and (b) on-off control.

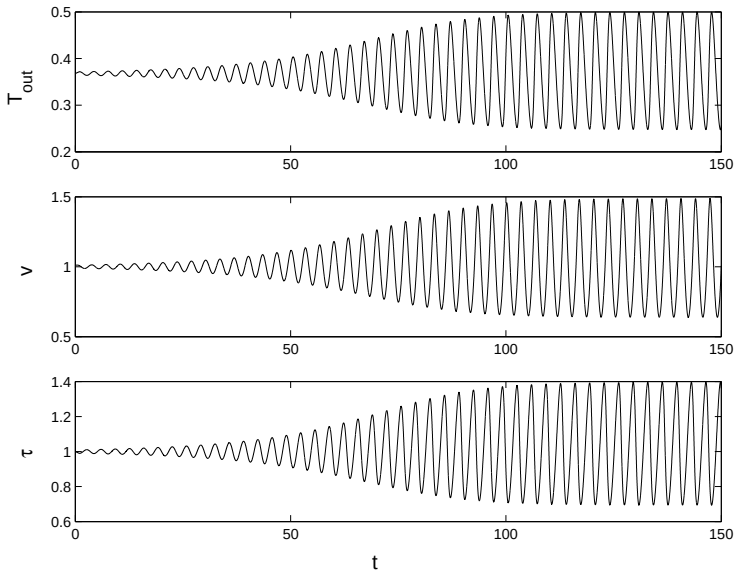

Figure 4.9: Outlet temperature, velocity and residence time for $K_i = -5$ and $K_p = 2.5$ [4].

2. Two bodies at temperatures $T_1(t)$ and $T_2(t)$, respectively, are in thermal contact with each other and with the environment. The temperatures are governed by

$$M_1 c_1 \frac{dT_1}{dt} + h_c A_c (T_1 - T_2) + hA(T_1 - T_\infty(t)) = Q_1(t)$$
$$M_2 c_2 \frac{dT_2}{dt} + h_c A_c (T_2 - T_1) + hA(T_2 - T_\infty(t)) = Q_2(t)$$

   where Q_1 and Q_2 are internal heat generation sources, each one of which can be independently controlled. Using on-off control, show analytical or numerical results for the temperature responses of the two bodies. If you do the problem analytically, take the ambient temperature, T_∞, to be constant, but if you do it numerically, then you can take it to be (a) constant, and (b) oscillatory. For $Q_1 = Q_2 = 0$, find the steady state $(\bar{T}_1, \bar{T}_2)$ and determine its stability.

3. Two lumped bodies A and B in thermal contact (contact thermal resistance R_c) exchange heat between themselves by conduction and with the surroundings by convection (see Fig. 3.7). It is desired to control their temperatures at T_A and T_B using separate internal heat inputs Q_A and Q_B.

   (a) Check that the system is controllable.

   (b) Set up a PID controller where its constants are matrices. Determine the condition for linear stability of the control system. Show that the case of two independent bodies is recovered as $R_c \to \infty$.

   (c) Calculate and plot $T_A(t)$ and $T_B(t)$ for chosen values of the controller constants.

4. Apply an on-off controller to the previous problem. Plot $T_A(t)$ and $T_B(t)$ for selected values of the parameters. Check for phase synchronization.

5. A number of identical rooms are arranged in a circle as shown in Fig. 4.10, with each at a uniform temperature $T_i(t)$. Each room exchanges heat by convection with the outside which is at T_∞, and with its neighbors with a conductive thermal resistance R. To maintain temperatures, each room has a heater that is controlled by independent but identical proportional controllers. (a) Derive the governing equations for the system, and nondimensionalize. (b) Find the steady state temperatures. (c) Write the dynamical system in the form

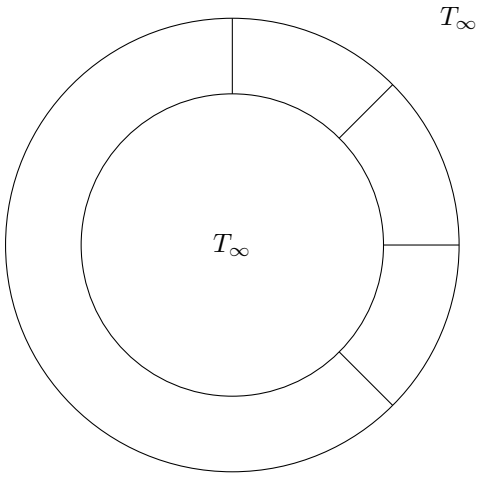

Figure 4.10: Rooms arranged in the form of a circle.

$\dot{\mathbf{x}} = \mathbf{A}\mathbf{x}$ and determine the condition for stability[1].

[1]Eigenvalues of an $N \times N$, circulant, banded matrix of the form

$$\begin{bmatrix} b & c & 0 & \dots & 0 & a \\ a & b & c & \dots & 0 & 0 \\ 0 & a & b & \dots & 0 & 0 \\ \vdots & \vdots & \vdots & \vdots & \vdots & \\ 0 & \dots & 0 & a & b & c \\ c & 0 & \dots & 0 & a & b \end{bmatrix}$$

are $\lambda_j = b + (a+c)\cos\{2\pi(j-1)/N\} - i(a-c)\sin\{2\pi(j-1)/N\}$, where $j = 1, 2, \dots, N$.

Chapter 5

Physics of heat transfer

sectionMicroscale heat transfer

[115] is a review of microscale heat exchangers, and [36] of photonic devices.

[90, 127, 187, 196, 212, 230]

5.1 Phonons

5.1.1 Single atom type

A lattice of atoms of a single type is shown in Fig. 5.5. The mass of each atom is m, the spring constants are c, and a is the mean distance between the atoms. For a typical atom n, Newton's second law gives

$$\begin{aligned} m\frac{d^2x_n}{dt^2} &= c(x_{n+1} - x_n) - c(x_n - x_{n-1}) \\ &= c(x_{n+1} - 2x_n + x_{n-1}). \end{aligned}$$

Let

$$x_i = \widehat{x}e^{i(nka-\omega t)},$$

then the dispersion relation is

$$\omega = \left(\frac{2c}{m}\right)^{1/2} (1 - \cos ka)^{1/2}.$$

The phase velocity is

$$v_p = \left(\frac{2c}{mk^2}\right)^{1/2} (1 - \cos ka)^{1/2},$$

Figure 5.1: Lattice of atoms of a single type

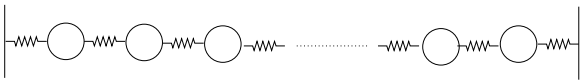

Figure 5.2: Lattice of atoms of a single type

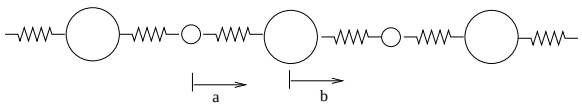

Figure 5.3: Lattice of atoms of two different type

and the group velocity is

$$v_g = \left(\frac{c}{2m}\right)^{1/2} \frac{a \sin ka}{(1 - \cos ka)^{1/2}}.$$

For $ka \to 0$, we have

$$v_g = a \left(\frac{c}{m}\right)^{1/2}.$$

The thermal conductivity

$$k = k_e + k_p$$

where k_e and k_p are those due to electron and phonon transports. We can also write

$$k = \frac{1}{3} c v_g l$$

where c is the specific heat, and l is the mean free path.

5.1.2 Two atom types

Newton's second law gives

$$\begin{aligned} m_1 \frac{d^2 x_i}{dt^2} &= c(y_i - x_i) - c(x_i - y_{i-1}) \\ &= c(y_i - 2x_i + y_{i-1}), \\ m_2 \frac{d^2 y_i}{dt^2} &= c(x_{i+1} - y_i) - c(y_i - x_i) \\ &= c(x_{i+1} - 2y_i + x_i). \end{aligned}$$

Let

$$\begin{aligned} x_i &= \widehat{x} e^{i(nka - \omega t)}, \\ y_i &= \widehat{y} e^{i(nka - \omega t)}, \end{aligned}$$

Table 5.1: Flow regimes

$Kn \to 0$	continuum, no viscous diffusion
$Kn \leq 10^{-3}$	continuum, Navier-Stokes, no-slip at boundaries
$10^{-3} \leq Kn \leq 10^{-1}$	continuum-transition, Navier-Stokes, slip at boundaries
$10^{-1} \leq Kn \leq 10$	transition
$10 \leq Kn$	free molecular flow

so that

$$-m_1\widehat{x}\omega^2 = c\left(\widehat{y} - 2\widehat{x} + \widehat{y}e^{-ika}\right),$$
$$-m_2\widehat{y}\omega^2 = c\left(\widehat{x}e^{ika} - 2\widehat{y} + \widehat{x}\right),$$

which can also be written as

$$\begin{bmatrix} 2c - m_1\omega^2 & -c(1+e^{-ika}) \\ -c(1+e^{ika}) & 2c - m_2\omega^2 \end{bmatrix} \begin{bmatrix} \widehat{x} \\ \widehat{y} \end{bmatrix} = \begin{bmatrix} 0 \\ 0 \end{bmatrix}.$$

This means that

$$(2c - m_1\omega^2)(2c - m_2\omega^2) - c^2(1+e^{-ika})(1+e^{ika}) = 0,$$

which simplifies to

$$m_1m_2\omega^4 - 2c(m_1+m_2)\omega^2 + 2c^2(1-\cos ka) = 0.$$

The solution is

$$\omega^2 = \frac{1}{2m_1m_2}\left[2c(m_1+m_2) \pm 2c\sqrt{m_1^2 + m_2^2 + 2m_1m_2\cos ka}\right].$$

The positive sign corresponds to the optical and the negative to the acoustic mode.

5.2 Rarefied gases

Knudsen number is defined as

$$Kn = \frac{\lambda}{L},$$

where λ is the mean free path, and L is a characteristic length. From statistical mechanics it can be shown that it is related to the Reynolds and Mach numbers by $Kn \sim Ma/Re$. The different flow regimes are shown in Table 5.1.

5.3 Thin films

5.4 Heat carriers

[110]

5.4.1 Free electrons and holes

Free electrons, as opposed to the valence electrons, move with an applied potential field, and contribute to transport of electrical current and heat.

5.4.2 Phonons

These are vibrations of atoms that propagate in a wave-like manner. There is more on this in Section 5.8.

5.4.3 Material particles

This transport is due to the bulk motion of a material which could be a solid, liquid or gas. For a gas, the motion of the atoms is usually what transports heat. For a continuum, it is usually referred to as advection, and will be discussed in detail in the Chapters on convection.

5.4.4 Photons

This is a particle that corresponds to an electromagnetic wave and is thus what enables radiation. There is more on this in Section 5.6.

5.5 Maxwell-Boltzmann distribution

Different distributions apply for different types of particles. The one that applies to classical particles is the Maxwell-Boltzmann distribution: for a single oscillator in a system of oscillators, the probability $p(E)$ of possessing energy between E and $E + dE$ is proportional to $e^{-E/kT}\ dE$.

5.6 Planck's radiation law

[1]

Planck assumed that the energy of each oscillator is a multiple of $\hbar\omega$, i.e. $E = n\hbar\omega$, so that

$$\begin{aligned} p(E) &= \frac{e^{-n\hbar\omega/kT}}{\sum_{n=0}^{\infty} e^{-n\hbar\omega/kT}}, \\ &= (1 - e^{-\hbar\omega/kT})\ e^{-n\hbar\omega/kT}, \text{ since } \sum_{n=0}^{\infty} y^n = \frac{1}{1-y}. \end{aligned}$$

[1] Quantum Mechanics with Applications, D.B. Beard and G.B. Beard, Allyn and Bacon, Boston, 1970

The average energy of each mode of oscillation is

$$\begin{aligned}\langle E\rangle &= \sum_{n=0}^{\infty} E\ p(E),\\ &= (1-e^{-\hbar\omega/kT})\sum_{k=0}^{\infty} n\hbar\omega e^{-n\hbar\omega/kT},\\ &= (1-e^{-\hbar\omega/kT})\hbar\omega\frac{e^{-\hbar\omega/kT}}{(1-e^{-\hbar\omega/kT})^2},\\ &= \frac{\hbar\omega}{e^{\hbar\omega/kT}-1}\end{aligned}$$

The number of vibrational modes per unit volume having frequency between ω and $\omega + d\omega$ is [To be clarified.]

$$N(\omega)\ d\omega = \frac{\omega^2}{\pi^2 c^3}\ d\omega.$$

Thus

$$N(\omega)\langle E\rangle\ d\omega = \frac{\omega^2}{\pi^2 c^3}\ \frac{\hbar\omega}{e^{\hbar\omega/kT}-1}\ d\omega$$

The energy density per unit volume per unit frequency is

$$S = \frac{\omega^2}{\pi^2 c^3}\ \frac{\hbar\omega}{e^{\hbar\omega/kT}-1}$$

The density above is for thermal equilibrium, so setting inward=outward gives a factor of 1/2 for the radiated power outward. Then one must average over all angles, which gives another factor of 1/2 for the angular dependence which is the square of the cosine. Thus the radiated power per unit area from a surface at this temperature is $Sc/4$. [To be clarified.]

Spectral radiance is

$$B_\nu(\nu,T) = \frac{2h\nu^3}{c^2}\frac{1}{e^{h\nu/kT}-1} \qquad \text{per unit frequency.}$$

This can be converted to

$$B_\lambda(\lambda,T) = \frac{2hc^2}{\lambda^5}\frac{1}{e^{hc/\lambda kT}-1} \qquad \text{per unit wavelength,}$$

where $c = \nu\lambda$ and $B_\nu(\nu,T)\ d\nu = -B_\lambda(\lambda,T)\ d\lambda$.

5.7 Diffusion by random walk

5.7.1 Brownian motion

Langevin equation

$$m\frac{d^2\mathbf{x}}{dt^2} = -\lambda\frac{d\mathbf{x}}{dt} + \mathbf{F}_R(t).$$

for a particle of mass m, position $\mathbf{x}$ that is undergoing a viscous drag of $\lambda(d\mathbf{x}/dt)$ and a random force $\mathbf{F}_R(t)$. At the two extremes of time, the solutions are
(a) Short time $t \ll m/\lambda$: ballistic

$$\langle x^2 \rangle - \langle x_0^2 \rangle = \frac{kT}{m}\, t^2$$

(b) Long time $t \gg m/\lambda$: viscous fluid

$$\langle x^2 \rangle - \langle x_0^2 \rangle = -\frac{2kT}{\lambda}\, t$$

The Fokker-Planck equation for the evolution of a probability density function $P(\mathbf{x}, t)$ is

$$\frac{\partial P}{\partial t} + \nabla \cdot (\mathbf{u}P) = \frac{1}{2}\nabla^2 \mathbf{D}P$$

5.7.2 One-dimensional

Consider a walker along an infinite straight line, as shown inFig. 5.4, moving with a step size ΔX taken forward or backward with equal probability in a time interval Δt. Let the current position of the walker be $x = X$, and the probability that the walker is in an interval $[X - dX/2, X + dX/2]$ be $P(X, t)$. Since there is equal probability of the walker in the previous time step to have been in the interval $[X - \Delta X - dX/2, X - \Delta X + dX/2]$ or $[X + \Delta X - dX/2, x + \Delta X + dX/2]$, we have

$$P(X, t) = \frac{1}{2}\left[P(X - \Delta X, t - \Delta t) + P(X + \Delta X, t - \Delta t\right]. \tag{5.1}$$

Assuming that ΔX and Δt are small, Taylor series expansions give

$$\begin{aligned} P(X \pm \Delta X, t - \Delta t) = P &\pm \frac{\partial P}{\partial x}\Delta X - \frac{\partial P}{\partial t}\Delta t + \frac{1}{2}\frac{\partial^2 P}{\partial x^2}(\Delta X)^2 \pm \frac{\partial^2 P}{\partial x \partial t}\Delta X \Delta t + \frac{1}{2}\frac{\partial^2 P}{\partial t^2}(\Delta t)^2 \\ &\pm \frac{1}{6}\frac{\partial^3 P}{\partial x^3}(\Delta x)^3 - \frac{1}{2}\frac{\partial^3 P}{\partial x^2 \partial t}(\Delta x)^2 \Delta t \pm \frac{1}{2}\frac{\partial^3 P}{\partial x \partial t^2}\Delta x (\Delta t)^2 - \frac{1}{6}\frac{\partial^3 P}{\partial t^3}(\Delta t)^3 \\ &+ \ldots, \end{aligned}$$

where the terms on the right side are evaluated at (X, t). Substituting in Eq. (5.1) we get

$$\frac{\partial P}{\partial t} - D\frac{\partial^2 P}{\partial x^2} = \frac{1}{2}\frac{\partial^2 P}{\partial t^2}\Delta t - \frac{1}{2}\frac{\partial^3 P}{\partial x^2 \partial t}(\Delta x)^2 + \ldots,$$

where $D = (\Delta x)^2/2\Delta t$. If we let $\Delta x \to 0$ and $\Delta t \to 0$ such that D is constant, we get the diffusion equation

$$\frac{\partial P}{\partial t} = D\frac{\partial^2 P}{\partial x^2}.$$

5.7.3 Multi-dimensional

Let $P = P(\mathbf{r}, t)$, and $\Delta\mathbf{r}$ be a step in any direction where $|\Delta\mathbf{r}|$ is a constant. Then

$$P(\mathbf{r}, t) = \int_S P(\mathbf{r} + \Delta\mathbf{r}, t - \Delta t)\; dS$$

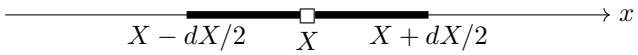

Figure 5.4: Random walker with current position at □.

Figure 5.5: Lattice of atoms of a single type

where S is a sphere of radius $|\Delta\mathbf{r}|$ centered on $\mathbf{r}$. Also

$$P(\mathbf{r}+\Delta\mathbf{r}, t-\Delta t) = P + \frac{\partial P}{\partial r_i}\Delta r_i - \frac{\partial P}{\partial t}\Delta t\frac{1}{2}\frac{\partial^2 P}{\partial r_i \partial r_i} + \dots$$

etc.

5.8 Phonons

Phonons are lattice vibrations that can be considered to be quasi-particles. [115] is a review of microscale heat exchangers, and [36] of photonic devices.

[90, 127, 187, 196, 212, 230]

5.8.1 Single atom type

A lattice of atoms of a single type is shown in Fig. 5.5. The mass of each atom is m, the spring constants are c, and a is the mean distance between the atoms. For a typical atom n, Newton's second law gives

$$\begin{aligned} m\frac{d^2x_n}{dt^2} &= c(x_{n+1}-x_n) - c(x_n - x_{n-1}) \\ &= c(x_{n+1} - 2x_n + x_{n-1}). \end{aligned}$$

Let

$$x_i = \widehat{x}e^{i(nka-\omega t)},$$

then the dispersion relation is

$$\omega = \left(\frac{2c}{m}\right)^{1/2}(1-\cos ka)^{1/2}.$$

The phase velocity is

$$v_p = \left(\frac{2c}{mk^2}\right)^{1/2}(1-\cos ka)^{1/2},$$

and the group velocity is

$$v_g = \left(\frac{c}{2m}\right)^{1/2}\frac{a\sin ka}{(1-\cos ka)^{1/2}}.$$

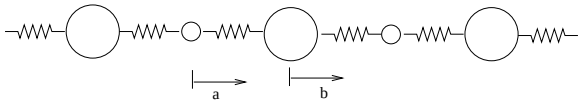

Figure 5.6: Lattice of atoms of two different type

For $ka \to 0$, we have

$$v_g = a\left(\frac{c}{m}\right)^{1/2}.$$

The thermal conductivity

$$k = k_e + k_p$$

where k_e and k_p are those due to electron and phonon transports. We can also write

$$k = \frac{1}{3}cv_g l$$

where c is the specific heat, and l is the mean free path.

5.8.2 Two atom types

Newton's second law gives

$$\begin{aligned} m_1\frac{d^2x_i}{dt^2} &= c(y_i - x_i) - c(x_i - y_{i-1}) \\ &= c(y_i - 2x_i + y_{i-1}), \\ m_2\frac{d^2y_i}{dt^2} &= c(x_{i+1} - y_i) - c(y_i - x_i) \\ &= c(x_{i+1} - 2y_i + x_i). \end{aligned}$$

Let

$$\begin{aligned} x_i &= \widehat{x}e^{i(nka-\omega t)}, \\ y_i &= \widehat{y}e^{i(nka-\omega t)}, \end{aligned}$$

so that

$$\begin{aligned} -m_1\widehat{x}\omega^2 &= c\left(\widehat{y} - 2\widehat{x} + \widehat{y}e^{-ika}\right), \\ -m_2\widehat{y}\omega^2 &= c\left(\widehat{x}e^{ika} - 2\widehat{y} + \widehat{x}\right), \end{aligned}$$

which can also be written as

$$\begin{bmatrix} 2c - m_1\omega^2 & -c(1+e^{-ika}) \\ -c(1+e^{ika}) & 2c - m_2\omega^2 \end{bmatrix} \begin{bmatrix} \widehat{x} \\ \widehat{y} \end{bmatrix} = \begin{bmatrix} 0 \\ 0 \end{bmatrix}.$$

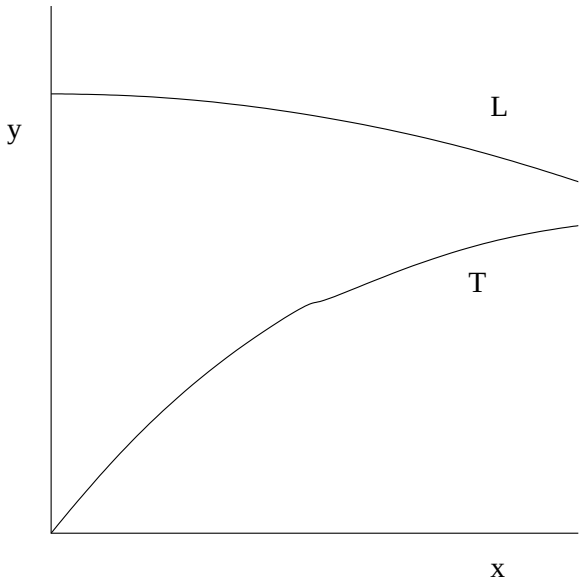

Figure 5.7: Schematic of dispersion relations; A = acoustic phonons, O = optical phonons.

This means that

$$(2c - m_1\omega^2)(2c - m_2\omega^2) - c^2(1 + e^{-ika})(1 + e^{ika}) = 0,$$

which simplifies to

$$m_1 m_2 \omega^4 - 2c(m_1 + m_2)\omega^2 + 2c^2(1 - \cos ka) = 0.$$

The solution is

$$\omega^2 = \frac{1}{2m_1 m_2}\left[2c(m_1 + m_2) \pm 2c\sqrt{m_1^2 + m_2^2 + 2m_1 m_2 \cos ka}\right].$$

The positive sign corresponds to the optical and the negative to the acoustic mode.

5.8.3 Types of phonons

- Frequency
  - Optical: high frequency
  - Acoustic: low frequency
- Direction of oscillation
  - Longitudinal: in direction of velocity
  - Transverse: normal to velocity

5.8.4 Heat transport

Phonons contribute to the internal energy of a material. In the Debye model for a monotomic crystallind solid

$$c_{v,p} = 9\frac{kT}{m}\left(\frac{kT}{\hbar\omega_D}\right)^3 n\int_0^{\hbar\omega_D/kT}\frac{x^4e^x}{e^x-1}\,dx,$$

where m is the mass of an atom, n is the number of atoms per unit volume, ω is the angular frequency of the phonon, and ω_D is the Debye frequency, i.e. the maximum frequency of vibration.

Phonons also participate in the transport of heat from one location to the other. The thermal conductivity k is

$$k = \frac{1}{3}nc_v u\lambda$$

where u is the average speed of the carrier, and λ is its mean free path.

5.9 Molecular dynamics

This is the technique of following individual molecules using Newtonian mechanics and appropriate intermolecular forces. One such commonly used force field is provided by the Lennard-Jones potential

$$V_{LJ} = 4\varepsilon\left[\left(\frac{\sigma}{r}\right)^{12} - \left(\frac{\sigma}{r}\right)^{6}\right]$$

5.10 Thin films

5.11 Boltzmann transport equation

The classical distribution function $f(\mathbf{r},\mathbf{v},t)$ is defined as number of particles in the volume $d\mathbf{r}\,d\mathbf{v}$ in the six-dimensional space of coordinates $\mathbf{r}$ and velocity $\mathbf{v}$. Following a volume element in this space, we have the balance equation [116, 131, 132], usually called the BTE:

$$\frac{\partial f}{\partial t} + \mathbf{v}\cdot\nabla f + \mathbf{a}\cdot\frac{\partial f}{\partial \mathbf{v}} = \left(\frac{\partial f}{\partial t}\right)_{scat}, \tag{5.2}$$

where $\mathbf{a} = d\mathbf{v}/dt$ is the acceleration due to an external force. The term on the right side is due to collisions and scattering. The heat flux is then

$$\mathbf{q}(\mathbf{r},t) = \int \mathbf{v}(\mathbf{r},t)f(\mathbf{r},\varepsilon,t)\varepsilon D\,d\varepsilon, \tag{5.3}$$

where $D(\varepsilon)$ is the density of energy states ε.

5.11.1 Relaxation-time approximation

Under this approximation

$$\left(\frac{\partial f}{\partial t}\right)_{scat} = \frac{f_0 - f}{\tau}, \tag{5.4}$$

where $\tau = \tau(\mathbf{r}, \mathbf{v})$. Thus

$$\frac{\partial f}{\partial t} + \mathbf{v} \cdot \nabla f + \mathbf{a} \cdot \frac{\partial f}{\partial \mathbf{v}} = \frac{f_0 - f}{\tau}. \tag{5.5}$$

Several further approximations can be made.

(a) Fourier's law

Assume $\partial/\partial t = 0$, $\mathbf{a} = 0$ and $\nabla f = \nabla f_0$ in the left side of Eq. (5.5) so that

$$f = f_0 - \tau \mathbf{v} \cdot \nabla f_0. \tag{5.6}$$

Introducing explicitly the dependence of f on temperature, we can write

$$\nabla f_0 = \frac{df_0}{dT} \nabla T. \tag{5.7}$$

Using Eqs. (5.6) and (5.7) in (5.3), we get

$$\mathbf{q} = -k \nabla T, \tag{5.8}$$

where

$$k = \int \mathbf{v} \left(\tau \mathbf{v} \cdot \frac{df_0}{dT} \right) \varepsilon D \, d\varepsilon, \tag{5.9}$$

since

$$\int \mathbf{v} f_0 \varepsilon D \, d\varepsilon = 0.$$

(b) Cattaneo's equation

Assume $\tau =$ constant and $\nabla f = (df_0/dT)\nabla T$. Multiply Eq. (5.5) by $\mathbf{v}\varepsilon D \, d\varepsilon$ and integrate to get

$$\frac{\partial}{\partial t} \int \mathbf{v} f \varepsilon D \, d\epsilon + \int \left(\mathbf{v} \cdot \frac{df_0}{dT} \nabla T \right) \mathbf{v} \varepsilon D \, d\varepsilon = -\frac{1}{\tau} \int \mathbf{v} f \varepsilon D \, d\varepsilon.$$

Using Eq. (5.3), this gives

$$\mathbf{q} + \tau \frac{\partial \mathbf{q}}{\partial t} = -k \nabla T,$$

where k is given by Eq. (5.9). This is Cattaneo's equation that can be compared to Fourier's law, Eq. (5.8).

5.12 Interactions and collisions

The heat carriers can all interact or collide with each other and with themselves, leaading to a contribution to the $(\partial f/\partial t)_{scat}$ term in the BTE. In addition solids have impurities, grain bvoundaries and dislocations with which they can interact as well.

5.13 Moments of the BTE

Eq. (5.2) can be multiplied by $\mathbf{v}^n$ to get the n-th moment of the BTE. These are the conservation equations: conservation of mass for $n = 0$, of momentum for $n = 1$, of mechanical energy for $n = 2$, and so on.

5.14 Rarefied gas dynamics

Knudsen number

$$Kn = \frac{\lambda}{L}$$

5.15 Radiation

5.15.1 Electromagnetics

[182]

Electromagnetic radiation travels at the speed of light $c = 2.998 \times 10^8$ m/s. Thermal radiation is the part of the spectrum in the 0.1–100 μm range. The frequency f and wavelength λ of a wave are related by

$$c = f\lambda$$

Maxwell's equations of electromagnetic theory are

$$\begin{aligned}
\boldsymbol{\nabla} \times \boldsymbol{H} &= \boldsymbol{J} + \frac{\partial \boldsymbol{D}}{\partial t} \\
\boldsymbol{\nabla} \times \boldsymbol{E} &= -\frac{\partial \boldsymbol{B}}{\partial t} \\
\boldsymbol{\nabla} \cdot \boldsymbol{D} &= \rho \\
\boldsymbol{\nabla} \cdot \boldsymbol{B} &= 0
\end{aligned}$$

where $\boldsymbol{H}$, $\boldsymbol{B}$, $\boldsymbol{E}$, $\boldsymbol{D}$, $\boldsymbol{J}$, and ρ are the magnetic intensity, magnetic induction, electric field, electric displacement, current density, and charge density, respectively. For linear materials $\boldsymbol{D} = \epsilon \boldsymbol{E}$, $\boldsymbol{J} = g\boldsymbol{E}$ (Ohm's law), and $\boldsymbol{B} = \mu \boldsymbol{H}$, where ϵ is the permittivity, g is the electrical conductivity, and μ is the permeability. For free space $\epsilon = 8.8542 \times 10^{-12}$ $\mathrm{C^2N^{-1}m^{-2}}$, and $\mu = 1.2566 \times 10^{-6}$ $\mathrm{NC^{-2}s^2}$,

For $\rho = 0$ and constant ϵ, g and μ, it can be shown that

$$\begin{aligned}
\nabla^2 \boldsymbol{H} - \epsilon\mu \frac{\partial^2 \boldsymbol{H}}{\partial t^2} - g\mu \frac{\partial \boldsymbol{H}}{\partial t} &= 0 \\
\nabla^2 \boldsymbol{E} - \epsilon\mu \frac{\partial^2 \boldsymbol{E}}{\partial t^2} - g\mu \frac{\partial \boldsymbol{E}}{\partial t} &= 0
\end{aligned}$$

The speed of an electromagnetic wave in free space is $c = 1/\sqrt{\mu\epsilon}$.

The radiation can also be considered a particles called phonons with energy

$$E = \hbar f$$

where $\hbar$ is Planck's constant.

5.16 Monte Carlo methods

[220]

[230] is a review of the radiative properties of semiconductors.

5.17 Participating media

Volumetric absorption: Beer's law

$$\frac{I_{\lambda,L}}{I_{\lambda,0}} = e^{-\kappa_\lambda L}$$

Radiative transfer equation:

$$\frac{1}{c}\frac{\partial}{\partial t}I_\nu + \hat{\Omega}\cdot\nabla I_\nu + (k_{\nu,s}+k_{\nu,a})I_\nu = j_\nu + \frac{1}{4\pi c}k_{\nu,s}\int_\Omega I_\nu d\Omega$$

Bibliography

D.B. Beard and G.B. Beard, *Quantum Mechanics with Applications,* Allyn and Bacon, Boston, 1970.

M. Kaviany, *Heat Transfer Physics,* Cambridge University Press, 2008.

C. Kittel and H. Kroemer, *Thermal Physics,* W.H. Freeman & Co., 1980.

H. Ibach and H. Lüth, *Solid-State Physics,* Springer, 1990.

A. Majumdar, *Microscale Energy Transport in Solids,* in Microscale Energy Transport, (Eds.) C.-L. Tien, A. Majumdar, F.M. Gerner, Taylor and Francis, 1998.

Problems

1. Consider an unsteady n-body radiative problem. The temperature of the ith body is given by
$$\begin{aligned} M_j c_j \frac{dT_j}{dt} &= -\sum_{i=1}^{n} A_i F_{ij}\sigma(T_i^4 - T_j^4) + Q_j \\ &= A_j \sum_{i=1}^{n} F_{ji}\sigma(T_i^4 - T_j^4) + Q_j \end{aligned}$$
What kind of dynamic solutions are possible?
2. The steady-state temperature distribution in a one-dimensional radiative fin is given by
$$\frac{dT}{dx} + hT^4 = 0$$
Is the solution unique and always possible?
3. Show that between one small body 1 and its large surroundings 2, the dynamics of the small-body temperature is governed by
$$M_1 c_1 \frac{dT_1}{dt} = -A_1 F_{12}\sigma(T_1^4 - T_2^4) + Q_1.$$
4. Plot all real $\overline{\theta}(\beta,\epsilon)$ surfaces for the convection with radiation problem, and comment on the existence of solutions.
5. Complete the problem of radiation in an enclosure (linear stability, numerical solutions).

Chapter 6

Conduction in rods (one-dimensional)

6.1 Fins

- *Fin effectiveness ϵ_f:* This is the ratio of the fin heat transfer rate to the rate that would be if the fin were not there.
- *Fin efficiency η_f:* This is the ratio of the fin heat transfer rate to the rate that would be if the entire fin were at the base temperature.

Longitudinal heat flux

$$q''_x = O(k_s \frac{T_b - T_\infty}{L})$$

Transverse heat flux

$$q''_t = O(h(T_b - T_\infty))$$

The transverse heat flux can be neglected compared to the longitudinal if

$$q''_x \gg q''_t$$

which gives a condition on the Biot number

$$Bi = \frac{hL}{k} \ll 1$$

Consider the fin shown shown in Fig. 6.1. The energy flows are indicated in Fig. 6.2. The conductive heat flow along the fin, the convective heat loss from the side, and the radiative loss from the side are

$$\begin{aligned} q_k &= -k_s A \frac{dT}{dx} \\ q_h &= h dA_s (T - T_\infty) \\ q_r &= \sigma dA_s (T^4 - T_\infty^4) \end{aligned}$$

where, for a small enough slope, $P(x) \approx dA_s/dx$ is the perimeter. Heat balance gives

$$\rho Ac \frac{\partial T}{\partial t} + \frac{\partial q_k}{\partial x} dx + q_h + q_r = 0 \tag{6.1}$$

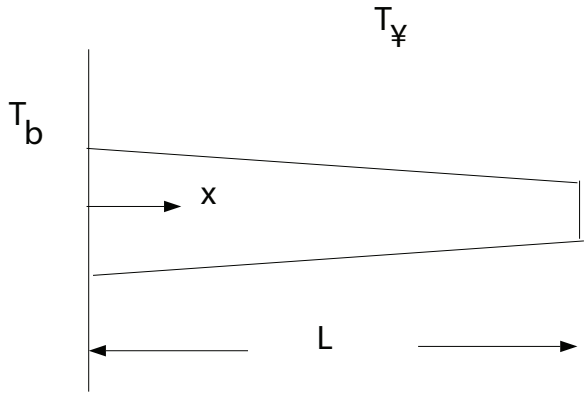

Figure 6.1: Schematic of a fin.

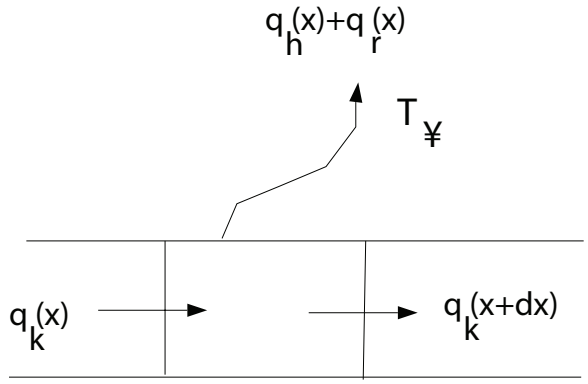

Figure 6.2: Energy balance.

from which

$$\rho Ac\frac{\partial T}{\partial t} - k_s\frac{\partial}{\partial x}(A\frac{\partial T}{\partial x}) + Ph(T - T_\infty) + \sigma P(T^4 - T_\infty^4) = 0$$

where k_s is taken to be a constant.

The initial temperature is $T(x, 0) = T_i(x)$. Usually the base temperature T_b is known. A surface cannot store energy, so that at a surface the heat flux coming in must be equal to that going out. The different types of boundary conditions for the tip are:

- Convective: $\partial T/\partial x = a$ at $x = L$
- Adiabatic: $\partial T/\partial x = 0$ at $x = L$
- Known tip temperature: $T = T_L$ at $x = L$
- Long fin: $T = T_\infty$ as $x \to \infty$

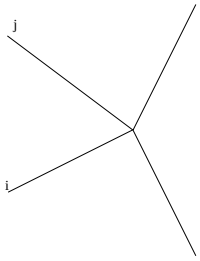

Figure 6.3: Complex conductive structures.

Taking

$$\theta = \frac{T - T_\infty}{T_b - T_\infty}, \quad \tau = \frac{k_s t}{L^2 \rho c} \text{ (Fourier modulus)}, \quad \xi = \frac{x}{L},$$
$$a(\xi) = \frac{A}{A_b}, \quad p(\xi) = \frac{P}{P_b}$$

where the subscript indicates quantities at the base, the fin equation becomes

$$a\frac{\partial \theta}{\partial \tau} - \frac{\partial}{\partial \xi}\left(a\frac{\partial \theta}{\partial \xi}\right) + m^2 p\theta + \epsilon p\left[(\theta+\beta)^4 - \beta^4\right] = 0$$

where

$$m^2 = \frac{P_b h L^2}{k_s A_b}$$
$$\epsilon = \frac{\sigma P_b L^2 (T_b - T_\infty)^3}{k_s A_b}$$
$$\beta = \frac{T_\infty}{T_b - T_\infty}$$

6.1.1 Structures

Fig. 6.3 shows a complex shape consisting of conductive bars. At each node

$$\sum_i q_i = 0$$

For each branch

$$\sum_i \frac{k_i A_i}{L_i}(T_i - T_0) = 0$$

from which

$$T_0 = \frac{\sum_i \frac{k_i A_i}{L_i} T_i}{\sum_i \frac{k_i A_i}{L_i}}$$

Example 6.1

A thick plate, shown in Fig. 6.4, has a lower surface kept at constant temperature T_0, and has convection to a fluid at temperature T_∞ at its upper surface. Find the temperature distribution in the plate.

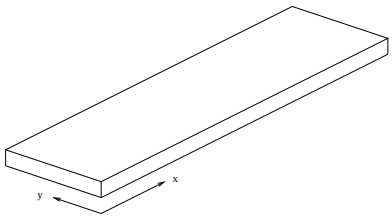

Figure 6.4: *Example 1.*

Assume: (a) Infinite in two dimensions. (b) Fourier conduction with constant thermal conductivity in plate. (c) Convective heat transfer coefficient h known.

Variables: $T(x)$ = temperature distribution, x = coordinate measured upward from the bottom of the plate, L = thickness of plate.

Steady-state temperature distribution $T(x)$ is governed by

$$k\frac{d^2T}{dx^2} = 0,$$

Integrating twice

$$\frac{dT}{dx} = a,$$
$$T = ax + b. \tag{6.2}$$

At bottom and top

$$T_0 = b,$$
$$T(L) = aL + b,$$

so that

$$a = \frac{T(L) - T_0}{L}, \tag{6.3}$$
$$b = T_0. \tag{6.4}$$

Equating the conductive and convective heat flux at the top surface

$$-k\frac{T(L) - T_0}{L} = h(T(L) - T_\infty),$$
$$T(L)\left\{-\frac{k}{L} - h\right\} = -\frac{kT_0}{L} - hT_\infty,$$
$$T(L) = \frac{kT_0 + hLT_\infty}{k + hL}. \tag{6.5}$$

The temperature distribution is Eq. (6.2), with a, b and $T(L)$ given by Eqs. (6.3), (6.4) and (6.5).

Example 6.2

The temperatures of the inner and outer surfaces of a wall composed of two concentric cylindrical layers of different thermal conductivities are known. What is the steady-state heat flux? See Fig. 6.5.

Assume: (a) Fourier conduction with constant thermal conductivity in each material. (b) No thermal resistance at interface between cylinders.

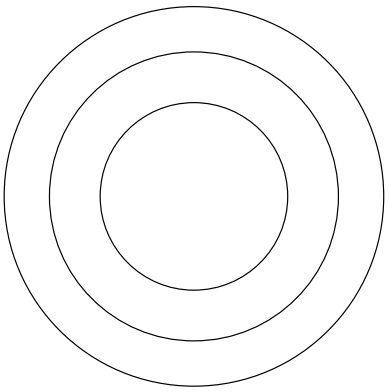

Figure 6.5: *Example 2*

Variables: q = conductive heat rate, T_1 and T_2 = the temperatures of the inner and outer surfaces, respectively; r_1, r_i and r_2 = the radii of the inner surface, the interface, and the outer surfaces, respectively; L = length of the cylinders; k_1 and k_2 = thermal conductivities of the inner and outer cylinders, respectively; R_1 and R_2 are the thermal resistances of the inner and outer cylinders, respectively.

Then

$$q = \frac{T_1 - T_2}{R_1 + R_2},$$
$$R_1 = \frac{\ln(r_i/r_1)}{2\pi L k_1},$$
$$R_2 = \frac{\ln(r_2/r_i)}{2\pi L k_2}.$$

Thus

$$q = \frac{T_1 - T_2}{\frac{\ln(r_i/r_1)}{2\pi L k_1} + \frac{\ln(r_2/r_i)}{2\pi L k_2}}.$$

6.1.2 Fin theory

Long time solution

$$a\frac{\partial\theta}{\partial\tau} - \frac{\partial}{\partial\xi}\left(a\frac{\partial\theta}{\partial\xi}\right) + f(\theta) = 0 \tag{6.6}$$

where $f(\theta)$ includes heat transfer from the sides due to convection and radiation. The boundary conditions are either Dirichlet or Neumannn type at $\xi = 0$ and $\xi = 1$. The steady state is determined from

$$-\frac{d}{d\xi}\left(a\frac{d\theta}{d\xi}\right) + f(\overline{\theta}) = 0 \tag{6.7}$$

with the same boundary conditions. Substituting $\theta = \overline{\theta} + \theta'$ in equation (6.6) and subtracting (6.7), we have

$$a\frac{\partial\theta'}{\partial\tau} - \frac{\partial}{\partial\xi}\left(a\frac{\partial\theta'}{\partial\xi}\right) + \left[f(\overline{\theta}+\theta') - f(\overline{\theta})\right] = 0$$

where θ' is the perturbation from the steady state. The boundary conditions for θ' are homogeneous. Multiplying by θ' and integrating from $\xi = 0$ to $\xi = 1$, we have

$$\frac{dE}{d\tau} = I_1 + I_2 \tag{6.8}$$

where

$$E = \frac{1}{2}\int_0^1 a(\theta')^2 \, d\xi \tag{6.9}$$

$$I_1 = \int_0^1 \theta' \frac{\partial}{\partial\xi}\left(a\frac{\partial\theta'}{\partial\xi}\right) \, d\xi \tag{6.10}$$

$$I_2 = -\int_0^1 \theta' \left[f(\overline{\theta}+\theta') - f(\overline{\theta})\right] \, d\xi \tag{6.11}$$

Integrating by parts we can show that

$$I_1 = \theta' a\frac{\partial\theta'}{\partial\xi}\bigg|_0^1 - \int_0^1 a\left(\frac{d\theta'}{d\xi}\right)^2 \, d\xi \tag{6.12}$$

$$= -\int_0^1 a\left(\frac{d\theta'}{d\xi}\right)^2 \, d\xi \tag{6.13}$$

since the first term on the right side of equation (6.12) is zero due to boundary conditions. Thus we know from the above that I_1 is nonpositive and from equation (6.9) that E is nonnegative. If we also assume that

$$I_2 \le 0 \tag{6.14}$$

then equation (6.8) tells us that E must decrease with time until reaching zero. Thus the steady state is globally stable. Condition (6.14) holds if [θ' and $f(\overline{\theta}+\theta') - f(\overline{\theta})$] are of the same sign or both zero; this is a consequence of the Second Law of Thermodynamics.

Example 6.3

What is the steady-state temperature distribution in a fin with a radiation boundary condition at the tip?

Assume: (a) Base temperature is known. (b) Tip is blackbody.
Variables: $T(x)$ = temperature distribution; x = coordinate along fin measured from the base.
The steady-state fin equation is

$$\frac{d^2T}{dx^2} - m^2(T - T_\infty) = 0,$$

where $m^2 = hA/(kA)$ with the solution

$$T = C_1\, e^{mx} + C_2\, e^{-mx}.$$

Boundary conditions are

$$T(0) = T_b,$$
$$-k\frac{dT}{dx}\Big|_{x=L} = \sigma[T(L)^4 - T_\infty^4].$$

so that

$$T_b = C_1 + C_2,$$
$$-k\left(C_1 m e^{mL} - C_2 e^{-mL}\right) = \sigma\left[(C_1\ e^{mL} + C_2\ e^{-mL})^4 - T_\infty^4\right],$$

which can be numerically solved for C_1 and C_2 if values of m, L and T_∞ are given.

Example 6.4

Show that there is a critical insulation radius which minimizes heat transfer from an insulation-covered pipe.

[cf. Example 3.5, 7th Ed.]

Variables: r_i = inner radius of insulation, r = outer radius of insulation, k = thermal conductivity of insulation material, h = external convective heat transfer coefficient.

The thermal resistance per unit length of the pipe is

$$R'_{tot} = \frac{\ln(r/r_1)}{2\pi k} + \frac{1}{2\pi r h},$$

and the heat rate per unit length is

$$q' = \frac{T_\infty - T_i}{R'_{tot}}$$

The maximum heat rate is obtained by minimizing q' or maximizing R'_{tot}. With the latter

$$0 = \frac{dR'_{tot}}{dr_{cr}},$$
$$= \frac{1}{2\pi r_{cr} k} - \frac{1}{2\pi r_{cr}^2 h},$$

from which $r_{cr} = k/h$. This is the critical radius of the insulation above and below which the heat rate is higher.

Example 6.5

If the temperature distribution inside a wall ($0 \le x \le L$) is $T(x) = a + bx + cx^2$, find the rate of heat generation in the wall.

Assume: (a) One-dimensional Fourier conduction. (b) Steady state. (c) Uniform thermal conductivity.

Variables: $T(x)$ = temperature distribution; x = coordinate through the wall; Q_g = heat generation per unit volume; k = thermal conductivity of wall.

The temperature distribution is given by

$$\frac{d^2T}{dx^2} + \frac{Q_g}{k} = 0$$

from which

$$g = -k\frac{d^2T}{dx^2},$$
$$= -2ck.$$

Example 6.6

The steady-state temperatures at different distances along a fin (6061 aluminum, 0.5 in diameter, 12 in long, ambient air temperature 20.8 °C) are measured to be the following.

x [m]	T [°C]
0.2794	42.3
0.2540	43.8
0.2286	47.2
0.2032	52.7
0.1778	59.1
0.1524	65.1
0.1270	72.2
0.1016	86.0
0.0762	104.5
0.0508	128.3
0.0254	154.7

Find the convective heat transfer coefficient.

Assume: Convective heat transfer along side and at tip.

Variables: x = distance from base, x_0 = x-coordinate of origin, L = distance between origin and tip of fin, θ = normalized temperature, T_∞ = ambient temperature, ξ = normalized distance.

At a distance of 0.0254 m from the base the temperature is 154.7 °C. We will take this point to be $x = x_0$ and the temperature there to be $T = T_0$. We define

$$\xi = \frac{x - x_0}{L},$$
$$\theta = \frac{T - T_0}{T_0 - T_\infty}.$$

The experimental data are plotted in Fig. 6.6. The theoretical temperature distribution

$$\frac{\theta}{\theta_0} = \frac{\cosh mL(1-\xi) + (h/mk)\sinh mL(1-\xi)}{\cosh mL + (h/mk)\sinh mL}$$

is also plotted in the figure. We can see that $h \approx 450$ W/m^{2}K fits the data well.

Example 6.7

1.5 kg/s of water enters a 10 cm diameter, 10 m long pipe at 40 °C. What is the exit temperature of the water if the inner wall of the pipe is uniformly at 20 °C?

Assume: (a) Heat rate depends on local temperature difference between the bulk temperature of the water and the temperature of the wall.

Variables: $\dot{m}$ = mass flow rate; c = specific heat; $T(x)$ = bulk temperature of water as a function of x; x = distance along the pipe; T_{in} = bulk temperature of water at inlet $x = 0$; T_w = inner wall temperature; D = diameter of pipe; h = convective heat transfer coefficient for heat transfer from water to pipe wall.

The governing equation is

$$\dot{m}c\ dT = h\pi D(T_w - T)\ dx,$$
$$\frac{dT}{dx} + \frac{h\pi D}{\dot{m}}T = \frac{h\pi D}{\dot{m}}T_w.$$

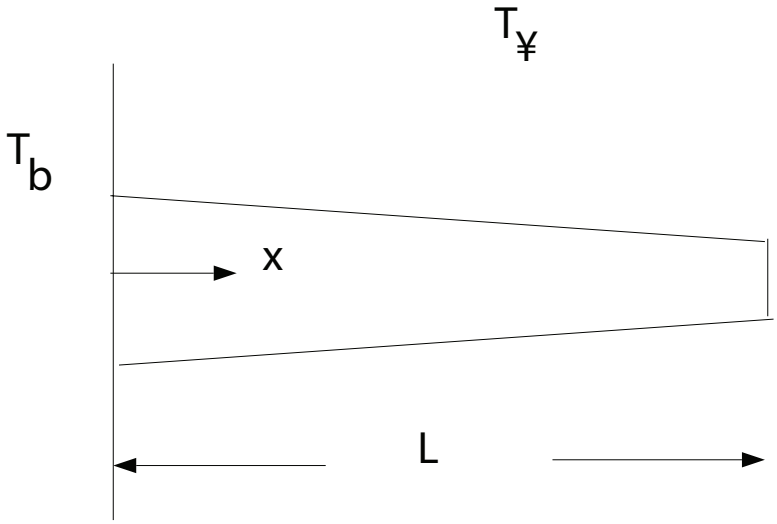

Figure 6.6: Points: measured temperature distribution; continuous line: theoretical temperature distribution for $h = 450$ W/m^{2}K.

The solution is

$$T(x) = T_w + Ae^{-h\pi Dx/\dot{m}}$$

The boundary condition is $T(x) = T_{in}$ at $x = 0$. This gives

$$\begin{aligned} T_{in} &= T_w + A, \\ A &= T_{in} - T_w, \end{aligned}$$

so that

$$T(x) = T_w + (T_{in} - T_w)e^{-h\pi Dx/\dot{m}}.$$

At $x = L$, the exit temperature T_{out} is

$$T_{out} = T_w + (T_{in} - T_w)e^{-h\pi DL/\dot{m}}.$$

Shape optimization of convective fin

Consider a rectangular fin of length L and thickness δ as shown in Fig. 6.7. The dimensional equation is

$$\frac{d^2T}{dx^2} - m^2(T - T_\infty) = 0$$

where

$$m = \left(\frac{2h}{k_s\delta}\right)^{1/2}$$

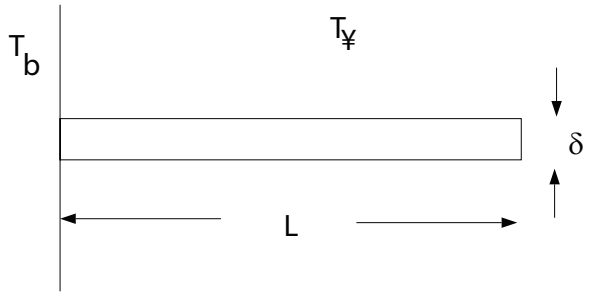

Figure 6.7: Rectangular fin.

We will take the boundary conditions

$$T(0) = T_b$$
$$\frac{dT}{dx}(L) = 0$$

The solution is

$$T = T_\infty - (T - T_\infty)\left[\tanh mL \sinh mx - \cosh mx\right]$$

The heat rate through the base per unit width is

$$\begin{aligned} q &= -k_s \delta \left.\frac{dT}{dx}\right|_{x=0} \\ &= k_s \delta (T_b - T_\infty) m \tanh mL \end{aligned}$$

Writing $L = A_p/\delta$, we get

$$q = k_s \delta \left(\frac{2h}{k_s \delta}\right)^{1/2} (T_b - T_\infty) \tanh \left[\frac{A_p}{\delta}\left(\frac{2h}{k_s \delta}\right)^{1/2}\right]$$

Keeping A_p constant, i.e. constant fin volume, the heat rate can be maximized if

$$\delta_{opt}^{1/2} \mathrm{sech}^2 \left[\frac{A_p}{\delta}\left(\frac{2h}{k_s \delta_{opt}}\right)\right] A_p \frac{2h}{k_s}^{1/2} (-\frac{3}{2}) \delta_{opt}^{-5/2} + \frac{1}{2}\delta_{opt}^{-1/2} \tanh \left[\frac{A_p}{\delta}\left(\frac{2h}{k_s \delta_{opt}}\right)^{1/2}\right] = 0$$

This is equivalent to

$$3\beta_{opt} \mathrm{sech}^2 \beta_{opt} = \tanh \beta_{opt}$$

where

$$\beta_{opt} = \frac{A_p}{\delta_{opt}}\left(\frac{2h}{k_s \delta_{opt}}\right)$$

Numerically, we find that $\beta_{opt} = 1.4192$. Thus

$$\delta_{opt} = \left[\frac{A_p}{\beta_{opt}} \left(\frac{k_s A_p}{2h} \right)^{1/2} \right]^{2/3}$$
$$L_{opt} = \left[\beta_{opt} \left(\frac{k_s A_p}{2h} \right)^{1/2} \right]^{2/3}$$

6.1.3 Fin structure

Consider now Fig. 6.3 with convection.

6.1.4 Fin with convection and radiation

Steady state solutions

Equation (6.6) reduces to

$$-\frac{d}{d\xi}\left(a \frac{d\theta}{d\xi} \right) + m^2 p\theta + \epsilon p \left[(\theta + \beta)^4 - \beta^4 \right] = 0$$

Uniform cross section

For this case $a = p = 1$, so that

$$-\frac{d^2\theta}{d\xi^2} + m^2\theta + \epsilon \left[(\theta + \beta)^4 - \beta^4 \right] = 0$$

Convective

With only convective heat transfer, we have

$$-\frac{d^2\theta}{d\xi^2} + m^2\theta = 0$$

the solution to whiich is

$$\theta = C_1 \sinh m\xi + C_2 \cosh m\xi$$

the constants are determined from the boundary conditions. For example, if

$$\theta(0) = 1$$
$$\frac{d\theta}{d\xi}(1) = 0$$

we get

$$\theta = -\tanh m \sinh m\xi + \cosh m\xi$$

Example 6.8

If

$$T(0) = T_0$$
$$T(L) = T_1$$

then show that

$$T(x) = \left[T_1 - T_0 \cosh\left(L\sqrt{\frac{hP}{kA}}\right)\right] \frac{\sinh\left(x\sqrt{\frac{hP}{kA}}\right)}{\sinh\left(L\sqrt{\frac{hP}{kA}}\right)} + T_0 \cosh\left(x\sqrt{\frac{hP}{kA}}\right)$$

Radiative

The fin equation is

$$-\frac{d^2\theta}{d\xi^2} + \epsilon\left[(\theta+\beta)^4 - \beta^4\right] = 0$$

Let

$$\phi = \theta + \beta$$

so that

$$-\frac{d^2\phi}{d\xi^2} + \epsilon\phi^4 = -\epsilon\beta^4$$

As an example, we will find a perturbation solution with the boundary conditions

$$\phi(0) = 1 + \beta$$
$$\frac{d\phi}{d\xi}(1) = 0$$

We write

$$\phi = \phi_0 + \epsilon\phi_1 + \epsilon^2\phi_2 + \ldots$$

The lowest order equation is

$$\frac{d_0^\phi}{d\xi^2} = 0, \quad \phi_0(0) = 1 + \beta, \quad \frac{d\phi_0}{d\xi}(1) = 0$$

which gives

$$\phi_0 = 1 + \beta$$

To the next order

$$\frac{d_1^\phi}{d\xi^2} = \phi_0^4 - \beta^4, \quad \phi_1(0) = 0, \quad \frac{d\phi_1}{d\xi}(1) = 0$$

with the solution

$$\phi_1 = [(1+\beta)^4 - \beta^4]\frac{\xi^2}{2} - [(1+\beta)^4 - \beta^4]\xi$$

The complete solution is

$$\phi = (1+\beta) + \epsilon\left\{[(1+\beta)^4 - \beta^4]\frac{\xi^2}{2} - [(1+\beta)^4 - \beta^4]\xi\right\} + \ldots$$

so that

$$\theta = 1 + \epsilon\left\{[(1+\beta)^4 - \beta^4]\frac{\xi^2}{2} - [(1+\beta)^4 - \beta^4]\xi\right\} + \ldots$$

Convective and radiative

?

Annular fin

Example 6.9

Show that under suitable conditions, the temperature distribution in a two-dimensional rectangle tends to that given by a one-dimensional approximation.

Extended surfaces

$$\eta_0 = 1 - \frac{A_f}{A}(1 - \eta_f)$$

where η_0 is the total surface temperature effectiveness, η_f is the fin temperature effectiveness, A_f is the HX total fin area, and A is the HX total heat transfer area.

6.1.5 Fin analysis

Analysis of Kraus (1990) for variable heat transfer coefficients.

6.2 Perturbations of one-dimensional conduction

6.2.1 Temperature-dependent conductivity

[13]

The governing equation is

$$\frac{d}{dx}\left(k(T)\frac{dT}{dx}\right) - \frac{Ph}{A}(T - T_\infty) = 0$$

with the boundary conditions

$$T(0) = T_b$$
$$\frac{dT}{dx}(L) = 0$$

we use the dimensionless variables

$$\theta = \frac{T - T_\infty}{T_b - T_\infty}$$
$$\xi = \frac{x}{L}$$

Consider the special case of a linear variation of conductivity

$$k(T) = k_0 \left(1 + \epsilon \frac{T - T_\infty}{T_b - T_\infty}\right)$$

so that

$$\begin{aligned} (1 + \epsilon\theta) \frac{d^2\theta}{d\xi^2} + \epsilon \left(\frac{d\theta}{d\xi}\right)^2 - m^2\theta = 0 \\ \theta(0) = 1 \\ \frac{d\theta}{d\xi}(L) = 0 \end{aligned}$$

where

$$m^2 = \frac{PhL^2}{Ak_0(T_b - T_\infty)}$$

Introduce

$$\theta(\xi) = \theta_0(\xi) + \epsilon\theta_1(\xi) + \epsilon\theta_2(\xi) + \ldots$$

Collect terms of $O(\epsilon^0)$

$$\begin{aligned} \frac{d^2\theta_0}{d\xi^2} - m^2\theta = 0 \\ \theta_0(0) = 1 \\ \frac{d\theta_0}{d\xi}(1) = 0 \end{aligned}$$

The solution is

$$\theta(\xi) = \cosh m\xi - \tanh m \sinh m\xi$$

To $O(\epsilon^1)$

$$\begin{aligned} \frac{d^2\theta_1}{d\xi^2} - m^2\theta_1 &= -\theta_0 \frac{d^2\theta_0}{d\xi^2} - \left(\frac{d\theta_0}{d\xi}\right)^2 \\ &= -m^2(1 - \tanh^2 m) \cosh 2m\xi - m^2 \tanh m \ \sinh 2m\xi \\ \theta_1(0) &= 0 \\ \frac{d\theta_1}{d\xi}(1) &= 0 \end{aligned}$$

The solution is

6.2.2 Eccentric annulus

Steady-state conduction in a slightly eccentric annular space, as shown in Fig. 6.8 can be solved by regular perturbation [13]. The radii of the two circles are r_1 and r_2.

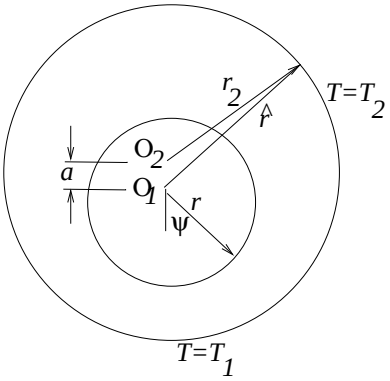

Figure 6.8: Eccentric annulus.

We will use polar coordinates (r, ψ) with the center of the small circle as origin. The two circles are at $r = r_1$ and $r = \widehat{r}$, where

$$r_2^2 = a^2 + \widehat{r}^2 + 2a\widehat{r}\cos\psi.$$

Solving for $\widehat{r}$, we have

$$\widehat{r} = \sqrt{r_2^2 - a^2(1 - \cos^2\psi)} - a\cos\psi.$$

In the quadratic solution, the positive sign corresponding to the geometry shown in the figure has been kept.

The governing equation for the temperature is

$$\left(\frac{\partial^2}{\partial r^2} + \frac{1}{r}\frac{\partial}{\partial r} + \frac{1}{r^2}\frac{\partial^2}{\partial \psi^2}\right) T(r, \psi) = 0.$$

The boundary conditions are

$$\begin{aligned} T(r_1, \psi) &= T_1, \\ T(\widehat{r}, \psi) &= T_2. \end{aligned}$$

With the variables

$$\begin{aligned} \theta &= \frac{T - T_2}{T_1 - T_2}. \\ R &= \frac{r - r_1}{r_2 - r_1}. \\ d &= \frac{r_1}{r_2 - r_1}. \\ \epsilon &= \frac{a}{r_2 - r_1}, \end{aligned}$$

we get

$$\left(\frac{\partial^2}{\partial R^2} + \frac{1}{R + d}\frac{\partial}{\partial R} + \frac{1}{(R + d)^2}\frac{\partial^2}{\partial \psi^2}\right) \theta(R, \psi) = 0,$$

and

$$\theta(0,\psi) = 1,$$
$$\theta(\widehat{R},\psi) = 0,$$

where

$$\begin{aligned}\widehat{R}(\psi) &= \frac{\widehat{r} - r_1}{r_2 - r_1} \\ &= \sqrt{(1+d)^2 - \epsilon^2(1-\cos^2\psi)} - \epsilon\cos\psi - d,\end{aligned}$$

The perturbation expansion is

$$\theta(R,\psi) = \theta_0(R,\psi) + \epsilon\theta_1(R,\psi) + \epsilon^2\theta_2(R,\psi) + \ldots.$$

Substituting in the equations, we get

$$\left(\frac{\partial^2}{\partial R^2} + \frac{1}{R+d}\frac{\partial}{\partial R} + \frac{1}{(R+d)^2}\frac{\partial^2}{\partial\psi^2}\right)\left(\theta_0 + \epsilon\theta_1 + \epsilon^2\theta_2 + \ldots\right) = 0, \tag{6.15}$$

$$\widehat{R}(\psi) = 1 - \epsilon\cos\psi - \frac{\epsilon^2}{2}(1-\cos^2\psi) + \ldots, \tag{6.16}$$

$$\theta_0(0,\psi) + \epsilon\theta_1(0,\psi) + \epsilon^2\theta_2(0,\psi) + \ldots = 1, \tag{6.17}$$

$$\theta_0(\widehat{R},\psi) + \epsilon\theta_1(\widehat{R},\psi) + \epsilon^2\theta_2(\widehat{R},\psi) + \ldots = 0. \tag{6.18}$$

Using Eq. (6.16), (6.18) can be further expanded in a Taylor series around $\widehat{R} = 1$ to give

$$\theta_0(1,\psi) + \epsilon\left(\theta_1(1,\psi) - \cos\psi\frac{d\theta_0}{dR}(1,\psi)\right) + \ldots = 0.$$

Collecting terms to order $O(\epsilon^0)$, we get

$$\left(\frac{\partial^2}{\partial R^2} + \frac{1}{R+d}\frac{\partial}{\partial R} + \frac{1}{(R+d)^2}\frac{\partial^2}{\partial\psi^2}\right)\theta_0 = 0,$$
$$\theta_0(0,\psi) = 1,$$
$$\theta_0(1,\psi) = 0,$$

which has the solution

$$\theta_0(R,\psi) = 1 - \frac{\ln(1+R/h)}{\ln(1+1/h)}.$$

To order $O(\epsilon^1)$

$$\left(\frac{\partial^2}{\partial R^2} + \frac{1}{R+d}\frac{\partial}{\partial R} + \frac{1}{(R+d)^2}\frac{\partial^2}{\partial\psi^2}\right)\theta_1 = 0,$$
$$\theta_1(0,\psi) = 0,$$
$$\begin{aligned}\theta_1(1,\psi) &= \cos\psi\frac{d\theta_0}{dR}(1,\psi), \\ &= \frac{\cos\psi}{(1+h)\ \ln(1+1/h)}.\end{aligned}$$

The solution is

$$\theta_1(R,\psi) = \pm\frac{R\cos\psi}{(1+2h)\ \ln(1+1/h)}\ \frac{R-2h}{R+h}.$$

6.3 Transient

The one-dimensional heat equation is

$$\rho c \, \frac{\partial T}{\partial t} = k_s \, \frac{\partial^2 T}{\partial x^2},$$

where $T = T(x,t)$. The spatial average of the temperature can be defined as

$$\bar{T}(t) = \frac{1}{L} \int_0^L T(x,t) \, dx.$$

Integrating the heat equation with respect to x and dividing by L gives

$$\begin{aligned} \rho c \, \frac{d\bar{T}}{dt} &= k_s \, \left. \frac{\partial T}{\partial x} \right|_0^L, \\ &= -q(L) + q(0). \end{aligned}$$

Derivatives and integrals commute on the left side since the integrals are basically limits of summations.

There are two time scales: the short (conductive) $\tau_0^k = L^2 \rho c / k_s$ and the long (convective) $\tau_0^h = L \rho c / h$. In the short time scale conduction within the slab is important, and convection from the sides is not. In the long scale, the temperature within the slab is uniform, and changes due to convection. The ratio of the two $\tau_0^k / \tau_0^h = Bi$. In the long time scale it is possible to show that

$$L \rho_s c \frac{dT}{dt} + h_1 (T - T_{\infty,1}) + h_2 (T - T_{\infty,2}) = 0$$

where $T = T_{w,1} = T_{w,2}$.

Let us propose a similarity solution of the transient conduction equation

$$\frac{\partial^2 T}{\partial x^2} - \frac{1}{\kappa} \frac{\partial T}{\partial t} = 0 \tag{6.19}$$

(6.20)

as

$$T = \text{ erf } \left(\frac{x}{2\sqrt{\kappa t}} \right) \tag{6.21}$$

Taking derivatives we find[1] [Clarify]

$$\frac{\partial T}{\partial x} = \frac{1}{\sqrt{\pi\kappa t}} \exp\left(-\frac{x^2}{4\kappa t}\right)$$
$$\frac{\partial^2 T}{\partial x^2} = -\frac{x}{2\sqrt{\pi\kappa^3 t^3}} \exp\left(-\frac{x^2}{4\kappa t}\right)$$
$$\frac{\partial T}{\partial t} = -\frac{x}{2\sqrt{\pi\kappa t^3}} \exp\left(-\frac{x^2}{4\kappa t}\right)$$

so that substitution verifies that equation (6.21) is a solution to equation (6.19).

Alternatively

$$T(x,t) = \frac{1}{\sqrt{4\pi\kappa t}} \exp\left(-\frac{x^2}{4\kappa t}\right)$$

In fact all multiples, derivatives and integrals of a solution of Eq. (6.19) are also solutions. They differ in the boundary conditions that they satisfy.

6.4 Green's functions

For bounded domains

`http://people.math.gatech.edu/~xchen/teach/pde/heat/Heat-Green.pdf`

6.5 Duhamel's principle

For inhomogeneous equations in infinite domains

The solution of the ODE

$$\frac{dy}{dt} - ay = g(t), \quad y(0) = x$$

is

$$y(t) = S(x,t) + \int_0^t S(g(s), t-s)ds,$$

where $S(x,t)$ is the solution of

$$\frac{dS}{dt} - aS = 0, \quad S(0) = x$$

[1] The error function is defined to be

$$\text{erf}\,(x) = \frac{2}{\pi}\int_0^x e^{-t^2}\,dt.$$

so that

$$\frac{d}{dx}\text{erf}\,(x) = \frac{2}{\pi}e^{-x^2}.$$

Similarly, the solution of [Clarify]

$$\frac{\partial T}{\partial t} - \kappa \frac{\partial^2 T}{\partial x^2} = g(x,t), \quad T(x,0) = f(x) \tag{6.22}$$

is obtained from the solution $S(x,t)$ of

$$\frac{\partial S}{\partial t} - \kappa \frac{\partial^2 S}{\partial x^2} = 0, \quad S(x,0) = f(x), \tag{6.23}$$

which is

$$S(f,t) = \int_{-\infty}^{\infty} f(y) G(x-y, 2\kappa t)\ dy.$$

where

$$G(x,t) = \frac{1}{\sqrt{4\pi\kappa t}} \exp\left(-\frac{x^2}{4\kappa t}\right)$$

is the Gaussian kernel. The solution of the inhomogeneous equation is then

$$\begin{aligned} T(x,t) &= S(f,t)(x) + \int_0^t S(g(\cdot,s), t-s)\ ds, \\ &= \int_{-\infty}^{\infty} f(y) G(x-y, 2\kappa t)\ dy + \int_0^t g(y,s) G(x-y, t-s)\ dy\ ds. \end{aligned}$$

6.6 Linear diffusion

Let $T = T(x,t)$ and

$$\frac{\partial T}{\partial t} = \alpha \frac{\partial^2 T}{\partial x^2}$$

in $0 \le x \le L$, with the boundary and initial conditions $T(0,t) = T_1$, $T(L,t) = T_2$, and $T(x,0) = f(x)$. The steady state solution is

$$\overline{T}(x) = T_1 + \frac{T_2 - T_1}{L} x.$$

With

$$T'(x,t) = T - \overline{T}$$

we have the same equation

$$\frac{\partial T'}{\partial t} = \alpha \frac{\partial^2 T'}{\partial x^2} \tag{6.24}$$

but with the conditions: $T'(0,t) = 0$, $T'(L,t) = 0$, and $T'(x,0) = f(x) - \overline{T}$.

Following the methodology outlined in Section **??**, we consider the eigenvalue problem

$$\frac{d^2\phi}{dx^2} = \lambda\phi$$

with $\phi(0) = \phi(L) = 0$. The operator is self-adjoint. Its eigenvalues are

$$\lambda_i = -\frac{i^2\pi^2}{L^2},$$

and its orthonormal eigenfunctions are

$$\phi_i(x) = \sqrt{\frac{2}{L}}\ \sin\frac{i\pi x}{L}.$$

Thus we let

$$\theta(x,t) = \sum_{i=1}^{\infty} a_i(t)\phi_i(x),$$

so that

$$\frac{da_j}{dt} = -\alpha\left(\frac{j\pi}{L}\right)^2 a_j,$$

with the solution

$$a_j = C_j \exp\left\{-\alpha\left(\frac{j\pi}{L}\right)^2 t\right\}.$$

Thus

$$T'(x,t) = \sum_{i=1}^{\infty} C_j \exp\left\{-\alpha\left(\frac{j\pi}{L}\right)^2 t\right\}\sqrt{\frac{2}{L}}\ \sin\frac{i\pi x}{L}. \tag{6.25}$$

The solution shows that $T' \to 0$, as $t \to \infty$. Thus $\theta = 0$ is a stable solution of the problem. It must be noted that there has been no need to linearize, since Eq. (6.24) was already linear.

6.7 Nonlinear diffusion

The following diffusion problem with heat generation is considered in [85]

$$\frac{\partial T}{\partial t} = \epsilon\frac{\partial^2 T}{\partial x^2} + f(T),$$

with $-\infty < x < \infty$, $t \geq 0$, and $\epsilon \ll 1$. The initial condition is taken to be

$$T(x,0) = g(x) \tag{6.26}$$

$$= \frac{1}{1+e^{\lambda x}}. \tag{6.27}$$

Consider two time scales, a fast, short one $t_1 = t$, and a slow, long scale $t_2 = \epsilon t$. Thus

$$\frac{\partial}{\partial t} = \frac{\partial}{\partial t_1} + \epsilon\frac{\partial}{\partial t_2}.$$

Assuming an asymptotic expansion of the type

$$T = T_0(x, t_1, t_2) + \epsilon T_1(x, t_1, t_2) + \dots$$

we have a Taylor series expansion

$$f(T) = f(T_0) + \epsilon f'(T_0) + \dots$$

Substituting and collecting terms of $O(\epsilon^0)$, we get

$$\frac{\partial T_0}{\partial t_1} = f(T_0), \tag{6.28}$$

with the solution

$$\int_{1/2}^{T_0} \frac{dr}{f(r)} = t_1 + \theta(x, t_2). \tag{6.29}$$

The lower limit of the integral is simply a convenient value at which $g(x) = 0.5$. Applying the initial condition gives

$$\theta = \int_{1/2}^{g(x)} \frac{dr}{f(r)}.$$

The terms of $O(\epsilon)$ are

$$\frac{\partial T_1}{\partial t_1} = f'(T_0)T_1 + \frac{\partial^2 T_0}{\partial x^2} - \frac{\partial T_0}{\partial t_2} \tag{6.30}$$

Differentiating Eq. 6.29 with respect to x gives

$$\frac{\partial T_0}{\partial x} = f(T_0)\frac{\partial \theta}{\partial x},$$

so that

$$\begin{aligned}\frac{\partial^2 T_0}{\partial x^2} &= f'(T_0)\frac{\partial T_0}{\partial x}\frac{\partial \theta}{\partial x} + f(T_0)\frac{\partial^2 \theta}{\partial x^2} \\ &= f'(T_0)f(T_0)\left(\frac{\partial \theta}{\partial x}\right)^2 + f(T_0)\frac{\partial @2\theta}{\partial x^2}\end{aligned}$$

Also, differentiating with respect to t_2 gives

$$\frac{\partial T_0}{\partial t_2} = f(T_0)\frac{\partial \theta}{\partial t_2}$$

Substituting in Eq. 6.30,

$$\frac{\partial T_1}{\partial t_1} = f'(T_0)T_1 + f(T_0)\left[\frac{\partial^2 \theta}{\partial x^2} - \frac{\partial \theta}{\partial t_2} + f'(T_0)\left(\frac{\partial \theta}{\partial x}\right)^2\right].$$

Since

$$\begin{aligned}\frac{\partial}{\partial t_1}\ln f(T_0) &= \frac{f'(T_0)}{f(T_0)}\frac{\partial T_0}{\partial t_1}\\ &= f'(T_0)\end{aligned}$$

we have

$$\frac{\partial T_1}{\partial t_1} = f'(T_0)T_1 + f(T_0)\left[\frac{\partial^2\theta}{\partial x^2} - \frac{\partial\theta}{\partial t_2} + \frac{\partial}{\partial t_1}\ln f(T_0)\right].$$

The solution is

$$T_1 = \left[A(x,t_2) + t_1\left(\frac{\partial^2\theta}{\partial x^2} - \frac{\partial\theta}{\partial t_2} + \left(\frac{\partial\theta}{\partial x}\right)^2 \ln f(T_0)\right)\right] f(T_0) \tag{6.31}$$

which can be checked by differentiation since

$$\begin{aligned}\frac{\partial T_1}{\partial t_1} &= \left[\frac{\partial^2\theta}{\partial x^2} - \frac{\partial\theta}{\partial t_2} + f'(T_0)\left(\frac{\partial\theta}{\partial x}\right)^2\right] f(T_0)\\ &\quad + \left[A + t_1\left(\frac{\partial^2\theta}{\partial x^2} - \frac{\partial\theta}{\partial t_2}\right) + \left(\frac{\partial\theta}{\partial x}\right)^2 \ln f(T_0)\right] f'(T_0)\frac{\partial T_0}{\partial t_1}\\ &= \left[\frac{\partial^2\theta}{\partial x^2} - \frac{\partial\theta}{\partial t_2} + f'(T_0)\left(\frac{\partial\theta}{\partial x}\right)^2\right] f(T_0) + T_1 f'(T_0).\end{aligned}$$

where Eq. 6.28 has been used.

To suppress the secular term in Eq. 6.31, we take

$$\frac{\partial^2\theta}{\partial x^2} - \frac{\partial\theta}{\partial t_2} + \kappa(x,t_1)\left(\frac{\partial\theta}{\partial x}\right)^2 = 0.$$

where $\kappa = f'(T_0)$. Let

$$w(x,t_2) = e^{\kappa\theta},$$

so that its derivatives are

$$\begin{aligned}\frac{\partial w}{\partial x} &= \kappa e^{\kappa\theta}\frac{\partial\theta}{\partial x}\\ \frac{\partial^2 w}{\partial x^2} &= \kappa^2 e^{\kappa\theta}\left(\frac{\partial\theta}{\partial x}\right)^2 + \kappa e^{\kappa\theta}\frac{\partial^2\theta}{\partial x^2}\\ \frac{\partial w}{\partial t_2} &= \kappa e^{\kappa\theta}\frac{\partial\theta}{\partial t_2}\end{aligned}$$

We find that

$$\begin{aligned}\frac{\partial^2 w}{\partial x^2} - \frac{\partial w}{\partial t_2} &= \kappa e^{\kappa\theta}\left[\frac{\partial^2\theta}{\partial x^2} - \frac{\partial\theta}{\partial t_2} + \kappa\left(\frac{\partial\theta}{\partial x}\right)^2\right]\\ &= 0.\end{aligned}$$

The solution is

$$w = \frac{1}{\sqrt{\pi}} \int_{\infty}^{\infty} R(x + 2r\sqrt{t_2}) e^{-r^2} \, dr, \tag{6.32}$$

where $R(x) = w(x, 0)$. This can be confirmed by finding the derivatives

$$\begin{aligned}
\frac{\partial^2 w}{\partial x^2} &= \frac{1}{\sqrt{\pi}} \int_{\infty}^{\infty} R''(x + 2r\sqrt{t_2}) e^{-r^2} \, dr \\
\frac{\partial w}{\partial t_2} &= \frac{1}{\sqrt{\pi}} \int_{\infty}^{\infty} R'(x + 2r\sqrt{t_2}) \frac{r}{\sqrt{t_2}} e^{-r^2} \, dr \\
&= -\frac{1}{2\sqrt{\pi}} \left[R'(x + 2r\sqrt{t_2}) \Big|_{\infty}^{\infty} - \int_{\infty}^{\infty} R''(x + 2r\sqrt{t_2}) 2\sqrt{t_2} e^{-r^2} \, dr \right] \\
&= \frac{1}{\sqrt{\pi}} \int_{\infty}^{\infty} R''(x + 2r\sqrt{t_2}) e^{-r^2} \, dr
\end{aligned}$$

and substituting. Also,

$$\begin{aligned}
R(x) &= \exp\left[\kappa \theta(x, 0)\right] \\
&= \exp\left[\kappa \int_{1/2}^{g(x)} \frac{dr}{f(r)} \right]
\end{aligned}$$

so that the final (implicit) solution is

$$\int_{1/2}^{T_0} \frac{dr}{f(r)} = t_1 + \frac{1}{\kappa} \ln \left[\frac{1}{\sqrt{\pi}} \int_{\infty}^{\infty} R(x + 2r\sqrt{t_2}) e^{-r^2} \, dr \right]$$

Fisher's equation: As an example, we take $f(T) = T(1 - T)$, so that the integral in Eq. 6.29 is

$$\int_{1/2}^{T_0} \frac{dr}{r(1 - r)} = \ln \frac{T_0}{T_0 - 1}$$

Substituting in the equation, we get

$$\begin{aligned}
T_0 &= \frac{1}{1 + e^{-(t_1 + \theta)}} \\
&= \frac{w}{w + e^{-t_1}}
\end{aligned}$$

Thus

$$w = \frac{T_0 e^{-t_1}}{1 - T_0}$$

and from Eq. 6.27,

$$\begin{aligned}
R(x) &= w(x, 0) \\
&= e^{-\lambda x}
\end{aligned}$$

Substituting in Eq. 6.32 and integrating,

$$w = \exp\left(-\lambda x + \lambda^2 t_2\right)$$

so that

$$T_0 = \frac{1}{1 + \exp\left[x - t(1 + \lambda^2\epsilon)/\lambda\right]}$$

This is a wave that travels with a phase speed of $(1 + \lambda^2\epsilon)/\lambda$.

6.8 Stability by energy method

6.8.1 Linear

As an example consider the same problem as in Section 6.6. The deviation from the steady state is governed by

$$\frac{\partial T'}{\partial t} = \alpha \frac{\partial^2 T'}{\partial x^2}$$

with $T'(0,t) = 0$, $T'(L,t) = 0$.

Define

$$E(t) = \frac{1}{2}\int_0^L T'^2 \, dx$$

so that $E \geq 0$. Also

$$\begin{aligned}
\frac{dE}{dt} &= \int_0^L T' \frac{\partial T'}{\partial t} \, dx \\
&= \alpha \int_0^L T' \frac{\partial^2 T'}{\partial x^2} \, dx \\
&= \alpha \left[\int_0^L T' \frac{\partial T'}{\partial x} \bigg|_0^L - \int_0^L \left(\frac{\partial T'}{\partial x}\right)^2 \, dx \right] \\
&= -\alpha \int_0^L \left(\frac{\partial T'}{\partial x}\right)^2 \, dx
\end{aligned}$$

so that

$$\frac{dE}{dt} \leq 0.$$

Thus $E \to 0$ as $t \to \infty$ whatever the initial conditions.

6.8.2 Nonlinear

Let us now re-do the problem for a bar with temperature-dependent conductivity. Thus

$$\frac{\partial T}{\partial t} = \frac{\partial}{\partial x}\left\{k(T)\frac{\partial T}{\partial x}\right\},$$

with $T(0,t) = T_1$ and $T(L,t) = T_2$. The steady state, $\overline{T}(x)$, is governed by

$$\frac{d}{dx}\left\{k(\overline{T})\frac{d\overline{T}}{dx}\right\} = 0.$$

Let the deviation from the steady state be

$$\theta(x,t) = T(x,t) - \overline{T}(x).$$

Thus

$$\frac{\partial\theta}{\partial t} = \frac{\partial}{\partial x}\left\{k(\theta)\frac{\partial\theta}{\partial x}\right\},$$

where $\theta = \theta(x,t)$, with $\theta(0,t) = \theta(L,t) = 0$. The steady state is $\theta = 0$. Let

$$E(t) = \frac{1}{2}\int_0^L \theta^2\, dx.$$

so that $E \geq 0$. Then

$$\begin{aligned}\frac{dE}{dt} &= \int_0^L \theta\frac{\partial\theta}{\partial t}\, dx \\ &= \int_0^L \theta\frac{\partial}{\partial x}\left\{k(\theta)\frac{\partial\theta}{\partial x}\right\}\, dx \\ &= \theta k(\theta)\frac{\partial\theta}{\partial x}\bigg|_0^L - \int_0^L k(\theta)\left(\frac{\partial\theta}{\partial x}\right)^2\, dx.\end{aligned}$$

Due to boundary conditions the first term on the right is zero, so that $dE/dt \leq 0$. Thus $E \to 0$ as $t \to \infty$.

6.9 Self-similar structures

Consider the large-scale structure shown in Fig. 6.9 in which each line i (indicated by $i = 0, 1, \ldots$) is a conductive bar. The length of each bar is $L_i = L/\beta^i$ and its diameter is $D_i = D/\beta^i$. The beginning is at temperature T_0 and the ambient is T_∞.

The total length of the structure is

$$\begin{aligned}L_T &= L_0 + 2L_1 + 4L_2 + 8L_3 + \ldots \\ &= \ldots\end{aligned}$$

The total volume of the material is

$$\begin{aligned}V_T &= \frac{\pi}{4}\left(D_0^2 L_0 + 2D_1^2 L_1 + 4D_2^2 L_2 + 8D_3^2 L_3 + \ldots\right) \\ &= \ldots\end{aligned}$$

Both of these are finite if $\beta < \beta_c = \ldots$.

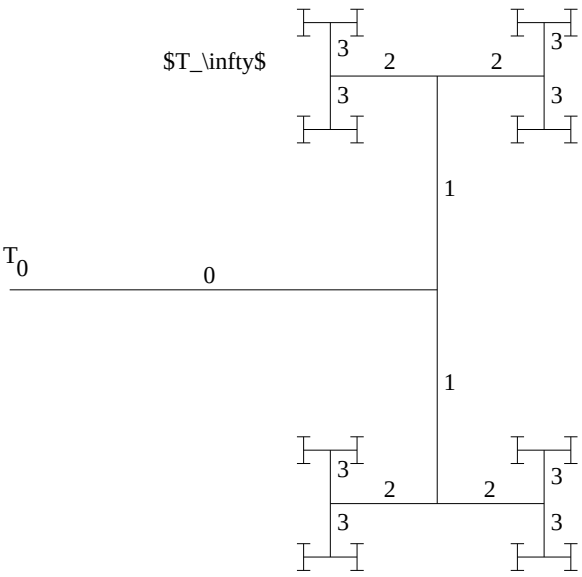

Figure 6.9: Large-scale self-similar structure.

6.10 Non-Cartesian coordinates

Toroidal, bipolar.

6.10.1 Radial cylindrical

$$\rho\Big[\pi(r+dr)^2-\pi r^2\Big]L\ c\ \frac{\partial T}{\partial t}=Q_r(r)-Q_r(r+dr).$$

Since

$$\begin{aligned}\pi(r+dr)^2-\pi r^2&=2\pi r\ dr+\pi\ dr^2\\ Q_r(r+dr)&=Q_r(r)+\frac{\partial Q_r}{\partial r}\ dr+\ldots\\ Q_r(r)&=q_r(r)\ 2\pi rL,\end{aligned}$$

we have

$$\begin{aligned}Q_r(r)-Q_r(r+dr)&=-\frac{\partial Q_r}{\partial r}\ dr\\ &=-\frac{\partial}{\partial r}(q_r\ 2\pi rL)\ dr\end{aligned}$$

so that

$$\rho\big(2\pi r\ dr+\pi\ dr^2\big)L\ c\ \frac{\partial T}{\partial t}=-\frac{\partial}{\partial r}(q_r\ 2\pi rL)\ dr+g\big(2\pi r\ dr+\pi\ dr^2\big)L,$$

which, on dividing by $2\pi r\ dr\ L$ and taking the limit of $dr\to 0$, simplifies to

$$\rho c\frac{\partial T}{\partial t}+\frac{1}{r}\frac{\partial}{\partial r}(rq_r)=0.$$

6.10.2 Radial spherical

Similarly we can show that

$$\rho c \frac{\partial T}{\partial t} + \frac{1}{r^2}\frac{\partial}{\partial r}(r^2 q_r) = 0.$$

6.11 Thermal control

Partial differential equations (PDEs) are an example of infinite-dimensional systems that are very common in thermal applications [2, 117]. *Exact* controllability exists if the function representing the state can be taken from an initial to a final target state, and is *approximate* if it can be taken to a neighborhood of the target [126]. Determination of approximate controllability is usually sufficient for practical purposes.

Consider a system governed by

$$\frac{\partial X}{\partial t} = \mathcal{A}X + \mathcal{B}u, \tag{6.33}$$

with homogeneous boundary and suitable initial conditions, where $\mathcal{A}$ is a bounded semi-group operator [2], and $\mathcal{B}$ is a another linear operator. The state $X(\xi, t)$ is a function of spatial coordinates ξ and time t. If $\mathcal{A}$ is self-adjoint, then it has real eigenvalues and a complete orthonormal set of eigenfunctions $\phi_m(\xi)$, with $m = 0, 1, 2\ldots$, which forms a complete spatial basis for X. It is known [117] that the system is approximately state controllable if and only if all the inner products

$$\langle \mathcal{B}, \phi_m \rangle \neq 0. \tag{6.34}$$

The lumped approximation in this chapter, valid for $Bi \ll 1$, is frequently not good enough for thermal systems, and the spatial variation of the temperature must be taken into account. The system is then described by PDEs that represent a formidable challenge for control analysis. The simplest examples occur when only one spatial dimension is present.

Fig. 6.10 shows a fin of length L with convection to the surroundings [4]. It is thin and long enough such that the transverse temperature distribution may be neglected. The temperature field is governed by

$$\frac{\partial T}{\partial t} = \alpha \frac{\partial^2 T}{\partial \xi^2} - \zeta(T - T_\infty), \tag{6.35}$$

where $T(\xi, t)$ is the temperature distribution that represents the state of the system, T_∞ is the temperature of the surroundings, t is time, and ξ is the longitudinal coordinate measured from one end. The thermal diffusivity is α, and $\zeta = hP/\rho c A_c$ where h is the convective heat transfer coefficient, A_c is the constant cross-sectional area of the bar, P is the perimeter of the cross section, ρ is the density, and c is the specific heat. For simplicity it will be assumed that ζ is independent of ξ. The end $\xi = 0$ will be assumed to be adiabatic so that $(\partial T/\partial \xi)(0, t) = 0$.

Since a linear system that is controllable can be taken from any state to any other, we can arbitrarily assume the fin to be initially at a uniform temperature. There are two ways in which the temperature distribution on the bar can be controlled: in *distributed* control[2] the surrounding temperature T_∞ is the control input and in *boundary* control it is the temperature of the other end $T(L, t)$ of the fin.

[2]This term is also used in other senses in control theory.

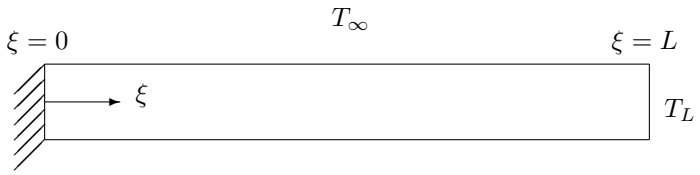

Figure 6.10: One-dimensional fin with convection.

(a) *Distributed control:* The boundary temperature $T(L,t) = T_L$ is fixed. Using it as a reference temperature and defining $\theta = T - T_L$, Eq. (6.35) becomes,

$$\frac{\partial \theta}{\partial t} = \alpha \frac{\partial^2 \theta}{\partial \xi^2} - \zeta\theta + \zeta\theta_\infty(t) \tag{6.36}$$

with the homogeneous boundary and initial conditions $(\partial\theta/\partial\xi)(0,t) = 0$, $\theta(L,t) = 0$, and $\theta(\xi,0) = 0$.

The operators in Eq. (6.33) are $\mathcal{A} = \alpha\partial^2/\partial\xi^2 - \zeta$, $\mathcal{B} = \zeta$, and $u = \theta_\infty$. $\mathcal{A}$ is a self-adjoint operator with the eigenvalues and eigenfunctions

$$\beta_m = -\frac{(2m+1)^2\pi^2}{4L^2} - \zeta,$$
$$\phi_m = \sqrt{\frac{2}{L}}\ \cos\frac{(2m+1)\pi\xi}{2L},$$

respectively. Inequality (6.34) is satisfied for all m, so the system is indeed state controllable. It can be shown that the same problem can also be analyzed using a finite-difference approximation [5].

(b) *Boundary control:* Using the constant outside temperature T_∞ as reference and defining $\theta = T - T_\infty$, Eq. (6.35) becomes

$$\frac{\partial \theta}{\partial t} = \alpha \frac{\partial^2 \theta}{\partial \xi^2} - \zeta\theta, \tag{6.37}$$

with the initial and boundary conditions $(\partial\theta/\partial\xi)(0,t) = 0$, $\theta(L,t) = T_L(t) - T_\infty$, and $\theta(\xi,0) = 0$.

To enable a finite-difference approximation [5], the domain $[0,L]$ is divided into n equal parts of size $\Delta\xi$, so that Eq. (6.37) becomes

$$\frac{d\theta_i}{dt} = \sigma\theta_{i-1} - (2\sigma+\zeta)\theta_i + \sigma\theta_{i-1},$$

where $\sigma = \alpha/\Delta\xi^2$. The nodes are $i = 1, 2, \ldots, n+1$, where $i = 1$ is at the left and $i = n+1$ at the right end of the fin in Fig. 6.10. With this Eq. (6.37) can be discretized to take the form of Eq. (4.6), where x is the vector of unknown θ_i. Thus we find

$$A = \begin{bmatrix} -(2\sigma+\zeta) & 2\sigma & 0 & \cdots & 0 \\ \sigma & -(2\sigma+\zeta) & \sigma & & \vdots \\ 0 & \ddots & \ddots & \ddots & \\ \vdots & & & & \sigma \\ 0 & \cdots & 0 & \sigma & -(2\sigma+\zeta) \end{bmatrix} \in \mathbb{R}^{n\times n},$$

$$B = [0, \cdots, \sigma]^T \in \mathbb{R}^n.$$

The boundary conditions have been applied to make A non-singular: at the left end the fin is adiabatic, and at the right end θ_{n+1} is the control input u.

The controllability matrix M is

$$M = \begin{bmatrix} 0 & \cdots & \cdots & 0 & \sigma^n \\ 0 & \cdots & 0 & \sigma^{n-1} & \cdots \\ \vdots & \vdots & \vdots & \vdots & \vdots \\ 0 & 0 & \sigma^3 & \cdots & \cdots \\ 0 & \sigma^2 & -2\sigma^2(2\sigma+\zeta) & \cdots & \cdots \\ \sigma & -\sigma(2\sigma+\zeta) & \sigma^3+\sigma(2\sigma+\zeta)^2 & \cdots & \cdots \end{bmatrix}$$

The rank of M is n, indicating that the state of the system is also boundary controllable.

6.12 Multiple scales

Solve

$$\frac{\partial T_1}{\partial t} = \alpha \frac{\partial^2 (T_1 - T_2)}{\partial x^2}$$
$$\frac{\partial T_2}{\partial t} = R\alpha \frac{\partial^2 (T_2 - T_1)}{\partial x^2}$$

where $\epsilon \ll 1$, and with a step change in temperature at one end. Let

$$t = t_0 + \epsilon t_1$$

6.13 Stefan moving boundary problems

[44]

The two phases, indicated by subscripts 1 and 2, are separated by an interface at $x = X(t)$. In each phase, the conduction equation is

$$\frac{\partial^2 T_1}{\partial x^2} - \frac{1}{\kappa_1}\frac{\partial T_1}{\partial t} = 0 \tag{6.38}$$
$$\frac{\partial^2 T_2}{\partial x^2} - \frac{1}{\kappa_2}\frac{\partial T_2}{\partial t} = 0 \tag{6.39}$$
$$\tag{6.40}$$

At the interface the temperature should be continuous, so that

$$T_1(X,t) = T_2(X,t) \tag{6.41}$$

Furthermore the difference in heat rate into the interface provides the energy required for phase change. Thus

$$k_1 \frac{\partial T_1}{\partial x} - k_2 \frac{\partial T_2}{\partial x} = L\rho \frac{dX}{dt} \tag{6.42}$$

6.13.1 Neumann's solution

The material is initially liquid at $T = T_0$. The temperature at the $x = 0$ end is reduced to zero for $t > 0$. Thus

$$T_1 = 0 \quad \text{at} \quad x = 0 \tag{6.43}$$

$$T_2 \to T_0 \quad \text{as} \quad x \to \infty \tag{6.44}$$

Assume $T_1(x, t)$ to be

$$T_1 = A \text{ erf } \frac{x}{2\sqrt{\kappa_1 t}}$$

so that it satisfies equations (6.38) and (6.43). Similarly

$$T_1 = A \text{ erf } \frac{x}{2\sqrt{\kappa_1 t}}$$
$$T_2 = T_0 - B \text{ erf } \frac{x}{2\sqrt{\kappa_2 t}}$$

satisfies equation (6.39) and (6.44). The, condition (6.41) requires that

$$A \text{ erf } \frac{x}{2\sqrt{\kappa_1 t}} = T_0 - B \text{ erf } \frac{x}{2\sqrt{\kappa_2 t}} = T_1$$

This shows that

$$X = 2\lambda\sqrt{\kappa_1 t}$$

where λ is a constant. Using the remaining condition (6.42), we get

$$k_1 A e^{-\lambda^2} - k_2 B \sqrt{\frac{\kappa_1}{\kappa_2}} e^{-\kappa_1 \lambda^2/\kappa_2} = \lambda L \kappa_1 \rho \sqrt{\pi}$$

This can be written as

$$\frac{e^{-\lambda^2}}{\text{erf } \lambda} - \frac{k_2 \sqrt{\kappa_1^2}(T_0 - T_1) e^{-\kappa_2 \lambda^2/\kappa_2}}{k_1 \sqrt{\kappa_2} T_1 \text{ erfc}(\lambda\sqrt{\kappa_1/\kappa_2})} = \frac{\lambda L \sqrt{\pi}}{c_1 T_1 s}$$

The temperatures are

$$T_1 = \frac{T_1}{\text{erf } \lambda} \text{ erf } (\frac{x}{2\sqrt{\kappa_1 t}})$$
$$T_2 = T_0 - \frac{T_0 - T_1}{\text{erfc}(\lambda\sqrt{\kappa_1/\kappa_2})} \text{ erfc}(\frac{x}{2\sqrt{\kappa_2 t}})$$

6.13.2 Goodman's integral

Bibliography

J. Crank, *Free and Moving Boundary Problems,* Clarendon Press, Oxford, U.K., 1984.

B. Straughan, *The Energy Method, Stability, and Nonlinear Convection,* 2nd Ed., Springer, 2003.

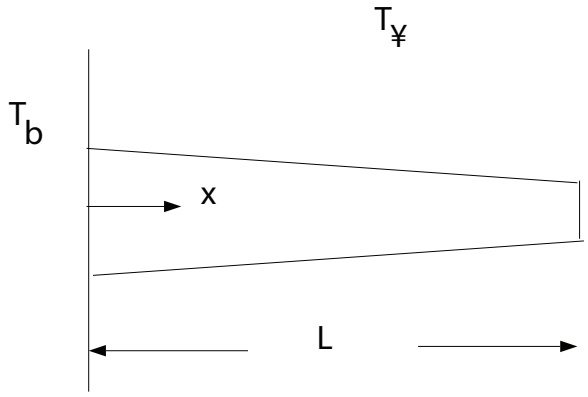

Figure 6.11: Longitudinal fin of concave parabolic profile.

Problems

1. From the governing equation for one-dimensional conduction

$$\frac{d}{dx}\left[k(x,T)\ \frac{dT}{dx}\right] = 0,$$

with boundary conditions

$$T(0) = \overline{T} + \frac{\Delta T}{2},$$
$$T(L) = \overline{T} - \frac{\Delta T}{2}.$$

show that the magnitude of the heat rate is independent of the sign of ΔT if we can write $k(x,T) = A(x)\ \lambda(T)$.

2. Consider a rectangular fin with convection, radiation and Dirichlet boundary conditions. Calculate numerically the evolution of an initial temperature distribution at different instants of time. Graph the results for several values of the parameters.

3. Consider a longitudinal fin of concave parabolic profile as shown in the figure, where $\delta = [1-(x/L)]^2\delta_b$. δ_b is the thickness of the fin at the base. Assume that the base temperature is known. Neglect convection from the thin sides. Find (a) the temperature distribution in the fin, and (b) the heat flow at the base of the fin. Optimize the fin assuming the fin volume to be constant and maximizing the heat rate at the base. Find (c) the optimum base thickness δ_b, and (d) the optimum fin height L.

4. Consider a longitudinal fin of concave parabolic profile as shown in the figure, where $\delta = [1-(x/L)]^2\delta_b$. δ_b is the thickness of the fin at the base. Assume that the base temperature is known. Neglect convection from the thin sides. Find (a) the temperature distribution in the fin, and (b) the heat flow at the base of the fin. Optimize the fin assuming the fin volume to be constant and maximizing the heat rate at the base. Find (c) the optimum base thickness δ_b, and (d) the optimum fin height L.

5. Analyze an annular fin with a prescribed base temperature and adiabatic tip. Determine its fin efficiency and plot.

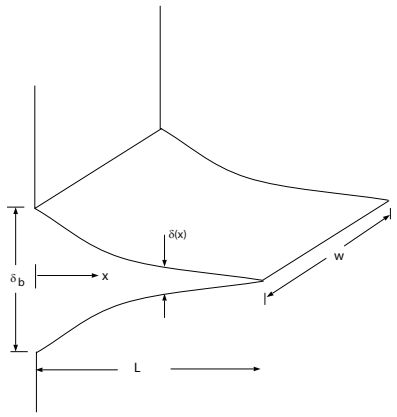

Figure 6.12: Longitudinal fin of concave parabolic profile.

Chapter 7

Convection in ducts (one-dimensional)

In this chapter we will consider heat transfer in pipe flows shown in Fig. 7.1. We will take a one-dimensional approach and neglect transverse variations in the velocity and temperature. In addition, for simplicity, we will assume that fluid properties are constant and that the area of the pipe is also constant.

7.1 Balance equations

7.1.1 Mass

For a control volume

$$\rho \int_{CV} V \, dA = \text{constant}.$$

Consider an elemental control volume as shown in Fig. 7.2. The mass fluxes in and out, m^- and m^+ respectively, are related by

$$m^+ = m^- + \frac{\partial m}{\partial s} \, ds.$$

For a fluid of constant density, there is no accumulation of mass within an elemental control volume, $\partial m/\partial s = 0$, and so the mass flow rate into and out of the control volume must be the same, i.e. $m^- = m^+ = m$. If V is uniform across the cross-section, then $m = \rho \, V A$. If not, then $\bar{V} = m/(\rho A)$ is the definition of the mean velocity; thus the mean velocity of the fluid, $\bar{V}$, is also constant.

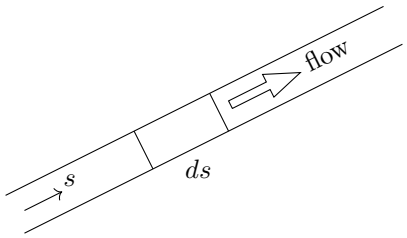

Figure 7.1: Flow in an inclined duct with a fluid element of length ds.

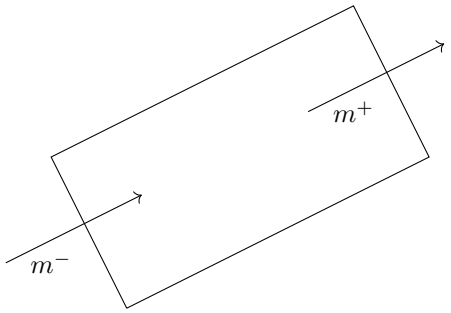

Figure 7.2: Mass balance in a fluid element.

7.1.2 Momentum

The total force on an element of length ds, shown in Fig. 7.3, in the positive s direction is $f = f_v + f_p + f_g$, where f_v = the viscous force, f_p = the pressure force, and f_g = the component of the gravity force. We can write

$$\begin{aligned} f_v &= -\tau_w \ P \ ds, \\ f_p &= -A\frac{\partial p}{\partial s}ds, \\ f_g &= -\rho A \ ds \ \tilde{g}, \end{aligned}$$

where τ_w is the wall shear stress, p is the pressure in the fluid, and $\tilde{g}$ is the component of gravity along the pipe axis in the negative s direction.

Since the mass of the element is $\rho A \ ds$, we can write the momentum equation as

$$\rho A \ ds \ \frac{dV}{dt} = f_v + f_p + f_g,$$

from which we get

$$\frac{dV}{dt} + \frac{\tau_w P}{\rho A} + \tilde{g} = -\frac{1}{\rho}\frac{\partial p}{\partial s}.$$

Integrating over the length L of a pipe and then dividing by L, we have

$$\frac{dV}{dt} + \frac{\tau_w P}{\rho A} + \tilde{g} = -\frac{p_2 - p_1}{\rho L},$$

where p_1 and p_2 are the pressures at the inlet and outlet respectively.

In the steady state, there is no acceleration and $dV/dt = 0$. The pressure drop is then given by

$$p_1 - p_2 = \frac{\tau_w P L}{A} + \tilde{g}\rho L.$$

The wall shear stress τ_w is estimated below for laminar and turbulent flows. Some assumptions must be made to enable that. It is impossible to determine the viscous force f_v through a one-dimensional analysis, since it is the velocity profile in the duct that is responsible for the shear stress at the wall.

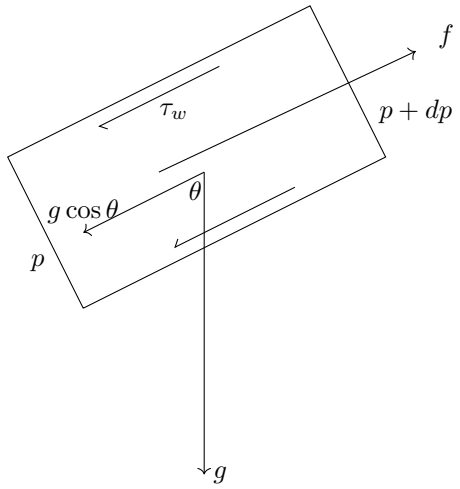

Figure 7.3: Forces on a fluid element; p is the pressure, g is gravity and $\tilde{g}$ is its component in the flow direction, τ is wall shear stress.

Frictional force

For fully developed flow τ_w is a function of V. It depends on the velocity profile and acts in a direction opposite to V. For empirical correlations the expression

$$\tau_w = \frac{f}{4}\ \frac{1}{2}\rho|V|V$$

is used. Here f is the Darcy-Weisbach friction factor[1]. Thus for a horizontal pipe in the steady state

$$\begin{aligned} p_1 - p_2 &= f\ \frac{L}{4A/P}\ \frac{1}{2}\rho V^2, \\ &= f\ \frac{L}{D}\ \frac{1}{2}\rho|V|V, \end{aligned}$$

which is commonly used to calculate pressure drops in pipe flow. For non-circular ducts one can use the the hydraulic diameter defined by $4A/P$.

Laminar

The fully developed laminar velocity profile in a circular duct is given by the Poiseuille flow result

$$V_s(r) = V_m\left(1 - \frac{4r^2}{D^2}\right),$$

where V_s is the local velocity in the axial direction, r is the radial coordinate, V_m is the maximum velocity at the centerline, and D is the diameter of the duct. The mean velocity is given by

$$\bar{V} = \frac{4}{\pi D^2}\int_0^{D/2} V_s(r)\ 2\pi r\ dr.$$

[1]Sometimes, confusingly, the Fanning friction factor, which is one-fourth the Darcy-Weisbach value, is used in the literature.

Substituting the velocity profile, we get

$$\bar{V} = \frac{V_m}{2}$$

The shear stress at the wall τ_w is given by

$$\begin{aligned}\tau_w &= -\mu \frac{\partial V_s}{\partial r}\bigg|_{r=D/2}, \\ &= \mu V_m \frac{4}{D}, \\ &= \frac{8\mu\bar{V}}{D}.\end{aligned}$$

The wall shear stress is linear relationship

$$\tau_w = \alpha\bar{V}, \tag{7.1}$$

where

$$\alpha = \frac{8\mu}{D},$$

which is equivalent to

$$f = \frac{64}{Re},$$

where the Reynolds number is $Re = |V|D/\nu$.

For laminar flow then, we can assume a linear relationship between the wall shear stress and the mean fluid velocity. Even if we do not exactly have Poiseuille flow, the proportionality constant given by it gives an order of magnitude value.

Turbulent

For turbulent flow empirical correlations are usually used. A couple of these are the Blasius equation for smooth pipes

$$f = \frac{0.3164}{Re^{1/4}},$$

and the Colebrook equation for rough pipes

$$\frac{1}{f^{1/2}} = -2.0\ \log\left(\frac{e/D_h}{3.7} + \frac{2.51}{Re\ f^{1/2}}\right),$$

where e is the roughness at the wall. There are many other similar expressions.

Example 7.1

Consider a long, thin pipe with pressures p_1 and p_2 ate either end. For $t \leq 0$, $p_1 - p_2 = 0$ and there is no flow. For $t > 0$, $p_1 - p_2$ is a nonzero constant. Find the resulting time-dependent flow. Make the assumption that the axial velocity is only a function of radial position and time.

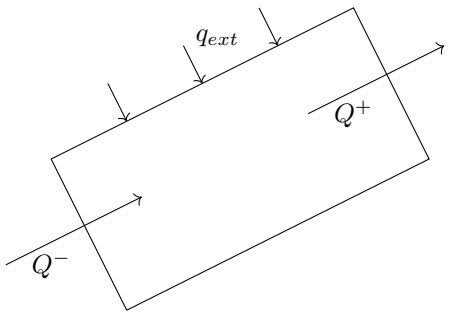

Figure 7.4: Energy balance in a fluid element.

Gravity force

Buoyancy is important in natural convection where the density change due to temperature has to be taken into account. In Fig. 7.3 the local component of the acceleration due to gravity along a pipe can be written as

$$\begin{aligned} \tilde{g}(s) &= g\cos\theta, \\ &= g\frac{dz}{ds}, \end{aligned} \tag{7.2}$$

where g is the usual acceleration in the vertical direction, $\tilde{g}$ is its component in the negative s direction, and dz is the difference in height at the two ends of the element, with z being measured upwards.

7.1.3 Energy

Conservation of energy for an element of width ds in Fig. 7.4 gives

$$\rho Ac\ ds\ \frac{\partial T}{\partial t} = Q^- - Q^+ + q_{ext}\ ds,$$

where q_{ext} is the external heat input per unit length. A Taylor series expansion of $Q(s)$ gives

$$Q^+ = Q^- + \frac{\partial Q}{\partial s}\ ds + \ldots$$

so that

$$\rho Ac\ \frac{\partial T}{\partial t} = -\frac{\partial Q}{\partial s} + q_{ext}.$$

The heat rate is

$$Q = \rho AVcT - kA\frac{\partial T}{\partial s}, \tag{7.3}$$

where the first and second terms on the right are due to the advective and conductive transports respectively. From this point on the conductive term will be neglected except in Section 7.6.

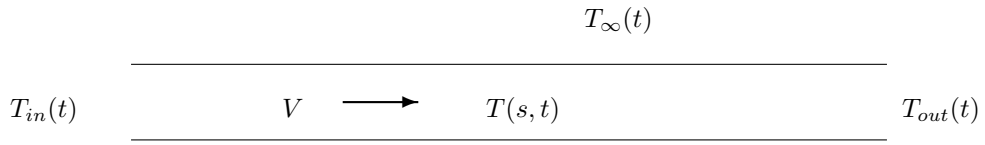

Figure 7.5: Fluid duct with heat loss.

Since $\rho AV = m$ is constant, the energy equation is thus

$$\frac{\partial T}{\partial t} + V\frac{\partial T}{\partial s} = \frac{q_{ext}}{\rho A c}.$$

There are two different types of external heating to consider: known heat rate and convective heat exchange with exterior.

7.2 Validity of one-dimensional approximation

Neglecting axial conduction, the mass, momentum and energy balance equations are

$$\begin{aligned} m &= \text{constant}, \\ \frac{dV}{dt} + \frac{\tau_w P}{\rho A} + \tilde{g} &= -\frac{1}{\rho}\frac{\partial p}{\partial s}, \\ \frac{\partial T}{\partial t} + V\frac{\partial T}{\partial s} &= \frac{q_{ext}}{\rho A c}, \end{aligned}$$

where

$$\tau_w \sim \begin{cases} V & \text{laminar} \\ V|V| & \text{turbulent} \end{cases}$$

7.2.1 No entrance length

It is shown in Section 9.2.1 that for high Reynolds numbers flows there is a small entrance length; this length will be neglected here.

7.2.2 No axial conduction

Conduction heat transfer will be neglected compared to advection. The effect of small axial conduction is analyzed below. There is a small boundary layer near the outlet of order α/V which will be neglected. As a result, the energy equation is first-order in space and can only satisfy one boundary condition which is the temperature at the entrance.

7.3 Forced convection in ducts

Consider the duct that is schematically shown in Fig. 7.5. The inlet temperature is $T_{in}(t)$, and the outlet temperature is $T_{out}(t)$, and the fluid velocity is V. The duct is subject to heat loss through its surface of the form $UP\,(T - T_\infty)$ per unit length, where the local fluid temperature is $T(s,t)$ and the ambient temperature is $T_\infty(t)$. U is the overall heat transfer coefficient and P the cross-sectional perimeter of the duct.

We assume that the flow is one-dimensional, and neglect axial conduction through the fluid and the duct. Using the same variables to represent non-dimensional quantities, the governing non-dimensional equation is

$$\frac{\partial T^*}{\partial t^*} + \frac{\partial T^*}{\partial x^*} + HT^* = 0$$

where the nondimensional variables are

$$x^* = \frac{s}{L}, \quad t^* = \frac{tV}{L}, \quad T^* = \frac{T - \bar{T}_\infty}{\Delta T}$$

The characteristic time is the time taken to traverse the length of the duct, i.e. the residence time. The ambient temperature is

$$T_\infty(t) = \bar{T}_\infty + \widetilde{T}_\infty(t)$$

where the time-averaged and fluctuating parts have been separated. Notice that the nondimensional mean ambient temperature is, by definition, zero. The characteristic temperature difference ΔT will be chosen later. The parameter $\gamma = UPL/\rho AVc$ represents the heat loss to the ambient.

7.3.1 Steady state

The solution of the equation

$$\frac{dT^*}{dx^*} + H(T^* - 1) = 0$$

with boundary condition $T^*(0) = 0$ is

$$T^*(x^*) = 1 - e^{-Hx^*}$$

7.3.2 Unsteady dynamics

The general solution of this equation is

$$T(s,t) = \left[f(s-t) + \gamma \int_0^t e^{Ht'} \widetilde{T}_\infty(t')\, dt' \right] e^{-Ht} \tag{7.4}$$

The boundary conditions $T(0,t) = T_{in}(t)$ and $T(s,0) = T_0(s)$ are shown in Fig. 7.6. The solution becomes

$$T(s,t) = \begin{cases} T_{in}(t-s)e^{-Hs} + He^{-Ht} \int_{t-s}^t e^{Ht'} \widetilde{T}_\infty(t')\, dt' & \text{for } t \geq s \\ T_0(s-t)e^{-Ht} + He^{-Ht} \int_0^t e^{Ht'} \widetilde{T}_\infty(t')\, dt' & \text{for } t < s \end{cases} \tag{7.5}$$

The $t < s$ part of the solution is applicable to the brief, transient period of time in which the fluid at time $t = 0$ has still not left the duct. The later $t > s$ part depends on the temperature of the fluid entering at $s = 0$. The temperature, $T_{out}(t)$, at the outlet section, $s = 1$, is given by

$$T_{out}(t) = \begin{cases} T_{in}(t-1)e^{-H} + He^{-Ht} \int_{t-1}^t e^{Ht'} \widetilde{T}_\infty(t')\, dt' & \text{for} \quad t \geq 1 \\ T_0(1-t)e^{-Ht} + He^{-Ht} \int_0^t e^{Ht'} \widetilde{T}_\infty(t')\, dt' & \text{for} \quad t < 1 \end{cases} \tag{7.6}$$

It can be observed that, after an initial transient, the inlet and outlet temperatures are related by a unit delay. The outlet temperature is also affected by the heat loss parameter, γ, and the ambient temperature fluctuation, $\widetilde{T}_\infty$. The following are some special cases of equation (7.6).

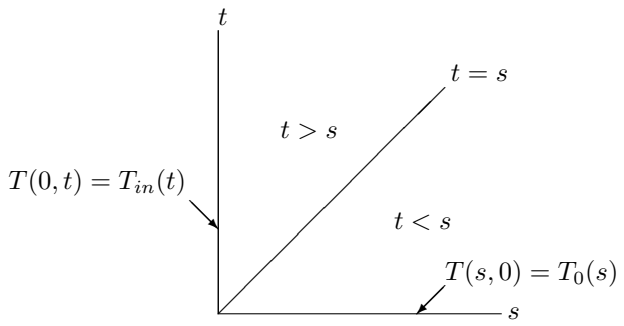

Figure 7.6: Solution in s-t space.

7.3.3 Perfectly insulated duct

If $H = 0$ the outlet temperature simplifies to

$$T_{out}(t) = \begin{cases} T_{in}(t-1) & \text{for } t \geq 1 \\ T_0(1-t) & \text{for } t < 1 \end{cases}$$

The outlet temperature is the same as the inlet temperature, but at a previous instant in time.

7.3.4 Constant ambient temperature

For this $\widetilde{T}_\infty = 0$, and equation (7.6) becomes

$$T_{out}(t) = \begin{cases} T_{in}(t-1)e^{-H} & \text{for } t \geq 1 \\ T_0(1-t)e^{-Ht} & \text{for } t < 1 \end{cases}$$

This is similar to the above, but with an exponential drop due to heat transfer.

7.3.5 Periodic inlet and ambient temperature

We take

$$T_{in}(t) = \bar{T}_{in} + \widehat{T}_{in} \sin \omega t \tag{7.7}$$

$$\widetilde{T}_\infty(t) = \widehat{T}_\infty \sin \Omega t \tag{7.8}$$

so that equation (7.6) becomes

$$T_{out}(t) = \begin{cases} \left[\bar{T}_{in} + \widehat{T}_{in} \sin \omega(t-1)\right] e^{-H} + \widehat{T}_\infty H \sqrt{\frac{-2e^{-H}\cos 1 + e^{-2H}}{H^2+\Omega^2}} \sin(\Omega t + \phi) & \text{for } t \geq 1 \\ T_0(1-t)e^{-Ht} + \frac{H}{H^2+\Omega^2}\widehat{T}_\infty \sqrt{H^2+\Omega^2} \sin(\Omega t + \phi') & \text{for } t < 1 \end{cases}$$

where

$$\tan \phi = -\frac{H(1 - e^{-H}\cos 1) + e^{-H}\Omega \sin 1}{\Omega(1 - e^{-H}\cos 1) - He^{-H}\sin 1}$$

$$\tan \phi' = -\frac{\Omega}{H}$$

The outlet temperature has frequencies which come from oscillations in the inlet as well as the ambient temperatures. A properly-designed control system that senses the outlet temperature must take

the frequency dependence of its amplitude and phase into account. There are several complexities that must be considered in practical applications to heating or cooling networks, some of which are analyzed below.

7.3.6 Long time behavior

Consider the flow in a single duct of finite length with a constant driving pressure drop. The governing equation for the flow velocity is equation (**??**). The flow velocity in the steady state is a solution of

$$T(\bar{V})\bar{V} = \beta\ \Delta p \tag{7.9}$$

where Δp and $\bar{V}$ are both of the same sign, say nonnegative. We can show that under certain conditions the steady state is globally stable. Writing $V = \bar{V} + V'$, equation (**??**) becomes

$$\frac{dV'}{dt} + T(\bar{V} + V')(\bar{V} + V') = \beta\ \Delta p$$

Subtracting equation (7.9), we get

$$\frac{dV'}{dt} = -T(\bar{V} + V')(\bar{V} + V') + T(\bar{V})(\bar{V})$$

Defining

$$E = \frac{1}{2}V'^2$$

so that $E \geq 0$, we find that

$$\begin{aligned}\frac{dE}{dt} &= V'\frac{dV'}{dt} \\ &= -V'\left[T(\bar{V} + V')(\bar{V} + V') - T(\bar{V})\bar{V}\right] \\ &= -V'\bar{V}\left[T(\bar{V} + V') - T(\bar{V})\right] - V'^2 T(\bar{V} + V')\end{aligned}$$

If we assume that $T(V)$ is a non-decreasing function of V, we see that

$$V'\bar{V}\left[T(\bar{V} + V') - T(\bar{V})\right] \geq 0 \tag{7.10}$$

regardless of the sign of either V' or $\bar{V}$, so that

$$\frac{dE}{dt} \leq 0$$

Thus, $E(V)$ is a Lyapunov function, and $V = \bar{V}$ is globally stable to all perturbations.

7.3.7 Effect of wall

The governing equations are

$$\rho A c\frac{\partial T}{\partial t} + \rho V A c\frac{\partial T}{\partial x} - kA\frac{\partial^2 T}{\partial x^2} + h_i P_i(T - T_\infty) = 0$$

$$\rho_w A_w c_w \frac{\partial T_w}{\partial t} - k_w A_w \frac{\partial^2 T_w}{\partial x^2} + h_i P_i(T_w - T) + h_o P_o(T_w - T_\infty) = 0$$

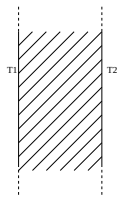

Figure 7.7: Effect of wall.

Nondimensionalize, using

$$x^* = \frac{x}{L}, \quad t^* = \frac{tV}{L}, \quad T^* = \frac{T - T_\infty}{T_i - T_\infty}, \quad T_w^* = \frac{T_w - T_\infty}{T_i - T_\infty}$$

we get

$$\frac{\partial T^*}{\partial t^*} + \frac{\partial T^*}{\partial x^*} - \lambda \frac{\partial^2 T^*}{\partial x^{*2}} + H_{in}(T^* - T_w^*) = 0$$
$$\frac{\partial T_w^*}{\partial t^*} - \lambda_w \frac{\partial^2 T_w^*}{\partial x^{*2}} + H_{in}(T_w^* - T^*) + H_{out} T_w^* = 0$$

where

$$\lambda_w = \frac{k_w}{\rho_w V A_w c_w L}, \quad H_{in} = \frac{h_{in} P_{in} L}{\rho_w A_w c_w V}, \quad H_{out} = \frac{h_{out} P_{out} L}{\rho_w A_w c_w V}$$

In the steady state and with no axial conduction in the fluid

$$\frac{dT^*}{dx^*} + H_{in}(T^* - T_w^*) = 0,$$
$$-\lambda_w \frac{d^2 T_w^*}{dx^{*2}} + H_{in}(T_w^* - T^*) + H_{out} T_w^* = 0$$

If we assume $\lambda_w = 0$ also, we get

$$T_w^* = \frac{H_{in}}{H_{in} + H_{out}} T^*$$

The governing equation is

$$\frac{dT^*}{dx^*} + H_w T^* = 0$$

where

$$H_w = \frac{H_{in}^w H_{out}^w}{H_{in}^w + H_{out}^w}.$$

Example 7.2

Find the temperature distribution along the finned heat exchanger with two tubes shown in Fig. 7.8. The over-tube flow is normal to the plane of the tubes.

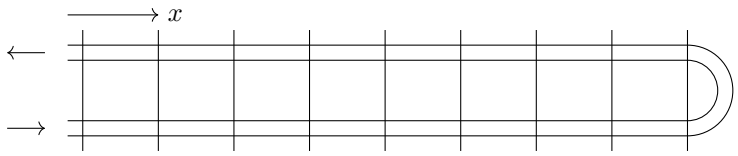

Figure 7.8: Finned heat exchanger with two tubes

Assumptions: One dimensional, steady state, constant properties, constant U, effect of conduction through fin uniform along tubes.

Variables: $T_1(x)$ and $T_2(x)$ are the in-tube temperatures in the lower and upper tubes respectively, m is the in-tube mass flow rate, c is the in-tube fluid specific heat, x is the coordinate measured from the entrance and exit plane, L is the length from left to right of each tube, U is the overall heat transfer coefficient between the in-tube and over-tube fluids, P is the perimeter of the tubes, T_∞ is the temperature of the over-tube fluid, P_f is the perimeter of a section of a fin, and R is the thermal resistance between $T_1(x)$ and $T_2(x)$.

Heat balance gives

$$\begin{aligned} mc\frac{dT_1}{dx} + UP(T_1 - T_\infty) &= \frac{P_f}{R}(T_2 - T_1), \\ -mc\frac{dT_2}{dx} + UP(T_2 - T_\infty) &= \frac{P_f}{R}(T_1 - T_2), \end{aligned}$$

With

$$T_1^* = \frac{T_1 - T_\infty}{T_{in} - T_\infty}; \quad T_2^* = \frac{T_2 - T_\infty}{T_{in} - T_\infty}; \quad x^* = \frac{x}{L},$$

we have

$$\begin{aligned} \frac{dT_1^*}{dx^*} + HT_1^* &= \epsilon(T_2^* - T_1^*), \\ -\frac{dT_2^*}{dx^*} + HT_2^* &= \epsilon(T_1^* - T_2^*), \end{aligned}$$

where

$$H = \frac{UPL}{mc}; \quad \epsilon = \frac{P_f L}{mcR}.$$

Adding and subtracting give

$$\begin{aligned} \frac{d}{dx}(T_1^* - T_2^*) &= -H(T_1^* + T_2^*), \\ \frac{d}{dx}(T_1^* + T_2^*) &= -H(T_1^* - T_2^*) + 2\epsilon(T_2^* - T_1^*), \\ &= -(H + 2\epsilon)(T_1^* - T_2^*), \end{aligned}$$

respectively. Differentiating the first

$$\begin{aligned} \frac{d^2}{dx^{*2}}(T_1^* - T_2^*) &= -H\frac{d}{dx^*}(T_1^* + T_2^*) \\ &= -H\big[H + 2\epsilon\big](T_1^* - T_2^*) \quad \text{using the second.} \end{aligned}$$

The solution is

$$T_1^* - T_2^* = Ae^{rx} + Be^{-rx},$$

where $r^2 = H(H + 2\epsilon)$. Also

$$\begin{aligned} T_1^* + T_2^* &= -\frac{1}{H}\frac{d}{dx^*}(T_1^* - T_2^*), \\ &= -\frac{r}{H}\big[Ae^{rx} - Be^{-rx}\big]. \end{aligned}$$

The sum and difference give

$$T_1^* = \frac{1}{2}(1 - \frac{r}{H})\big[Ae^{rx} - Be^{-rx}\big],$$
$$T_2^* = -\frac{1}{2}(1 + \frac{r}{H})\big[Ae^{rx} - Be^{-rx}\big].$$

At $x = L$, $T_1^* = T_2^*$, so that

$$Ae^{rL} + Be^{-rL} = 0.$$

Also, at $x = 0$, $T_1^* = 1$, from which

$$\frac{1}{2}(1 - \frac{r}{H})\big[A - B\big] = 1.$$

Thus

$$A = \frac{2}{(1 - r/H)(1 + e^{2rL})},$$
$$B = -\frac{2e^{2rL}}{(1 - r/H)(1 + e^{2rL})}.$$

Limiting behavior

If $R \to \infty$, $\epsilon = 0$, the governing equations decouple. The temperatures are $T_1^* = e^{-Hx^*}$, $T_2^* =?$.
If $H = 0$, then $T_1* = T_2^* = T_{in}^*$.

Alternatively

For small ϵ, regular perturbation series for T_1^* and T_2^* give

$$T_1^* = T_{1,0}^* + \epsilon T_{1,1}^* + \epsilon^2 T_{1,2}^* + \ldots,$$
$$T_2^* = T_{2,0}^* + \epsilon T_{2,1}^* + \epsilon^2 T_{2,2}^* + \ldots,$$

from which

$$\frac{dT_{1,0}^*}{dx^*} + HT_{1,0}^* = 0,$$
$$-\frac{dT_{2,0}^*}{dx^*} + HT_{2,0}^* = 0,$$

and

$$\frac{dT_{1,1}^*}{dx^*} + HT_{1,1}^* = T_{2,0}^* - T_{1,0}^*,$$
$$-\frac{dT_{2,1}^*}{dx^*} + HT_{2,1}^* = T_{1,0}^* - T_{2,0}^*,$$

and so on. These can be easily solved.

7.4 Other forced convection problems

7.4.1 Two-fluid configuration

Consider the heat balance in Fig. 7.9. Neglecting axial conduction, we have

$$\rho_w A_w c_w \frac{\partial T_w}{\partial t} + h_1(T_w - T_1) + h_2(T_w - T_2) = 0,$$
$$\rho_1 A_1 c_1 \frac{\partial T_1}{\partial t} + \rho_1 V_1 c_1 \frac{\partial T_1}{\partial x} + h_1(T_1 - T_w) = 0,$$
$$\rho_2 A_2 c_2 \frac{\partial T_2}{\partial t} + \rho_2 V_2 c_2 \frac{\partial T_2}{\partial x} + h_2(T_2 - T_w) = 0.$$

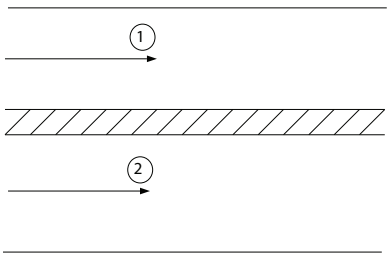

Figure 7.9: Two-fluids with wall.

7.4.2 Conjugate heat transfer

7.4.3 Flow between plates with viscous dissipation

Consider the steady, laminar flow of an incompressible, Newtonian fluid between fixed, flat plates at $y = -h$ and $y = h$. The flow velocity $u(y)$ is in the x-direction due to a constant pressure gradient $P < 0$. The plane walls are kept isothermal at temperature $T = T_0$, and the viscosity is assumed to decrease exponentially with temperature according to

$$\mu = \exp(1/T).) \tag{7.11}$$

The momentum equation is then

$$\frac{d}{dy}\left(\mu(T)\frac{du}{dy}\right) = P$$

with boundary conditions $u = 0$ at $y = \pm h$. Integrating, we get

$$\mu(T)\frac{du}{dy} = Py + C$$

Due to symmetry $du/dy = 0$ at $y = 0$ so that $C = 0$. There is also other evidence for this.

The energy equation can be written as

$$k\frac{d^2T}{dy^2} + \mu(T)\left(\frac{du}{dy}\right)^2 = 0$$

with $T = T_0$ at $y = \pm h$, where k has been taken to be a constant. The second term corresponds to viscous heating or dissipation, and the viscosity is assumed to be given by Eq. (7.11). We non-dimensionalize using

$$T^* = \beta(T - T_0), \quad y^* = \frac{y}{h}$$

The energy equation becomes

$$\frac{d^2T^*}{dy^{*2}} + a\ y^{*2}eT^* = 0 \tag{7.12}$$

where

$$a = \frac{\beta P^2 h^4}{k\mu_0}$$

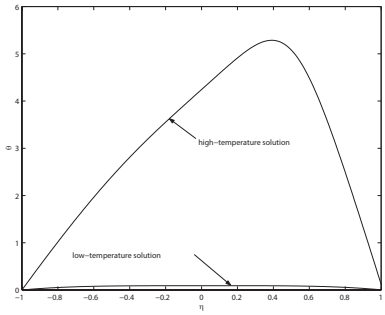

Figure 7.10: Two solutions of Eq. (7.12) with boundary conditions (7.13) for $a = 1$.

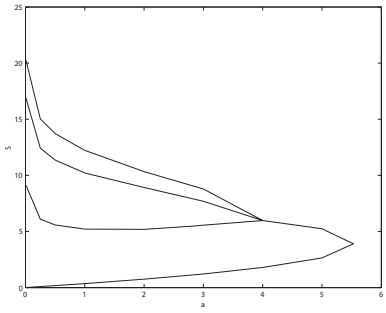

Figure 7.11: Bifurcation diagram.

The boundary conditions are

$$T^* = 0 \text{ for } y^* = \pm 1 \tag{7.13}$$

There are two solutions that can be obtained numerically (by the shooting method, for instance) for the boundary-value problem represented by Eqs. (7.12) and (7.13) for $a < a_c$ and above which there are none. There are other solutions also but they do not satisfy the boundary conditions on the velocity. As examples, two numerically obtained solutions for $a = 1$ are shown in Fig. 7.10.

The bifurcation diagram corresponding to this problem is shown in Fig. 7.11 where S is the slope of the temperature gradient on one wall.

7.4.4 Radial flow between disks

This is shown in Fig. 7.12.

$$u_r = \frac{C}{r}$$

$$q_r = u_r 2\pi r H T - k 2\pi r H \frac{dT}{dr}$$

where H is the distance between the disks. With $dq_r/dr = 0$, we get

$$\frac{d}{dr}(r u_r T) = k \frac{d}{dr}(r \frac{dT}{dr})$$

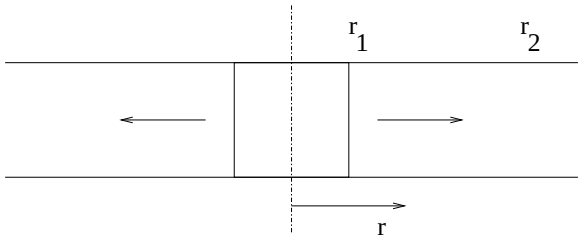

Figure 7.12: Flow between disks.

For the boundary conditions $T(r_1) = T_1$ and $T(r_2) = T_2$, the temperature field is

$$T(r) = \frac{T_1 \ln(r_2/r) - T_2 \ln(r_1/r)}{\ln(r_2/r_1)}$$

Example 7.3

Redo the previous problem with a slightly eccentric flow.

7.5 Natural convection in ducts

We will once again make a one-dimensional approximation. Furthermore we will make the Boussinesq approximation by which the fluid density is constant except in the buoyancy term. Temperature differences within the fluid lead to a change in density and hence a buoyancy force that creates a natural convection. The density in the gravity force term will be often be assumed to decrease linearly with temperature, so that

$$\rho = \rho_0 \big[1 - \beta(T - T_{ref})\big].$$

The mass, momentum and energy equations are

$$\begin{aligned} V &= V(t), \\ \frac{\partial V}{\partial t} &= -\frac{1}{\rho}\frac{\partial p}{\partial s} - + \frac{P\alpha}{\rho A} V - \big[1 - \beta(T - T_{ref})\big]\tilde{g}, \\ \frac{\partial T}{\partial t} + V\frac{\partial T}{\partial s} &= \frac{q_{ext}}{\rho A c}. \end{aligned}$$

7.5.1 Open ducts

Example 7.4

Consider a long, thin, vertical tube that is open at both ends, as shown in Fig. 7.13. The air in the tube is heated with an electrical resistance running down the center of the tube. Find the steady state temperature distribution and the velocity of the air due to natural convection.

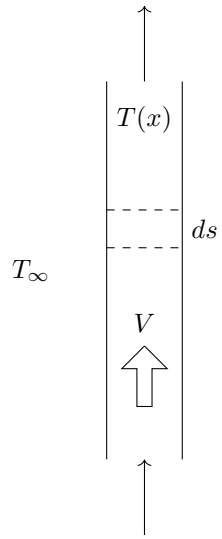

Figure 7.13: Vertical tube open at both tubes; an element of length ds is indicated by dashed lines.

Assumptions: One dimensional, Boussinesq approximation, constant q_{ext}.

Variables: V is mean velocity, $T(s)$ is temperature, s axial coordinate starting from $s = 0$ at lower end, P is the perimeter at a cross section, α is the proportionality constant between wall shear stress and velocity defined by Eq. (7.1); ρ is constant density, A is cross-sectional area, $p(s)$ is pressure, β is the coefficient of thermal expansion, T_{ref} is a reference temperature for density, $\tilde{g}$ is the component of gravity along the tube, and q_{ext} is the heat input per unit length.

The mass, momentum and energy equations equations for an element of length ds for a vertical tube are

$$V = \text{constant},$$

$$0 = -\frac{1}{\rho}\frac{dp}{ds} - \big[1 - \beta(T - T_\infty\big]g - \frac{P\alpha}{\rho A}V, , \tag{7.14}$$

$$V\frac{dT}{ds} = \frac{q_{ext}}{\rho Ac}, \tag{7.15}$$

where $T_{ref} = T_\infty$.

Integrating Eq. (7.15)

$$T = \frac{q_{ext}}{\rho VAc}s + C, \tag{7.16}$$

$$= \frac{q_{ext}}{\rho VAc}s + T_\infty, \tag{7.17}$$

where the condition $T = T_\infty$ at $s = 0$ at the inlet has been used.

Integrating Eq. (7.14) from $s = 0$ to L

$$\begin{aligned}
0 &= -\frac{1}{\rho}\int_0^L \frac{dp}{ds}\, ds - \int_0^L \big[1 - \beta(T - T_\infty\big]g\, ds - \int_0^L \frac{P\alpha V}{\rho A}\, ds, \\
&= -\frac{1}{\rho}\Big(p(L) - p(0)\Big) - gL + \beta g\int_0^L \underbrace{(T - T_\infty)}_{\text{use Eq. (7.17)}}\, ds - \frac{P\alpha V}{\rho A}L, \\
&= -\frac{1}{\rho}\Big(\cancel{-\rho gL}\Big) - \cancel{gL} + \beta g\int_0^L \frac{q_{ext}}{\rho VAc}s\, ds - \frac{P\alpha VL}{\rho A}, \\
&= \frac{\beta g q_{ext}}{\rho VAc}\frac{L^2}{2} - \frac{P\alpha VL}{\rho A},
\end{aligned}$$

so that

$$V = \sqrt{\frac{\beta g q_{ext} L}{2P\alpha c}}. \tag{7.18}$$

Only the positive square root is admissible since it does not make physical sense for the fluid inside the tube at a higher temperature and hence lighter than the fluid outside to fall; see (e) below.

Checks
(a) Dimensions: In Eq. (7.18)

$$[V] = LT^{-1}; \quad [\beta] = \Theta^{-1}; \quad [g] = LT^{-2}; \quad [q_{ext}] = MLT^{-3};$$
$$[L] = L; \quad [P] = L; \quad [\alpha] = ML^{-2}T^{-1}; \quad [c] = L^2T^{-2}\Theta^{-1},$$

so that

$$\begin{aligned}[V] &= \frac{(\Theta^{-1})(LT^{-2})(MLT^{-3})(L)}{(L)(ML^{-2}T^{-1})(L^2T^{-2}\Theta^{-1})},\\ &= L^2T^{-2}.\checkmark\end{aligned}$$

(b) Physical sense of final result: V should increase if any one of these parameters independently increases: β (fluid expands more), g (greater weight difference between inside and outside), q_{ext} (greater temperature difference between inside and outside), L (greater weight difference between inside and outside). Similarly V should decrease if any one of the following independently increases: $P\alpha$ (greater friction at wall), c (smaller in-tube temperature rise). ✓
(c) Physical sense of intermediate results: temperature distribution (increases linearly with distance from lower end). ✓
(d) Pressure distribution: Integrating Eq. (7.14) from 0 to s

$$\begin{aligned}0 &= -\frac{1}{\rho}\Big(p(s) - p(0)\Big) - gs + \beta g \int_0^s \Big(T(s') - T_\infty\Big)\, ds' - \frac{P\alpha V}{\rho A}s,\\ &= -\frac{1}{\rho}\Big(p(s) - p(0)\Big) - gs + \beta g \int_0^s \left(\frac{q_{ext}}{\rho V A c}s'\right) ds' - \frac{P\alpha V}{\rho A}s,\\ &= \dots\end{aligned}$$

(e) Reverse flow: A negative value of V implies that the inlet is at $s = L$ and so the condition to find C in Eq. (7.16) is that $T = T_\infty$ at $s = L$. Let us see what happens if we assume that the flow is downward. We can avoid redoing the algebra and use many of the same equations, including the boundary condition, if we take the s coordinate starting from the top and growing downward. The temperature distribution is the same, but gravity changes sign. Thus, in Eq. (7.18) the quantity under the square root is negative if q_{ext} is positive, and no real velocity is possible. If, however, the tube is cooled instead of being heated, a downward flow is set up due to natural convection.

7.5.2 Closed loops

Let us consider a closed loop, shown in Fig. 7.14, of length L and constant cross-sectional area A filled with a fluid. The loop is heated in some parts and cooled in others. The spatial coordinate is s, measured from some arbitrary origin and going around the loop in the counterclockwise direction. We will also approximate the behavior of the fluid using one spatial dimension. Thus, we will assume that the velocity V and temperature T are constant across a section of the loop. In general $T = T(s,t)$ but, for a loop of constant cross-sectional area, mass conservation implies that V is independent of s, and must be a function of t alone.

Compared to ducts that are open at both ends, there are some simplifications for closed loops.

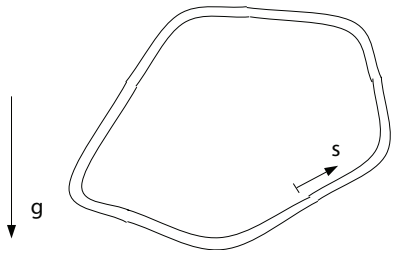

Figure 7.14: A general natural convective loop.

- From Eq. (7.2)

$$\int_0^L \tilde{g}(s)\, ds = \int_0^L g\frac{dz}{ds}\, ds, \\ = 0. \tag{7.19}$$

- The integral over a loop of the pressure term vanishes, i.e.

$$\int_0^L \frac{\partial p}{\partial s}\, ds = 0.$$

The integral of the momentum equation

$$\frac{\partial V}{\partial t} = -\frac{1}{\rho}\frac{\partial p}{\partial s} - \frac{P\alpha}{\rho A}V - \big[1 - \beta(T - T_{ref})\big]\tilde{g},$$

over a loop is thus

$$\frac{dV}{dt} + \frac{P\alpha}{\rho A}V = \frac{\beta}{L}\int_0^L T\tilde{g}(s)\, ds. \tag{7.20}$$

[173, 174] The simplest heating condition is when the heat rate per unit length, $q(s)$, is known all along the loop. For zero mean heating, we have

$$\int_0^L q_{ext}(s)\, ds = 0 \tag{7.21}$$

$q_{ext}(s) > 0$ indicates heating, and $q_{ext}(s) < 0$ cooling.

7.5.3 Steady state

The steady-state governing equations are

$$\frac{P\alpha}{\rho A}\bar{V} = \frac{\beta}{L}\int_0^L \bar{T}(s)\tilde{g}(s)\, ds \tag{7.22}$$

$$\bar{V}\frac{d\bar{T}}{ds} = \frac{q_{ext}(s)}{\rho A c} \tag{7.23}$$

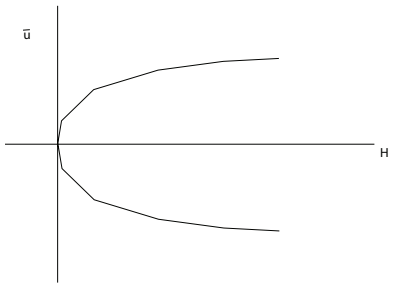

Figure 7.15: Bifurcation with respect to parameter H.

The solution of equation (7.23) gives us the temperature field

$$\bar{T}(s) = \frac{1}{\rho A c \bar{V}} \int_0^s \; q_{ext}(s') \; ds' + T_0$$

where $\bar{T}(0) = T_0$. Using equation (7.19) it can be checked that $T(L) = T_0$ also. Substituting in equation (7.22), we get

$$\frac{P\alpha}{\rho A} \bar{V} = \frac{\beta}{\rho A c L \bar{V}} \int_0^L \left[\int_0^s \; q_{ext}(s') \; ds' \right] \; \tilde{g}(s) \; ds \tag{7.24}$$

from which

$$\bar{V} = \pm \sqrt{\frac{\beta}{P\alpha L c} \int_0^L \left[\int_0^s \; q_{ext}(s') \; ds' \right] \; \tilde{g}(s) \; ds}$$

Two real solutions exist for

$$\int_0^L \left[\int_0^s \; q_{ext}(s') \; ds' \right] \; \tilde{g}(s) \; ds \geq 0$$

and none otherwise. Thus there is a bifurcation from no solution to two as the parameter H passes through zero, where

$$H = \int_0^L \left[\int_0^s \; q_{ext}(s') \; ds' \right] \; \tilde{g}(s) \; ds$$

The pressure distribution can be found from

$$\frac{d\bar{p}}{ds} = -\frac{P\alpha \bar{V}}{A} - \rho \left[1 - \beta(\bar{T} - T_0) \right] \tilde{g} \tag{7.25}$$

$$= -\frac{P\alpha \bar{V}}{A} - \rho \tilde{g} + \frac{\beta}{A c \bar{V}} \left[\int_0^s \; q_{ext}(s') \; ds' \right] \tilde{g} \tag{7.26}$$

from which

$$\bar{p}(s) = p_0 - \frac{P\alpha \bar{V}}{A} \; s - \rho \int_0^s \; \tilde{g}(s') \; ds' + \frac{\beta}{A c \bar{V}} \int_0^s \left[\int_0^{s''} \; q_{ext}(s') \; ds' \right] \tilde{g}(s'') \; ds''$$

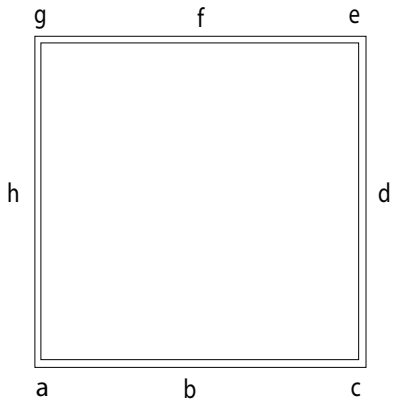

Figure 7.16: Geometry of a square loop.

where $\bar{p}(0) = p_0$. Using equations (7.19) and (7.24), it can be shown that $\bar{p}(L) = p_0$ also.

Example 7.5

Find the temperature distributions and velocities in the three heating and cooling distributions corresponding to Fig. 7.16. (a) Constant heating between points c and d, and constant cooling between h and a. (b) Constant heating between points c and d, and constant cooling between g and h. (c) Constant heating between points d and e, and constant cooling between h and a. (d) Constant heating between points a and c, and constant cooling between e and g. The constant value is $\hat{q}_{ext}$, and the total length of the loop is L.

Let us write

$$F(s) = \int_0^s q_{ext}(s')\, ds'$$
$$G(s) = F(s)\tilde{g}(s)$$
$$H = \int_0^L G(s)\, ds$$

so that

$$\begin{aligned}
\bar{V} &= \pm\sqrt{\frac{\beta}{P\alpha Lc}\int_0^L \left[\int_0^s q_{ext}(s')\, ds'\right] \tilde{g}(s)\, ds}, \\
&= \pm\sqrt{\frac{\beta}{P\alpha Lc}\int_0^L F(s)\, \tilde{g}(s)\, ds}, \\
&= \pm\sqrt{\frac{\beta}{P\alpha Lc}\int_0^L G(s)\, ds}, \\
&= \pm\sqrt{\frac{\beta H}{P\alpha Lc}}.
\end{aligned}$$

The functions $F(s)$ and $G(s)$ are shown in Fig. 7.17. The origin is at point a, and the coordinate s runs counterclockwise. The integral H in the four cases is: (a) $H = 0$, (b) $H = \hat{q}_{ext}L/8$, (c) $H = -\hat{q}_{ext}L/8$, (d) $H = \hat{q}_{ext}L/4$.

No real solution for the fluid velocity exists for case (c); the velocity is zero for (a); the other two cases have two solutions each, one positive and the other negative. The temperature distribution is given by

$$\bar{T} - T_0 = \frac{F(s)}{\rho Ac\bar{V}},$$

and the pressure distribution can be found from equation (7.26). Steady states are not possible for (a) and (c).

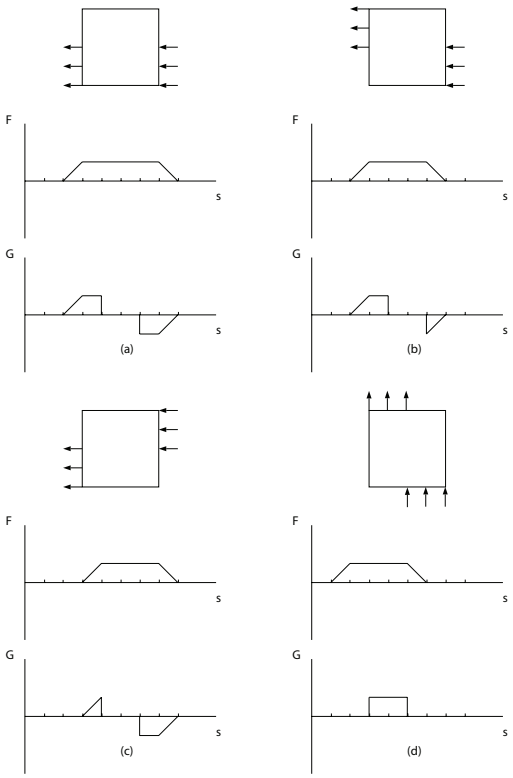

Figure 7.17: Functions $F(s)$ and $G(s)$ for the four cases.

Example 7.6

What is the physical interpretation of condition (7.25)?

Let us write

$$\begin{aligned} H &= \int_0^L \left[\int_0^s q_{ext}(s')\ ds'\right]\ \tilde{g}(s)\ ds \\ &= \int_0^L \left[\int_0^s q_{ext}(s')\ ds'\right]\ d\left[\int_0^s \tilde{g}(s')\ ds'\right] \\ &= \left[\int_0^s q_{ext}(s')\ ds'\right]_0^L \left[\int_0^s \tilde{g}(s')\ ds'\right]_0^L - \int_0^L \left[q_{ext}(s)\int_0^s \tilde{g}(s')\ ds'\right]\ ds \end{aligned}$$

The first term on the right vanishes due to equations (7.21) and (7.19). Using equation (7.2), we find that

$$H = -g\int_0^L q_{ext}(s)z(s)\ ds \tag{7.27}$$

The function $z(s)$ is another way of describing the geometry of the loop. We introduce the notation

$$q_{ext}(s) = q_{ext}^+(s) - q_{ext}^-(s) \tag{7.28}$$

where

$$q_{ext}^+ = \begin{cases} q_{ext}(s) & \text{for} \quad q_{ext}(s) > 0 \\ 0 & \text{for} \quad q_{ext}(s) \le 0 \end{cases}$$

and

$$q_{ext}^- = \begin{cases} 0 & \text{for} \quad q_{ext}(s) \ge 0 \\ -q_{ext}(s) & \text{for} \quad q_{ext}(s) < 0 \end{cases}$$

Equations (7.21) and (7.27) thus becomes

$$\int_0^L q_{ext}^+(s)\ ds = \int_0^L q_{ext}^-(s)\ ds \tag{7.29}$$

$$H = -g\left[\int_0^L q_{ext}^+(s)z(s)\ ds - \int_0^L q_{ext}^-(s)z(s)\ ds\right] \tag{7.30}$$

From these, condition (7.25) which is $H \ge 0$ can be found to be equivalent to

$$\frac{\int_0^L q_{ext}^+(s)z(s)\ ds}{\int_0^L q_{ext}^+(s)\ ds} < \frac{\int_0^L q_{ext}^-(s)z(s)\ ds}{\int_0^L q_{ext}^-(s)\ ds}$$

This implies that the height of the centroid of the heating rate distribution should be above that of the cooling.

7.6 Axial conduction effects

With axial conduction

$$\frac{\partial T}{\partial t} + V\frac{\partial T}{\partial s} = \frac{k}{\rho c}\frac{\partial^2 T}{\partial s^2} + \frac{q_{ext}}{\rho A c}.$$

The energy equation is

$$\frac{\partial T}{\partial t} + V\frac{\partial T}{\partial s} = \frac{q}{\rho_0 Ac} + \frac{k}{\rho_0 c}\frac{\partial^2 T}{\partial s^2}$$

Example 7.7

Analyze the longitudinal temperature field for small axial conduction.

We have

$$\lambda\frac{d^2T^*}{dx^{*2}} - \frac{dT^*}{dx^*} - H(T^* - 1) = 0$$

where $\lambda \ll 1$, and with the boundary conditions $T^*(0) = 0$ and $T^*(1) = T_1^*$.

We can use a boundary layer analysis for this singular perturbation problem. The outer solution is

$$T_{out}^* = 1 - e^{-Hx^*}$$

The boundary layer is near $x^* = 1$, where we make the transformation

$$X = \frac{x^* - 1}{\lambda}$$

This gives the equation

$$\frac{d^2T_{in}^*}{dX^2} - \frac{dT_{in}^*}{dX} - \lambda H(T_{in}^* - 1) = 0$$

To lowest order, we have

$$\lambda\frac{d^2T_{in}^*}{dX^2} - \frac{dT_{in}^*}{dX} = 0$$

with the solution

$$T_{in}^* = A + Be^X$$

The boundary condition $T_{in}^*(X = 0) = T_1^*$ gives $T_1^* = A + B$, so that

$$T_{in}^* = A + (T_1^* - A)e^X$$

The matching condition is

$$T_{outer}^*(x^* = 1) = T_{in}^*(X \to -\infty)$$

so that

$$A = 1 - e^{-H}$$

The composite solution is then

$$T^* = 1 - e^{-H} + (T_1^* - 1 + e^{-H})e^{(x^*-1)/\lambda} + \ldots$$

7.6.1 Nondimensionalization

For known heat rate, $q_{ext} = q(s)$, is known along the duct. Defining

$$s^* = \frac{s}{L}, \quad T^* = \frac{(T - T_i)\rho V A C}{Lq}, \quad t^* = \frac{tV}{L},$$

gives

$$\frac{\partial T^*}{\partial t^*} + \frac{\partial T^*}{\partial s^*} - \lambda \frac{\partial^2 T^*}{\partial s^{*2}} = 1$$

where

$$\lambda = \frac{k}{LV\rho c}$$

Suitable boundary conditions for this second-order equation may be $T^* = 0$ at $s^* = 0$, and $T^* = T_1^*$ at $s^* = 1$.

For convective heat exchange with an overall heat transfer coefficient U, and an external temperature of $T_\infty(s)$ gives

$$q_{ext} = PU(T_\infty - T).$$

Defining

$$x^* = \frac{x}{L}, \quad T^* = \frac{T - T_i}{T_\infty - T_i}, \quad t^* = \frac{tV}{L},$$

gives

$$\frac{\partial T^*}{\partial t^*} + \frac{\partial T^*}{\partial x^*} - \lambda \frac{\partial^2 T^*}{\partial x^{*2}} + HT^* = H,$$

where

$$\lambda = \frac{k}{LV\rho c}, \quad H = \frac{U\rho L}{\rho V A c}.$$

To nondimensionalize and normalize equations (7.20) and (**??**), we take

$$t^* = \frac{t'}{\tau} \quad s^* = \frac{s}{L}, \quad u^* = \frac{u}{VG^{1/2}}, \quad T^* = \frac{T - T_0}{\Delta T\ G^{1/2}}, \quad \tilde{g}^* = \frac{\tilde{g}}{g}, \quad q^* = \frac{q}{q_m}$$

where

$$V = \frac{P\alpha L}{\rho_0 A}, \quad \Delta T = \frac{P^2\alpha^2 L}{\beta g \rho_0^2 A^2}, \quad \tau = \frac{\rho_0 A}{P\alpha}, \quad G = \frac{q_m \beta g \rho_0^2 A^2}{P^3 \alpha^3 L c}$$

Substituting, we get

$$\frac{du^*}{dt^*} + u^* = \int_0^1 T^* \tilde{g}^*\ ds^* \tag{7.31}$$

$$\frac{\partial T^*}{\partial t^*} + G^{1/2} u^* \frac{\partial T^*}{\partial s^*} = G^{1/2} q^* + K \frac{\partial^2 T^*}{\partial s^{*2}} \tag{7.32}$$

where

$$K = \frac{kA}{P\alpha L^2 c}$$

The two nondimensional parameters which govern the problem are G and K.

Under steady-state conditions, and neglecting axial conduction, the temperature and velocity are

$$\bar{T}^*(s) = \frac{1}{\bar{u}^*} \int_0^{s^*} q^*(s_1^*)\ ds_1^*$$

$$\bar{u}^* = \pm\sqrt{\int_0^1 \left[\int_0^{s^*} q^*(s_1^*)\ ds_1^*\right]\ \tilde{g}^*(s^*)\ ds^*}$$

All variables are of unit order indicating that the variables have been appropriately normalized.

For $\alpha = 8\mu/D$, $A = \pi D^2/4$, and $P = \pi D$, we get

$$G = \frac{1}{8192\pi}\ \frac{Gr}{Pr}\ \left(\frac{D}{L}\right)^4$$

$$K = \frac{1}{32\ Pr}\ \left(\frac{D}{L}\right)^2$$

where the Prandtl and Grashof numbers are

$$Pr = \frac{\mu c}{k}$$

$$Gr = \frac{q_m g \beta L^3}{\nu^2 k}$$

respectively. Often the Rayleigh number defined by

$$Ra = Gr\ Pr$$

is used instead of the Grashof number.

Since $\bar{u}^*$ is of $O(1)$, the dimensional velocity is of order $(8\nu L/D^2)Gr^{1/2}$. The ratio of axial conduction to the advective transport term is

$$\epsilon = \frac{K}{G^{1/2}}$$

$$= \left(\frac{8\pi}{Ra}\right)^{1/2}$$

Taking typical numerical values for a loop with water to be: $\rho = 998$ kg/m^3, $\mu = 1.003 \times 10^{-3}$ kg/m s, $k = 0.6$ W/m K, $q_m = 100$ W/m, $g = 9.91$ m/s^2, $\beta = 0.207 \times 10^{-3}$ K^{-1}, $D = 0.01$ m, $L = 1$ m, $c = 4.18 \times 10^3$ J/kgK, we get the velocity and temperature scales to be

$$VG^{1/2} =$$

$$\Delta T G^{1/2} =$$

and the nondimensional numbers as

$$G = 1.86 \times 10^{-2} \tag{7.33}$$
$$K = 4.47 \times 10^{-7} \tag{7.34}$$
$$Gr = 3.35 \times 10^{11} \tag{7.35}$$
$$Ra = 2.34 \times 10^{12} \tag{7.36}$$
$$\epsilon = 3.28 \times 10^{-6} \tag{7.37}$$

Axial conduction is clearly negligible in this context.

For a steady state, equations (7.31) and (7.32) are

$$\bar{u}^* = \int_0^1 \bar{T}^* \tilde{g}^* \, ds^*$$
$$\epsilon \frac{d^2\bar{T}^*}{ds^{*2}} - \bar{u}^* \frac{d\bar{T}^*}{ds^*} = -q^*(s^*)$$

Integrating over the loop from $s^* = 0$ to $s^* = 1$, we find that continuity of $\bar{T}^*$ and equation (7.21) imply continuity of $d\bar{T}^*/ds^*$ also.

Conduction-dominated flow

If $\lambda = G^{1/2}/\epsilon \ll 1$, axial conduction dominates. We can write

$$\bar{u} = \bar{u}_0 + \lambda \bar{u}_1 + \lambda^2 \bar{u}_2 + \ldots$$
$$\bar{T}(s) = \bar{T}_0(s) + \lambda \bar{T}_1(s) + \lambda^2 \bar{T}_2(s) + \ldots$$

where, for convenience, the asterisks have been dropped. Substituting into the governing equations, and collecting terms of $O(\lambda^0)$, we have

$$\bar{u}_0 = \int_0^1 \bar{T}_0 \tilde{g} \, ds$$
$$\frac{d^2\bar{T}_0}{ds^2} = 0$$

The second equation, along with conditions that $\bar{T}_0$ and $d\bar{T}_0/ds$ have the same value at $s = 0$ and $s = 1$, gives $\bar{T}_0 =$ an arbitrary constant. The first equation gives $\bar{u}_0 = 0$.

The terms of $O(\lambda)$ give

$$\bar{u}_1 = \int_0^1 \bar{T}_1 \tilde{g} \, ds \tag{7.38}$$
$$\frac{d^2\bar{T}_1}{ds^2} = -q(s) + \bar{u}_0 \frac{d\bar{T}_0}{ds} \tag{7.39}$$

The second equation can be integrated once to give

$$\frac{d\bar{T}_1}{ds} = -\int_0^s q(s') \, ds' + A$$

and again

$$\bar{T}_1 = -\int_0^s \left[\int_0^{s''} q(s')\ ds'\right]\ ds'' + As + B$$

Continuity of $\bar{T}_1(s)$ and $d\bar{T}_1/ds$ at $s = 0$ and $s = 1$ give

$$B = -\int_0^1 \left[\int_o^{s''} q(s')\ ds'\right]\ ds'' + A + B$$
$$A = A$$

respectively, from which

$$A = \int_0^1 \left[\int_0^{s''} q(s')\ ds'\right]\ ds''$$

and that B can be arbitrary. Thus

$$\bar{T}_1 = \int_0^s \left[\int_0^{s''} q(s')\ ds'\right]\ ds'' + s\int_0^1 \left[\int_0^{s''} q(s')\ ds'\right]\ ds'' + T_1(0)$$

where $\bar{T}(0)$ is an arbitrary constant. Substituting in equation (7.38), gives

$$\bar{u}_1 = -\int_0^1 \left\{\int_0^s \left[\int_0^{s''} q(s')\ ds'\right]\ ds''\right\}\tilde{g}\ ds + \int_0^1 \left[\int_0^{s''} q(s')\ ds'\right]\ ds'' \int_0^1 s\tilde{g}\ ds$$

The temperature distribution is determined by axial conduction, rather than by the advective velocity, so that the resulting solution is unique.

Advection-dominated flow

The governing equations are

$$\bar{u} = \int_0^1 \bar{T}\tilde{g}\ ds$$
$$\bar{u}\frac{d\bar{T}}{ds} = q + \epsilon\frac{d^2\bar{T}}{ds^2}$$

where $\epsilon \ll 1$. Expanding in terms of ϵ, we have

$$\bar{u} = \bar{u}_0 + \epsilon\bar{u}_1 + \epsilon^2\bar{u}_2 + \ldots$$
$$\bar{T} = \bar{T}_0 + \epsilon\bar{T}_1 + \epsilon^2\bar{T}_2 + \ldots$$

To $O(\epsilon^0)$, we get

$$\bar{u}_0 = \int_0^1 \bar{T}_0\tilde{g}\ ds$$
$$\bar{u}_0\frac{d\bar{T}_0}{ds} = q$$

from which

$$\bar{T}_0 = \frac{1}{\bar{u}_0}\int_0^s q(s')\ ds'$$
$$\bar{u}_0 = \pm\int_0^1 \left[\int_0^s q(s')\ ds'\right]\tilde{g}\ ds$$

Axial conduction. therefore, slightly modifies the two solutions obtained without it.

7.7 Toroidal geometry

The dimensional gravity function can be expanded in a Fourier series in s, to give

$$\tilde{g}(s) = \sum_{n=1}^{\infty}\left[g_n^c\cos\frac{2\pi ns}{L} + g_1^s\sin\frac{2\pi ns}{L}\right]$$

The simplest loop geometry is one for which we have just the terms

$$\tilde{g}(s) = g_1^c\cos\frac{2\pi s}{L} + g_1^s\sin\frac{2\pi s}{L} \tag{7.40}$$

corresponds to a toroidal geometry. Using

$$g^2 = (g_1^c)^2 + (g_1^s)^2$$
$$\phi_0 = \tan^{-1}\frac{g_1^c}{g_1^s}$$

equation (7.40) becomes

$$\tilde{g}(s) = g\cos\left(\frac{2\pi s}{L} - \phi_0\right)$$

Without loss of generality, we can measure the angle from the horizontal, i.e. from the three o'clock point, and take $\phi_0 = 0$ so that

$$\tilde{g}(s) = g\cos(2\pi s/L)$$

The nondimensional gravity component is

$$\tilde{g} = \cos(2\pi s)$$

where the * has been dropped.

Assuming also a sinusoidal distribution of heating

$$q(s) = -\sin(2\pi s - \phi)$$

the momentum and energy equations are

$$\bar{V} = \int_0^1 T(s)\cos(2\pi s)\ ds \tag{7.41}$$
$$\bar{V}\frac{d\bar{T}}{ds} = -\sin(2\pi s - \phi) + \epsilon\frac{d^2\bar{T}}{ds^2} \tag{7.42}$$

The homogeneous solution is

$$\bar{T}_h = Be^{\bar{V}s/\epsilon} + A$$

The particular integral satisfies

$$\frac{d^2T_p}{ds^2} - \frac{\bar{V}}{\epsilon}\frac{d\bar{T}_p}{ds} = \frac{1}{\epsilon}\sin(2\pi s - \phi)$$

Integrating, we have

$$\begin{aligned}\frac{dT_p}{ds} - \frac{\bar{V}}{\epsilon}\bar{T}_p &= -\frac{1}{2\pi\epsilon}\cos(2\pi s - \phi) \\ &= -\frac{1}{2\pi\epsilon}\left[\cos(2\pi s)\cos\phi + \sin(2\pi s)\sin\phi\right]\end{aligned}$$

Take

$$\bar{T}_p = a\cos(2\pi s) + b\sin(2\pi s)$$

from which

$$\frac{d\bar{T}_p}{ds} = -2\pi a\sin(2\pi s) + 2\pi b\cos(2\pi s)$$

Substituting and collecting the coefficients of $\cos(2\pi s)$ and $\sin(2\pi s)$, we get

$$\begin{aligned}-\frac{\bar{V}}{\epsilon}a + 2\pi b &= -\frac{\cos\phi}{2\pi\epsilon} \\ -2\pi a - \frac{\bar{V}}{\epsilon}b &= -\frac{\sin\phi}{2\pi\epsilon}\end{aligned}$$

The constants are

$$\begin{aligned}a &= \frac{(\bar{V}/2\pi\epsilon^2)\cos\phi + (1/\epsilon)\sin\phi}{4\pi^2 + \bar{V}^2/\epsilon^2} \\ b &= \frac{-(1/\epsilon)\cos\phi + (\bar{V}/2\pi\epsilon^2)\sin\phi}{4\pi^2 + \bar{V}^2/\epsilon^2}\end{aligned}$$

The temperature field is given by

$$\bar{T} = \bar{T}_h + \bar{T}_p$$

Since $\bar{T}(0) = \bar{T}(1)$, we must have $B = 0$. Taking the other arbitrary constant A to be zero, we have

$$\bar{T} = \frac{1}{4\pi^2 + \bar{V}^2/\epsilon^2}\left[\left(\frac{\bar{V}}{2\pi\epsilon^2}\cos\phi + \frac{1}{\epsilon}\sin\phi\right)\cos(2\pi s) + \left(-\frac{1}{\epsilon}\cos\phi + \frac{\bar{V}}{2\pi\epsilon^2}\sin\phi\right)\sin(2\pi s)\right]$$

The momentum equation gives

$$\bar{V} = \frac{(\bar{V}/2\pi\epsilon^2)\cos\phi + (1/\epsilon)\sin\phi}{2(4\pi^2 + \bar{V}^2/\epsilon^2)}$$

which can be written as

$$\bar{V}^3 + \bar{V}\left(4\pi^2\epsilon^2 - \frac{1}{4\pi}\cos\phi\right) - \frac{\epsilon}{2}\sin\phi = 0 \tag{7.43}$$

Special cases are:

- $\epsilon = 0$

  Equations (7.41) and (7.42) can be solved to give

$$\bar{T} = \frac{1}{2\pi\bar{V}}\left[\cos(2\pi s)\cos\phi + \sin(2\pi s)\sin\phi\right]$$
$$\bar{V} = \pm\sqrt{\frac{\cos\phi}{4\pi}}$$

  On the other hand substituting $\epsilon = 0$ in equation (7.43) gives an additional spurious solution $\bar{V} = 0$.

- $\epsilon \to \infty$

  We get that $\bar{V} \to 0$.

- $\phi = 0$

  We get

$$\bar{V} = \begin{cases} 0 \\ \sqrt{\frac{1}{4\pi} - 4\pi^2\epsilon^2} \\ -\sqrt{\frac{1}{4\pi} - 4\pi^2\epsilon^2} \end{cases}$$

  The last two solutions exist only when $\epsilon < (16\pi^3)^{-1/2}$.

- $\phi = \pi/2$

  The velocity is a solution of

$$\bar{V}^3 + \bar{V}4\pi^2\epsilon^2 - \frac{\epsilon}{2} = 0$$

Figure 7.18 shows $\bar{V}$-ϕ curves for three different values of ϵ. Figure 7.19 and 7.20 show $\bar{V}$-ϵ curves for different values of ϕ. It is also instructive to see the curve V-Ra, shown in Figure 7.21, since the Rayleigh number is directly proportional to the strength of the heating.

The bifurcation set is the line dividing the regions with only one real solution and that with three real solutions. A cubic equation

$$x^3 + px + q = 0$$

has a discriminant

$$D = \frac{p^3}{27} + \frac{q^2}{4}$$

For $D < 0$, there are three real solutions, and for $D > 0$, there is only one. The discriminant for the cubic equation (7.43) is

$$D = \frac{1}{27}\left(4\pi^2\epsilon^2 - \frac{1}{4\pi}\cos\phi\right)^3 + \frac{1}{4}\left(\epsilon\sin\phi\right)^2$$

The result is shown in Fig. 7.22.

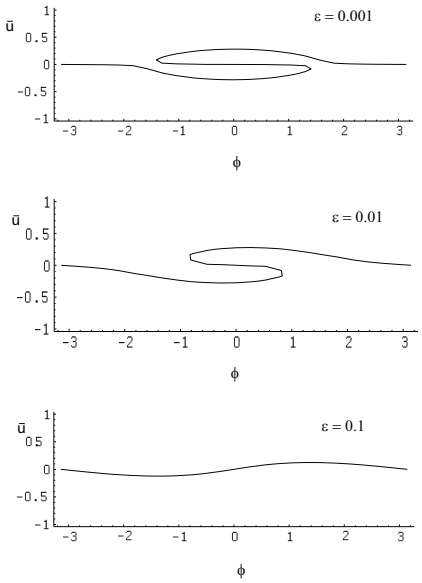

Figure 7.18: $\bar{V}$-ϕ curves.

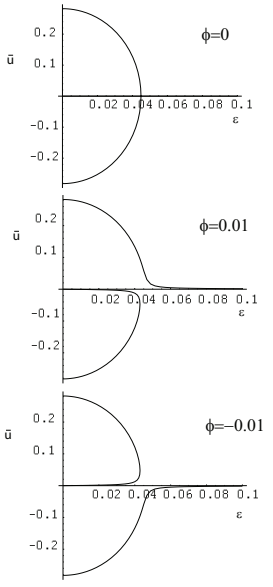

Figure 7.19: $\bar{V}$-ϵ curves.

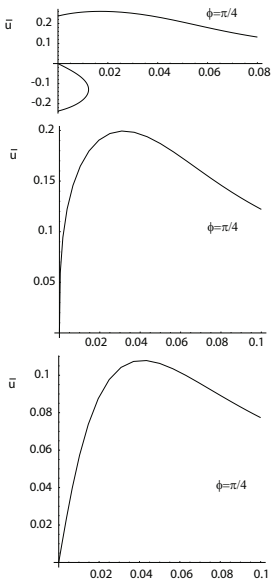

Figure 7.20: More $\bar{V}$-ϵ curves.

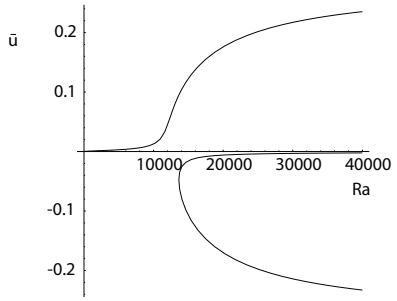

Figure 7.21: $\bar{V}$-Ra for $\phi = 0.01$ radians.

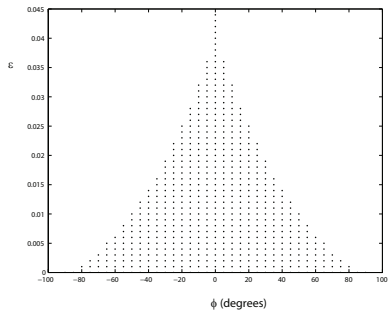

Figure 7.22: Region with three solutions.

7.7.1 Dynamic analysis

We rescale the nondimensional governing equations (7.31) and (7.32) by

$$V^* = \frac{1}{2\pi G^{1/2}}\ \widehat{V}$$
$$T^* = \frac{1}{2\pi G^{1/2}}\ \widehat{T}$$

to get

$$\frac{dV}{dt} + V = \int_0^1 T\tilde{g}\ ds$$
$$\frac{\partial T}{\partial t} + \frac{1}{2\pi}\ V\frac{\partial T}{\partial s} = Gq + \frac{G^{1/2}K}{2\pi}\frac{\partial^2 T}{\partial s^2}$$

where the hats and stars have been dropped.

We take $\tilde{g} = \cos(2\pi s)$ and $q = -\sin(2\pi s - \phi)$. Expanding the temperature in a Fourier series, we get

$$T(s,t) = T_0(t) + \sum_{n=1}^{\infty}\left[T_n^c(t)\cos(2\pi ns) + T_n^s(t)\sin(2\pi ns)\right]$$

Substituting, we have

$$\frac{dV}{dt} + V = \frac{1}{2}T_1^c$$

and

$$\frac{dT_0}{dt} + \sum_{n=1}^{\infty}\left[\frac{dT_n^c}{dt}\cos(2\pi ns) + \frac{dT_n^c}{dt}\sin(2\pi ns)\right] + V\sum_{n=1}^{\infty}\left[-nT_n^c\sin(2\pi ns) + nT_n^s\cos(2\pi ns)\right]$$
$$= -G\left[\sin(2\pi s)\cos\phi - \cos(2\pi s)\sin\phi\right] - 2\pi n^2 G^{1/2}K\sum_{n=1}^{\infty}\left[T_n^c\cos(2\pi ns) + T_n^s\sin(2\pi ns)\right]$$

Integrating, we get

$$\frac{dT_0}{dt} = 0$$

Multiplying by $\cos(2\pi ms)$ and integrating

$$\frac{1}{2}\frac{dT_m^c}{dt} + \frac{m}{2}VT_m^s = \frac{1}{2}G\sin\phi - \pi m^2 G^{1/2}KT_m^c$$

Now multiplying by $\sin(2\pi ms)$ and integrating

$$\frac{1}{2}\frac{dT_m^s}{dt} - \frac{m}{2}VT_m^c = -\frac{1}{2}G\cos\phi - \pi m^2 G^{1/2}KT_m^s$$

Choosing the variables

$$x = V, \quad y = \frac{1}{2}T_1^c, \quad z = \frac{1}{2}T_1^s$$

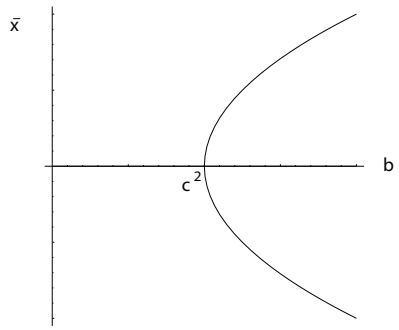

Figure 7.23: Bifurcation diagram for $\bar{x}$.

and the parameters

$$a = \frac{G}{2}\sin\phi \tag{7.44}$$

$$b = \frac{G}{2}\cos\phi \tag{7.45}$$

$$c = 2\pi G^{1/2} K \tag{7.46}$$

we get the dynamical system

$$\frac{dx}{dt} = y - x \tag{7.47}$$

$$\frac{dy}{dt} = a - xz - cy \tag{7.48}$$

$$\frac{dz}{dt} = -b + xy - cz \tag{7.49}$$

The physical significance of the variables are: x is the fluid velocity, y is the horizontal temperature difference, and z is the vertical temperature difference. The parameter c is positive, while a and b can have any sign.

The critical points are found by equating the vector field to zero, so that

$$\bar{y} - \bar{x} = 0 \tag{7.50}$$

$$a - \bar{x}\bar{z} - c\bar{y} = 0 \tag{7.51}$$

$$-b + \bar{x}\bar{y} - c\bar{z} = 0 \tag{7.52}$$

From equation (7.50), we have $\bar{y} = \bar{x}$, and from equation (7.52), we get $\bar{z} = (-b+\bar{x}^2)/c$. Substituting these in equation (7.51), we get

$$\bar{x}^3 + \bar{x}(c^2 - b) - ac = 0 \tag{7.53}$$

This corresponds to equation (7.43), except in different variables.

To analyze the stability of a critical point $(\bar{x}, \bar{y}, \bar{z})$ we add perturbations of the form

$$x = \bar{x} + x' \tag{7.54}$$

$$y = \bar{y} + y' \tag{7.55}$$

$$z = \bar{z} + z' \tag{7.56}$$

Substituting in equation (7.47)-(7.49), we get the local form

$$\frac{d}{dt}\begin{bmatrix} x' \\ y' \\ z' \end{bmatrix} = \begin{bmatrix} -1 & 1 & 0 \\ -\bar{z} & -c & -\bar{x} \\ \bar{y} & \bar{x} & -c \end{bmatrix} \begin{bmatrix} x' \\ y' \\ z' \end{bmatrix} + \begin{bmatrix} 0 \\ -x'z' \\ x'y' \end{bmatrix} \tag{7.57}$$

The linearized version is

$$\frac{d}{dt}\begin{bmatrix} x' \\ y' \\ z' \end{bmatrix} = \begin{bmatrix} -1 & 1 & 0 \\ -\bar{z} & -c & -\bar{x} \\ \bar{y} & \bar{x} & -c \end{bmatrix} \begin{bmatrix} x' \\ y' \\ z' \end{bmatrix} \tag{7.58}$$

No tilt, with axial conduction $(a = 0, c \neq 0)$

From equation (7.53), for $a = 0$ we get

$$\bar{x}^3 + \bar{x}(c^2 - b) = 0$$

from which

$$\bar{x} = \bar{y} = \begin{cases} 0 \\ \sqrt{b - c^2} \\ -\sqrt{b - c^2} \end{cases}$$

The z coordinate is

$$\bar{z} = \begin{cases} -b/c \\ -c \\ -c \end{cases}$$

The bifurcation diagram is shown in Figure 7.23.

Stability of conductive solution

The critical point is $(0, 0, -b/c)$. To examine its linear stability, we look at the linearized equation (7.58) to get

$$\frac{d}{dt}\begin{bmatrix} x' \\ y' \\ z' \end{bmatrix} = \begin{bmatrix} -1 & 1 & 0 \\ b/c & -c & 0 \\ 0 & 0 & -c \end{bmatrix} \begin{bmatrix} x' \\ y' \\ z' \end{bmatrix} \tag{7.59}$$

The eigenvalues of the matrix are obtained from the equation

$$\begin{vmatrix} -(1+\lambda) & 1 & 0 \\ b/c & -(c+\lambda) & 0 \\ 0 & 0 & -(c+\lambda) \end{vmatrix} = 0$$

which simplifies to

$$(c + \lambda)\left[(1 + \lambda)(c + \lambda) - \frac{b}{c}\right] = 0$$

One eigenvalue is

$$\lambda_1 = -c$$

Since $c \geq 0$ this eigenvalue indicates stability. The other two are solutions of

$$\lambda^2 + (c+1)\lambda + (c - \frac{b}{c}) = 0$$

which are

$$\lambda_2 = \frac{1}{2}\left[-(c+1) - \sqrt{(c+1)^2 - 4(c - \frac{b}{c})}\right]$$
$$\lambda_3 = \frac{1}{2}\left[-(c+1) + \sqrt{(c+1)^2 - 4(c - \frac{b}{c})}\right]$$

λ_2 is also negative and hence stable. λ_3 is negative as long as

$$-(c+1) + \sqrt{(c+1)^2 - 4(c - \frac{b}{c})} < 0$$

which gives

$$b < c^2$$

This is the condition for stability.

In fact, one can also prove global stability of the conductive solution. Restoring the nonlinear terms in equation (7.57) to equation (7.59), we have

$$\frac{dx'}{dt} = y' - x'$$
$$\frac{dy'}{dt} = \frac{b}{c}x' - cy' - x'z'$$
$$\frac{dz'}{dt} = -cz' + x'y'$$

Let

$$E(x, y, z) = \frac{b}{c}x'^2 + y'^2 + z'^2$$

Thus

$$\begin{aligned}\frac{1}{2}\frac{dE}{dt} &= \frac{b}{c}x'\frac{dx'}{dt} + y'\frac{dy'}{dt} + z'\frac{dz'}{dt} \\ &= -\frac{b}{c}x'^2 + \frac{2b}{c}x'y' - cy'^2 - cz'^2 \\ &= -\frac{b}{c}(x' - y')^2 - (c - \frac{b}{c})y'^2 - cz'^2\end{aligned}$$

Since

$$E \geq 0$$
$$\frac{dE}{dt} \leq 0$$

for $0 \le b \le c^2$, E is a Liapunov function, and the critical point is stable to all perturbations in this region. The bifurcation at $b = c^2$ is thus supercritical.

Stability of convective solution

For $b > c^2$, only one critical point $(\sqrt{b-c^2}, \sqrt{b-c^2}, -c)$ will be considered, the other being similar. We use the linearized equations (7.58). Its eigenvalues are solutions of

$$\begin{vmatrix} -(1+\lambda) & 1 & 0 \\ c & -(c+\lambda) & -\sqrt{b-c^2} \\ \sqrt{b-c^2} & \sqrt{b-c^2} & -(c+\lambda) \end{vmatrix} = 0$$

This can be expanded to give

$$\lambda^3 + \lambda^2(1+2c) + \lambda(b+c) + 2(b-c^2) = 0$$

The Hurwitz criteria for stability require that all coefficients be positive, which they are. Also the determinants

$$D_1 = 1 + 2c$$
$$D_2 = \begin{vmatrix} 1+2c & 2(b-c^2) \\ 1 & b+c \end{vmatrix}$$
$$D_3 = \begin{vmatrix} 1+2c & 2(b-c^2) & 0 \\ 1 & b+c & 0 \\ 0 & 1+2c & 2(b-c^2) \end{vmatrix}$$

should be positive. This requires that

$$b < \frac{c(1+4c)}{1-2c} \quad \text{if} \quad c < 1/2$$
$$b > \frac{c(1+4c)}{1-2c} \quad \text{if} \quad c > 1/2$$

With tilt, no axial conduction ($a \neq 0$, $c = 0$)

The dynamical system (7.47)-(7.49) simplifies to

$$\frac{dx}{dt} = y - x$$
$$\frac{dy}{dt} = a - xz$$
$$\frac{dz}{dt} = -b + xy$$

The critical points are $\pm(\sqrt{b}, \sqrt{b}, a/\sqrt{b})$. The linear stability of the point P^+ given by $(\sqrt{b}, \sqrt{b}, a/\sqrt{b})$ will be analyzed. From equation (7.58), the solutions of

$$\begin{vmatrix} -(1+\lambda) & 1 & 0 \\ -a/\sqrt{b} & -\lambda & -\sqrt{b} \\ \sqrt{b} & \sqrt{b} & -\lambda \end{vmatrix} = 0$$

are the eigenvalues. This simplifies to

$$\lambda^3 + \lambda^2 + \lambda(b + \frac{a}{\sqrt{b}}) + 2b = 0 \tag{7.60}$$

For stability the Hurwitz criteria require all coefficients to be positive, which they are. The determinants

$$D_1 = 1$$
$$D_2 = \begin{vmatrix} 1 & 2b \\ 1 & b + a/\sqrt{b} \end{vmatrix}$$
$$D_3 = \begin{vmatrix} 1 & 2b & 0 \\ 1 & b + a/\sqrt{b} & 0 \\ 0 & 1 & 2b \end{vmatrix}$$

should also be positive. This gives the condition $(b + a/\sqrt{b}) - 2b > 0$, from which, we have

$$a > b^{3/2} \tag{7.61}$$

for stability. The stable and unstable region for P^+ is shown in Figure 7.24. Also shown is the stability of the critical point P^- with coordinates $-(\sqrt{b}, \sqrt{b}, a/\sqrt{b})$. The dashed circles are of radius $G/2$, and the angleof tile ϕ is also indicated. Using equations (7.44) and (7.45), the stability condition (7.61) can be written as

$$\frac{\sin\phi}{\cos^{3/2}\phi} > \left(\frac{G}{2}\right)^{1/2}$$

As a numerical example, for the value of G in equation (7.33), P^+ is stable for the tilt angle range $\phi > 7.7°$, and P^- is stable for $\phi < -7.7°$. In fact, for $G \ll 1$, the stability condition for P^+ can be approximated as

$$\phi > \left(\frac{G}{2}\right)^{1/2}$$

The same information can be shown in slightly different coordinates. Using $\bar{x} = \sqrt{b}$ for P^+ and equation (7.45), we get

$$\frac{G}{2} = \frac{\bar{x}^2}{\cos\phi}$$

The stability condition (7.61) thus becomes

$$\tan\phi < \bar{x}$$

The stability regions for both $P+$ and P^- are shown in Figure 7.25.

The loss of stability is through imaginary eigenvalues. In fact, for P^+, substituting $a = b^{3/2}$ in equation (7.60), the equation can be factorized to give the three eigenvalues $-1, \pm i\sqrt{2b}$. Thus the nondimensional radian frequency of the oscillations in the unstable range is approximately $\sqrt{2b}$.

The effect of a small nonzero axial conduction parameter c is to alter the Figure 7.61 in the zone $0 < b < c$.

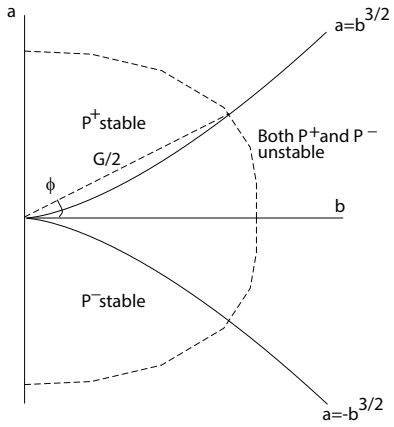

Figure 7.24: Stability of critical points P^+ and P^- in (b, a) space.

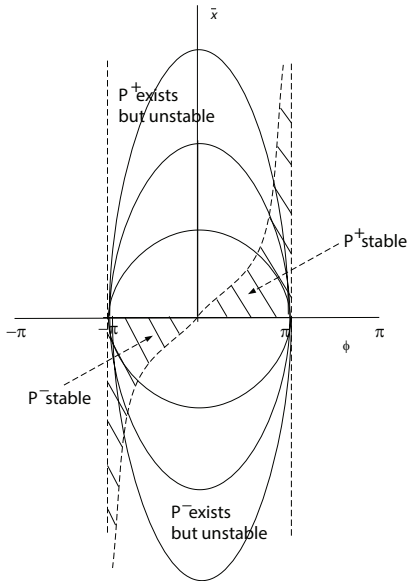

Figure 7.25: Stability of critical points P^+ and P^- in $(\phi, \bar{x})$ space.

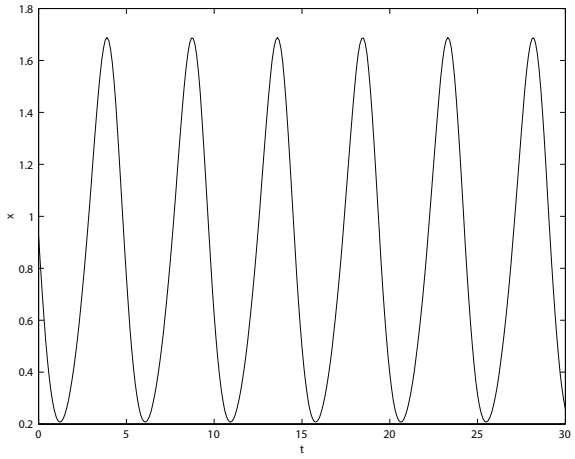

Figure 7.26: x-t for $a = 0.9$, $b = 1$.

7.7.2 Nonlinear analysis

Numerical

Let us choose $b = 1$, and reduce a. Figures 7.26 and 7.27 show the x-t and phase space representation for $a = 0.9$, Figures 7.28 and 7.29 for $a = 0.55$, and Figures 7.30 and 7.31 for $a = 0.53$. The strange attractor is shown in Figures 7.32 and 7.33. Comparison of the three figures in Figures 7.34 shows that vestiges of the shape of the closed curves for $a = -0.9$ and $a = 0.9$ can be seen in the trajectories in $a = 0$.

Analytical

See Appendix.

7.7.3 Known wall temperature

The heating is now convective with a heat transfer coefficient U, and an external temperature of $T_w(s)$. Thus,

$$q = PU(T - T_w)$$

Neglecting axial conduction

$$\frac{P\alpha}{\rho_0 A}\bar{V} = \frac{\beta}{L}\int_0^L \bar{T}(s)\tilde{g}(s)\, ds \tag{7.62}$$

$$\bar{V}\frac{d\bar{T}}{ds} = \gamma\left[\bar{T} - T_w(s)\right] \tag{7.63}$$

where $\gamma = UP/\rho_0 Ac^2$. Multiplying the second equation by $e^{-\gamma s/\bar{V}}/\bar{V}$, we get

$$\frac{d}{ds}\left(e^{-\gamma s/\bar{V}}\bar{T}\right) = -\frac{\gamma}{\bar{V}}e^{-\gamma s/\bar{V}}T_w$$

[2]The sign of γ appears to be wrong.

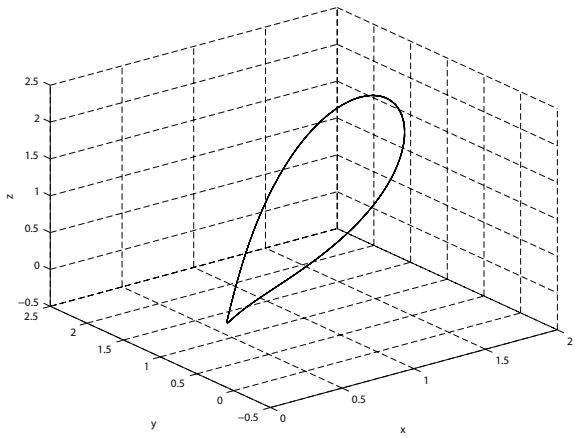

Figure 7.27: Phase-space trajectory for $a = 0.9$, $b = 1$.

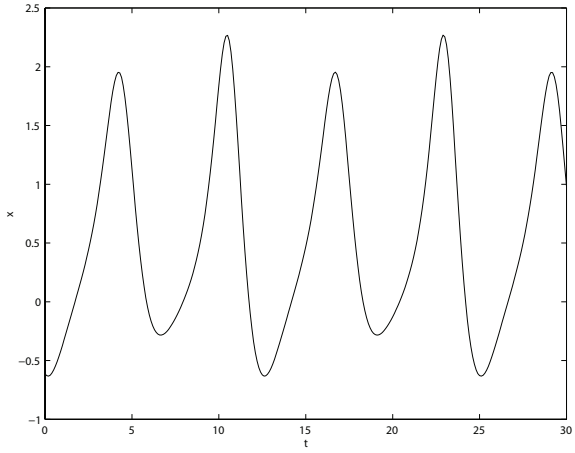

Figure 7.28: x-t for $a = 0.55$, $b = 1$.

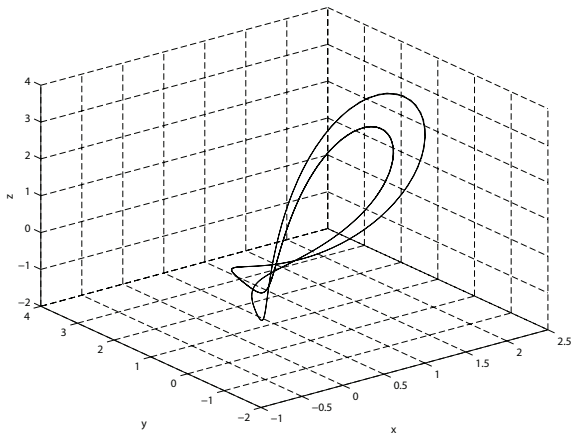

Figure 7.29: Phase-space trajectory for $a = 0.55$, $b = 1$.

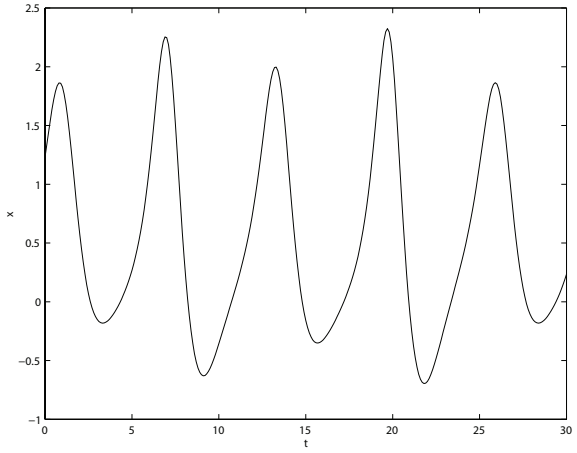

Figure 7.30: x-t for $a = 0.53$, $b = 1$.

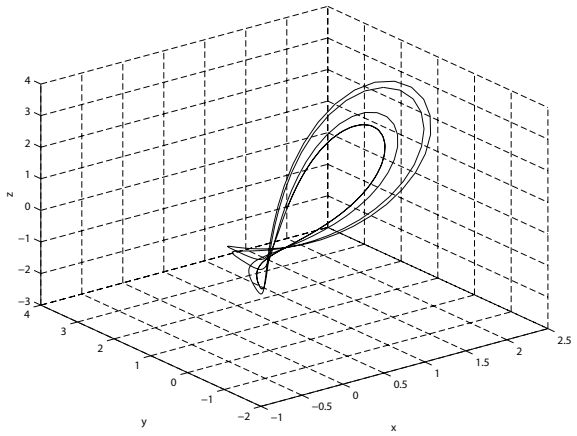

Figure 7.31: Phase-space trajectory for $a = 0.53$, $b = 1$.

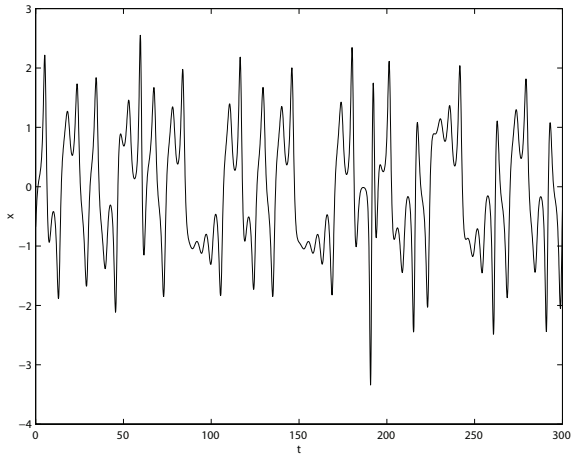

Figure 7.32: x-t for $a = 0$, $b = 1$.

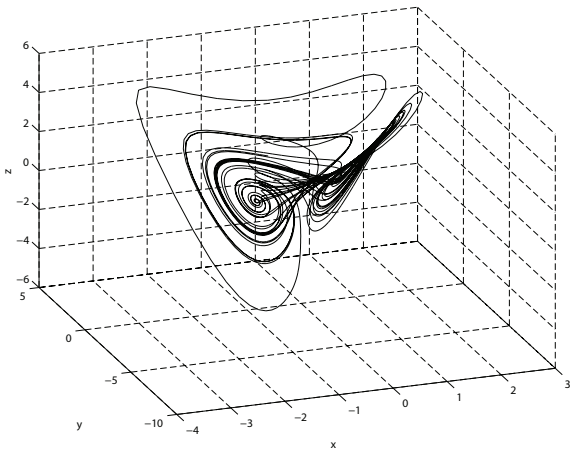

Figure 7.33: Phase-space trajectory for $a = 0$, $b = 1$.

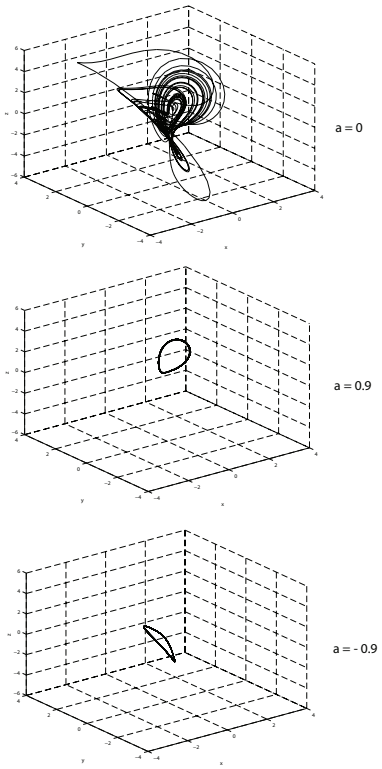

Figure 7.34: Phase-space trajectories for $b = 1$.

Integrating, we get

$$\bar{T} = e^{\gamma s/\bar{V}} \left[-\frac{\gamma}{\bar{V}} \int_0^s e^{-\gamma s'/\bar{V}} T_w(s') \, ds' + T_0 \right]$$

Since $\bar{T}(L) = \bar{T}(0)$, we get

$$T_0 = \frac{\gamma}{\bar{V}} \, \frac{e^{\gamma L/\bar{V}} \int_0^L e^{-\gamma s'/\bar{V}} T_w(s') \, ds'}{e^{\gamma L/\bar{V}} - 1}$$

The velocity is obtained from

$$\frac{P\alpha}{\rho_0 A} \bar{V} = \frac{\beta}{L} \int_0^L \left[e^{\gamma s/\bar{V}} \left\{ -\frac{\gamma}{\bar{V}} \int_0^s e^{-\gamma s'/\bar{V}} T_w(s') \, ds' + T_0 \right\} \right] \tilde{g}(s) \, ds$$

This is a transcendental equation that may have more than one real solution.

Example 7.8

Show that there is no motion if the wall temperature is uniform.

Take T_w to be a constant. Then equation (7.63) can be written as

$$\frac{d(\bar{T} - T_w)}{\bar{T} - T_w} = \frac{\gamma}{\bar{V}} \, ds$$

The solution to this is

$$\bar{T} = T_w + K \, e^{\gamma s/\bar{V}}$$

where K is a constant. Continuity of T at $s = 0$ and $s = L$ gives $K = 0$. Hence $T = T_w$, and, from equation (7.62), $\bar{V} = 0$.

Assume the wall temperature to be

$$T_w(s) = -\sin(2\pi s - \phi)$$

The temperature field is

$$T = \frac{b}{r_2 - r_1} \left(\frac{\cos(2\pi s - \phi)}{2\pi(1 + r_2^2/4\pi^2)} \right) - \left(\frac{\cos(2\pi s - \phi)}{2\pi(1 + r_1 62/4\pi^2)} \right)$$

Bibliography

A.S. Dorfman, *Conjugate Problems in Convective Heat Transfer,* CRC Press, Boca Raton, FL, 2010.

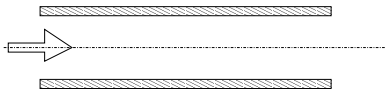

Figure 7.35: Flow in tube with non-negligible wall thickness.

Problems

1. Determine the single duct solutions for heat loss by radiation $q = P\epsilon\sigma(T_{sur}^4 - T^4)$.
2. A sphere, initially at temperature T_i is being cooled by natural convection to fluid at T_∞. Churchill's correlation for natural convection from a sphere is

$$\bar{Nu} = 2 + \frac{0.589\ Ra_D^{1/4}}{\left[1 + (0.469/Pr)^{9/16}\right]^{4/9}},$$

where

$$Ra_D = \frac{g\beta(T_s - T_\infty)D^3}{\nu\alpha}.$$

Assume that the temperature within the sphere $T(t)$ is uniform, and that the material properties are all constant. Derive the governing equation, and find a two-term perturbation solution.

3. The velocity field, $u(r)$, for forced convection in a cylindrical porous medium is given by

$$u'' + r^{-1}u' - s^2u + s^2\ Da = 0,$$

where s and the Darcy number Da are parameters. A WKB solution for small Da has been reported as[3]

$$u = Da\left[1 - \frac{e^{-s(1-r)}}{\sqrt{r}}\right].$$

Re-do to check the analysis.

4. Consider one-dimensional steady-state flow along a pipe with advection and conduction in the fluid and lateral convection from the side. The fluid inlet and outlet temperatures given. Use the nondimensional version of the governing equation to find the inner and outer matched temperature distributions if the fluid thermal conductivity is small.
5. Plot the exact analytical and the approximate boundary layer solutions for Problem 4 for a small value of the conduction parameter.
6. Show that no solution is possible in Problem 4 if the boundary layer is assumed to be on the wrong side.
7. Consider one-dimensional unsteady flow in a tube with a non-negligible wall thickness, as shown in Fig. E.34. There is conduction along the fluid as well as along the wall of the tube. There is also convection from the outer surface of the tube to the environment as well as from its inner surface to the fluid. Find the governing equations and their boundary conditions. Nondimensionalize.
8. Consider the hydrodynamic and thermal boundary layers in a flow over a flat plate at constant temperature. Starting from the boundary layer equations

$$\frac{\partial u}{\partial x} + \frac{\partial v}{\partial y} = 0 \tag{7.64}$$

$$u\frac{\partial u}{\partial x} + v\frac{\partial u}{\partial y} = \nu\frac{\partial^2 u}{\partial y^2} \tag{7.65}$$

$$u\frac{\partial T}{\partial x} + v\frac{\partial T}{\partial y} = \alpha\frac{\partial^2 T}{\partial y^2} \tag{7.66}$$

change to variables $f(\eta)$ and $T^*(\eta)$ and derive the boundary layer equations

$$2f''' + ff'' = 0 \tag{7.67}$$

$$T^{*\prime\prime} + \frac{Pr}{2}fT^{*\prime} = 0 \tag{7.68}$$

[3]K. Hooman and A.A. Ranjbar-Kani, Forced convection in a fluid-saturated porous-medium tube with isoflux wall, International Communcications in Heat and Mass Transfer, Vol. 30, No. 7, pp. 1015–1026, 2003.

and the boundary conditions. Solve equations (7.67) and (7.68) numerically by the shooting method for different Pr and compare with results in the literature.

9. For Problem 1, derive the momentum and energy integral equations. Using cubic expansions for u/u_∞ and T^*, derive expressions for the boundary layer thicknesses. [Explain Momentum integral method?]

10. For natural convection near a vertical plate, show that the governing boundary layer equations

$$\frac{\partial u}{\partial x} + \frac{\partial v}{\partial y} = 0$$
$$u\frac{\partial u}{\partial x} + v\frac{\partial u}{\partial y} = g\beta(T - T_\infty) + \nu\frac{\partial^2 u}{\partial y^2}$$
$$u\frac{\partial T}{\partial x} + v\frac{\partial T}{\partial y} = \alpha\frac{\partial^2 T}{\partial y^2}$$

can be reduced to

$$f''' + 3ff'' - 2(f')^2 + T^* = 0 \tag{7.69}$$
$$T^{*''} + 3\ Pr\ f\ T^{*'} = 0 \tag{7.70}$$

with appropriate boundary conditions. Solve equations (7.69) and (7.70) numerically by the shooting method for different Pr and compare with results in the literature.

11. Find the pressure distributions for the different cases of the square loop problem.

12. Consider the same square loop but tilted through an angle T^* where $0 \le T^* < 2\pi$. There is constant heating between points a and c, and constant cooling between e and g. For the steady-state problem, determine the temperature distribution and the velocity as a function of T^*. Plot (a) typical temperature distributions for different tilt angles, and (b) the velocity as a function of tilt angle.

13. Find the steady-state temperature field and velocity for known heating if the loop has a variable cross-sectional area $A(s)$.

14. Find the temperature field and velocity for known heating if the total heating is not zero.

15. Find the velocity and temperature fields for known heating if the heating and cooling takes place at two different points. What the condition for the existence of a solution?

16. What is the effect on the known heat rate solution of taking a power-law relationship between the frictional force and the fluid velocity?

17. For known wall temperature heating, show that if the wall temperature is constant, the temperature field is uniform and the velocity is zero.

18. Study the steady states of the toroidal loop with known wall temperature including nondimensionalization of the governing equations, axial conduction and tilting effects, multiplicity of solutions and bifurcation diagrams. Illustrate typical cases with appropriate graphs.

19. For a thin, vertical pipe compare the wall shear stress to mean flow velocity relation obtained from a two-dimensional analysis to that from Poiseuille flow.

20. Find the combination of fluid parameters that determines the rate of heat transfer from a closed loop with known temperature distribution. Compare the cooling rate achieved by an ionic liquid to water in the same loop and operating under the same temperature difference.

21. Consider a tall natural circulation loop shown in Fig. 7.36 consisting of two vertical pipes of circular cross sections. The heating pipe has a diameter D, and that of the cooling side is $2D$. The heat rate per unit length coming in and going out are both q. Find the steady state velocity in the loop. Neglect the small horizontal sections and state your other assumptions.

22. Set up a controller for PID control of the velocity x to a given value, x_s, in the toroidal natural convection loop equations

$$\frac{dx}{dt} = y - x \tag{7.71}$$
$$\frac{dy}{dt} = a\sin\phi - xz \tag{7.72}$$
$$\frac{dz}{dt} = -b\cos\phi + xy \tag{7.73}$$

where a and b are held constant. Use the tilt angle ϕ as control input, and show numerical results.

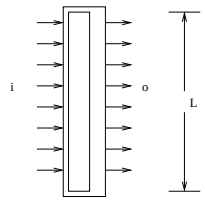

Figure 7.36: Tall natural circulation loop.

23. For a duct of varying area $A(s)$, show that

$$\rho\left(\frac{\partial V}{\partial t} + V\frac{\partial V}{\partial s}\right) + \frac{P}{A}\,\tau_w = 0.$$

where τ_w is the wall stress and P is the sectional perimeter.

Chapter 8

Multidimensional conduction

8.1 Separation of variables

Steady-state conduction in a rectangular plate.

$$\nabla^2 T = 0$$

Let $T(x, y) = X(x)Y(y)$. See Table 8.1.

8.1.1 Similarity variable

$$\frac{\partial T}{\partial t} = \alpha \frac{\partial^2 T}{\partial x^2}$$

8.2 Steady-state problems

See [216].

8.3 Transient problems

8.3.1 Two-dimensional fin

The governing equation is

$$c\rho dx\ dyL\frac{\partial T}{\partial t} = Lk\left(\frac{\partial^2 T}{\partial x^2} + \frac{\partial^2 T}{\partial y^2}\right) - hdx\ dy(T - T_\infty)$$

which simplifies to

$$\frac{1}{\alpha}\frac{\partial T}{\partial t} = \frac{\partial^2 T}{\partial x^2} + \frac{\partial^2 T}{\partial y^2} - m^2(T - T_\infty)$$

where $m^2 = h/kL$, the Biot number.

Table 8.1: Summary of PDE solutions with separation of variables

Equation type $\longrightarrow$	*Parabolic*	*Hyperbolic*	*Elliptic*
Equation	$\alpha \dfrac{\partial^2 u}{\partial x^2} = \dfrac{\partial u}{\partial t}$	$a^2 \dfrac{\partial^2 u}{\partial x^2} = \dfrac{\partial^2 u}{\partial t^2}$	$\dfrac{\partial^2 u}{\partial x^2} + \dfrac{\partial^2 u}{\partial y^2} = 0$
Name of equation	Heat equation	Wave equation	Laplace's equation
Variables	$u(x,t)$	$u(x,t)$	$u(x,y)$
Independent variable 1	$0 \le x \le L$	$0 \le x \le L$	$0 \le x \le L_x$
Independent variable 2	$t \ge 0$	$t \ge 0$	$0 \le y \le L_y$
Condition 1(a)	$u(0,t) = 0$ (homogeneous)	$u(0,t) = 0$ (homogeneous)	$u(0,y) = 0$ (homogeneous)
Condition 1(b)	$u(L,t) = 0$ (homogeneous)	$u(L,t) = 0$ (homogeneous)	$u(L_x,y) = 0$ (homogeneous)
Condition 2(a)	$u(x,0) = f(x)$ (inhomogeneous)	$u_t(x,0) = 0$ (homogeneous)	$u(x,0) = 0$ (homogeneous)
Condition 2(b)	–	$u(x,0) = f(x)$ (inhomogeneous)	$u(x,L_y) = f(x)$ (inhomogeneous)
Separation of variables	$u(x,t) = X(x)T(t)$	$u(x,t) = X(x)T(t)$	$u(x,y) = X(x)Y(y)$
ODE 1	$X'' + \lambda^2 X = 0$	$X'' + \lambda^2 X = 0$	$X'' + \lambda^2 X = 0$
Homogeneous conditions	$X(0) = X(L) = 0$	$X(0) = X(L) = 0$	$X(0) = X(L_x) = 0$
Eigenvalues	$\lambda_n = \dfrac{n\pi}{L},\ n = 1,2,3,\ldots$	$\lambda_n = \dfrac{n\pi}{L},\ n = 1,2,3,\ldots$	$\lambda_n = \dfrac{n\pi}{L_x},\ n = 1,2,3,\ldots$
Eigenfunctions	$X_n = A_n \sin(\lambda_n x)$	$X_n = A_n \sin(\lambda_n x)$	$X_n = A_n \sin(\lambda_n x)$
ODE 2	$T_n' + \alpha\lambda_n^2 T_n = 0$	$T_n'' + a^2\lambda_n^2 T_n = 0$	$Y_n'' - \lambda_n^2 Y_n = 0$
General solution	$T_n = B_n \exp(-\alpha\lambda_n^2 t)$	$T_n = B_n \cos(a\lambda_n t) + C_n \sin(a\lambda_n t)$	$Y_n = B_n \cosh(\lambda_n y) + C_n \sinh(\lambda$
Homogeneous condition	–	$T_n'(0) = 0 \Rightarrow C_n = 0$	$Y_n(0) = 0 \Rightarrow B_n = 0$
Solution	$T_n = B_n \exp(-\alpha\lambda_n^2 t)$	$T_n = B_n \cos(a\lambda_n t)$	$Y_n = C_n \sinh(\lambda_n y)$
Typical solution	$u_n = c_n \sin(\lambda_n x) \exp\left(-\alpha\lambda_n^2 t\right)$	$u_n = c_n \sin(\lambda_n x) \cos(a\lambda_n t)$	$u_n = c_n \sin(\lambda_n x) \sinh(\lambda_n y)$
General solution	$u = \sum_{n=1}^{\infty} u_n$	$u = \sum_{n=1}^{\infty} u_n$	$u = \sum_{n=1}^{\infty} u_n$
Inhomogeneous condition	$f(x) = \sum_{n=1}^{\infty} c_n \sin(\lambda_n x)$	$f(x) = \sum_{n=1}^{\infty} c_n \sin(\lambda_n x)$	$f(x) = \sum_{n=1}^{\infty} c_n \sin(\lambda_n x) \sinh(\lambda_n L$
Euler-Fourier formula	$c_n = \dfrac{2}{L}\int_0^L f(x) \sin(\lambda_n x)\ dx$	$c_n = \dfrac{2}{L}\int_0^L f(x) \sin(\lambda_n x)\ dx$	$c_n = \dfrac{2}{L_x \sinh(\lambda_n L_y)} \int_0^{L_x} f(x)$

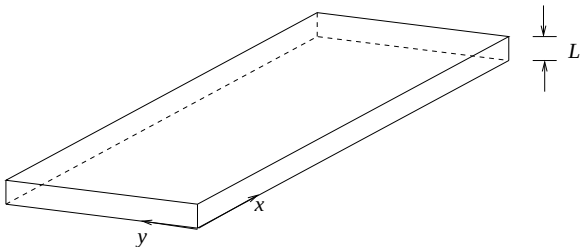

Figure 8.1: Two-dimensional fin.

In the steady state

$$\frac{\partial^2 T}{\partial x^2} + \frac{\partial^2 T}{\partial y^2} - m^2(T - T_\infty)$$

Consider a square of unit side with $\theta = T - T_\infty$ being zero all around, except for one edge where it is unity.

Let

$$\theta(x, y) = X(x)Y(y)$$

so that

$$\frac{1}{X}\frac{d^2X}{dx^2} = -\frac{1}{X}\frac{d^2Y}{dy^2} + m^2 = -\lambda^2$$

This leads to one equation

$$\frac{d^2X}{dx^2} + \lambda^2 X = 0$$

with $X(0) = X(1) = 1$. Thus

$$X(x) = A\sin\lambda x + B\cos\lambda x$$

where due to the boundary conditions, $B = 0$ and $\lambda = n\pi$, $n = 1, 2, \ldots$. Another equation is

$$\frac{d^2Y}{dy^2} - \left(m^2 + \lambda^2\right) Y = 0$$

with

$$Y(y) = A\sinh\sqrt{m^2 + n^2\pi^2}y + B\cosh\sqrt{m^2 + n^2\pi^2}y$$

The condition $Y(0) = 0$ gives $B = 0$. Thus

$$\theta(x, y) = \sum A_n \sin n\pi x \sinh\sqrt{m^2 + n^2\pi^2}y$$

Example 8.1

Find the steady state temperature distribution in a square plate with uniform heat generation and uniform temperature at the boundary.

Variables: $T(x,y)$ = temperature distribution; (x,y) = coordinates of a point on the plate with x and y coordinates parallel to the sides and the origin at one corner; Q_g = heat generation per unit volume; k = thermal conductivity of plate.

The problem

$$\frac{\partial^2 T}{\partial x^2} + \frac{\partial^2 T}{\partial y^2} = -\frac{Q_g}{k},$$
$$\text{BCs:} \quad T(0,y) = T(L,y) = T(x,0) = T(x,L) = T_0,$$

can be written as

$$\frac{\partial^2 \theta}{\partial X^2} + \frac{\partial^2 \theta}{\partial Y^2} = -1,$$
$$\text{BCs:} \quad \theta(0,Y) = \theta(1,Y) = \theta(X,0) = \theta(X,1) = 0,$$

where

$$X = \frac{x}{L}, \quad Y = \frac{y}{L}, \quad \theta = \frac{Q_g}{k}(T - T_0).$$

(a) *First method*

The equation can be written as

$$\frac{\partial^2 \Theta}{\partial X^2} + \frac{\partial^2 \Theta}{\partial Y^2} = 0,$$

where

$$\Theta = \theta + \frac{Q_g}{2k} X^2.$$

with boundary conditions

$$\Theta(0,Y) = 0,\ \Theta(X,0) = \frac{Q_g}{2k} X^2,\ \Theta(L,y) = \frac{g}{2k},\ \Theta(X,1) = \frac{Q_g}{2k} X^2,$$

This can be split up into four problems: the same equation with each one of the following boundary conditions.

$$\Theta(0,Y) = 0,\ \Theta(X,0) = 0,\ \Theta(L,y) = 0,\ \Theta(X,1) = 0,$$
$$\Theta(0,Y) = 0,\ \Theta(X,0) = \frac{Q_g}{2k} X^2,\ \Theta(L,y) = 0,\ \Theta(X,1) = 0,$$
$$\Theta(0,Y) = 0,\ \Theta(X,0) = 0,\ \Theta(L,y) = \frac{Q_g}{2k},\ \Theta(X,1) = 0,$$
$$\Theta(0,Y) = 0,\ \Theta(X,0) = 0,\ \Theta(L,y) = 0,\ \Theta(X,1) = \frac{Q_g}{2k} X^2.$$

Each of the four problems can be solved by separation of variables, and the results added.

(b) *Second method*[1]

The solution can be written as

$$\theta(X,Y) = \theta_h(X,Y) + \theta_p(X,Y),$$

where

$$\frac{\partial^2 \theta_h}{\partial X^2} + \frac{\partial^2 \theta_h}{\partial Y^2} = 0, \qquad \theta_h = \text{homogeneous solution}$$
$$\frac{\partial^2 \theta_p}{\partial X^2} + \frac{\partial^2 \theta_p}{\partial Y^2} = -1, \qquad \theta_p = \text{particular solution.}$$

[1]From P.A. Ramachandran, Advanced Transport Phenomena: Analysis, Modeling, and Computations, Cambridge University Press, Cambridge, U.K., 2014.

The particular solution is not unique. For example one can take

$$\theta_p = \frac{1}{2}(1 - x^2).$$

From separation of variables, the homogeneous solution is

$$\theta_h = \sum_{n=0}^{\infty} A_n \cosh(\lambda y) \cos(\lambda x).$$

The complete solution is

$$\theta = \frac{1}{2}(1 - x^2) + \sum_{n=0}^{\infty} A_n \cosh(\lambda y) \cos(\lambda x),$$

where

$$\lambda = \frac{\pi}{2}(n + 1).$$

From the Fourier expansion of the boundary condition at $y = 1$

$$A_n = -\frac{16h^2}{n^3\pi^3} \frac{\sin(n\pi/2)}{\cosh(n\pi/2)}$$

(b) *Third method*[2]

$$T(x, y) = \sum_{n=1}^{\infty} \{C_n \sin \lambda_n x \cosh \lambda_n y\} + \frac{gL^2}{2k} \left\{ \frac{x}{L} - \left(\frac{x}{L}\right)^2 \right\}$$

Example 8.2

Computer problem: Use a finite difference method to calculate the temperature field in the previous problem (choose specific numerical values of the constants).

8.4 Radiating fins

8.5 Non-Cartesian coordinates

Toroidal, bipolar.

Shape factor.

Moving boundary problem at a corner.

Bibliography

M.N. Ozisik, *Heat Conduction,* John Wiley, 1980.

[2]From D.W. Hahn and M.N. ́Ozişik, Heat Conduction, John Wiley, New York, 2012.

Problems

1. Show that the separation of variables solution for $\nabla^2 T = 0$ for a rectangle can also be obtained through an eigenfunction expansion procedure.
2. Consider steady-state conduction in bipolar coordinates shown in

   http://mathworld.wolfram.com/BipolarCylindricalCoordinates.html

   with $a = 1$. The two cylindrical surfaces shown as $v = 1$ and $v = 2$ are kept at temperatures T_1 and T_2, respectively. Sketch the geometry of the annular material between $v = 1$ and $v = 2$ and find the temperature distribution in it by solving the Laplace's equation $\nabla^2 T = 0$.
3. Set up and solve a conduction problem similar to Problem 2, but in parabolic cylindrical coordinates. Use Morse and Feshbach's notation as shown in

   http://www.math.sdu.edu.cn/mathency/math/p/p059.htm
4. Consider an unsteady one-dimensional fin of constant area with base temperature known and tip adiabatic. Use the eigenfunction expansion method to reduce the governing equation to an infinite set of ODEs and solve.
5. Consider conduction in a square plate with Dirichlet boundary conditions. Find the appropriate eigenfunctions for the Laplacian operator for this problem.
6. Consider a square plate of side 1 m. The temperatures on each side are (a) 10°C, (b) 10°C, (c) 10°C, and (d) $10 + \sin(\pi x)$ °C, where x is the coordinate along the edge. Find the steady-state temperature distribution analytically. Write a computer program to do the problem numerically using finite differences and compare with the analytical results. Choose different grid sizes and show convergence.
7. A plane wall initially at a uniform temperature is suddenly immersed in a fluid at a different temperature. Find the temperature profile as a function of time. Assume all parameter values to be unity. Write a computer program to do the problem numerically using finite differences and compare with the analytical results.

Chapter 9

Multidimensional convection

See [216].

9.1 Governing equations

The following equations are for constant density and viscosity. The sources (or drivers) are terms that generate momentum or heat. The boundary conditions can also be drivers.

Mass:

$$\boldsymbol{\nabla} \cdot \boldsymbol{V} = 0. \tag{9.1}$$

Momentum:

$$\rho \, \frac{\partial \boldsymbol{V}}{\partial t} + \rho \, \boldsymbol{V} \cdot \boldsymbol{\nabla} \boldsymbol{V} = \boldsymbol{\nabla} \cdot \boldsymbol{\tau} + \rho \, \boldsymbol{f},$$

where $\boldsymbol{f}$ is the body force per unit mass. A common case is gravity for which $\boldsymbol{f} = \boldsymbol{g}$, the acceleration due to gravity. For a Newtonian fluid

$$\boldsymbol{\tau} = -p\boldsymbol{I} + \mu\Big(\boldsymbol{\nabla} \boldsymbol{V} + (\boldsymbol{\nabla} \boldsymbol{V})^T\Big),$$

which gives the Navier-Stokes equation

$$\underbrace{\rho \, \frac{\partial \boldsymbol{V}}{\partial t}}_{\text{accumulation}} + \underbrace{\rho \, \boldsymbol{V} \cdot \boldsymbol{\nabla} \boldsymbol{V}}_{\text{advection}} = \underbrace{\mu \nabla^2 \boldsymbol{V}}_{\text{diffusion}} \underbrace{- \boldsymbol{\nabla} p + \tilde{\rho} \, \boldsymbol{f}}_{\text{sources}}, \tag{9.2}$$

where

$$\tilde{\rho} = \begin{cases} \rho\big[1 - \beta(T - T_{\text{ref}})\big] & \text{for natural convection} \\ \rho & \text{otherwise} \end{cases}.$$

The Boussinesq approximation in natural convection allows for density change due to temperature in the body force term while keeping it constant elsewhere.

Energy: For a Fourier fluid

$$\underbrace{\rho c \frac{\partial T}{\partial t}}_{\text{accumulation}} + \underbrace{\rho c \boldsymbol{V}\cdot\boldsymbol{\nabla} T}_{\text{advection}} = \underbrace{k\nabla^2 T}_{\text{diffusion}} + \underbrace{Q_g + \Phi}_{\text{sources}}, \tag{9.3}$$

where Q_g and

$$\begin{aligned}\Phi &= \mu\Big(\boldsymbol{\nabla V} + \big(\boldsymbol{\nabla V}\big)^T\Big) : \boldsymbol{\nabla V} \\ &= \mu\left(\frac{\partial V_i}{\partial x_j} + \frac{\partial V_j}{\partial x_i}\right)\frac{\partial V_i}{\partial x_j}\end{aligned}$$

are the generation of heat and viscous dissipation per unit volume respectively.

9.1.1 Nondimensionalization

Using x_c and t_c as the characteristic length and time scales, respectively, we have

$$t = t^* t_c; \quad x = x^* x_c,$$

so that Eqs. (9.1), (9.2), and (9.3) for a constant density fluid become

$$\begin{aligned}\boldsymbol{\nabla}^*\cdot\boldsymbol{V}^* &= 0,\\ \frac{\partial \boldsymbol{V}^*}{\partial t^*} + \boldsymbol{V}^*\cdot\boldsymbol{\nabla}^*\boldsymbol{V}^* &= \frac{1}{Re}\nabla^{*2}\boldsymbol{V}^* - \boldsymbol{\nabla}^* p^* + \boldsymbol{f}^*,\\ \frac{\partial T^*}{\partial t^*} + \boldsymbol{V}^*\cdot\boldsymbol{\nabla}^* T^* &= \frac{1}{Pe}\nabla^{*2} T^* + Q_g^* + \Phi^*,\\ \frac{\partial T^*}{\partial t^*} + \boldsymbol{V}^*\cdot\boldsymbol{\nabla}^* T^* &= \frac{1}{Pe}\nabla^{*2} T^* + Q_g^* + \frac{Ec}{Re}\Phi^*,\end{aligned}$$

where

$$\begin{gathered}\boldsymbol{V} = \boldsymbol{V}^* V_c; \quad V_c = x_c/t_c; \quad p = p^*\rho x_c^2/t_c^2;\\ \boldsymbol{\nabla} = \boldsymbol{\nabla}^*/x_c; \quad T^* = (T - T_{ref})/\Delta T; \quad \boldsymbol{f}^* = \frac{t_c^2}{x_c}\,\frac{\tilde{\rho}}{\rho}\boldsymbol{f};\\ Q_g^* = \frac{t_c}{\rho c \Delta T} Q_g; \quad \Phi^* = \Big(\boldsymbol{\nabla}^*\boldsymbol{V}^* + \big(\boldsymbol{\nabla}^*\boldsymbol{V}^*\big)^T\Big) : \boldsymbol{\nabla}^*\boldsymbol{V}^*;\end{gathered}$$

$$Re = \frac{V_c x_c}{\nu}\ \text{(Reynolds number)};\ Pe = \frac{V_c x_c}{\alpha}\quad \text{(Péclet number)}; Ec = \frac{V_c^2}{c\Delta T}\quad \text{(Eckert number)}.$$

The momentum and thermal diffusivities are $\nu = \mu/\rho$ and $\alpha = k/\rho c$ respectively. Sometimes $Re\ Pr$ is used instead of Pe, where the Prandtl number $Pr = \nu/\alpha$.

9.1.2 Advection and diffusion

Advection is transfer that is due to bodily motion of the material. The relation between the transfer length ℓ_a and the transfer time t_a is the velocity V so that $\ell_a = V t_a$. Both solids and fluids can thus transfer heat due to advection. Diffusion, on the other hand, is transfer due to molecular motion. The property that governs its rate is the thermal diffusivity α. The diffusion length ℓ_d and time t_d are related by $\ell_d^2 = \alpha t_d$.

Advection and diffusion can both be present. Consider a cube of fluid of side L that is at a higher temperature ΔT than the rest. Assume first that the cube moves at velocity V without the heat diffusing. The rate of heat transfer due to advection is then

$$Q_{adv} = (\rho L^3)(c\Delta T)(V/L).$$

If, on the other hand, the cube did not move and the heat merely diffused, the rate of heat transfer by conduction would be of the order of

$$Q_{diff} = k(6L^2)(\Delta T/L).$$

The ratio is

$$\begin{aligned}\frac{Q_{adv}}{Q_{diff}} &= \frac{(\rho L^3)(c\Delta T)(V/L)}{k(6L^2)(\Delta T/L)}, \\ &= \frac{1}{6}\frac{VL}{\alpha}, \\ &= \frac{Pe}{6}.\end{aligned}$$

As a numerical example, for air with $V = 1$ m/s, $L = 0.1$ m, $Pe = 5000$. In forced convection it is common for the advective heat transfer to be much larger than the diffusive.

Similar diffusion processes also occur with momentum (for which the appropriate ratio is the Reynolds number) and mass (mass Péclet number). The ratio of the momentum to heat transfer is the Prandtl number $Pr = \nu/\alpha$; the ratio of the thermal to mass diffusion is the Lewis number Le. Turbulence greatly enhances diffusion, and turbulent diffusivity is much higher than its laminar counterpart.

9.2 Flows

9.2.1 High Reynolds number flows

See Fig. 9.1. The time t taken by a fluid particle to traverse a distance x along the plate is roughly x/V. In this time interval the lateral spread of momentum due to diffusion is the hydrodynamic boundary layer thickness $\delta \sim (\nu x/V)^{1/2}$. The thermal boundary layer thickness is $\delta_T \sim (\alpha x/V)^{1/2}$.

In a pipe there is growth of the boundary layers from all sides until they meet at the centerline. The hydrodynamic and thermal entrance lengths for developing flow in a pipe of diameter D are thus $x_{e,h} \sim (D/2)^2 V/\nu$ and $x_{e,t} \sim (D/2)^2 V/\alpha$, respectively. Empirical relations are

$$\frac{x_{e,h}}{D} = \begin{cases} 0.05(VD/\nu) & \text{laminar} \\ 1.359(VD/\nu)^{1/4} & \text{turbulent} \end{cases}$$

and

$$\frac{x_{e,t}}{D} = \begin{cases} 0.05(VD/\nu)\ Pr & \text{laminar} \\ 10 & \text{turbulent} \end{cases}$$

Beyond this point the flow is fully developed hydrodynamically or thermally.

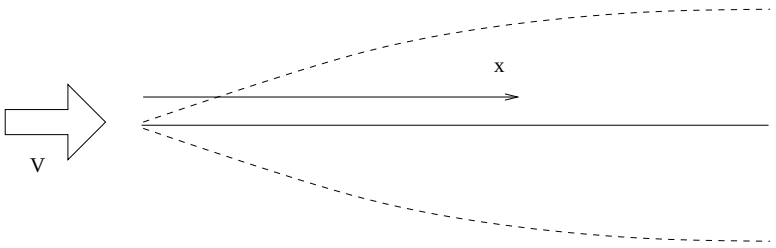

Figure 9.1: Boundary layer on a flat plate.

9.2.2 Low Reynolds number flows

Example 9.1

(From Incropera et al.) 20 °C air at 40 m/s flows parallel to a 0.2 m by 0.2 m thin, flat plate which is at 100 °C. The air flows both above and below the plate. The drag force parallel to the plate is measured to be 0.075 N. What is the rate of heat transfer from the plate?

Assume: Modified Reynolds analogy.

Variables: ν = the dynamic viscosity; T_s = the temperature of the plate; T_∞ = the temperature of the air flow; U_∞ = the velocity of the air flow; F_d = the drag force; C_f = the friction coefficient; Pr = Prandtl number; h = convective heat transfer coefficient.

The friction coefficient can be determined by the following relation that as

$$F_d = C_f \frac{\rho U_\infty^2}{2} A,$$
$$C_f = \frac{2F_d}{\rho U_\infty^2 A}.$$

Then the convective heat transfer coefficient h can be determined through

$$\begin{aligned}
\frac{C_f}{2} &= \text{St } \text{Pr}^{2/3}, \\
&= \left(\frac{h}{\rho U_\infty c_p}\right) \text{Pr}^{2/3}, \\
h &= \frac{C_f \rho U_\infty c_p}{2\text{Pr}^{2/3}}, \\
&= \frac{2F_d}{\rho U_\infty^2 A} \frac{\rho U_\infty c_p}{2\text{Pr}^{2/3}}, \\
&= \frac{F_d c_p}{U_\infty A \text{Pr}^{2/3}}.
\end{aligned}$$

Then the heat rate is given by

$$Q = 2hA(T_s - T_\infty).$$

Example 9.2

For fully-developed laminar flow determine the relation between the maximum and the bulk temperature in (a) a circular pipe, and (b) flow between flat plates.

Example 9.3

Consider the wing of an aircraft as a flat plate of length 2.5 m in the flow direction. The plane is moving at 100 m/s in air at 0.7 bar, $-10°$C. The top surface of the wing absorbs solar radiation at a rate of 800 W/m^2. Estimate the steady-state temperature of the wing, assuming it to be uniform.

[Clarify this.]

Variables: ν = the dynamic viscosity; T_s = the temperature of the plate; T_∞ = the temperature of the air flow; U_∞ = the velocity of the air flow; h = convective heat transfer coefficient.

The Reynolds number is

$$\mathrm{Re} = \frac{u_\infty L}{\nu} = 1.404 \times 10^7;$$

so that the flow is turbulent. Using

$$\mathrm{Nu}_L = 0.037 \mathrm{Re}^{4/5} \mathrm{Pr}^{1/3};$$

and

$$h = \frac{\mathrm{Nu}_L k}{L}; \tag{9.4}$$

the convective heat coefficient h_L can be determined.

Then considering the energy balance :

$$Q_{absorb} = Q_{conv} = 2 h_l A (T_s - T_\infty); \tag{9.5}$$

the temperature of the plate T_s can be determined.

Example 9.4

Measurements show the following Reynolds and Nusselt numbers for convection from a heated object.

Re	Nu
40.0	3.38
126.5	5.79
400	9.89
1265	16.92
4000	28.93

Show that the data fit a power law of the form $\mathrm{Nu} = C\mathrm{Re}^m$, and find C and m.

Since $\ln Nu = \ln C + m \ln Re$, we expand the table to get

Re	$\ln Re$	Nu	$\ln Nu$
40.0	3.6889	3.38	1.2179
126.5	4.8402	5.79	1.7561
400	5.9915	9.89	2.2915
1265	7.1428	16.92	2.8285
4000	8.2940	28.93	3.3649

A linear regression of $\ln \mathrm{Re}$ and $\ln \mathrm{Nu}$ obtained using MATLAB (shown in Fig. 9.2) gives: $\ln C = -0.5$, and $m = 0.47$, so that the linear best fit is

$$\ln \mathrm{Nu} = -0.5 + 0.47 \ln \mathrm{Re},$$

$$\mathrm{Nu} = 0.6065\ \mathrm{Re}^{0.47}.$$

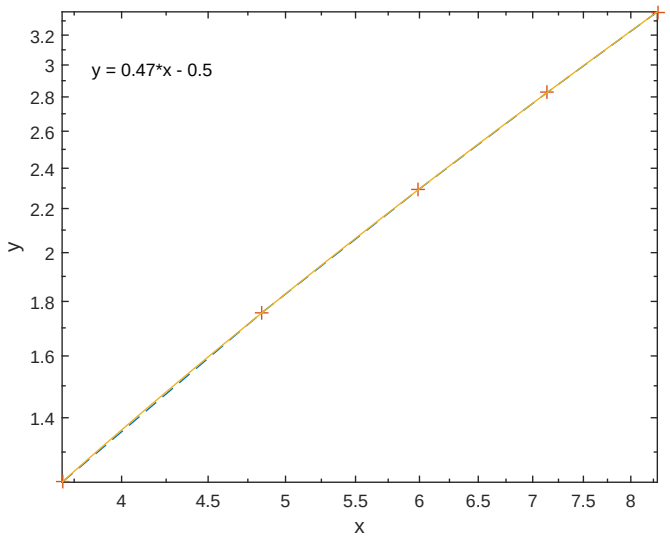

Figure 9.2: Linear regression between $x = \ln \mathrm{Re}$ and $y = \ln \mathrm{Nu}$.

Example 9.5

Computer problem: Write a computer program to determine the temperature profile in a flat plate laminar boundary layer for $\mathrm{Pr} = 0.7$.

9.2.3 Potential flow

[178]

If the heat flux is written as

$$\mathbf{q} = \rho c \mathbf{u} T - k \nabla T$$

the energy equation is

$$\nabla \cdot \mathbf{q} = 0$$

Heat flows along heatlines given by

$$\frac{dx}{\rho c T u_x - k(\partial T/\partial x)} = \frac{dy}{\rho c T u_y - k(\partial T/\partial y)} = \frac{dz}{\rho c T u_z - k(\partial T/\partial z)}$$

The tangent to heatlines at every point is the direction of the heat flux vector.

Two-dimensional flow

9.3 Leveque's solution

Leveque (1928)

9.4 Multiple solutions

See [175].

9.5 Boundary layers

9.5.1 Flat plate

Example 9.6

From the governing equations for an incompressible fluid (continuity, Navier-Stokes, energy), derive the ODEs for the hydrodynamic and thermal boundary layers for laminar flow over a flat plate.

Assume: steady state and boundary layers.
Governing equations:

$$\begin{aligned} \frac{\partial u}{\partial x} + \frac{\partial v}{\partial y} &= 0 && \text{continuity} \\ u\frac{\partial u}{\partial x} + v\frac{\partial u}{\partial y} &= \nu\frac{\partial^2 u}{\partial y^2} && \text{momentum,} \\ u\frac{\partial T}{\partial x} + v\frac{\partial T}{\partial y} &= \alpha\frac{\partial^2 T}{\partial y^2} && \text{energy.} \end{aligned}$$

To obtain the ODEs, define a stream function $\psi(x, y)$ as

$$\begin{aligned} u &= \frac{\partial \psi}{\partial y}, \\ v &= -\frac{\partial \psi}{\partial x}, \end{aligned}$$

which will satisfy the continuity equation. Then define

$$f(\eta) = \frac{\psi}{u_\infty}\sqrt{\frac{u_\infty}{\nu x}},$$

where

$$\eta = y\sqrt{\frac{u_\infty}{\nu x}}.$$

Using chain rule we get

$$\begin{aligned} u &= \frac{\partial \psi}{\partial y}, \\ &= \frac{\partial \psi}{\partial \eta}\frac{\partial \eta}{\partial y}, \\ &= u_\infty\sqrt{\frac{\nu x}{u_\infty}}\frac{df}{d\eta}\sqrt{\frac{u_\infty}{\nu x}}, \\ &= u_\infty\frac{df}{d\eta}, \end{aligned}$$

and

$$\begin{aligned} v &= -\frac{\partial \psi}{\partial y}, \\ &= -\left(u_\infty \sqrt{\frac{\nu x}{u_\infty}} \frac{\partial f}{\partial x} + \frac{u_\infty}{2} \sqrt{\frac{\nu}{u_\infty x}} f \right), \\ &= \frac{1}{2} \sqrt{\frac{\nu u_\infty}{x}} \left(\eta \frac{df}{d\eta} - f \right). \end{aligned}$$

Differentiating these

$$\begin{aligned} \frac{\partial u}{\partial x} &= -\frac{u_\infty}{2x} \eta \frac{d^2 f}{d\eta^2}, \\ \frac{\partial u}{\partial y} &= u_\infty \sqrt{\frac{u_\infty}{\nu x}} \frac{d^2 f}{d\eta^2}, \\ \frac{\partial^2 u}{\partial y^2} &= \frac{u_\infty^2}{\nu x} \frac{d^3 f}{d\eta^3}. \end{aligned}$$

Substituting back into the momentum equation and we get

$$2\frac{d^3 f}{d\eta^3} + f\frac{d^2 f}{d\eta^2} = 0, \text{ with } f = \frac{df}{d\eta} = 0 \text{ at } \eta = 0, \frac{df}{d\eta} = 1 \text{ at } \eta \to \infty.$$

Use

$$T^* = \frac{T - T_s}{T_\infty - T_s}$$

and $T^* = T^*(\eta)$ in the energy equation to get

$$\frac{d^2 T^*}{d\eta^2} + \frac{\Pr}{2} f \frac{dT^*}{d\eta} = 0, \text{ with } T^*(0) = 0, T^*(\infty) = 1.$$

9.5.2 Falkner-Skan

9.6 Heat exchangers

[112, 163]

Shell and tube heat exchangers are commonly used for large industrial applications. Compact heat exchangers are also common in industrial and engineering applications that exchanger heat between two separated fluids. The term *compact* is understood to mean a surface to volume ratio of more than about 700 m^2/m^3. The advantages are savings in cost, weight and volume of the heat exchanger.

The fin efficiency concept was introduced by Harper and Brown (1922). The effectiveness-NTU method was introduced by London and Seban in 1941.

A possible classification of HXs is shown in Table 9.1.

9.6.1 Parallel- and counter-flow

We define the subscripts h and c to mean hot and cold fluids, i and o for inlet and outlet, 1 the end where the hot fluids enters, and 2 the other end. Energy balances give

$$dq = U(T_h - T_c)\, dA \tag{9.6}$$

$$dq = \pm \dot{m}_c C_c\, dT_c \tag{9.7}$$

$$dq = -\dot{m}_h C_h\, dT_h \tag{9.8}$$

Table 9.1: Classification of HX (due to Shah [179], 1981

According to	*Types of HXs*	*Examples*
Transfer processes	Direct contact	
	Indirect contact	(a) direct transfer, (b) storage, (c) fluidized bed
Surface compactness	Compact	
	Non-compact	
Construction	Tubular	(a) double pipe (b) shell and tube (c) spiral tube
	Plate	(a) gasketed, (b) spiral, (c) lamella
	Extended surface	(a) plate fin, (b) tube fin
	Regenerative	(a) rotary disk (b) rotary drum (c) fixed matrix
Flow arrangement	Single pass	(a) parallel flow (b) counterflow (c) crossflow
	Multipass	(a) extended surface cross counter flow, (b) extended surface cross parallel flow, (c) shell and tube parallel counterflow shell and tube mixed, (d) shell and tube split flow, (e) shell and tube divided flow Plate
Number of fluids	Two fluid	
	Three fluid	
	Multifluid	
Heat transfer	Single-phase convection mechanisms on both sides	
	Single-phase convection on one side, two-phase convection on other side	
	Two-phase convection on both sides	
	Combined convection and radiative heat transfer	

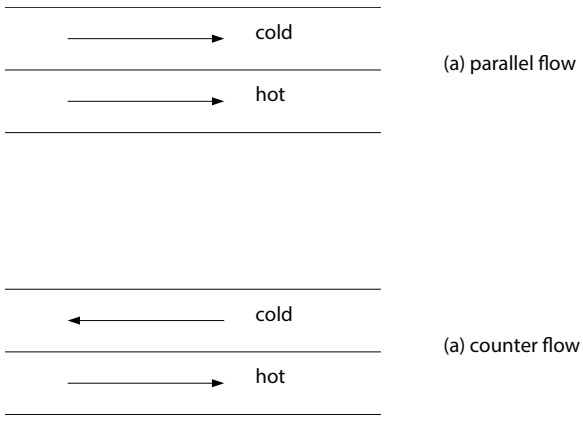

Figure 9.3: Parallel and counter flow.

where the upper and lower signs are for parallel and counterflow, respectively. From equations (9.7) and (9.8), we get

$$-dq\left(\frac{1}{\dot{m}_h C_h} \pm \frac{1}{\dot{m}_c C_c}\right) = d(T_h - T_c) \tag{9.9}$$

Using (9.6), we find that

$$-U\ dA\left(\frac{1}{\dot{m}_h C_h} \pm \frac{1}{\dot{m}_c C_c}\right) = \frac{d(T_h - T_c)}{T_h - T_c}$$

which can be integrated from 1 to 2 to give

$$-UA\left(\frac{1}{\dot{m}_h C_h} \pm \frac{1}{\dot{m}_c C_c}\right) = \ln\frac{(T_h - T_c)_1}{(T_h - T_c)_2}$$

From equation (9.9), we get

$$-q_T\left(\frac{1}{\dot{m}_h C_h} + \frac{1}{\dot{m}_c C_c}\right) = (T_h - T_c)_2 - (T_h - T_c)_1$$

where q_T is the total heat transfer rate. The last two equations can be combined to give

$$q_T = UA\Delta T_{lmtd}$$

where

$$\Delta T_{lmtd} = \frac{(T_h - T_c)_1 - (T_h - T_c)_2}{\ln[(T_h - T_c)_1/(T_h - T_c)_2]}$$

is the logarithmic mean temperature difference.

For parallel flow, we have

$$\Delta T_{lmtd} = \frac{(T_{h,i} - T_{c,i}) - (T_{h,o} - T_{c,o})}{\ln[(T_{h,i} - T_{c,i})/(T_{h,o} - T_{c,o})]}$$

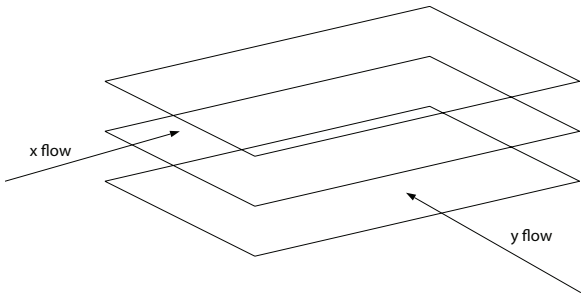

Figure 9.4: Schematic of crossflow plate HX.

while for counterflow it is

$$\Delta T_{lmtd} = \frac{(T_{h,i} - T_{c,o}) - (T_{h,o} - T_{c,i})}{\ln[(T_{h,i} - T_{c,o})/(T_{h,o} - T_{c,i})]}$$

We an write the element of area dA in terms of the perimeter P as $dA = P\ dx$, so that

$$T_c(x) = T_{c,1} \pm \frac{q(x)}{\dot{m}_c C_c}$$
$$T_h(x) = T_{h,1} - \frac{q(x)}{\dot{m}_h C_h}$$

Thus

$$\frac{dq}{dx} + qUP\left(\frac{1}{\dot{m}_h C_h} \pm \frac{1}{\dot{m}_c C_c}\right)$$

With the boundary condition $q(0) = 0$, the solution is

$$q(x) = \frac{T_{h,1} - T_{c,1}}{\frac{1}{\dot{m}_h C_h} \pm \frac{1}{\dot{m}_c C_c}} \left\{1 - \exp\left[-UP\left(\frac{1}{\dot{m}_h C_h} \pm \frac{1}{\dot{m}_c C_c}\right)\right]\right\}$$

9.6.2 Plate heat exchangers

There is flow on the two sides of a plate, 1 and 2, with an overall heat transfer coefficient of U. Consider a rectangular plate of size $L_x \times L_y$ in the x- and y-directions, respectively, as shown in Fig. 9.4. The flow on one side of the plate is in the x-direction with a temperature field $T_x(x, y)$. The mass flow rate of the flow is m_x per unit transverse length. The flow in the other side of the plate is in the y-direction with the corresponding quantities $T_y(x, y)$ and m_y. The overall heat transfer coefficient between the two fluids is U, which we will take to be a constant.

For the flow in the x-direction, the steady heat balance on an elemental rectangle of size $dx \times dy$ gives

$$c_x\ m_x\ dy\ \frac{\partial T_x}{\partial x}\ dx = U\ dx\ dy\ (T_y - T_x)$$

where c_x is the specific heat of that fluid. Simplifying, we get

$$2C_x R \frac{\partial T_x}{\partial x} = T_y - T_x \tag{9.10}$$

where $R = 1/2U$ is proportional to the thermal resistance between the two fluids, and $C_x = c_x m_x$. For the other fluid

$$2C_y R\frac{\partial T_y}{\partial y} = T_x - T_y \tag{9.11}$$

These equations have to be solved with suitable boundary conditions to obtain the temperature fields $T_x(x, y)$ and $T_y(x, y)$.

From equation (9.11), we get

$$T_x = T_y + C_y R\frac{\partial T_y}{\partial y} \tag{9.12}$$

Substituting in equation (9.10), we have

$$\frac{1}{C_y}\frac{\partial T_y}{\partial x} + \frac{1}{C_x}\frac{\partial T_y}{\partial y} + 2R\frac{^2T_y}{\partial x \partial y} = 0$$

Nusselt (Jakob, 1957) gives an interesting solution in the following manner. Let the plate be of dimensions L and W in the x- and y-directions. Nondimensional variables are

$$\xi = \frac{x}{L}$$
$$\eta = \frac{y}{W}$$
$$\theta_x = \frac{T_x - T_{y,i}}{T_{x,i} - T_{y,i}}$$
$$\theta_y = \frac{T_y - T_{y,i}}{T_{x,i} - T_{y,i}}$$
$$a = \frac{UWL}{C_x}$$
$$b = \frac{UWL}{C_y}$$

The governing equations are then

$$a(\theta_x - \theta_y) = -\frac{\partial \theta_x}{\partial \xi} \tag{9.13}$$
$$b(\theta_x - \theta_y) = \frac{\partial \theta_y}{\partial \eta} \tag{9.14}$$

with boundary conditions

$$\theta_x = 1 \quad \text{at } \xi = 0 \tag{9.15}$$
$$\theta_y = 0 \quad \text{at } \eta = 0 \tag{9.16}$$

Equation (9.14) can be written as

$$\frac{\partial \theta_y}{\partial \eta} + b\theta_y = b\theta_x$$

Solving for θ_y we get

$$\theta_y = e^{-b\eta}\left(C(\xi) + b\int_0^\eta \theta_x(\xi,\eta')e^{b\eta'}\ d\eta'\right)$$

From the boundary condition (9.16), we get

$$C = 0$$

so that

$$\theta_y(\xi,\eta) = be^{-b\eta}\int_0^\eta \theta_x(\xi,\eta')e^{b\eta'}\ d\eta'$$

Using the same procedure, from equation (9.13) we get

$$\theta_x(\xi,\eta) = e^{-a\xi} + ae^{-a\xi}\int_0^\xi \theta_y(\xi',\eta)e^{a\xi'}\ d\xi'$$

Substituting for θ_y, we find the Volterra integral equation

$$\theta_x(\xi,\eta) = e^{-a\xi} + abe^{-(a\xi+b\eta)}\int_0^\xi\int_0^\eta \theta_x(\xi',\eta')e^{a\xi'+b\eta'}\ d\xi'\ d\eta'$$

for the unknown θ_x.

We will first solve the Volterra equation for an arbitrary λ, where

$$\theta_x(\xi,\eta) = e^{-a\xi} + ab\lambda e^{-(a\xi+b\eta)}\int_0^\xi\int_0^\eta \theta_x(\xi',\eta')e^{a\xi'+b\eta'}\ d\xi'\ d\eta'$$

Let us express the solution in terms of a finite power series

$$\theta_x(\xi,\eta) = \phi_0(\xi,\eta) + \lambda\phi_1(\xi,\eta) + \lambda^2\phi_2(\xi,\eta) + \ldots + \lambda^n\phi_n(\xi,\eta) \tag{9.17}$$

This can be substituted in the integral equation. Since λ is arbitrary, the coefficient of each order of λ must vanish. Thus

$$\begin{aligned}
\phi_0(\xi,\eta) &= e^{-a\xi}\\
\phi_1(\xi,\eta) &= abe^{-(a\xi+b\eta)}\int_0^\xi\int_0^\eta \phi_0(\xi',\eta')e^{a\xi'+b\eta'}\ d\xi'\ d\eta'\\
\phi_2(\xi,\eta) &= abe^{-(a\xi+b\eta)}\int_0^\xi\int_0^\eta \phi_1(\xi',\eta')e^{a\xi'+b\eta'}\ d\xi'\ d\eta'\\
&\vdots\\
\phi_n(\xi,\eta) &= abe^{-(a\xi+b\eta)}\int_0^\xi\int_0^\eta \phi_{n-1}(\xi',\eta')e^{a\xi'+b\eta'}\ d\xi'\ d\eta'
\end{aligned}$$

The solutions are

$$\begin{aligned}
\phi_0 &= e^{-a\xi} \\
\phi_1 &= a\xi e^{-a\xi}(1 - e^{-b\eta}) \\
\phi_2 &= \frac{1}{2}a^2\xi^2 e^{-a\xi}(1 - e^{-b\eta} - b\eta e^{-b\eta}) \\
\phi_3 &= \frac{1}{2\times 3}a^3\xi^3 e^{-a\xi}(1 - e^{-b\eta} - b\eta e^{-b\eta} - \frac{1}{2}b^2\eta^2 e^{-b\eta}) \\
&\vdots \\
\phi_n &= \frac{1}{n!}a^n\xi^n e^{-a\xi}(1 - e^{-b\eta} - b\eta e^{-b\eta} - \ldots - \frac{1}{(n-1)!}b^{n-1}\eta^{n-1}e^{-b\eta})
\end{aligned}$$

Substituting into the expansion, equation (9.17), and taking $\lambda = 1$, we get

$$\theta_x(\xi,\eta) = \phi_0(\xi,\eta) + \phi_1(\xi,\eta) + \phi_2(\xi,\eta) + \ldots + \phi_n(\xi,\eta)$$

where the ϕs are given above.

Example 9.7

Find a solution of the same problem by separation of variables.
Taking

$$T_y(x,y) = X(x)Y(y)$$

Substituting and dividing by XY, we get

$$\frac{1}{C_x}\frac{\partial T_x}{\partial x} + \frac{1}{C_y}\frac{dY}{dy} + 2R = 0$$

Since the first term is a function only of x, and the second only of y, each must be a constant. Thus we can write

$$\begin{aligned}
\frac{dX}{dx} + \frac{1}{c_x m_x(a+R)}X &= 0 \\
\frac{dY}{dy} + \frac{1}{c_y m_y(a-R)}Y &= 0
\end{aligned}$$

where a is a constant. Solving the two equations and taking their product, we have

$$T_y = \frac{c}{a+R}\exp\left[-\frac{x}{c_x m_x(a+R)} + \frac{y}{c_y m_y(a-R)}\right]$$

where c is a constant. Substituting in equation (9.12), we get

$$T_x = \frac{c}{a-R}\exp\left[-\frac{x}{c_x m_x(a+R)} + \frac{y}{c_y m_y(a-R)}\right]$$

The rate of heat transfer over the entire plate, Q, is given by

$$\begin{aligned}
Q &= C_x\int_0^{L-y}\left[T_x(L_x,y) - T_x(0,y)\right]\,dy \\
&= cC_xC_y\exp\left[-\frac{l_x}{C_x(a+R)} - \frac{L_y}{C_2(a-R)} - 2\right]
\end{aligned}$$

The heat rate can be maximized by varying either of the variables C_x or C_y.

9.6.3 HX relations

The HX effectiveness is

$$\begin{aligned}\epsilon &= \frac{Q}{Q_{max}} \\ &= \frac{C_h(T_{h,i} - T_{h,o})}{C_{min}(T_{h,i} - T_{c,i})} \\ &= \frac{C_c(T_{c,o} - T_{c,i})}{C_{min}(T_{h,i} - T_{c,i})}\end{aligned}$$

where

$$C_{min} = \min(C_h, C_c)$$

Assuming U to be a constant, the number of transfer units is

$$NTU = \frac{AU}{C_{min}}$$

The heat capacity rate ratio is $C_R = C_{min}/C_{max}$.

Effectiveness-NTU relations

In general, the effectiveness is a function of the HX configuration, its NTU and the C_R of the fluids.
(a) Counterflow

$$\epsilon = \frac{1 - \exp[-NTU(1 - C_R)]}{1 - C_R \exp[-NTU(1 - C_R)]}$$

so that $\epsilon \to 1$ as $NTU \to \infty$.
(b) Parallel flow

$$\epsilon = \frac{1 - \exp[-NTU(1 - C_R)]}{1 + C_R}$$

(c) Crossflow, both fluids unmixed
Series solution (Mason, 1954)
(d) Crossflow, one fluid mixed, the other unmixed
If the unmixed fluid has $C = C_{min}$, then

$$\epsilon = 1 - \exp[-C_R(1 - \exp\{-NTUC_r\})]$$

But if the mixed fluid has $C = C_{min}$

$$\epsilon = C_R(1 - \exp\{-C_R(1 - e^{-NTU})\})$$

(e) Crossflow, both fluids mixed
(f) Tube with wall temperature constant

$$\epsilon = 1 - \exp(-NTU)$$

Pressure drop

It is important to determine the pressure drop through a heat exchanger. This is given by

$$\frac{\Delta p}{p_1} = \frac{G^2}{2\rho_1 p_1}\left[(K_c + 1 - \sigma^2) + 2(\frac{\rho_1}{\rho_2} - 1) + f\frac{A\rho_1}{A_c\rho_m} - (1 - \sigma^2 - K_e)\frac{\rho_1}{\rho_2}\right]$$

where K_c and K_e are the entrance and exit loss coefficients, and σ is the ratio of free-flow area to frontal area.

9.6.4 Design methodology

Mean temperature-difference method: Given the inlet temperatures and flow rates, this method enables one to find the outlet temperatures, the mean temperature difference, and then the heat rate.

Effectiveness-NTU method: The order of calculation is NTU, ϵ, q_{max} and q.

9.7 Porous medium analogy

See Nield and Bejan, p. 87 [138].

9.8 Heat transfer augmentation

9.9 Maldistribution effects

Rohsenow (1981)

9.10 Microchannel heat exchangers

Phillips (1990).

9.11 Radiation effects

See Ozisik (1981).

Shah (1981)

9.12 Transient behavior

Ontko and Harris (1990)

For both fluids mixed

$$Mc\frac{dT}{dt} + \dot{m}_1 c_1(T_1^{in} - T_1^{out}) + \dot{m}c_2(T_2^{in} - T_2^{out}) = 0$$

For one fluid mixed and the other unmixed, we have

$$\rho A c_2\frac{\partial T_2}{\partial t} + \rho V_2 A c_2\frac{\partial T_2}{\partial x} + hP(T - T_1) = 0$$

9.13 Correlations

9.13.1 Least squares method

Possible correlations are

$$y(x) = \sum_{k=0}^{n} a_k x^k$$
$$y(x) = a_0 + a_{1/2}x^{1/2} + a_1 x + a_{3/2}x^{3/2} + a_2 x^2 + \dots$$
$$y(x) = ax^m + bx^n + \dots$$
$$y(x) = \int_{k=0}^{n} a(k)x^k \, dk \qquad \text{where } -1 < x < 1$$

A power-law correlation of the form

$$y = cx^n$$

satisfies the invariance condition given by equation (**??**).

9.14 Compressible flow

9.15 Natural convection

9.15.1 Governing equations

9.15.2 Cavities

9.15.3 Marangoni convection

See [214].

Example 9.8

A beverage can 150 mm long and 60 mm in diameter is initially at 27 °C and is to be cooled by placement in a refrigerator at 4 °C. In the interest of maximizing the cooling rate, should the can be laid horizontally or vertically?

Assume: (a) Heat transfer from the can is by natural convection. (b) neglect heat transfer from the sides. (c) Heat transfer from a vertical cylinder is assumed to be as from a vertical flat plate.

Variables: g = acceleration due to gravity; β = coefficient of volumetric expansion; T_s = exterior temperature of cylinder; T_∞ = refrigerator temperature; ν = coefficient of dynamic viscosity; α = thermal diffusivity; D = diameter of cylinder; L = length of cylinder; $Pr = \nu/\alpha$ = Prandtl number; k = thermal conductivity of air.

Horizontal cylinder

$$Ra_D = \frac{g\beta(T_s - T_\infty)D^3}{\nu\alpha},$$
$$\overline{Nu}_D = \left\{ 0.60 + \frac{0.387 Ra_D^{1/6}}{\left[1 + (0.559/Pr)^{9/16}\right]^{8/27}} \right\},$$
$$\overline{h} = \frac{\overline{Nu}_D k}{D},$$
$$Q_h = \overline{h}\pi DL(T_s - T_\infty)$$

Vertical cylinder

$$
\begin{aligned}
Ra_L &= \frac{g\beta(T_s - T_\infty)L^3}{\nu\alpha}, \\
\overline{Nu}_L &= \left\{ 0.825 + \frac{0.387 Ra_L^{1/6}}{\left[1 + (0.492/Pr)^{9/16}\right]^{4/9}} \right\}^2, \\
\overline{h} &= \frac{\overline{Nu}_L k}{L}, \\
Q_v &= \overline{h}\pi DL(T_s - T_\infty)
\end{aligned}
$$

The optimum orientation of the can depends on whether Q_h or Q_h is greater.

Bibliography

S. Chandrasekhar, Hydrodynamic and Hydromagnetic Stability, Dover, New York, 1981.

P.G. Drazin and W.H. Reid, Hydrodynamic Stability, Cambridge, 1981.

R.K. Shah and A.L. London, *Laminar flow forced convection in ducts, a source book for compact heat exchanger analytical data*, Academic Press, 1978.

W.M. Kays and A.L. London, *Compact Heat Exchangers,* 3rd Ed., McGraw-Hill, 1984.

W.M. Kays and M.E. Crawford, *Convective Heat and Mass Transfer,* McGraw-Hill, 3rd Ed., McGraw-Hill, 1993.

Problems

1. For parallel and counterflow heat exchangers, I obtained the temperature distributions

$$T_h(x) = T_{h,1} - \frac{T_{h,1} - T_{c,1}}{1 \pm (\dot{m}_h c_h/\dot{m}_c c_c)} \left[1 - \exp\{-UP\left(\frac{1}{\dot{m}_h c_h} \pm \frac{1}{\dot{m}_c c_c}\right) x\}\right], \tag{9.18}$$

$$T_c(x) = T_{c,1} \pm \frac{T_{h,1} - T_{c,1}}{(\dot{m}_c c_c/\dot{m}_h c_h) \pm 1} \left[1 - \exp\{-UP\left(\frac{1}{\dot{m}_h c_h} \pm \frac{1}{\dot{m}_c c_c}\right) x\}\right] \tag{9.19}$$

   for the hot and cold fluids, respectively. As usual the upper sign is for parallel and the lower for counterflow; 1 is the end where the hot fluid enters (from where x is measured) and 2 is where it leaves. Please check.

2. For a counterflow heat exchanger, derive the expression for the effectiveness as a function of the NTU, and also the NTU as function of the effectiveness.

3. (From Incropera and DeWitt) A single-pass, cross-flow heat exchanger uses hot exhaust gases (mixed) to heat water (unmixed) from 30 to 80°C at a rate of 3 kg/s. The exhaust gases, having thermophysical properties similar to air, enter and exit the exchanger at 225 and 100°C, respectively. If the overall heat transfer coefficient is 200 W/m^{2}K, estimate the required area.

4. (From Incropera and DeWitt) A cross-flow heat exchanger used in cardiopulmonary bypass procedure cools blood flowing at 5 liters/min from a body temperature of 37°C to 25°C in order to induce body hypothermia, which reduces metabolic and oxygen requirements. The coolant is ice water at 0°C and its flow rate is adjusted to provide an outlet temperature of 15°C. The heat exchanger operates with both fluids unmixed, and the overall heat transfer coefficient is 750 W/m^{2}K. The density and specific heat of the blood are 1050 kg/m^2 and 3740 J/kg K, respectively. (a) Determine the heat transfer rate for the exchanger. (b) Calculate the water flow rate. (c) What is the surface area of the heat exchanger?

Chapter 10

Porous media

[109, 138, 211]

10.1 Governing equations

The continuity equation for incompressible flow in a porous medium is

$$\nabla \cdot \mathbf{V} = 0 \tag{10.1}$$

10.1.1 Darcy's equation

Consider the porous medium schematically shown in Fig. 10.1. The flow is in between the granular solid, and so the corresponding length scale is the free space between them. The Reynolds number in Eq. (9.2) is thus small and so inertia terms on the left side can be neglected. Taking, furthermore, the viscous stress to be proportional to the velocity, we get the simplest model for the momentum equation in a porous medium, which is Darcy's law

$$\nabla p = -\frac{\mu}{K}\mathbf{V} + \rho\mathbf{f} \tag{10.2}$$

where $\mathbf{f}$ is the body force per unit mass. Here K is called the permeability of the medium and has units of inverse area. It is similar to the incompressible Navier-Stokes equation with constant properties where the inertia terms are dropped and the viscous force per unit volume is represented by $-(\mu/K)\mathbf{V}$. Sometimes a term $c\rho_0\partial\mathbf{V}/\partial t$ is added to the left side for transient problems, but it is normally left out because it is small. The condition on the velocity is that of zero normal velocity at a boundary, allowing for slip in the tangential direction.

From equations (10.1) and (10.2), for $\mathbf{f} = 0$ we get

$$\nabla^2 p = 0$$

from which the pressure distribution can be determined.

10.1.2 Forchheimer's equation

Forchheimer's equation which is often used instead of Darcy's equation is

$$\nabla p = -\frac{\mu}{K}\mathbf{V} - c_f K^{-1/2}\rho|\mathbf{V}|\mathbf{V} + \rho\mathbf{f}$$

where c_f is a dimensionless constant. There is still slip at a boundary.

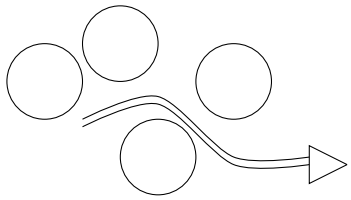

Figure 10.1: Schematic of porous medium.

10.1.3 Brinkman's equation

Another alternative is Brinkman's equation

$$\nabla p = -\frac{\mu}{K}\mathbf{V} + \tilde{\mu}\nabla^2\mathbf{V} + \rho\mathbf{f}$$

where $\tilde{\mu}$ is another viscous coefficient. In this model there is no slip at a solid boundary.

10.1.4 Energy equation

The energy equation is

$$(\rho c)_m \frac{\partial T}{\partial t} + \rho c_p \mathbf{V}\cdot\nabla T = k_m \nabla^2 T$$

where k_m is the effective thermal conductivity, and

$$(\rho c)_m = \phi\rho c_p + (1-\phi)(\rho c)_m$$

is the average heat capacity. The subscripts m refers to the solid matrix, and ϕ is the porosity of the material. An equivalent form is

$$\sigma\frac{\partial T}{\partial t} + \mathbf{V}\cdot\nabla T = \alpha_m \nabla^2 T$$

where

$$\alpha_m = \frac{k_m}{\rho c_p}$$
$$\sigma = \frac{(\rho c)_m}{\rho c_p}$$

See [1].

10.2 Forced convection

10.2.1 Plane wall at constant temperature

The solution to

$$\frac{\partial u}{\partial x} + \frac{\partial v}{\partial y} = 0$$
$$u = -\frac{K}{\mu}\frac{\partial p}{\partial x}$$
$$v = -\frac{K}{\mu}\frac{\partial p}{\partial y}$$

is

$$u = U$$
$$v = 0$$

For

$$\frac{Ux}{\alpha_m} = Pe_x \gg 1$$

the energy equation is

$$u\frac{\partial T}{\partial x} + v\frac{\partial T}{\partial y} = \alpha_m \frac{\partial^2 T}{\partial y^2}$$

or

$$U\frac{\partial T}{\partial x} = \alpha_m \frac{\partial^2 T}{\partial y^2}$$

The boundary conditions are

$$T(0) = T_w$$
$$T(\infty) = T_\infty$$

Writing

$$\eta = y\sqrt{\frac{U}{\alpha_m x}}$$
$$\theta(\eta) = \frac{T - T_w}{T_\infty - T_w}$$

we get

$$\begin{aligned}
\frac{\partial T}{\partial x} &= (T_\infty - T_w)\,\frac{d\theta}{d\eta}\frac{\partial \eta}{\partial x} \\
&= (T_\infty - T_w)\,\frac{d\theta}{d\eta}\left(-y\sqrt{\frac{U}{\alpha_m}}\frac{1}{2}x^{-3/2}\right) \\
\frac{\partial T}{\partial y} &= (T_\infty - T_w)\,\frac{d\theta}{d\eta}\frac{\partial \eta}{\partial y} \\
&= (T_\infty - T_w)\,\frac{d\theta}{d\eta}\sqrt{\frac{U}{\alpha_m x}} \\
\frac{\partial^2 T}{\partial y^2} &= (T_\infty - T_w)\,\frac{d^2\theta}{d\eta^2}\frac{U}{\alpha_m x}
\end{aligned}$$

so that the equation becomes

$$\theta'' + \frac{1}{2}\eta\ \theta' = 0$$

with

$$\begin{aligned}
\theta(0) &= 0 \\
\theta(\infty) &= 1
\end{aligned}$$

We multiply by the integrating factor $e^{\eta^2/4}$ to get

$$\frac{d}{d\eta}\left(e^{\eta^2/4}\theta'\right) = 0$$

The first integral is

$$\theta' = C_1 e^{-\eta^2/4}$$

Integrating again we have

$$\theta = C_1 \int_0^\eta e^{-\eta'^2/4}\ d\eta' + C_2$$

With the change in variables $x = \eta'/2$, the solution becomes

$$\theta = 2C_1 \int_0^{\eta/2} e^{-x^2}\ dx$$

Applying the boundary conditions, we find that $C_1 = 1/\sqrt{\pi}$ and $C_2 = 0$. Thus

$$\begin{aligned}
\theta &= \frac{2}{\sqrt{\pi}} \int_0^{\eta/2} e^{-x^2}\ dx \\
&= \ \mathrm{erf}\ \frac{\eta}{2}
\end{aligned}$$

The heat transfer coefficient is defined as

$$\begin{aligned} h &= \frac{q''}{T_w - T_\infty} \\ &= -\frac{k_m}{T_w - T_\infty}\frac{\partial T}{\partial y} \\ &= k_m \frac{\partial \theta}{\partial y} \end{aligned}$$

The local Nusselt number is given by

$$\begin{aligned} Nu_x &= \frac{hx}{k_m} \\ &= x\frac{\partial \theta}{\partial y}\bigg|_{y=0} \\ &= \frac{1}{\sqrt{\pi}}\sqrt{\frac{Ux}{\alpha_m}} \\ &= \frac{1}{\sqrt{\pi}} Pe_x^{-1/2} \end{aligned}$$

Example 10.1

Find the temperature distribution for flow in a porous medium parallel to a flat plate with uniform heat flux.

10.2.2 Stagnation-point flow

For flow in a porous medium normal to an infinite flat plate, the velocity field is

$$\begin{aligned} u &= Cx \\ v &= -Cy \end{aligned}$$

The energy equation is

$$Cx\frac{\partial T}{\partial x} - Cy\frac{\partial T}{\partial y} = \alpha_m \frac{\partial^2 T}{\partial y^2}$$

10.2.3 Thermal wakes

Line source

For $Pe_x \gg 1$, the governing equation is

$$U\frac{\partial T}{\partial x} = \alpha_m \frac{\partial^2 T}{\partial y^2}$$

where the boundary conditions are

$$\frac{\partial T}{\partial y} = 0 \text{ at } y = 0 \tag{10.3}$$

$$q' = (\rho c_p) U \int_{-\infty}^{\infty} (T - T_\infty)\, dy \tag{10.4}$$

Writing

$$\eta = y\sqrt{\frac{U}{\alpha_m x}}$$

$$\theta(\eta) = \frac{T - T_\infty}{q'/k_m}\sqrt{\frac{Ux}{\alpha_m}}$$

we find that

$$\frac{\partial T}{\partial x} = \theta \frac{q'}{k_m}\sqrt{\frac{\alpha_m}{U}}\left(-\frac{1}{2}x^{-3/2}\right) + \frac{d\theta}{d\eta} y \sqrt{\frac{U}{\alpha_m}}\left(-\frac{1}{2}x^{-3/2}\frac{q'}{k_m}\sqrt{\frac{\alpha_m}{Ux}}\right)$$

$$\frac{\partial T}{\partial y} = \frac{q'}{k_m}\sqrt{\frac{\alpha_m}{Ux}}\frac{d\theta}{d\eta}\sqrt{\frac{U}{\alpha_m x}}$$

$$\frac{\partial^2 T}{\partial y^2} = \frac{q'}{k_m}\sqrt{\frac{\alpha_m}{Ux}}\frac{d\theta}{d\eta}\frac{U}{\alpha_m x}$$

Substituting in the equation, we get

$$\theta'' = -\frac{1}{2}(\theta + \eta\theta') \tag{10.5}$$

The conditions (10.3)-(10.4) become

$$\frac{\partial \theta}{\partial \eta} = 0 \text{ at } \eta = 0$$

$$\int_{-\infty}^{\infty} \theta\, dy = 1$$

The equation (10.5) can be written as

$$\theta'' = -\frac{1}{2}\frac{d}{d\eta}(\eta\theta)$$

which integrates to

$$\theta' = -\frac{1}{2}\eta\theta + C_1$$

Since $\theta' = 0$ at $\eta = 0$, we find that $C_1 = 0$. Integrating again, we get

$$\theta = C_2 e^{-\eta^2/4}$$

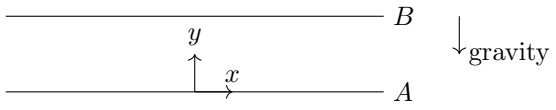

Figure 10.2: Stability of horizontal porous layer; the surfaces A and B are a distance H apart.

Substituting in the other boundary condition

$$1 = \int_{-\infty}^{\infty} \theta \; d\eta = C_2 \int_{-\infty}^{\infty} e^{-\eta^2/4} \; d\eta = 2\sqrt{\pi} C_2$$

from which

$$C_2 = \frac{1}{2\sqrt{\pi}}$$

Thus the solution is

$$\theta = \frac{1}{2\sqrt{\pi}} e^{-\eta^2/4}$$

or

$$T - T_\infty = \frac{1}{2\sqrt{\pi}} \frac{q'}{k_m} \sqrt{(\frac{\alpha_m}{Ux})} \exp(\frac{-Uy^2}{4\alpha_m x})$$

Example 10.2

Show that for a point source

$$T - T_\infty = \frac{q}{4\pi k x} \exp(\frac{-Ur^2}{4\alpha_m x})$$

10.3 Natural convection

10.3.1 Linear stability

This is often called the Horton-Rogers-Lapwood problem, and consists of finding the stability of a horizontal layer of fluid in a saturated porous medium heated from below. The two-dimensional geometry is shown in Fig. 10.2.

The governing equations are

$$\nabla \cdot \mathbf{V} = 0$$
$$-\nabla p - \frac{\mu}{K} \mathbf{V} + \rho \mathbf{g} = 0$$
$$\sigma \frac{\partial T}{\partial t} + \mathbf{V} \cdot \nabla T = \alpha_m \nabla^2 T$$
$$\rho = \rho_0 \left[1 - \beta \left(T - T_0\right)\right]$$

where $\mathbf{g} = -g\mathbf{j}$. The basic steady solution is

$$\begin{aligned}\bar{\mathbf{V}} &= 0\\ \bar{T} &= T_0 + \Delta T\left(1 - \frac{y}{H}\right)\\ p &= p_0 - \rho_0 g\left[y + \frac{1}{2}\beta\Delta T\left(\frac{y^2}{H} - 2y\right)\right]\end{aligned}$$

For constant heat flux $\Delta T = q_s''/k_m$. We apply a perturbation to each variable as

$$\begin{aligned}\mathbf{V} &= \bar{\mathbf{V}} + \mathbf{V}'\\ T &= \bar{T} + T'\\ p &= \bar{p} + p'\end{aligned}$$

Substituting and linearizing

$$\begin{aligned}\nabla\cdot\mathbf{V}' &= 0\\ -\nabla p' - \frac{\mu}{K}\mathbf{V}' - \beta\rho_0 T'\mathbf{g} &= 0\\ \frac{\partial T'}{\partial t} - \frac{\Delta T}{H}w' &= \alpha_m\nabla^2 T'\end{aligned}$$

Using the nondimensional variables

$$\begin{aligned}\mathbf{x}^* &= \frac{\mathbf{x}}{H}, \quad t^* = \frac{\alpha_m t}{\sigma H^2},\\ \mathbf{V}'^* &= \frac{H\mathbf{V}'}{\alpha_m}, \quad T'^* = \frac{T'}{\Delta T}, \quad p'^* = \frac{Kp'}{\mu\alpha_m}\end{aligned}$$

the equations become, on dropping $'$s and *s

$$\begin{aligned}\nabla\cdot\mathbf{V} &= 0\\ -\nabla p - \mathbf{V} + Ra\ T\mathbf{k} &= 0\\ \frac{\partial T}{\partial t} - w &= \nabla^2 T\end{aligned}$$

where

$$Ra = \frac{\rho_0 g\beta K H\Delta T}{\mu\alpha_m}$$

From these equations we get

$$\nabla^2 w = Ra\nabla_H^2 T$$

where

$$\nabla_H = \frac{\partial^2}{\partial x^2}$$

Using separation of variables

$$\begin{aligned}w(x,y,z,t) &= W(y)\exp\left(st + ik_x x\right)\\ T(x,y,z,t) &= \Theta(y)\exp\left(st + ik_x x\right)\end{aligned}$$

Substituting into the equations we get

$$\left(\frac{d^2}{dy^2} - k^2 - s\right)\Theta = -W$$
$$\left(\frac{d^2}{dy^2} - k^2\right)W = -k^2 Ra\ \Theta$$

where

$$k^2 = k_x^2 + k_y^2$$

Isothermal boundary conditions

The boundary conditions are $W = \Theta = 0$ at either wall. For the solutions to remain bounded as $x, y \to \infty$, the wavenumbers k_x and k_y must be real. Furthermore, since the eigenvalue problem is self-adjoint, as shown below, it can be shown that s is also real.

For a self-adjoint operator L, we must have

$$(u, Lv) = (Lu, v)$$

If

$$vL(u) - uL(v) = \frac{\partial P}{\partial x} + \frac{\partial Q}{\partial y}$$

then

$$\begin{aligned}\int_V \left[vL(u) - uL(v)\right]\ dV &= \int \left(\frac{\partial P}{\partial x} + \frac{\partial Q}{\partial y}\right)\ dV \\ &= \int_V \nabla \cdot (P\mathbf{i} + Q\mathbf{j})\ dV \\ &= \int_S \mathbf{n} \cdot (P\mathbf{i} + Q\mathbf{j})\end{aligned}$$

If $\mathbf{n}\cdot(P\mathbf{i}+Q\mathbf{j}) = 0$ at the boundaries (i.e. impermeable), which is the case here, then L is self-adjoint.

Thus, marginal stability occurs when $s = 0$, for which

$$\left(\frac{d^2}{dy^2} - k^2\right)\Theta = -W$$
$$\left(\frac{d^2}{dy^2} - k^2\right)W = -k^2 Ra\ \Theta$$

from which

$$\left(\frac{d^2}{dy^2} - k^2\right)^2 W = k^2 Ra\ W$$

The eigenfunctions are

$$W = \sin n\pi y$$

where $n = 1, 2, 3, \ldots$, as long as

$$Ra = \left(\frac{n^2\pi^2}{k} + k \right)^2$$

For each n there is a minimum value of the critical Rayleigh number determined by

$$\frac{dRa}{dk} = 2\left(\frac{n^2\pi^2}{k} + k \right)\left[-\frac{n^2\pi^2}{k^2} + 1 \right]$$

The lowest critical Ra is with $k = \pi$ and $n = 1$, which gives

$$Ra_c = 4\pi^2$$

for the onset of instability.

Constant heat flux conditions

Here $W = d\Theta/dy = 0$ at the walls. We write

$$W = W_0 + \alpha^2 W_1 + \ldots$$
$$\Theta = \Theta_0 + \alpha^2 \Theta_1 + \ldots$$
$$Ra = Ra_0 + \alpha^2 Ra_1 + \ldots$$

For the zeroth order system

$$\frac{d^2 W_0}{dy^2} = 0$$

with $W_0 = d\Theta_0/dy = 0$ at the walls. The solutions is $W_0 = 0$, $\Theta_0 = 1$. To the next order

$$\frac{d^2 W_1}{dy^2} = W_0 - Ra_0 \Theta_0$$
$$\frac{d^2 \Theta_1}{dy^2} + W_1 = \Theta_0$$

with $W_1 = d\Theta_1/dy = 0$ at the walls. Finally, we get $Ra_c = 12$.

10.3.2 Steady-state inclined layer solutions

Consider an inclined porous layer of thickness H at angle ϕ with respect to the horizontal shown in Fig. 10.3

Introducing the streamfunction $\psi(x, y)$, where

$$u = \frac{\partial \psi}{\partial y},$$
$$v = -\frac{\partial \psi}{\partial x},$$

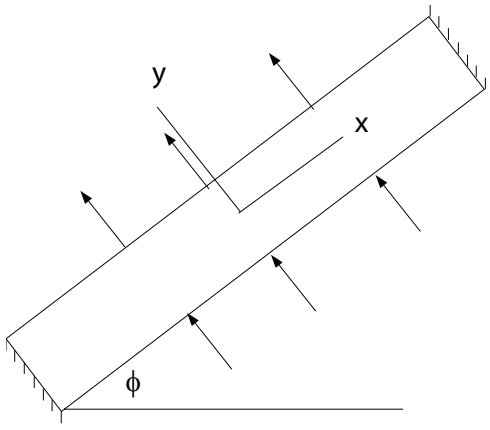

Figure 10.3: Inclined porous layer.

satisfies the continuity equation. Darcy's equation becomes

$$-\frac{\partial p}{\partial x} - \frac{\mu}{K}\frac{\partial \psi}{\partial y} = \rho_0 g\left[1-\beta(T-T_0)\right]\sin\phi,$$
$$-\frac{\partial p}{\partial y} + \frac{\mu}{K}\frac{\partial \psi}{\partial x} = \rho_0 g\left[1-\beta(T-T_0)\right]\cos\phi.$$

Taking $\partial/\partial y$ of the first and $\partial/\partial x$ of the second and subtracting, we have

$$\frac{\partial^2\psi}{\partial x^2} + \frac{\partial^2\psi}{\partial y^2} = -\frac{\rho_0 g\beta K}{\mu}\left(\frac{\partial T}{\partial x}\cos\phi - \frac{\partial T}{\partial y}\sin\phi\right).$$

The energy equation is

$$\left(\frac{\partial\psi}{\partial y}\frac{\partial T}{\partial x} - \frac{\partial\psi}{\partial x}\frac{\partial T}{\partial y}\right) = \alpha_m\left(\frac{\partial^2 T}{\partial x^2} + \frac{\partial^2 T}{\partial y^2}\right).$$

Side-wall heating

The non-dimensional equations are

$$\frac{\partial^2\psi}{\partial x^2} + \frac{\partial^2\psi}{\partial y^2} = -Ra\,\left(\frac{\partial T}{\partial x}\cos\phi - \frac{\partial T}{\partial y}\sin\phi\right),$$
$$\frac{\partial\psi}{\partial y}\frac{\partial T}{\partial x} - \frac{\partial\psi}{\partial x}\frac{\partial T}{\partial y} = \frac{\partial^2 T}{\partial x^2} + \frac{\partial^2 T}{\partial y^2}.$$

The boundary conditions are

$$\psi = 0,\ \frac{\partial T}{\partial x} = 0 \quad \text{at} \quad x = \pm\frac{A}{2},$$
$$\psi = 0,\ \frac{\partial T}{\partial y} = -1 \quad \text{at} \quad y = \pm\frac{1}{2}.$$

With a parallel-flow approximation, we assume [176]

$$\psi = \psi(y)$$
$$T = Cx + \theta(y)$$

The governing equations become

$$\frac{\partial^2 \psi}{\partial y^2} - Ra \ \sin\phi \frac{d\theta}{dy} + RC\cos\phi = 0$$
$$\frac{d^2\theta}{dy^2} - C\frac{d\psi}{dy} = 0$$

An additional constraint is the heat transported across a transversal section should be zero. Thus

$$\int_{-1/2}^{1/2} \left(uT - \frac{\partial T}{\partial x} \right) \ dy = 0 \tag{10.6}$$

Let us look at three cases.

(a) *Horizontal layer*

For $\phi = 0°$ the temperature and streamfunction are

$$T = Cx - y\left[1 + \frac{RaC^2}{24}\left(4y^2 - 3\right)\right]$$
$$\psi = -\frac{RaC}{8}\left(4y^2 - 1\right)$$

Substituting in condition (10.6), we get

$$C\left(10R - Ra^2C^2 - 120\right) = 0$$

the solutions of which are

$$C = 0$$
$$C = \frac{1}{Ra}\sqrt{10(Ra - 12)}$$
$$C = -\frac{1}{Ra}\sqrt{10(Ra - 12)}$$

The only real solution that exists for $Ra \leq 12$ is the conductive solution $C = 0$. For $C > 12$, there are two nonzero values of C which lead to convective solutions, for which

$$\psi_c = \frac{RaC}{8}$$
$$Nu = \frac{12}{12 - RaC^2}$$

For $\phi = 180°$, the only real value of C is zero, so that only the conductive solution exists.

(b) *Natural circulation*

Let us take $C\sin\phi > 0$, for which we get

$$\psi_c = \frac{B}{C}\left(1 - \cosh\frac{\alpha}{2}\right)$$
$$Nu = -\frac{\alpha}{2B\sinh\frac{\alpha}{2} + \alpha C\cot\phi}$$

where

$$\alpha^2 = RC\sin\phi$$
$$B = -\frac{1 + C\cot\phi}{\cosh\frac{\alpha}{2}}$$

and the constant C is determined from

$$C - \frac{B^2}{2C}\left(\frac{\sinh\alpha}{\alpha} - 1\right) - B\cot\phi\left(\cosh\frac{\alpha}{2} - \frac{2}{\alpha}\sinh\frac{\alpha}{2}\right) = 0$$

(c) *Antinatural circulation*

For $C\sin\phi < 0$, for which we get

$$\psi_c = \frac{B}{C}\left(1 - \cosh\frac{\beta}{2}\right)$$
$$Nu = -\frac{\beta}{2B\sinh\frac{\beta}{2} + \beta C\cot\phi}$$

where

$$\beta^2 = -RC\sin\phi$$
$$B = -\frac{1 + C\cot\phi}{\cosh\frac{\beta}{2}}$$

and the constant C is determined from

$$C - \frac{B^2}{2C}\left(\frac{\sin\beta}{\beta} - 1\right) - B\cot\phi\left(\cosh\frac{\beta}{2} - \frac{2}{\beta}\sinh\frac{\beta}{2}\right) = 0$$

End-wall heating

Darcy's law is

$$\nabla^2\psi = R\left(\frac{\partial T}{\partial x}\sin\phi + \frac{\partial T}{\partial y}\cos\phi\right)$$

The boundary conditions are

$$\psi = 0,\ \frac{\partial T}{\partial x} = -1 \quad \text{at} \quad x = \pm\frac{A}{2}$$
$$\psi = 0,\ \frac{\partial T}{\partial y} = 0 \quad \text{at} \quad x = \pm\frac{1}{2}$$

With a parallel-flow approximation, we assume

$$\psi = \psi(y)$$
$$T = Cx + \theta(y)$$

The governing equations become

$$\frac{d^2\theta}{dy^2} - C\frac{d\psi}{dy} = 0$$
$$\frac{\partial^2\psi}{\partial y^2} - R\cos\phi\frac{d\theta}{dy} - RC\sin\phi = 0$$

An additional constraint is the heat transported across a transversal section. Thus

$$\int_{-1/2}^{1/2}\left(uT - \frac{\partial T}{\partial x}\right)\,dy = 1 \tag{10.7}$$

Let us look at three cases.

(a) *Vertical layer*
For $\phi = 0°$ the temperature and streamfunction are

$$T = Cx + \frac{B_1}{\alpha}\sin(\alpha y) - \frac{B_2}{\alpha}\cos(\alpha y)$$
$$\psi = \frac{B_1}{C}\cos(\alpha y) + \frac{B_2}{C}\sin(\alpha y) + B_3$$

where

$$\alpha^2 = -RC$$

Substituting in condition (10.6), we get

$$C\left(10R - R^2C^2 - 120\right) = 0$$

the solutions of which are

$$C = 0$$
$$C = \frac{1}{R}\sqrt{10(R-12)}$$
$$C = -\frac{1}{R}\sqrt{10(R-12)}$$

The only real solution that exists for $R \leq 12$ is the conductive solution $C = 0$. For $C > 12$, there are two nonzero values of C which lead to convective solutions, for which

$$\psi_c = \frac{RC}{8}$$
$$Nu = \frac{12}{12 - RC}$$

For $\phi = 180°$, the only real value of C is zero, so that only the conductive solution exists.

(b) *Natural circulation*
Let us take $C\sin\phi > 0$, for which we get

$$\psi_c = \frac{B}{C}\left(1 - \cosh\frac{\alpha}{2}\right)$$
$$Nu = -\frac{\alpha}{2B\sinh\frac{\alpha}{2} + \alpha C\cot\phi}$$

where

$$\alpha^2 = RC\sin\phi$$
$$B = -\frac{1 + C\cot\phi}{\cosh\frac{\alpha}{2}}$$

and the constant C is determined from

$$C - \frac{B^2}{2C}\left(\frac{\sinh\alpha}{\alpha} - 1\right) - B\cot\phi\left(\cosh\frac{\alpha}{2} - \frac{2}{\alpha}\sinh\frac{\alpha}{2}\right) = 0$$

(c) *Antinatural circulation*
For $C\sin\phi > 0$, for which we get

$$\psi_c = \frac{B}{C}\left(1 - \cosh\frac{\beta}{2}\right)$$
$$Nu = -\frac{\beta}{2B\sinh\frac{\beta}{2} + \beta C\cot\phi}$$

where

$$\beta^2 = -RC\sin\phi$$
$$B = -\frac{1 + C\cot\phi}{\cosh\frac{\beta}{2}}$$

and the constant C is determined from

$$C - \frac{B^2}{2C}\left(\frac{\sin\beta}{\beta} - 1\right) - B\cot\phi\left(\cosh\frac{\beta}{2} - \frac{2}{\beta}\sinh\frac{\beta}{2}\right) = 0$$

Bibliography

M. Kaviany, *Principles of Heat transfer in Porous Media,* 2nd Ed., Springer-Verlag, 1955.

D.A. Nield and A. Bejan, *Convection in Porous Media,* 2nd Ed., Springer-Verlag, 1999.

Problems

1. This is a problem.

Appendix A

Fractional derivatives

Cauchy's formula for repeated integration is

$$\begin{aligned} I^n &= \int_a^x \int_a^{\sigma_1} \dots \int_a^{\sigma_{n-1}} f(\sigma_n)\ d\sigma_n \dots d\sigma_1, \\ &= \frac{1}{(n-1)!} \int_a^x (x-y)^{n-1} f(y)\ dy. \end{aligned}$$

Generalize n to real number, and factorial to gamma function to get the Riemann-Liouville fractional integral

$$I_{RL}^{\alpha} f(x) = \frac{1}{\Gamma(\alpha)} \int_a^x \frac{f(t)}{(x-t)^{1-\alpha}}\ dt.$$

Differentiating n times we have the Riemann-Liouville fractional derivative

$$D_{RL}^{\alpha} f(x) = \frac{1}{\Gamma(n-\alpha)} \frac{d^n}{dx^n} \int_a^x \frac{f(t)}{(x-t)^{1+\alpha-n}}\ dt, \quad n-1 \leq \alpha < n.$$

The Caputo fractional derivative is

$$D_{C}^{\alpha} f(x) = \frac{1}{\Gamma(n-\alpha)} \int_a^x \frac{f^{(n)}(t)}{(x-t)^{1+\alpha-n}}\ dt, \quad n-1 \leq \alpha < n.$$

The Grünwald-Letnikov fractional derivative is

$$D_{G}^{\alpha} f(x) = \lim_{h \to 0} \frac{1}{h^{\alpha}} \sum_{m=0}^{(x-a)/h} (-1)^m \frac{\Gamma(\alpha+1)}{m!\ \Gamma(\alpha-m+1)} f(x-mh).$$

Examples of fractional derivative are in Fig. A.1.

A.1 Experiments with shell-and-tube heat exchanger

For this experiment [**?**], a shell-and-tube heat exchanger, shown in Fig. A.2, was tested and the inlet and outlet temperatures on both the cold and hot side were recorded. The inlet flow rates were

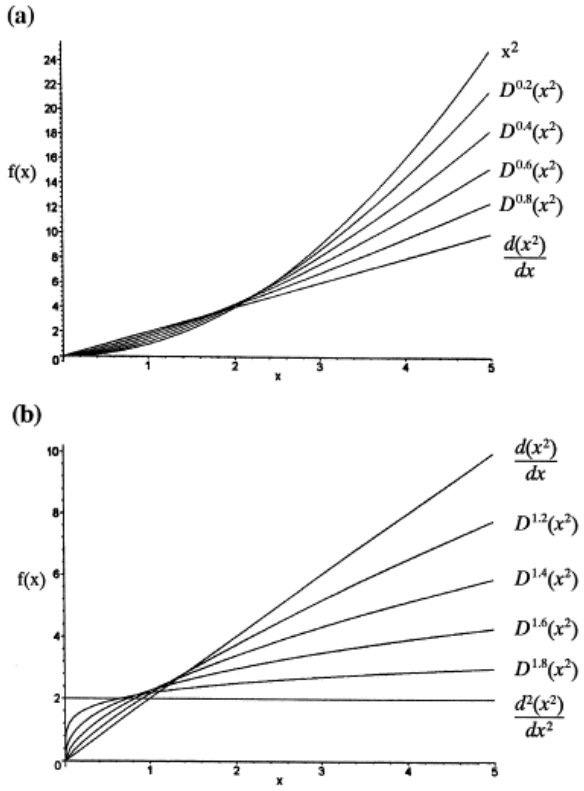

Figure A.1: Fractional derivatives $D^{\alpha}_{RL}f(x)$ of x^2; (a) $\alpha = 0.2, 0.4, 0.6, 0.8, 1.0$. (b) $\alpha = 1, 1.2, 1.4, 1.6, 1.8, 2.0$. From Schumer et al. (2001)

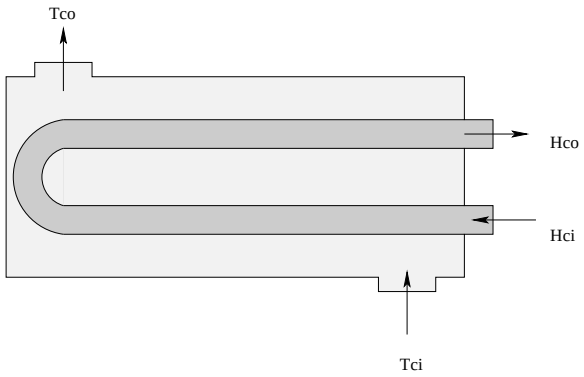

Figure A.2: Shell-and-tube heat exchanger.

held constant in both the cold and hot sides and the inlet temperatures were controlled to remain constant. After the system reached equilibrium for a given set of conditions, a step change (on-off) in the flow rate of the cold-side was applied. Experimental results of two tests are shown in Fig. A.3, where the non-dimensional temperature is given by

$$T^*(t) = \frac{T_{h,o}(t) - T_{h,o}(0)}{T_{h,o}(\infty) - T_{h,o}(0)},$$

and time is non-dimensionalized by

$$t^* = \frac{t}{\tau_r},$$

where τ_r is the rise time, defined as the time required for $T_{h,o}(t)$ to reach 85% of $T_{h,o}(\infty)$.

The approximations are the following.

$$\text{first-order} \quad c_1 D^1 y(t) + c_2 y(t) = u(t) \tag{A.1a}$$

$$\text{second-order} \quad c_1 D^2 y(t) + c_2 D^1 y(t) + c_3 y(t) = u(t) \tag{A.1b}$$

$$\text{fractional-order} \quad c_1 D^\alpha y(t) + c_2 y(t) = u(t) \text{ [Sol. } \frac{1}{c_1} t^\alpha E_{\alpha,\alpha+1}(-\frac{c_2}{c_1} t^\alpha)] \tag{A.1c}$$

Data Set #1

Model	c_1	c_2	c_3	α	$\sum \text{error}^2$
First-order	1.0401	0.028554			3.5284e-03
Second-order	0.097011	0.59086	0.89968		7.6902e-04
Fractional-order	0.22381	2.1700		1.8911	9.5609e-05
$\alpha = 1.8196$	0.24855	2.0221			1.3355e-04

Data Set #2

Model	c_1	c_2	c_3	α	$\sum \text{error}^2$
First-order	1.2536	-0.32904			1.4135e-03
Second-order	0.12359	0.65039	0.85564		1.0973e-04
Fractional-order	0.33183	1.8782		1.7481	2.7757e-05
$\alpha = 1.8196$	0.2976	2.0476			4.9404e-05

The three models proposed in Eq. A.1 were used to find best fit approximations. In both data sets, the fractional-order model resulted in a better approximation than either the first or second order models. Data set #1 is shown to be fit best with a derivative of order $\alpha = 1.8911$ and data set #2 with a derivative of order $\alpha = 1.7481$. The average $\alpha = 1.8196$ also outperforms both the first and second order models, despite the same number of free parameters.

A.2 Fractional time derivative in heat equation

Consider a semi-infinite body, $\infty < x \leq 0$, shown in Fig. A.4 [**?**]. The initial temperature is $T(0, x) = T_0$, and the surface temperature is $T(0, t) = T_s(t)$.

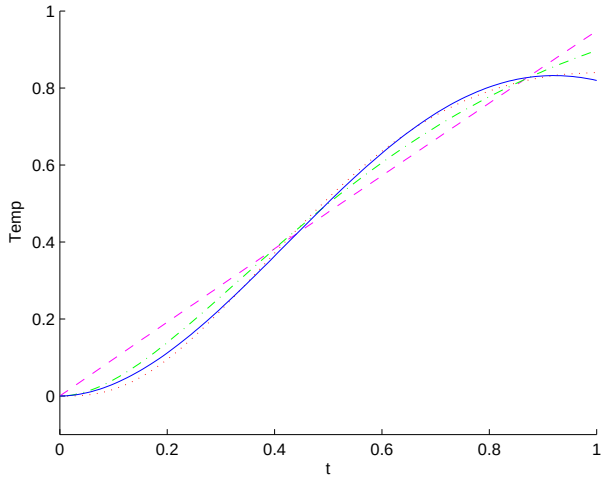

(a) Test data 1

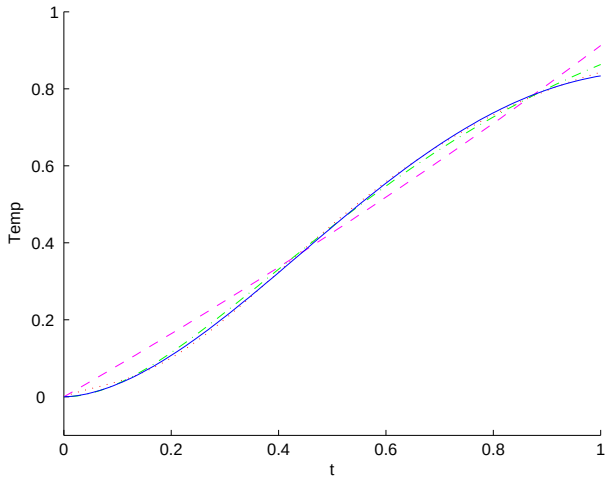

(b) Test data 2

Figure A.3: Best fit approximations to shell-and-tube data using first, second, and fractional-order models. Dotted line is filtered data, dashed line is first-order model, dash-dot is second-order model, and solid line is fractional-order model.

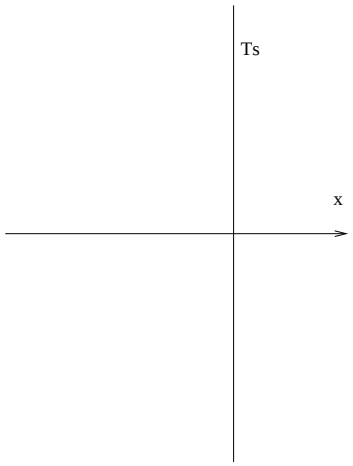

Figure A.4: Semi-infinite body.

Writing $T^*(t,x) = T(t,x) - T_0$,

$$\frac{\partial T^*}{\partial t} = \alpha \frac{\partial^2 T^*}{\partial x^2}, \quad t \geq 0, \quad -\infty < x \leq 0,$$
$$T^*(0,x) = 0,$$
$$T^*(t,0) = T_s^*(t),$$
$$\left| \lim_{x \to -\infty} T^*(t,x) \right| < 0.$$

The Laplace transform in time is $\widehat{T}^*(s,x)$, where[1]

$$s\ \widehat{T}^* = \alpha \frac{d^2 \widehat{T}^*}{dx^2}.$$

The solution that is bounded for $x \to -\infty$ is

$$\widehat{T}^* = \widehat{T}^*(s,0) \exp\left(x\sqrt{s/\alpha}\right).$$

From this

$$\frac{\partial \widehat{T}^*}{\partial x} = \widehat{T}^*(s,0)\sqrt{\frac{s}{\alpha}} \exp\left(x\sqrt{s/\alpha}\right),$$

so that at $x = 0$

$$\frac{1}{\sqrt{s}} \frac{\partial \widehat{T}^*}{\partial x}(s,0) = \frac{1}{\sqrt{\alpha}} \widehat{T}^*(s,0).$$

The inverse transform of this gives

$${}_0D_t^{-1/2} \left[\frac{\partial T^*}{\partial t}(t,0) \right] = \frac{1}{\sqrt{\alpha}} T^*(t,0),$$

[1]The Laplace transform of $f(t)$ is $F(s)$, and that of ${}_0D_t^{\alpha} f(t)$ is $s^{\alpha}F(s) - \sum_{k=0}^{n-1} s^k\ {}_0D_t^{\alpha-1-k} f(t)\big|_{t=0}$.

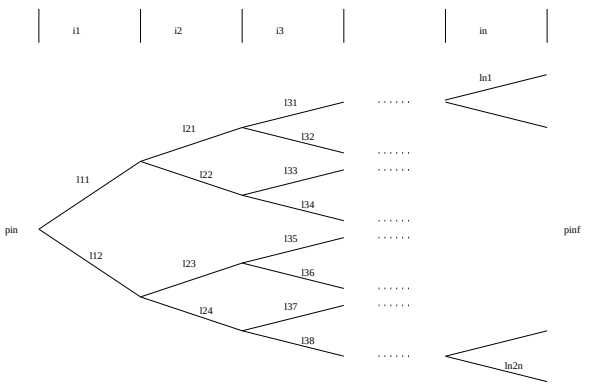

Figure A.5: n-generational tree.

from which

$$\frac{\partial T^*}{\partial x}(t,0) = \frac{1}{\sqrt{\alpha}}\ {}_0D_t^{1/2}\left[T^*(t,0)\right].$$

The heat flux at $x = 0$ is

$$\begin{aligned} q_s &= -k\frac{\partial T^*}{\partial x}(t,0), \\ &= -\frac{k}{\sqrt{\alpha}}\ {}_0D_t^{1/2}\left[\frac{\partial T^*}{\partial t}(t,0)\right]. \end{aligned}$$

Alternatively, since

$$\begin{aligned} D_t^{1/2}\ D_t^{1/2} &= D_t^1, \\ D_x^1\ D_x^1 &= D_x^2, \end{aligned}$$

we have

$$D_t^{1/2}\ T = \sqrt{\alpha}D_x^1\ \sqrt{\alpha}D_x^1\ T$$

A.3 Self-similar trees

See Fig. A.5.

Potential-driven flow

$$\Delta V = iZ \quad \text{where} \quad \begin{cases} \Delta V = \text{potential difference} \\ i = \text{flow rate} \\ Z = \text{impedance} \end{cases}$$

The equivalent impedance for a capacitor-resistor tree [**?**] called fractance, is in Fig. A.6.

$$\frac{1}{Z} = \frac{1}{(sC)^{-1} + Z} + \frac{1}{R + Z}$$

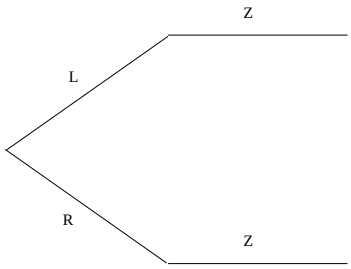

Figure A.6: Equivalent impedance for fractance.

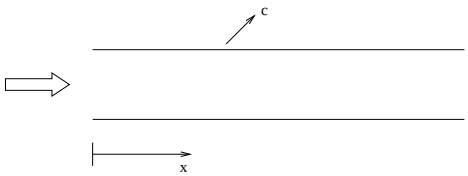

Figure A.7: CAPTION HERE.

from which

$$Z = \left(\frac{R}{sC}\right)^{1/2}$$

Converting back from the Laplace domain,

$$\Delta V(t) = \frac{(R/C)^{1/2}}{\Gamma(1/2)} \int_0^t \frac{i(t^*)}{(t-\tau)^{1/2}} dt^*,$$

Potential-driven flow networks [**?**]

$$L(q) = \Delta p$$

$$q_{i,j} = q_{i+1,2j-1} + q_{i+1,2j}$$

Overall behavior of tree

$$L_N q_N = p_{in} - p_{out},$$

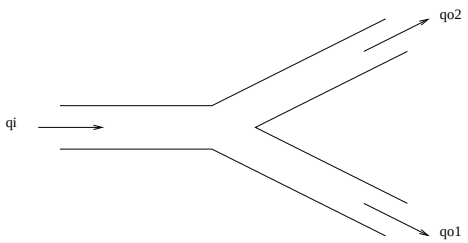

where

$$L_N = \cfrac{1}{\cfrac{1}{L_{1,1} + \cfrac{1}{\cfrac{1}{L_{2,1}+\ldots} + \cfrac{1}{L_{2,2}+\ldots}}}} + \cfrac{1}{L_{1,2} + \cfrac{1}{\cfrac{1}{L_{2,3}+\ldots} + \cfrac{1}{L_{2,4}+\ldots}}}.$$

Self-symmetric trees

$$L_N = \cfrac{1}{\cfrac{1}{L_1 + \cfrac{1}{\cfrac{1}{L_1+\ldots} + \cfrac{1}{L_2+\ldots}}}} + \cfrac{1}{L_2 + \cfrac{1}{\cfrac{1}{L_1+\ldots} + \cfrac{1}{L_2+\ldots}}}$$

For $N \to \infty$

$$L_\infty = \cfrac{1}{\cfrac{1}{L_1 + L_\infty} + \cfrac{1}{L_2 + L_\infty}}$$

$$L_\infty = \sqrt{L_1\ L_2}$$

A.4 Continued fractions

$$\begin{aligned} x &= \cfrac{1}{1 + \cfrac{1}{1 + \cfrac{1}{1+\cdots}}} \\ &= \frac{1}{1+x} \end{aligned}$$

$$x^2 + x - 1 = 0$$

$$x = \begin{cases} \dfrac{-1+\sqrt{5}}{2} & \text{golden mean} \\ \dfrac{-1-\sqrt{5}}{2} & \end{cases}$$

A.5 Mittag-Leffler functions

Define the two-parameter function

$$E_{\alpha,\beta}(z) = \sum_{k=0}^{\infty} \frac{z^k}{\Gamma(\alpha k + \beta)}$$

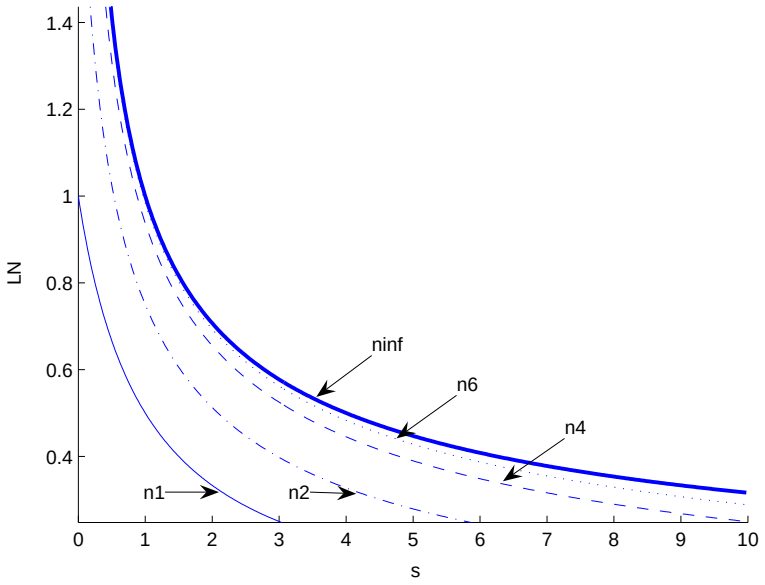

(a) $\mathcal{L}_1 = s$, $\mathcal{L}_2 = 1$

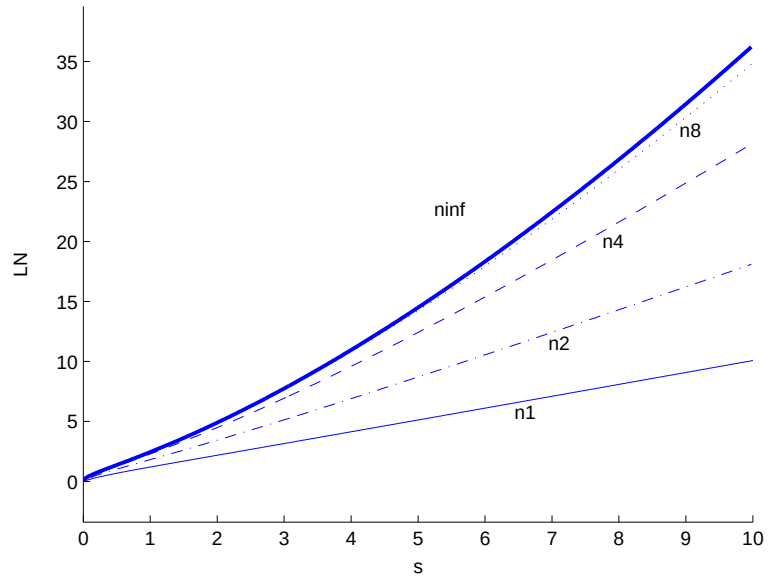

(b) $\mathcal{L}_1 = s + 1$, $\mathcal{L}_2 = s^2 + 2s$

Figure A.8: $\mathcal{L}_\infty$ shown with $\mathcal{L}_N$ for different values of N. As N increases, $\mathcal{L}_N$ converges to $\mathcal{L}_\infty$ in the Laplace domain while in the time domain L_N converges to L_∞.

Thus

$$E_{1,1}(z) = \sum_{k=0}^{\infty} \frac{z^k}{\Gamma(k+1)} = \sum_{k=0}^{\infty} \frac{z^k}{k!} = e^z.$$

Appendix B

More on natural circulation loops

B.1 Mixed heating

The following has been written by A. Pacheco-Vega.

It is common, especially in experiments, to have one part of the loop heated with a known heat rate and the rest with known wall temperature. Thus for part of the loop the wall temperature is known so that $q = PU(T - T_w(s))$, while $q(s)$ is known for the rest. As an example, consider

$$q = \begin{cases} PU(T - T_0) & \text{for} \quad \frac{\phi}{2\pi} \leq s \leq \pi + \frac{\phi}{2\pi} \\ q_0 & \text{for} \quad \pi + \frac{\phi}{2\pi} < s < 2\pi + \frac{\phi}{2\pi} \end{cases}$$

where T_0 and q_0 are constants.

B.2 Modeling

[1]

If we consider a one-dimensional incompressible flow, the equation of continuity indicates that the velocity v is a function of time alone. Thus,

$$v = v(t).$$

Taking an infinitesimal cylindrical control volume of fluid in the loop $\pi r^2 d\theta$, see Figure (B.1), the momentum equation in the θ-direction can be written as

$$\rho\pi r^2 R d\theta \frac{dv}{dt} = -\pi r^2 d\theta \frac{dp}{d\theta} - \rho g \pi r^2 R d\theta \cos(\theta + \alpha) - \tau_w 2\pi r R d\theta \tag{B.1}$$

Integrating Eq. (B.1) around the loop using the Boussinesq approximation $\rho = \rho_w[1 - \beta(T - T_w)]$, with the shear stress at the wall being approximated by that corresponding to Poiseuille flow in a straight pipe $\tau_w = 8\mu v/\rho_w r^2$, the expression of the balance in Eq. (B.1) modifies to

$$\frac{dv}{dt} + \frac{8\mu}{\rho_w r^2} v = \frac{\beta g}{2\pi} \int_0^{2\pi} (T - T_w) \cos(\theta + \alpha)\, d\theta \tag{B.2}$$

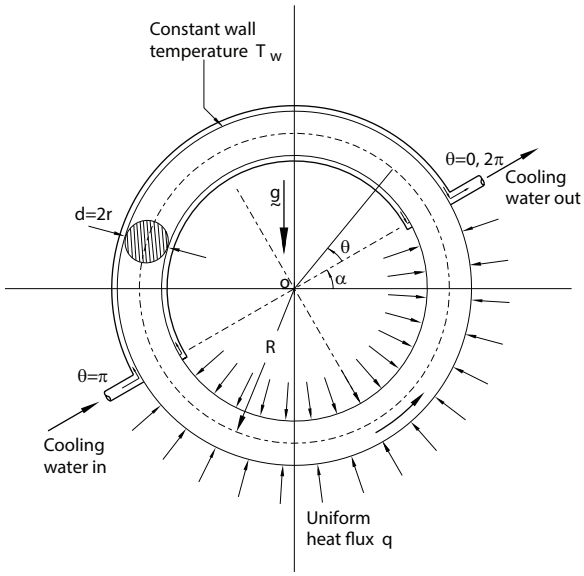

Figure B.1: Schematic of a convection loop heated with constant heat flux in one half and cooled at constant temperature in the other half.

Neglecting axial heat conduction, the temperature of the fluid satisfies the following energy balance equation

$$\rho_w c_p \left(\frac{\partial T}{\partial t} + \frac{v}{R} \frac{\partial T}{\partial \theta} \right) = \begin{cases} -\frac{2h}{r}(T - T_w), & 0 \le \theta \le \pi \\ \frac{2}{r} q, & \pi < \theta < 2\pi \end{cases} \tag{B.3}$$

Following the notation used by Greif et al. (1979), the nondimensional time, velocity and temperature are defined as

$$\tau = \frac{t}{2\pi R/V}, \quad w = \frac{v}{V}, \quad \phi = \frac{T - T_w}{q/h}$$

respectively, where

$$V = \left(\frac{g\beta R r q}{2\pi c_p \mu} \right)^{1/2}.$$

Accordingly, Eqs. (B.2) and (B.3) become

$$\frac{dw}{d\tau} + \Gamma w = \frac{\pi \Gamma}{4D} \int_0^{2\pi} \phi \, \cos(\theta + \alpha) \, d\theta \tag{B.4}$$

and

$$\frac{\partial \phi}{\partial \tau} + 2\pi w \frac{\partial \phi}{\partial \theta} = \begin{cases} -2D\phi, & 0 \le \theta \le \pi \\ 2D, & \pi < \theta < 2\pi \end{cases} \tag{B.5}$$

where the parameters D and Γ are defined by

$$D = \frac{2\pi R h}{\rho_w c_p r V} \qquad \Gamma = \frac{16\pi \mu R}{\rho_w r^2 V}$$

B.3 Steady State

The steady-state governing equations without axial conduction are

$$\overline{w} = \frac{\pi}{4D} \int_0^{2\pi} \overline{\phi}\, \cos(\theta + \alpha)\, d\theta \tag{B.6}$$

and

$$\frac{d\overline{\phi}}{d\theta} = \begin{cases} -\frac{D}{\pi \overline{w}}\, \overline{\phi}, & 0 \le \theta \le \pi \\ \frac{D}{\pi \overline{w}}, & \pi < \theta < 2\pi \end{cases} \tag{B.7}$$

where $\overline{w}$ and $\overline{\phi}$ are the steady-state values of velocity and temperature respectively. Eq. (B.7) can be integrated to give

$$\overline{\phi}(\theta) = \begin{cases} A\, e^{-(D\theta/\pi\overline{w})}, & 0 \le \theta \le \pi \\ \frac{D}{\pi \overline{w}}\, \theta + B, & \pi < \theta < 2\pi \end{cases}$$

Applying the condition of continuity in the temperature, such that $\phi(0) = \phi(2\pi)$ and $\phi(\pi^-) = \phi(\pi^+)$ the constants A and B can be determined. These are

$$A = \frac{D}{\overline{w}} \frac{1}{1 - e^{(-D/\overline{w})}} \qquad B = \frac{D}{\overline{w}} \left[\frac{2\, e^{(-D/\overline{w})} - 1}{1 - e^{(-D/\overline{w})}} \right]$$

The resulting temperature filed is

$$\overline{\phi}(\theta) = \begin{cases} \frac{D}{\overline{w}} \frac{e^{-(D\theta/\pi\overline{w})}}{1 - e^{-(D/\overline{w})}}, & 0 \le \theta \le \pi \\ \frac{D}{\overline{w}} \left[\frac{\theta}{\pi} + \frac{2e^{-(D/\overline{w})} - 1}{1 - e^{-(D/\overline{w})}} \right], & \pi < \theta < 2\pi \end{cases} \tag{B.8}$$

Substituion of Eq. (B.7) in Eq. (B.6), followed by an expansion of $\cos(\theta + \alpha)$, leads to

$$\begin{aligned} \overline{w} = {} & \frac{\pi}{4D} \cos\alpha \left\{ \int_0^{\pi} \frac{D}{\overline{w}} \frac{e^{-(D\theta/\pi\overline{w})}}{1 - e^{-(D/\overline{w})}}\, \cos\theta\, d\theta \right. \\ & \left. + \int_{\pi}^{2\pi} \frac{D}{\overline{w}} \left[\frac{\theta}{\pi} + \frac{2e^{-(D/\overline{w})} - 1}{1 - e^{-(D/\overline{w})}} \right] \cos\theta\, d\theta \right\} \\ & - \frac{\pi}{4D} \sin\alpha \left\{ \int_0^{\pi} \frac{D}{\overline{w}} \frac{e^{-(D\theta/\pi\overline{w})}}{1 - e^{-(D/\overline{w})}}\, \sin\theta\, d\theta \right. \\ & \left. + \int_{\pi}^{2\pi} \frac{D}{\overline{w}} \left[\frac{\theta}{\pi} + \frac{2e^{-(D/\overline{w})} - 1}{1 - e^{-(D/\overline{w})}} \right] \sin\theta\, d\theta \right\} \end{aligned}$$

and integration around the loop, gives the steady-state velocity as

$$\overline{w}^2 = \frac{\cos\alpha}{2} + \frac{(D/\overline{w})\cos\alpha + \pi(D/\overline{w})^2 \sin\alpha}{4\left[1 + \left(\frac{D}{\pi\overline{w}}\right)^2\right]} \left(\frac{1 + e^{-(D/\overline{w})}}{1 - e^{-(D/\overline{w})}} \right).$$

As a final step, multiplying the numerator and denominator by $e^{(D/2\overline{w})}$ and rearranging terms leads to the expresion for the function of the steady-state velocity

$$G(\overline{w},\alpha,D)=\overline{w}^2-\frac{\cos\alpha}{2}-\frac{(D/\overline{w})\cos\alpha+\pi(D/\overline{w})^2\sin\alpha}{4\left[1+\left(\frac{D}{\pi\overline{w}}\right)^2\right]}\coth(D/2\ \overline{w})=0 \tag{B.9}$$

For $\alpha=0$, symmetric steady-state solutions for the fluid velocity are possible since $G(w,0,D)$ is an even function of w. In this case Eq.(B.9) reduces to

$$\overline{w}^2=\frac{1}{2}+\frac{(D/\overline{w})\left[1+e^{-(D/\overline{w})}\right]}{4\left[1+\left(\frac{D}{\pi\overline{w}}\right)^2\right]\left[1-e^{-(D/\overline{w})}\right]}. \tag{B.10}$$

The steady-state solutions of the velocity field and temperature are shown next. Figure B.2 shows the $\overline{w}-\alpha$ curves for different values of the parameter D. Regions of zero, one, two and three solutions can be identified. The regions of no possible steady-state velocity are: $-180^\circ<\alpha<-147.5^\circ$ and $147.5^\circ<\alpha<180^\circ$. There is only one velocity for the ranges $-147.5^\circ<\alpha<-\alpha_0$ and $\alpha_0<\alpha<147.5^\circ$ where α_0 varies from 90° at a value of $D=0.001$ to $\alpha_0=32.5^\circ$ when $D=100$. Three velocities are obtained for $-\alpha_0<\alpha<-32.5^\circ$ and $32.5^\circ<\alpha<\alpha_0$, except for the zero-inclination case which has two possible steady-state velocities. The temperature distribution in the loop, for three values of the parameter D and $\alpha=0$ is presented in Figure B.3. From the $\overline{\phi}-\theta$ curves it can be seen the dependence of the temperature with D. As D increases the variation in temperature between two opposit points also increases. When has a value $D=0.1$ the heating and cooling curves are almost straight lines, while at a value of $D=1.0$ the temperature decays exponentially and rises linearly. Similar but more drastic change in temperature is seen when $D=2.5$. Figure B.4 shows the $\overline{\phi}-\theta$ curves for three different inclination angles with $D=2.5$. It can be seen the increase in the temperature as α takes values of $\alpha=0^\circ$, $\alpha=90^\circ$ and $\alpha=135^\circ$. This behaviour is somewhat expected since the steady-state velocity is decreasing in value such that the fluid stays longer in both parts of the loop. Figure B.5 shows the steady-state velocity as a function of D for different angles of inclination α. For $\alpha=0$ we have two branches of the velocity-curve which are symmetric. The positive and negative values of the velocity are equal in magnitude for any value of D. For $\alpha=45^\circ$, the two branches are not symmetric while for $\alpha=90^\circ$ and $\alpha=135^\circ$, only the positive branch exist.

B.4 Dynamic Analysis

The temperature can be expanded in Fourier series, such that

$$\phi=\phi_0+\sum_{n=1}^{\infty}\left[\phi_n^c(t)\cos(n\theta)+\phi_n^s(t)\sin(n\theta)\right] \tag{B.11}$$

Substituiting into Eqs. (B.4) and (B.5), we have

$$\frac{dw}{d\tau}+\Gamma w=\frac{\pi^2\Gamma}{4D}\cos\alpha\phi_1^c-\frac{\pi^2\Gamma}{4D}\sin\alpha\phi_1^s \tag{B.12}$$

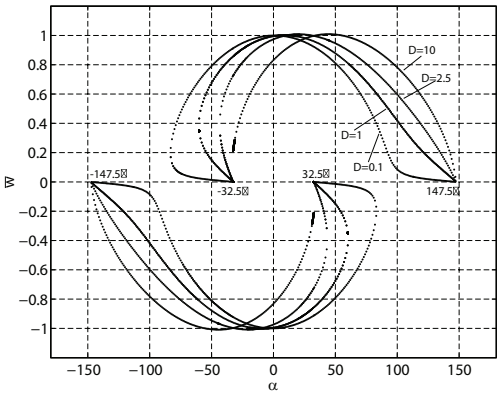

Figure B.2: Steady-State velocity field.

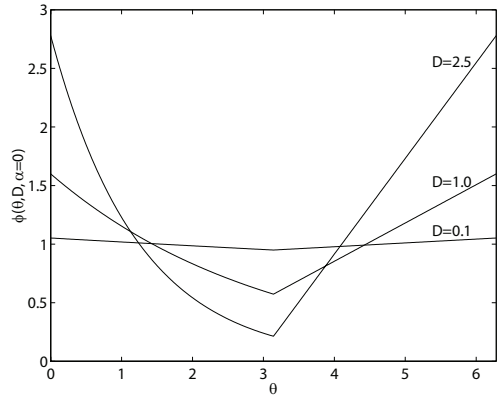

Figure B.3: Nondimensional temperature distribution as a function of the parameter D for $\alpha = 0$.

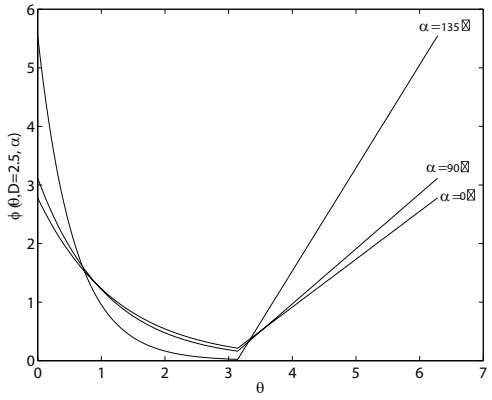

Figure B.4: Nondimensional temperature distribution as a function of thermosyphon inclination α for $D = 2.5$.

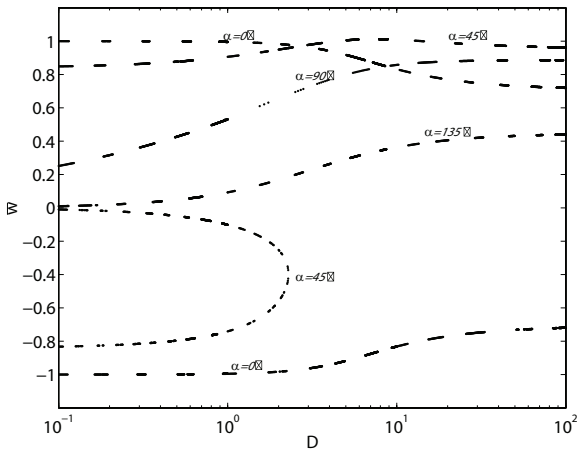

Figure B.5: Velocity $\overline{w}$ as a function of D for different thermosyphon inclinations α.

and

$$\begin{aligned}\frac{d\phi_0^c}{d\tau} + \sum_{n=1}^{\infty}\left[\frac{d\phi_n^c}{d\tau}\cos(n\theta) + \frac{d\phi_n^s}{d\tau}\sin(n\theta)\right] \\ +2\pi w\sum_{n=1}^{\infty}\left[-n\phi_n^c\sin(n\theta) + n\phi_n^s\cos(n\theta)\right] \\ = \begin{cases} -2D\left\{\phi_0^c + \sum_{n=1}^{\infty}\left[\phi_n^c(t)\cos(n\theta) + \phi_n^s(t)\sin(n\theta)\right]\right\}, & 0 \le \theta \le \pi \\ 2D, & \pi < \theta < 2\pi \end{cases}\end{aligned} \tag{B.13}$$

Integrating Eq. (B.13) from $\theta = 0$ to $\theta = 2\pi$ we get

$$\frac{d\phi_0^c}{d\tau} = -D\left[\phi_0^c - \frac{1}{\pi}\sum_{n=1}^{\infty}\frac{\phi_n^s}{n}\left[(-1)^n - 1\right] - 1\right] \tag{B.14}$$

Multiplying by $\cos(m\theta)$ and integrating from $\theta = 0$ to $\theta = 2\pi$

$$\frac{d\phi_m^c}{d\tau} + 2\pi m\, w\, \phi_m^s = -D\phi_m^c + \frac{D}{\pi}\sum_{\substack{n=1\\ n\neq m}}^{\infty}\phi_n^s\left[(-1)^{m+n} - 1\right]\frac{2n}{n^2 - m^2} \tag{B.15}$$

Now multiplying by $\sin(m\theta)$ and integrating from $\theta = 0$ to $\theta = 2\pi$

$$\begin{aligned}\frac{d\phi_m^s}{d\tau} - 2\pi m\, w\, \phi_m^c = -D\phi_m^s + \frac{D}{\pi}\sum_{\substack{n=0\\ n\neq m}}^{\infty}\phi_n^c\left[(-1)^{m+n} - 1\right]\frac{2m}{m^2 - n^2} \\ -\frac{2D}{\pi m}\left[1 - (-1)^m\right]\end{aligned} \tag{B.16}$$

for $m \geq 1$.

Choosing the variables

$$\begin{aligned} w &= w \\ C_0 &= \phi_0^c \\ C_m &= \phi_m^c \\ S_m &= \phi_m^s \end{aligned}$$

we get an infinte-dimensional dynamical system

$$\frac{dw}{d\tau} = -\Gamma w + \frac{\pi^2\Gamma}{4D}\cos\alpha\, C_1 - \frac{\pi^2\Gamma}{4D}\sin\alpha\, S_1 \tag{B.17}$$

$$\frac{dC_0}{d\tau} = -D\, C_0 + \frac{D}{\pi}\sum_{n=1}^{\infty}\frac{S_n}{n}\left[(-1)^n - 1\right] + D \tag{B.18}$$

$$\frac{dC_m}{d\tau} = -2\pi m\, w\, S_m - D\, C_m + \frac{D}{\pi}\sum_{\substack{n=1\\ n\neq m}}^{\infty}S_n\left[(-1)^{m+n} - 1\right]\frac{2n}{n^2 - m^2} \tag{B.19}$$

$$\begin{aligned}\frac{dS_m}{d\tau} = 2\pi m\, w\, C_m - D\, S_m + \frac{D}{\pi}\sum_{\substack{n=0\\ n\neq m}}^{\infty}C_n\left[(-1)^{m+n} - 1\right]\frac{2m}{m^2 - n^2} \\ + \frac{2D}{\pi m}\left[(-1)^m - 1\right]\end{aligned} \tag{B.20}$$

for $m \geq 1$. The physical significance of the variables are: w is the fluid velocity, C is the horizontal temperature difference, and S is the vertical temperature difference. The parameters of the system are D, Γ and α. D and Γ are positive, while α can have any sign.

The critical points are found by equating the vector filed to zero, so that

$$\begin{aligned}
\overline{w} - \frac{\pi^2}{4D}\cos\alpha\,\overline{C}_1 + \frac{\pi^2}{4D}\sin\alpha\,\overline{S}_1 &= 0 \\
(\overline{C}_0 - 1) - \frac{1}{\pi}\sum_{n=1}^{\infty}\frac{\overline{S}_n}{n}\left[(-1)^n - 1\right] &= 0 \\
2\pi m\,\overline{w}\,\overline{S}_m + D\,\overline{C}_m - \frac{D}{\pi}\sum_{\substack{n=1\\ n\neq m}}^{\infty}\overline{S}_n\left[(-1)^{m+n} - 1\right]\frac{2n}{n^2 - m^2} &= 0 \\
2\pi m\,\overline{w}\,\overline{C}_m - D\,\overline{S}_m + \frac{D}{\pi}\sum_{\substack{n=0\\ n\neq m}}^{\infty}\overline{C}_n\left[(-1)^{m+n} - 1\right]\frac{2m}{m^2 - n^2} & \\
+\frac{2D}{\pi m}\left[(-1)^m - 1\right] &= 0
\end{aligned}$$

However, a convenient alternative way to determine the critical points is by using a Fourier series expansion of the steady-state temperature field solution given in Eq. (B.8). The Fourier series expansion is

$$\overline{\phi} = \sum_{n=0}^{\infty}\left[\overline{C}_n\cos(n\theta) + \overline{S}_n\sin(n\theta)\right] \tag{B.21}$$

Performing the inner product between Eq. (B.8) and $\cos(m\theta)$ we have

$$\begin{aligned}
&\frac{D}{\overline{w}}\frac{1}{1 - e^{-(D/\overline{w})}}\int_0^{\pi} e^{-(D\theta/\pi\overline{w})}\,\cos(m\theta)\,d\theta \\
&+\frac{D}{\overline{w}}\int_{\pi}^{2\pi}\left[\frac{\theta}{\pi} + \frac{2e^{-(D/\overline{w})} - 1}{1 - e^{-(D/\overline{w})}}\right]\cos(m\theta)\,d\theta \\
&= \sum_{n=0}^{\infty}\overline{C}_n\int_0^{2\pi}\cos(n\theta)\cos(m\theta)\,d\theta + \sum_{n=0}^{\infty}\overline{S}_n\int_0^{2\pi}\sin(n\theta)\,\cos(m\theta)d\theta
\end{aligned}$$

Now the inner product between Eq. (B.8) and $\sin(m\theta)$ gives

$$\begin{aligned}
&\frac{D}{\overline{w}}\frac{1}{1 - e^{-(D/\overline{w})}}\int_0^{\pi} e^{-(D\theta/\pi\overline{w})}\,\sin(m\theta)\,d\theta \\
&+\frac{D}{\overline{w}}\int_{\pi}^{2\pi}\left[\frac{\theta}{\pi} + \frac{2e^{-(D/\overline{w})} - 1}{1 - e^{-(D/\overline{w})}}\right]\sin(m\theta)\,d\theta \\
&= \sum_{n=0}^{\infty}\overline{C}_n\int_0^{2\pi}\cos(n\theta)\sin(m\theta)\,d\theta + \sum_{n=0}^{\infty}\overline{S}_n\int_0^{2\pi}\sin(n\theta)\,\sin(m\theta)d\theta
\end{aligned}$$

from which we get

$$\overline{C}_0 = \frac{1}{2}\left[1 + \frac{D}{\overline{w}}\left(\frac{3}{2} + \frac{2e^{-(D/\overline{w})} - 1}{1 - e^{-(D/\overline{w})}}\right)\right] \tag{B.22}$$

$$\overline{C}_m = \frac{\left(\frac{D}{\pi\overline{w}}\right)^2}{\left[m^2 + \left(\frac{D}{\pi\overline{w}}\right)^2\right]} \frac{1 - e^{-(D/\overline{w})}\cos(m\pi)}{1 - e^{-(D/\overline{w})}} + \frac{D}{\pi^2 m^2 \overline{w}}\left[1 - \cos(m\pi)\right] \tag{B.23}$$

$$\overline{S}_m = -\left\{\frac{\left(\frac{D}{\pi\overline{w}}\right)^3}{m\left[m^2 + \left(\frac{D}{\pi\overline{w}}\right)^2\right]} \frac{1 - e^{-(D/\overline{w})}\cos(m\pi)}{1 - e^{-(D/\overline{w})}}\right\} \tag{B.24}$$

To analyze the stability of a critical point $(\overline{w}, \overline{C}_0, \overline{C}_1, \cdots, \overline{C}_m, \overline{S}_1, \cdots, \overline{S}_m)$ we add perturbations of the form

$$w = \overline{w} + w' \tag{B.25}$$

$$C_0 = \overline{C}_0 + C_0' \tag{B.26}$$

$$C_1 = \overline{C}_1 + C_1' \tag{B.27}$$

$$\vdots \tag{B.28}$$

$$C_m = \overline{C}_m + C_m' \tag{B.29}$$

$$S_1 = \overline{S}_1 + S_1' \tag{B.30}$$

$$\vdots \tag{B.31}$$

$$S_m = \overline{S}_m + S_m' \tag{B.32}$$

Substituting in Eqs. (B.17) to (B.20), we obtain the local form

$$\frac{dw'}{d\tau} = -\Gamma w' + \frac{\pi^2\Gamma}{4D}\cos\alpha\, C_1' - \frac{\pi^2\Gamma}{4D}\sin\alpha\, S_1' \tag{B.33}$$

$$\frac{dC_0'}{d\tau} = -D\, C_0' + \frac{D}{\pi}\sum_{n=1}^{\infty}\frac{(-1)^n - 1}{n} S_n' \tag{B.34}$$

$$\begin{aligned}\frac{dC_m'}{d\tau} &= -2\pi m\,\overline{w}\, S_m' - 2\pi m\,\overline{S}_m\, w' - D\, C_m' \\ &+ \frac{D}{\pi}\sum_{\substack{n=1\\ n\neq m}}^{\infty}\frac{2n}{n^2 - m^2}\left[(-1)^{m+n} - 1\right] S_n' - 2\pi m\, w'\, S_m' \qquad m \geq 1\end{aligned} \tag{B.35}$$

$$\begin{aligned}\frac{dS_m'}{d\tau} &= 2\pi m\,\overline{w}\, C_m' + 2\pi m\,\overline{C}_m\, w' - D\, S_m' \\ &+ \frac{D}{\pi}\sum_{\substack{n=0\\ n\neq m}}^{\infty}\frac{2m}{m^2 - n^2}\left[(-1)^{m+n} - 1\right] C_n' + 2\pi m\, w'\, C_m' \qquad m \geq 1\end{aligned} \tag{B.36}$$

The linearized version is

$$\frac{dw'}{d\tau} = -\Gamma w' + \frac{\pi^2\Gamma}{4D}\cos\alpha\, C_1' - \frac{\pi^2\Gamma}{4D}\sin\alpha\, S_1' \tag{B.37}$$

$$\frac{dC_0'}{d\tau} = -D\, C_0' + \frac{D}{\pi}\sum_{n=1}^{\infty}\frac{(-1)^n - 1}{n} S_n' \tag{B.38}$$

$$\begin{aligned}\frac{dC_m'}{d\tau} &= -2\pi m\,\overline{w}\, S_m' - 2\pi m\,\overline{S}_m\, w' - D\, C_m' \\ &+ \frac{D}{\pi}\sum_{\substack{n=1\\ n\neq m}}^{\infty}\frac{2n}{n^2-m^2}\left[(-1)^{m+n}-1\right] S_n' \qquad m \geq 1\end{aligned} \tag{B.39}$$

$$\begin{aligned}\frac{dS_m'}{d\tau} &= 2\pi m\,\overline{w}\, C_m' + 2\pi m\,\overline{C}_m\, w' - D\, S_m' \\ &+ \frac{D}{\pi}\sum_{\substack{n=0\\ n\neq m}}^{\infty}\frac{2m}{m^2-n^2}\left[(-1)^{m+n}-1\right] C_n' \qquad m \geq 1\end{aligned} \tag{B.40}$$

In general, the system given by Eqs. (B.17) to (B.20) can be written as

$$\frac{d\mathbf{x}}{dt} = \mathbf{f}(\mathbf{x}) \tag{B.41}$$

The eigenvalues of the linearized system given by Eqs. (B.37) to (B.40), and in general form as

$$\frac{d\mathbf{x}}{dt} = \mathbf{A}\mathbf{x} \tag{B.42}$$

are obtained numerically, such that

$$|\mathbf{A} - \lambda\mathbf{I}| = 0$$

where $\mathbf{A}$ is the Jacobian matrix corresponding to the vector field of the linearized system, $\mathbf{I}$ is the identity matrix, and λ are the eigenvalues. The neutral stability curve is obtained numerically from the condition that $\Re(\lambda) = 0$. A schematic of the neutral curve is presented in Figure B.6 for $\alpha = 0$. In this figure, the stable and unstable regions can be identified. Along the line of neutral stability, a Hopf-type of bifurcation occurs. Figure B.7 shows the plot of $\overline{w} - \alpha$ curve for a value of the parameters $D = 0.1$ and $\Gamma = 0.20029$. When $\alpha = 0$, a Hopf bifurcation for both the positive and negative branches of the curve can be observed, where stable and unstable regions can be identified. It is clear that the *natural* branches which correspond to the first and third quadrants are stable, whereas the *antinatural* branches, second and fourth quadrants are unstable. The symmetry between the first and third quadrants, and, between the second and fourth quadrants can be notice as well. The corresponding eigenvalues of the bifurcation point are shown in Figure B.8. The number of eigenvalues in this figure is 42 which are obtained from a dynamical system of dimension 42. This system results from truncating the infinite dimensional system at a number for which the value of the leading eigenvalues does not change when increasing its dimension. When we increase the size of the system, new eigenvalues appear in such a way that they are placed symmetrically farther from the real axis and aligned to the previous set of slave complex eigenmodes. This behaviour seems to

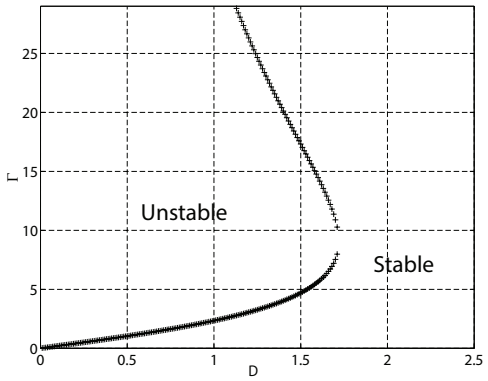

Figure B.6: Stability curve D and Γ for a thermosyphon inclination $\alpha = 0$.

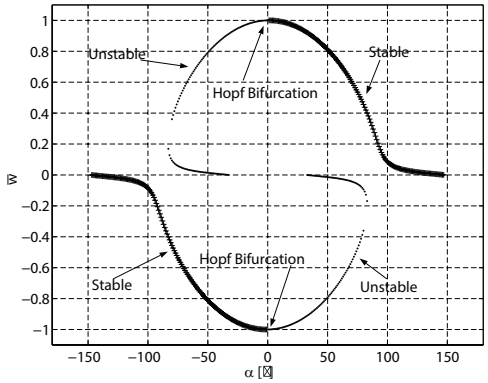

Figure B.7: Stability curve $\overline{w}$ vs. α for $D = 0.1$, and $\Gamma = 0.20029$.

be a characteristic of the dynamical system itself. Figure B.9 illustrates a view of several stability curves, each for a different value of the tilt angle α in a $D - \Gamma$ plane at $\alpha = 0$. In this plot, the neutral curves appear to unfold when decreasing the tilt angle from 75.5° to −32.5° increasing the region of instability. On the other hand, Figure B.10 illustrates the linear stability characteristics of the dynamical system in a $\overline{w} - \alpha$ plot for a fixed Γ and three values of the parameter D. The stable and unstable regions can be observed. Hopf bifurcations occur for each branch of ecah particular curve. However, it is to be notice that the bifurcation occurs at a higher value of the tilt angle when D is smaller.

B.5 Nonlinear analysis

Let us select $D = 1.5$, and increase Γ. Figures B.11 and B.12 show the $w - \tau$ time series and phase-space curves for $\Gamma = 0.95\Gamma_{cr}$, whereas Figures B.13 and B.14 show the results for $\Gamma = 1.01\Gamma_{cr}$. The plots suggest the appearance of a subcritical Hopf bifurcation. Two attractors coexist for $\Gamma \leq \Gamma_{cr}$, these being a critical point and a strange attractor of fractional dimension. For $\Gamma > \Gamma_{cr}$, the only presence is of a strange attractor.

Now we choose $D = 0.1$, and increase Γ. Figure B.15 presents a plot of the $\overline{w} - \tau$ curve for

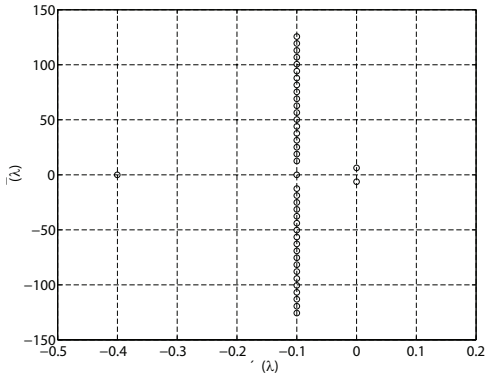

Figure B.8: Eigenvalues at the neutral curve for $D = 0.1$, $\Gamma = 0.20029$ and $\alpha = 0$.

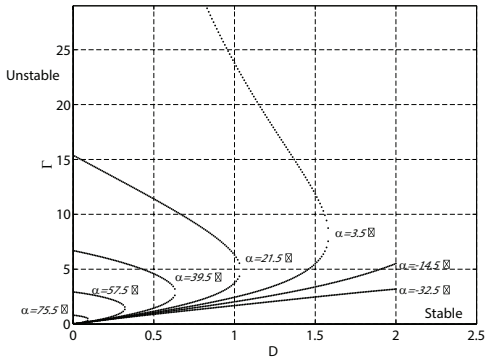

Figure B.9: Neutral stability curve for different values of the tilt angle α.

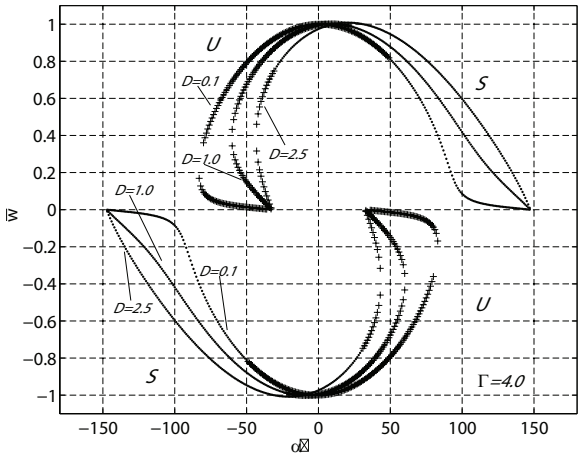

Figure B.10: Curve $\overline{w}$ vs. α $\Gamma = 4.0$ and $D = 0.1$,$D = 1.0$,$D = 2.5$.

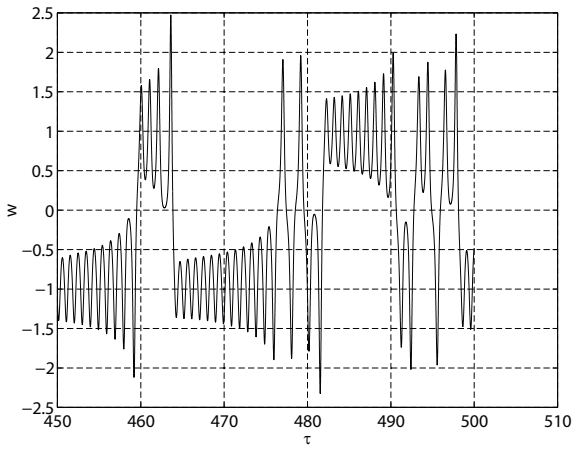

Figure B.11: Curve w vs. τ for $D = 1.5$, $\Gamma = 0.95\Gamma_{cr}$.

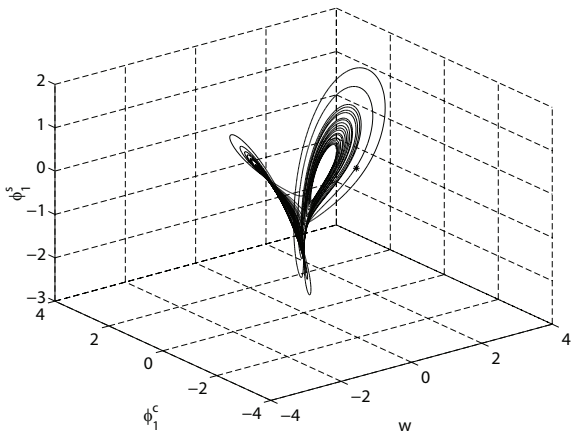

Figure B.12: Phase-space trajectory for $D = 1.5$, $\Gamma = 0.95\Gamma_{cr}$.

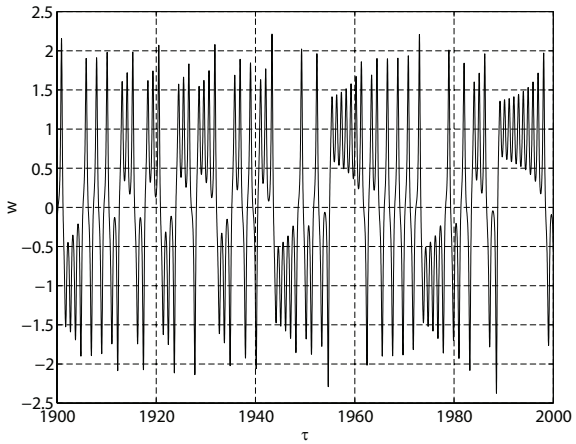

Figure B.13: Curve w vs. τ for $D = 1.5$, $\Gamma = 1.01\Gamma_{cr}$.

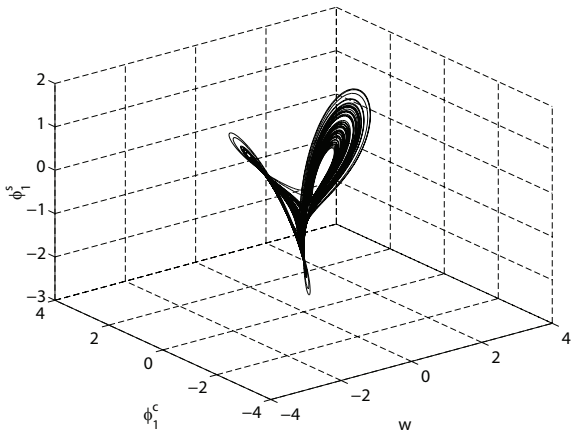

Figure B.14: Phase-space trajectory for $D = 1.5$, $\Gamma = 1.01\Gamma_{cr}$.

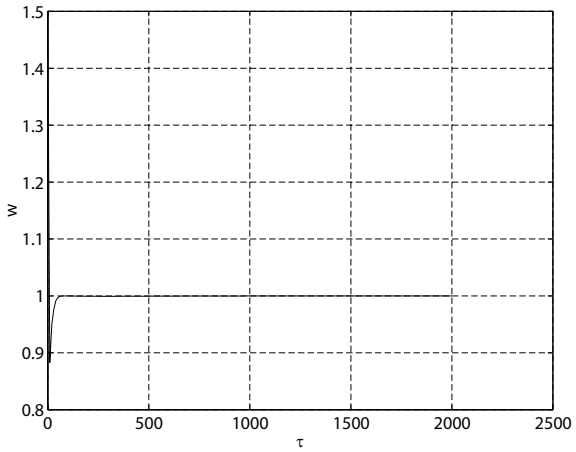

Figure B.15: Curve w vs. τ for $D = 0.1$, $\Gamma = 0.99\Gamma_{cr}$.

$\Gamma = 0.99\Gamma_{cr}$. Figures B.16 and B.17 show the time series plots and phase space representation for $\Gamma = 1.01\Gamma_{cr}$, and Figures B.18 and B.19 for $\Gamma = 20\Gamma_{cr}$. In this case, for $\Gamma < \Gamma_{cr}$ we have stable solutions. For $\Gamma = 1.01\Gamma_{cr}$ the figures show a possible limit cycle undergoes a period doubling. This implies a supercritical Hopf bifurcation. The strange attractor is shown in Figures B.20 and B.21.

B.6 Further nonlinear analysis

The following analysis is by W. Franco.

We start with the dynamical system which models a toroidal thermosyphon loop with known heat flux

$$\begin{aligned}\frac{dx}{dt} &= y - x\\ \frac{dy}{dt} &= a - zx\\ \frac{dz}{dt} &= xy - b\end{aligned}$$

For $b > 0$ two critical points P^+ and P^- appear

$$(\bar{x}, \bar{y}, \bar{z}) = \pm\left(\sqrt{b}, \sqrt{b}, \frac{a}{\sqrt{b}}\right)$$

The local form respect to P^+ is

$$\begin{aligned}\frac{dx'}{dt} &= y' - x'\\ \frac{dy'}{dt} &= -\frac{a}{\sqrt{b}}x' - \sqrt{b}z'\\ \frac{dz'}{dt} &= \sqrt{b}x' + \sqrt{b}y'\end{aligned}$$

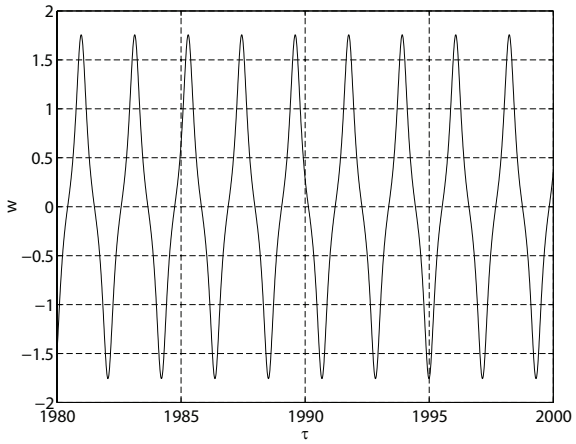

Figure B.16: Curve w vs. τ for $D = 0.1$, $\Gamma = 1.1\Gamma_{cr}$.

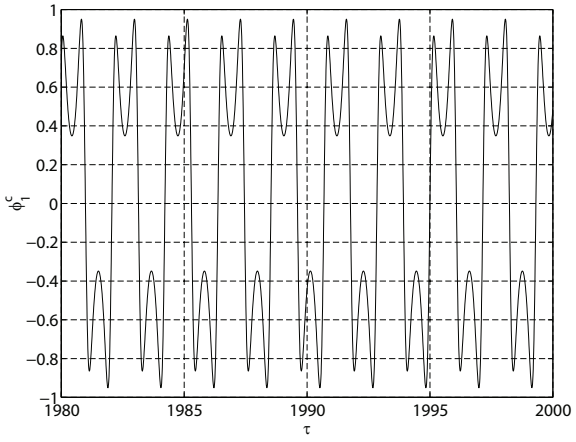

Figure B.17: Phase-space trajectory for $D = 0.1$, $\Gamma = 1.1\Gamma_{cr}$.

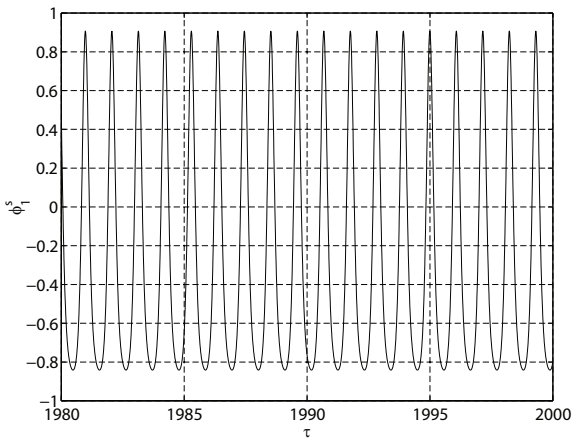

Figure B.18: Curve w vs. τ for $D = 0.1$, $\Gamma = 1.1\Gamma_{cr}$.

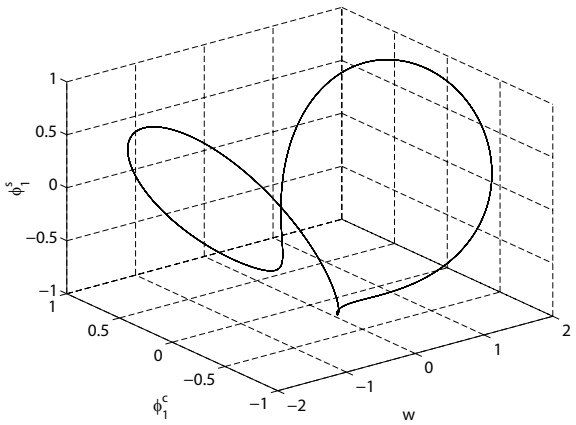

Figure B.19: Phase-space trajectory for $D = 0.1$, $\Gamma = 1.1\Gamma_{cr}$.

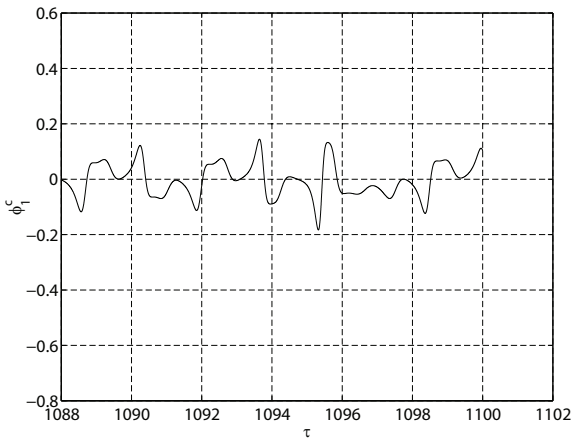

Figure B.20: Phase-space trajectory for $D = 0.1$, $\Gamma = 20\Gamma_{cr}$.

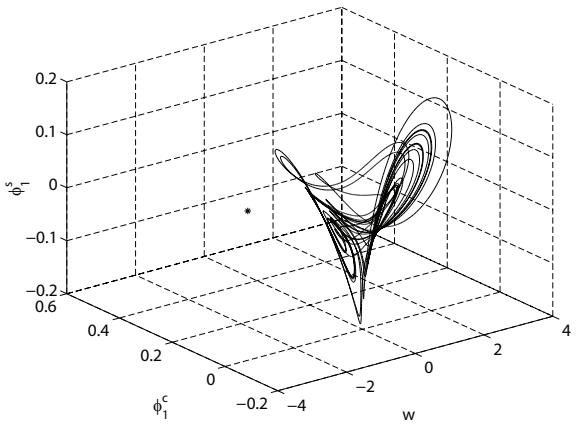

Figure B.21: Phase-space trajectory for $D = 0.1$, $\Gamma = 20\Gamma_{cr}$.

For stability $a > b^{\frac{3}{2}}$. At $a = b^{\frac{3}{2}}$ the eigenvalues are $-1,\pm\sqrt{2b}i$, thus a nonlinear analysis through the center manifold projection is possible. Let's introduce a perturbation of the form $a = b^{\frac{3}{2}} + \epsilon$ and the following change of variables

$$\alpha = \frac{a}{\sqrt{b}}$$
$$\beta = \sqrt{b}$$

rewriting the local form, dropping the primes and regarding the perturbation the system becomes

$$\frac{dx}{dt} = y - x$$
$$\frac{dy}{dt} = \left(\beta^2 + \frac{\epsilon}{\beta}\right) x - \beta z$$
$$\frac{dz}{dt} = \beta x - \beta y$$

for stability $\alpha > \beta^2$.

Let's apply the following transformation:

$$\begin{aligned} x &= w_1 + \frac{2}{2\beta^2+1} w_2 + \frac{2\beta\sqrt{2}}{2\beta^2+1} \\ y &= 2w_2 \\ z &= -\beta w_1 - \frac{2\beta}{2\beta^2+1} w_2 + \frac{2\sqrt{2}\left(\beta^2+1\right)}{2\beta^2+1} w_3 \end{aligned} \tag{B.43}$$

in the new variables

$$\dot{\mathbf{w}} = \begin{pmatrix} -1 & 0 & 0 \\ 0 & 0 & -\sqrt{2}\beta \\ 0 & \sqrt{2}\beta & 0 \end{pmatrix} \mathbf{w} + \hat{\mathbf{P}}\mathbf{w} + \mathbf{l}(\mathbf{w}) \tag{B.44}$$

The center manifold projection is convenient to use if the large-time dynamic behavior is of interest. In many dimensional systems, the system often settles into the same large-time dynamics irrespective of the initial condition; this is usually less complex than the initial dynamics and can be described by far simple evolution equations.

We first state the definition of an invariant manifold for the equation

$$\dot{x} = N(x) \tag{B.45}$$

where $x \in R^n$. A set $S \subset R^n$ is a local invariant manifold for (B.45) if for $x_0 \subset S$, the solution $x(t)$ of (B.45) is in S for $\mid t \mid < T$ where $T > 0$. If we can always choose $T = \infty$, then S is an invariant manifold. Consider the system

$$\begin{aligned} \dot{x} &= Ax + f(x,y) \\ \dot{y} &= By + g(x,y) \end{aligned} \tag{B.46}$$

where $x \in R^n$, $y \in R^m$ and A and B are constant matrices such that all the eigenvalues of A have zero real parts while all the eigenvalues of B have negative real parts. If $y = h(x)$ is an invariant

manifold for (**??**) and h is smooth, then it is called a center manifold if $h(0) = 0$,$h'(0) = 0$. The flow on the center manifold is governed by the n-dimensional system

$$\dot{x} = Ax + f(x, h(x))$$

The last equation contains all the necessary information needed to determine the asymptotic behavior of small solutions of (**??**).

Now we calculate, or at least approximate the center manifold $h(\mathbf{w})$. Substituting $w_1 = h(w_2, w_3)$ in the first component of (B.44) and using the chain rule, we obtain

$$\dot{w}_1 = \left(\frac{\partial h}{\partial w_2}, \frac{\partial h}{\partial w_3}\right) \begin{pmatrix} \dot{w}_2 \\ \\ \dot{w}_3 \end{pmatrix} = -h + l_1\left(w_2, w_3, h\right) \tag{B.47}$$

We seek a center manifold

$$h = aw_2^2 + bw_2w_3 + cw_3^2 + O(3)$$

substituting in (B.47)

$$(2aw_2 + bw_3, 2cw_3 + bw_2) \begin{pmatrix} -\sqrt{2}\beta w_3 \\ \\ \sqrt{2}\beta w_2 \end{pmatrix} = -\left(aw_2^2 + bw_2w_3 + cw_3^2\right) + \left(k_1w_2^2 + k_2w_2w_3 + k_3w_3^2\right) + O(3)$$

Equating powers of x^2,xy and y^2, we find that

$$\begin{aligned} a &= k_1 - b\sqrt{2}\beta \\ c &= k_3 + b\sqrt{2}\beta \\ b &= \frac{k_2 + 2\sqrt{2}\beta\left(k_1 - k_3\right)}{8\beta^2 + 1} \end{aligned}$$

The reduced system is therefore given by

$$\begin{aligned} \dot{w}_2 &= -\sqrt{2}\beta w_3 + s^2\left(w_2, w_3\right) \\ \dot{w}_3 &= \sqrt{2}\beta w_2 + s^3\left(w_2, w_3\right) \end{aligned} \tag{B.48}$$

Normal form: Now we carry out a smooth nonlinear coordinate transform of the type

$$\mathbf{w} = \mathbf{v} + \psi(\mathbf{v})$$

to simplify (B.48) by transforming away many nonlinear terms. The system in the new coordinates is

$$\dot{\mathbf{v}} = \begin{pmatrix} 0 & -\sqrt{2}\beta \\ \sqrt{2}\beta & 0 \end{pmatrix} + \begin{pmatrix} \left(\nu v_1 - \gamma v_2\right)\left(v_1^2 + v_2^2\right) \\ \\ \left(\nu v_2 + \gamma v_1\right)\left(v_1^2 + v_2^2\right) \end{pmatrix} \tag{B.49}$$

where ν and γ depend on the nonlinear part of (B.48). This is the unfolding of the Hopf bifurcation.

Although the normal form theory presented in class pertains to a Jacobian whose eigenvalues all lie on the imaginary axis, one can also present a perturbed version. The eigenvalues are then close to the imaginary axis but not quite on it. Consider the system

$$\dot{\mathbf{v}} = \mathbf{A}\mathbf{v} + \hat{\mathbf{A}}\mathbf{v} + \mathbf{f}(\mathbf{v}) \tag{B.50}$$

where the Jacobian $\mathbf{A}$ has been evaluated at a point in the parameter space where all its eigenvalues are on the imaginary axis, $\hat{\mathbf{A}}$ represents a linear expansion of order μ in the parameters above that point; a perturbed Jacobian. The perturbation parameter represents the size of the neighborhood in the parameter space. We stipulate the order of μ such that the real part of the eigenvalues of $\mathbf{A}+\hat{\mathbf{A}}$ is such that, to leading order, $\hat{\mathbf{A}}$ does not change the coefficients of the leading order nonlinear terms of the transformed equation. The linear part $\mathbf{A}+\hat{\mathbf{A}}$ of perturbed Hopf can always be transformed to

$$\begin{pmatrix} \mu & -\omega \\ \omega & \mu \end{pmatrix}$$

The required transformation is a near identity linear transformation

$$\mathbf{v} = \mathbf{u} + \mathbf{B}\mathbf{u}$$

such that the linear part of (B.50) is transformed to

$$\dot{\mathbf{u}} = \left(\mathbf{A} + \mathbf{A}\mathbf{B} - \mathbf{B}\mathbf{A} + \hat{\mathbf{A}}\right)\mathbf{z}$$

For the Hopf bifurcation if

$$\hat{\mathbf{A}} = \begin{pmatrix} a_1 & a_2 \\ a_3 & a_4 \end{pmatrix}$$

then

$$\mu = \frac{a1 + a4}{\omega}$$

Therefore for ϵ small we can write (B.49) as

$$\dot{\mathbf{v}} = \begin{pmatrix} 0 & -\sqrt{2}\beta \\ \sqrt{2}\beta & 0 \end{pmatrix}\mathbf{v} + \begin{pmatrix} p_{22} & p_{23} \\ p_{32} & p_{33} \end{pmatrix}\mathbf{v} + \begin{pmatrix} f_1(\mathbf{v}) \\ \\ f_2(\mathbf{v}) \end{pmatrix}$$

where the perturbation matrix comes from (B.44). Applying a near identity transformation of the form $\mathbf{v} = \mathbf{u} + \mathbf{B}\mathbf{u}$ the system becomes

$$\dot{\mathbf{u}} = \begin{pmatrix} \mu & -\sqrt{2}\beta \\ \sqrt{2}\beta & \mu \end{pmatrix}\mathbf{u} + \begin{pmatrix} (\nu u_1 - \gamma u_2)\left(u_1^2 + u_2^2\right) \\ \\ (\nu u_2 + \gamma u_1)\left(u_1^2 + u_2^2\right) \end{pmatrix}$$

which is the unfolding for the perturbed Hopf bifurcation. In polar coordinates we have

$$\begin{aligned} \dot{r} &= \mu r + \nu r^3 \\ \dot{\theta} &= \sqrt{2}\beta \end{aligned}$$

where

$$\mu = -\frac{\epsilon\sqrt{2}}{2\beta^2\left(2\beta^2 + 1\right)}$$

$$\nu = -\frac{40\beta^6 + 40\beta^4 + 12\beta^3 + 10\beta^2 + 12\beta + 3}{4\left(8\beta^2+1\right)\left(2\beta^2+1\right)^4}$$

Appendix

$$k_1 = -\frac{8\beta\left(\beta^2+1\right)}{\left(2\beta^2+1\right)^3}$$
$$k_2 = \frac{\left(\beta^2+1\right)\left(4\sqrt{2}-8\sqrt{2}\beta^2\right)}{\left(2\beta^2+1\right)^3}$$
$$k_3 = \frac{8\beta\left(\beta^2+1\right)}{\left(2\beta^2+1\right)^3}$$

$$p_{22} = -\frac{\epsilon}{\beta\left(2\beta^2+1\right)}$$
$$p_{23} = -\frac{\epsilon\sqrt{2}}{2\beta^2+1}$$

From the literature

$$\nu = \frac{1}{16}\left(f_{xxx} + f_{xyy} + g_{xxy} + g_{yyy}\right) + \frac{1}{16\omega}\left(f_{xy}(f_{xx}+f_{yy}) - g_{xy}(g_{xx}-g_{yy}) - f_{xx}g_{xx} - f_{yy}g_{yy}\right)$$

in our problem $f = f_1$, $g = f_2$, $x = v_1$, $y = v_2$ and $\omega = \sqrt{2}\beta$.

Appendix C

Networks

A network consists of a number of ducts that are united at certain points. At each junction, we must have

$$\sum_i A_i V_i = 0 \tag{C.1}$$

where A_i are the areas and V_i the fluid velocities in the ducts coming in, the sum being over all the ducts entering the junction. Furthermore, for each duct, the momentum equation is

$$\frac{dV_i}{dt} + T(V_i)V_i = \beta \ \left[p_i^{in} - p_i^{out} + \Delta p\right]$$

where Δp is the pressure developed by a pump, if there happens to be one on that line. We must distinguish between two possible geometries.

(a) Two-dimensional networks: A planar or two-dimensional network is one that is topologically equivalent to one on a plane in which every intersection of pipes indicates fluid mixing. For such a graph, we know that

$$E = V + F - 1$$

where E, V and F are the number of edges, vertices and faces, respectively. In the present context, these are better referred to as branches, junctions and circuits, respectively.

The unknowns are the E velocities in the ducts and the V pressures at the junctions, except for one pressure that must be known. The number of unknowns thus are $E+V-1$. The momentum equation in the branches produce E independent differential equations, while mass conservation at the juntions give $V-1$ independent algebraic relations. Thus the number of

(b) Three-dimensional networks: For a three-dimensioanl network, we have

$$E = V + F - 2$$

If there are n junctions, they can have a maximum of $n(n-1)/2$ lines connecting them. The number of circuits is then $(n^2 - 3n + 4)/2$. The number of equations to be solved is thus quite large if n is large.

C.1 Hydrodynamics

The global stability of flow in a network can be demonstrated in a manner similar to that in a finite-length duct. In a general network, assume that there are n junctions, and each is connected to all the rest. Also, p_i is the pressure at junction i, and V_{ij} is the flow velocity from junction i to j defined to be positive in that direction. The flow velocity matrix V_{ij} is anti-symmetric, so that V_{ii} which has no physical meaning is considered zero.

The momentum equation for V_{ij} is

$$\frac{dV_{ij}}{dt} + T_{ij}(V_{ij})V_{ij} = \beta_{ij}(p_i - p_j) \tag{C.2}$$

The network properties are represented by the symmetric matrix β_{ij}. The resistance T_{ij} may or may not be symmetric. To simplify the analysis the network is considered fully connected, but T_{ij} is infinite for those junctions that are not physically connected so that the flow velocity in the corresponding branch is zero. We take the diagonal terms in T_{ij} to be also infinite, so as to have $V_{ii} = 0$.

The mass conservation equation at junction j for all flows arriving there is

$$\sum_{i=1}^{n} A_{ij}V_{ij} = 0 \quad \text{for } j = 1, \ldots, n$$

where A_{ij} is a symmetric matrix. The symmetry of A_{ij} and antisymmetry of V_{ij} gives the equivalent form

$$\sum_{i=1}^{n} A_{ji}V_{ji} = 0 \quad \text{for } j = 1, \ldots, n \tag{C.3}$$

which is simply the mass conservation considering all the flows leaving junction j.

The steady states are solutions of

$$T_{ij}(\overline{V}_{ij})\overline{V}_{ij} = \beta_{ij}(\overline{p}_i - \overline{p}_j) \tag{C.4}$$

$$\sum_{i=1}^{n} A_{ij}\overline{V}_{ij}7 = 0 \quad \text{or} \quad \sum_{i=1}^{n} A_{ji}\overline{V}_{ji} = 0 \tag{C.5}$$

We write

$$V_{ij} = \overline{V}_{ij} + V'_{ij}$$
$$p_i = \overline{p} + p'_i$$

Substituting in equations (C.2)–(C.3), and subtracting equations (C.4) and (C.5) we get

$$\frac{dV'_{ij}}{dt} = -\left[T_{ij}(\overline{V}_{ij} + V'_{ij})(\overline{V}_{ij} + V'_{ij}) - T_{ij}(\overline{V}_{ij})\overline{V}_{ij}\right] + \beta_{ij}(p'_i - p'_j)$$

$$\sum_{i=1}^{n} A_{ij}V'_{ij} = 0 \quad \text{or} \quad \sum_{i=1}^{n} A_{ji}V'_{ji} = 0$$

Defining

$$E = \frac{1}{2}\sum_{j=1}^{n}\sum_{i=1}^{n} \frac{A_{ij}}{\beta_{ij}} V'^{2}_{ij}, \quad \beta_{ij} > 0$$

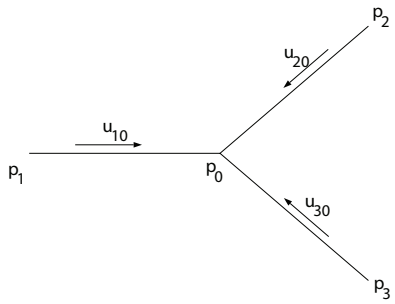

Figure C.1: Star network.

we get

$$\frac{dE}{dt} = \sum_{j=1}^{n}\sum_{i=1}^{n} \frac{A_{ij}}{\beta_{ij}} V'_{ij} \frac{dV'_{ij}}{dt} \tag{C.6}$$

$$= -\sum_{j=1}^{n}\sum_{i=1}^{n} \frac{A_{ij}}{\beta_{ij}} V'_{ij} \left[T_{ij}(\overline{V}_{ij} + V'_{ij})(\overline{V}_{ij} + V'_{ij}) - T_{ij}(\overline{V}_{ij})\overline{V}_{ij} \right] + \sum_{j=1}^{n}\sum_{i=1}^{n} A_{ij} V'_{ij}(p'_i - p'_j) \tag{C.7}$$

The pressure terms vanish since

$$\begin{aligned} \sum_{j=1}^{n}\sum_{i=1}^{n} A_{ij} V'_{ij} p'_i &= \sum_{i=1}^{n}\sum_{j=1}^{n} A_{ij} V'_{ij} p'_i \\ &= \sum_{i=1}^{n} \left(p'_i \sum_{j=1}^{n} A_{ij} V'_{ij} \right) \\ &= 0 \end{aligned}$$

and

$$\begin{aligned} \sum_{j=1}^{n}\sum_{i=1}^{n} A_{ij} V'_{ij} p'_j &= \sum_{j=1}^{n} \left(p'_j \sum_{i=1}^{n} A_{ij} V'_{ij} \right) \\ &= 0 \end{aligned}$$

The terms that are left in equation (C.7) are similar to those in equation (7.10) and satisfy the same inequality. Since $E \geq 0$ and $dE/dt \leq 0$, the steady state is globally stable. For this reason the steady state is also unique.

Example C.1

Show that the flow in the the star network shown in Fig. C.1 is globally stable. The pressures p_1, p_2 and p_3 are known while the pressure p_0 and velocities V_{10}, V_{20} and V_{30} are the unknowns.

For branches $i = 1, 2, 3$, equation (**??**) is

$$\frac{dV_{i0}}{dt} + T_{i0}(V_{i0})V_{i0} = \beta_{i0}(p_i - p_0) \tag{C.8}$$

Equation (C.1) at the junction gives

$$\sum_{i=1}^{3} A_{i0} V_{i0} = 0 \tag{C.9}$$

In the steady state

$$T_{i0}(\overline{V}_{i0})\overline{V}_{i0} = \beta_{i0}(p_i - \overline{p}_0) \tag{C.10}$$

$$\sum_{i=1}^{3} A_{i0} \overline{V}_{i0} = 0 \tag{C.11}$$

Substituting $V_{i0} = \overline{V}_{i0} + V'_{i0}$ and $p_0 = \overline{p}_0 + p'_0$ in equations (C.8) and (C.9) and subtracting equations (C.10) and (C.11), we find that

$$\frac{dV'_{i0}}{dt} = -\left[T_{i0}(\overline{V}_{i0} + V'_{i0})(\overline{V}_{i0} + V'_{i0}) - T_{i0}(\overline{V}_{i0})\overline{V}_{i0}\right] - \beta_{i0} p'_0 \tag{C.12}$$

$$\sum_{i=1}^{3} A_{i0} V'_{i0} = 0 \tag{C.13}$$

If we define

$$E = \frac{1}{2} \sum_{i=1}^{3} \frac{A_{i0}}{\beta_{i0}} {V'}_i^2$$

we find that

$$\begin{aligned} \frac{dE}{dt} &= \sum_{i=1}^{3} \frac{A_{i0}}{\beta_{i0}} V'_{i0} \frac{dV'_{i0}}{dt} \\ &= -\sum_{i=1}^{3} \frac{A_{i0}}{\beta_{i0}} V'_{i0} \left[T_{i0}(\overline{V}_{i0} + V'_{i0})(\overline{V}_{i0} + V'_{i0}) - T_{i0}(\overline{V}_{i0})\overline{V}_{i0}\right] - p'_0 \sum_{i=1}^{3} A_{i0} V'_{i0} \end{aligned}$$

The last term vanishes because of equation (C.13). Thus

$$\frac{dE}{dt} = -\sum_{i=1}^{3} \frac{A_{i0}}{\beta_{i0}} V'_{i0} \overline{V}_{i0} \left[T_{i0}(\overline{V}_{i0} + V'_{i0}) - T_{i0}(\overline{V}_{i0})\right] - \sum_{i=1}^{3} \frac{A_{i0}}{\beta_{i0}} {V'}_{i0}^2 T_{i0}(\overline{V}_{i0} + V'_{i0})$$

Since $E \geq 0$ and $dE/dt \leq 0$, E is a Lyapunov function and the steady state is globally stable.

C.2 Thermal networks

[63]

C.3 Control of complex thermal systems

The previous sections examined systems that were fairly simple in the sense that mathematical models could be written down and their behaviors studied. For most practical thermal systems, this is difficult to do with any degree of precision. In the following, we will look first at thermal components and then combine them in networks.

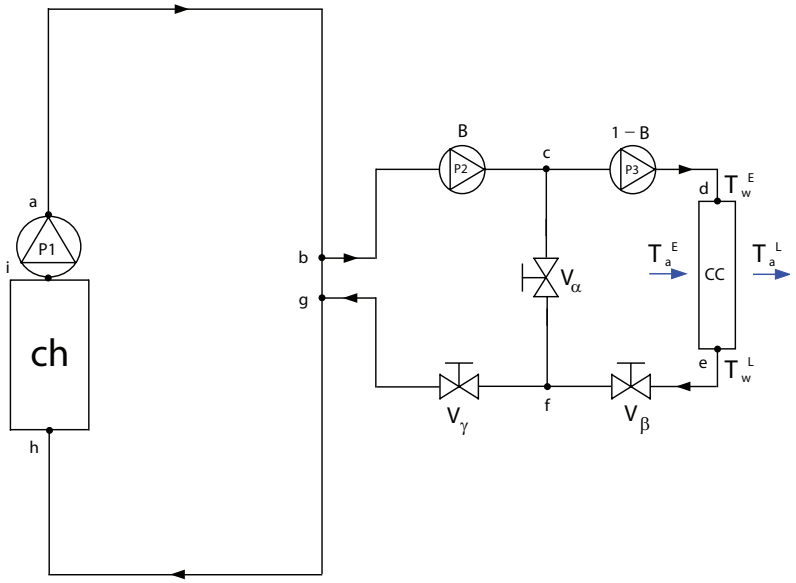

Figure C.2: Network used to study control strategies [63].

C.3.1 Hydronic networks

The science of networks of all kinds has been put forward as a new emerging science [15]. In the present context this means that a complete understanding of the behavior of components does not necessarily mean that large networks formed out of these components can be modeled and computed in real time for control purposes. Controllability issues of heat exchanger networks are reported in [213]. Mathematical models of the dynamics of a piping network lead to differential-algebraic systems [63]. The momentum equation governing the flow in each pipe is differential, while the conservation of mass condition at each of the junctions is algebraic. Thus, it turns out that only certain flow rates may be controllable, the others being dependent on these.

There are at present many different strategies for the thermal control of networks, and comparative studies based on mathematical models can be carried out. Fig. C.2 shows a network in which three specific control strategies can be compared [63, 64]; each control method works differently and are labeled VF, MCF and BT in the following figures (details are in [63]). The network has a primary loop, a secondary loop and a bypass that has the three strategies as special cases. The primary loop includes a chiller, while the secondary has a water-air cooling coil which serves as a thermal load. Integral controllers are used to operate the valves V_α, V_β, and V_γ to control the air temperature leaving the cooling coil, $T_a^L(t)$. Figs. C.3 and C.4 show the dynamic response of $T_a^L(t)$, the leaving water temperatures $T_w^L(t)$, and the bypass pressure difference Δp_{bp} to step changes in the air velocity over the coil. $\alpha(t)$, $\beta(t)$, and $\gamma(t)$ are the respective closing fractions of the valves which change dynamically in response to the error signal. There are some oscillations in all the variables before they settle down to stable, steady values.

Laboratory experiments with a network of water-to-water heat exchangers have been reported in [63–65]; the configuration is shown in Fig. C.5. The hot water flow is diminished by changing its controller set point. Figure C.6 shows the secondary hot water flow rates q_8, q_7 and q_4 to the heat exchangers for the three different control strategies. Each curve represents one independent run; that is, water flow to HX_{BT} and HX_{CF} is zero when testing VF, and so on. The system is taken

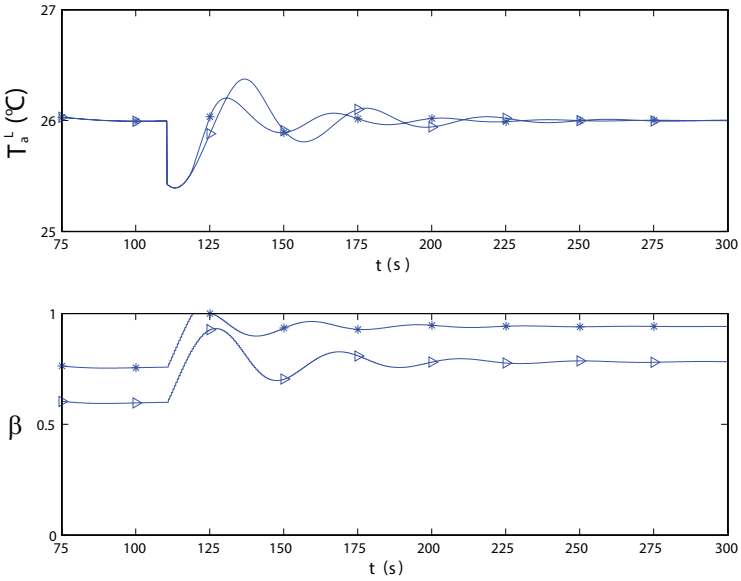

Figure C.3: Dynamic response of control system to drop in air velocity, $-*-$ method VF, and $-\triangleright-$ method MCF; $T^L_{a,set} = 26°\text{C}$, $T^E_a = 30°\text{C}$ [63].

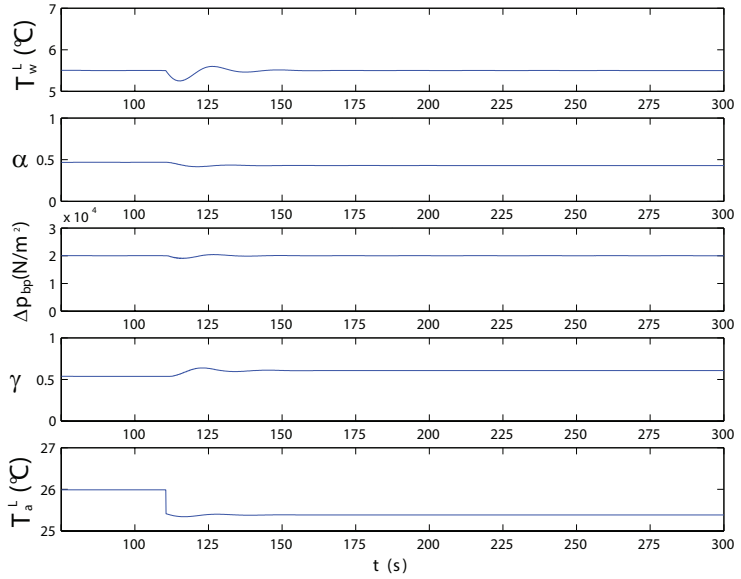

Figure C.4: Dynamic response of control system to drop in air velocity with method BT; $T^L_{w,set} = 5.5°\text{C}$, $\Delta p_{bp,set} = 20000$ (N/m^2); $T^E_a = 30°\text{C}$ [63].

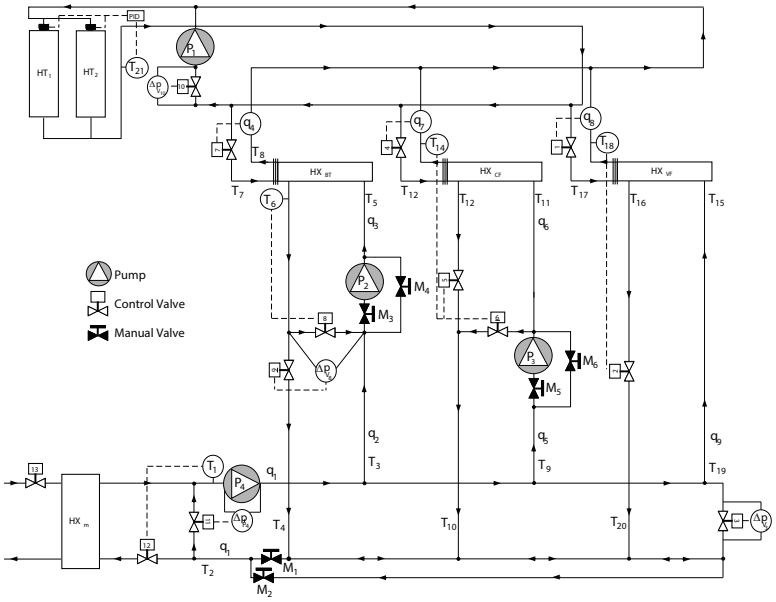

Figure C.5: Layout of hydronic network [63].

to the nominal operating conditions, and then the hot water flow is decreased by a constant value every 1800 s. The controls drive the system to different operational points while coping with the changes. The input voltages v_7, v_4 and v_1 that control flow and the hot water temperature at the heat exchanger inlet T_{21} are also shown. It is seen that for certain control parameters, the system is becomes unstable and the variables oscillate in time.

C.3.2 Other applications

There are a large number of other thermal problems in which control theory has been applied. Agent-based controls have been proposed by complex thermal systems such as in buildings [224], microwave heating [128], thermal radiation [151], and materials processing and manufacturing [56, 169]. Control of convection is an important and active topic; this includes the study of convection loops [184, 185, 215, 226, 228], stabilization and control of convection in horizontal fluid layers [18, 87, 133, 153, 200–205], and in porous media [199].

C.4 Conclusions

This has been a very brief introduction to the theory of thermal control. The fundamental ideas in this subject are firmly grounded on the mathematics of systems and control theory which should be the starting point. There are, however, a few aspects that are particularly characteristic of thermal systems. Phenomena such as diffusion, convection and advection are common and the systems are usually complex, nonlinear and poorly predictable dynamically. The governing equations cover a wide range of possibilities, from ordinary and partial differential equations to functional and differential-algebraic systems. Furthermore, control theory itself is a vast subject, with specialized branches like optimal [83], robust [38], and stochastic control [37] that are well developed. Many of the tools in these areas find applications in thermal systems.

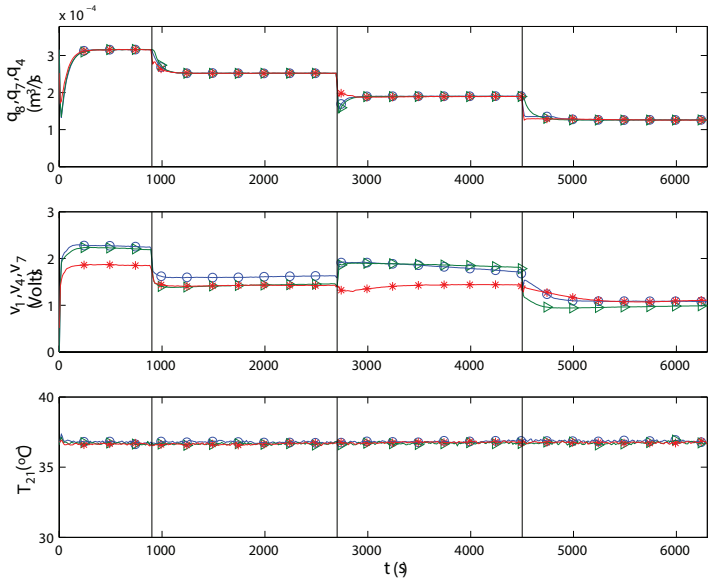

Figure C.6: Secondary hot water flows and T_{21}: $-\circ-BT$, $-\triangleright-CF$, $-*-VF$. The dashed vertical lines are instants at which the thermal load is changed [63].

The study of thermal control will continue to grow from the point of view of fundamentals as well as engineering applications. There are many outstanding problems and issues that need to be addressed. To cite one specific example, networking between a large number of coupled components will become increasingly important; it is known that unexpected synchronization may result even when multiple dynamical systems are coupled weakly [191]. It is hoped that the reader will use this brief overview as a starting point for further study and apply control theory in other thermal applications.

Appendix D

Soft computing

D.1 Genetic algorithms

[149]

D.2 Artificial neural networks

D.2.1 Heat exchangers

The most important of the components are heat exchangers, which are generally very complex in that they cannot be realistically computed in real time for control purposes [97, 162, 192]. An approach that is becoming popular in these cases is that of artificial neural networks (ANN) [76] for prediction of system behavior both for time-independent [49, 147, 148, 150] and time-dependent operation. It is particularly suitable for systems for which experimental information that can be used for training is available. Reviews of artificial neural network applications to thermal engineering [172, 177] and other soft control methodologies [32, 139, 231] and applications [227] are available.

A stabilized neurocontrol technique for heat exchangers has been described in [48, 50–53]. Fig. D.1 shows the test facility in which the experiments were conducted. The objective is to control the outlet air temperature T^a_{out}. Figs. D.2 shows the results of using neurocontrol compared with PID; both are effective. Fig. D.3 shows the result of an disturbance rejection experiment. The heat exchanger is stabilized at $T^a_{out} = 36°\text{C}$, and then the water flow is shut down between $t = 40\text{s}$ and $t = 70\text{s}$; after that the neurocontroller brings the system back to normal operation. A neural network-based controller is able to adapt easily to changing circumstances; in thermal systems this may come from effects such as the presence of fouling over time or from changes in system configuration as could happen in building heating and cooling systems.

[52, 175]

[171]

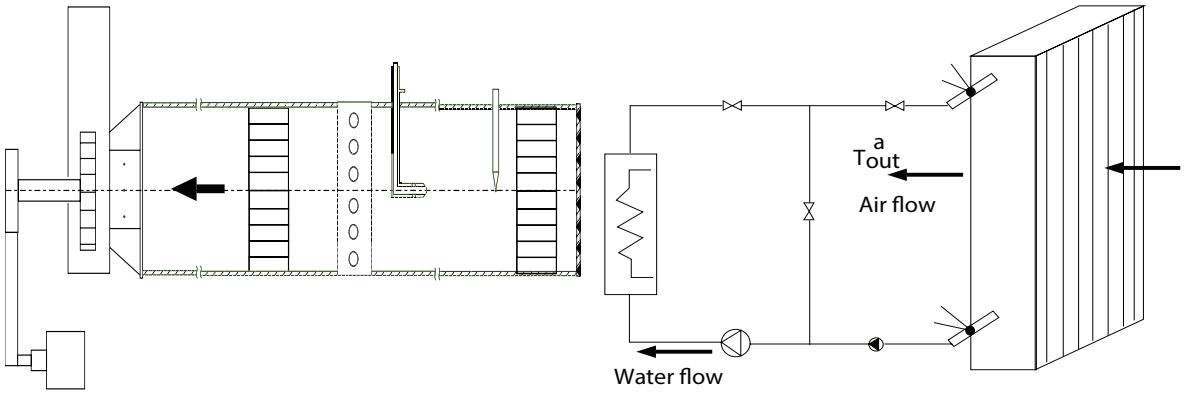

Figure D.1: Experimental setup: (a) heat exchanger test facility with wind tunnel and in-draft fan, (b) heat exchanger with water and air flows indicated; T^a_{out} is the air outlet temperature [48].

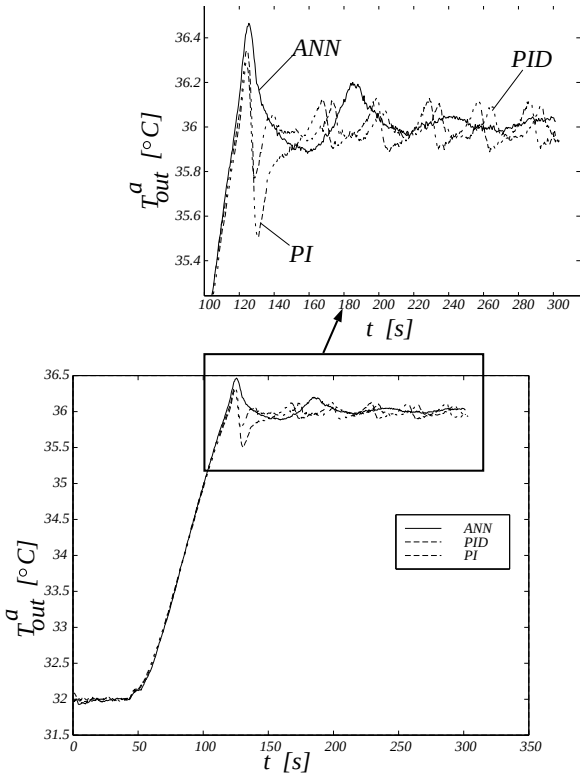

Figure D.2: Time-dependent behavior of heat exchanger using ANN, PID and PI control methodologies [48].

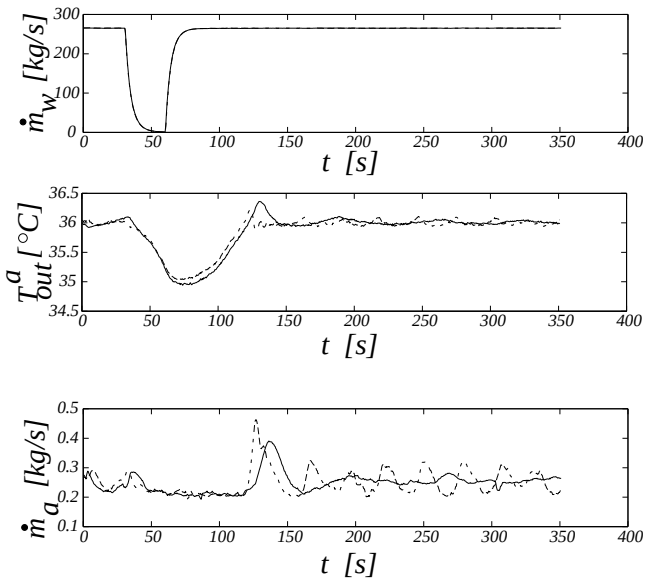

Figure D.3: Time-dependent behavior of heat exchanger with neurocontrol for disturbance rejection experiment showing flow rates and air outlet temperature [48].

Appendix E

Additional problems

1. Write the governing equations for natural convection flow in an inclined rectangular cavity, and nondimensionalize them. The thermal conditions at the walls of the cavity are: (a) AB heating with heat flux q_s'', (b) BC adiabatic, (c) CD cooling with heat flux q_s'', (d) DA adiabatic.

2. An "Aoki" curve is defined as shown in Fig. E.2. Show that when $n \to \infty$, the dimension of the curve is $D = 1$ and the length $L \to \infty$.

3. Consider conductive rods of thermal conductivity k joined together in the form of a fractal tree (generation $n = 3$ is shown in Fig. E.3; the fractal is obtained in the limit $n \to \infty$). The base and tip temperatures are T_0 and T_∞, respectively. The length and cross-sectional area of bar 0 is L and A, respectively, and those of bar 1 are $2L/\beta$ and A/β^2, where $1 \leq \beta < 2$, and so on. Show that the conductive heat transfer through rod 0 is

$$q = \frac{kA}{L}\left(T_0 - T_\infty\right)\left(1 - \frac{\beta}{2}\right)$$

4. The dependence of the rate of chemical reaction on the temperature T is often represented by the Arrhenius function $f(T) = e^{-E/T}$, where E is the activation energy. Writing $T^* = T/E$, show that $f(T^*)$ has a point of inflexion at $T^* = 1/2$. Plot $f(T^*)$ in the range $T^* = 1/16$ to

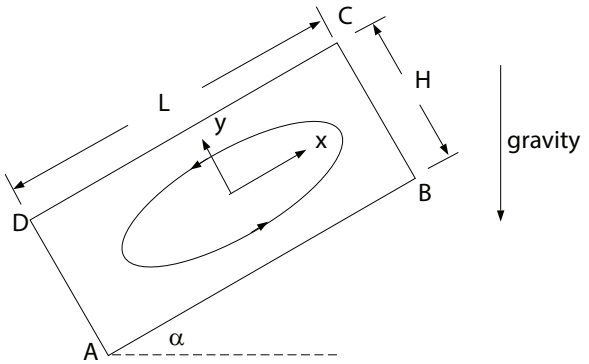

Figure E.1: Inclined rectangular cavity

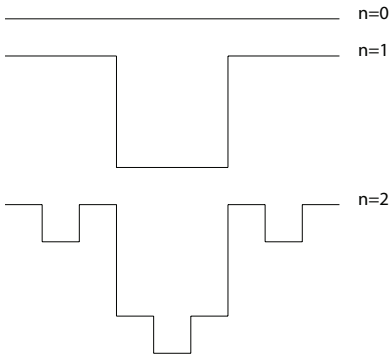

Figure E.2: Aoki curve.

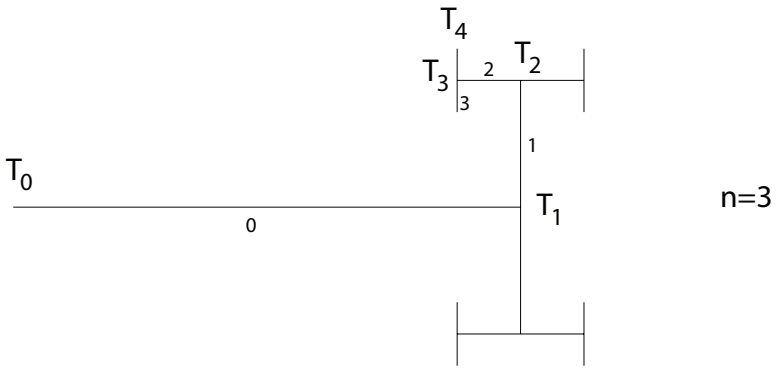

Figure E.3: Fractal tree.

$T^* = 4$ as well as its Taylor series approximation to various orders around $T^* = 1/2$. Plot also the L_2-error in the same range for different orders of the approximation.

5. Using a complete basis, expand the solution of the one-dimensional heat equation

$$\frac{\partial T}{\partial t} = \alpha \frac{\partial^2 T}{\partial x^2}$$

with boundary conditions

$$-k\frac{\partial T}{\partial x} = q_0 \text{ at } x = 0, \tag{E.1}$$

$$T = T_1 \text{ at } x = L \tag{E.2}$$

as an infinite set of ODEs.

6. Show that the governing equation of the unsteady, variable-area, convective fin can be written in the form

$$\frac{\partial T}{\partial t} - \frac{\partial}{\partial x}\left(a(x)\frac{\partial T}{\partial x}\right) + b(x)T = 0$$

Show that the steady-state temperature distribution with fixed temperatures at the two ends $x = 0$ and $x = L$ is globally stable.

7. Nondimensionalize and solve the radiative cooling problem

$$Mc\frac{dT}{dt} + \sigma A\left(T^4 - T_\infty^4\right) = 0$$

with $T(0) = T_i$. [Is this done elsewhere?]

8. For heat transfer from a heated body with convection and weak radiation, i.e. for

$$\frac{d\theta}{d\tau} + \theta + \epsilon\left\{(\theta + \beta)^4 - \beta^4\right\} = q$$

with $\theta(0) = 1$, using symbolic algebra determine the regular perturbation solution up to and including terms of order ϵ^4. Assuming $\epsilon = 0.1$, $\beta = 1$, $q = 1$, plot the five solutions (with one term, with two terms, with three terms, etc.) in the range $0 \le \tau \le 1$.

9. Consider a body in thermal contact with the environment

$$Mc\frac{dT}{dt} + hA(T - T_\infty) = 0$$

where the ambient temperature, $T_\infty(t)$, varies with time in the form shown below. Find (a) the long-time solution of the system temperature, $T(t)$, and (b) the amplitude of oscillation of the system temperature, $T(t)$, for a small period δt.

10. For a heated body in thermal contact with a constant temperature environment

$$Mc\frac{dT}{dt} + hA(T - T_\infty) = Q$$

analyze the conditions for linear stability of PID control.

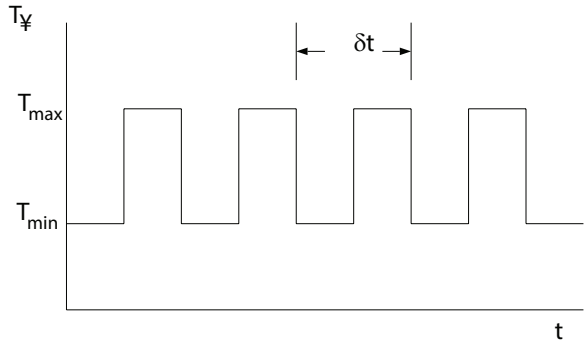

Figure E.4: Ambient temperature variation.

11. Show numerical results for the behavior of two heated bodies in thermal contact with each other and with a constant temperature environment for on-off control with (a) one thermostat, and (b) two thermostats.

12. Analyze the system controllability of two heated bodies in thermal contact with each other and with a constant temperature environment for (a) $Q_1(t)$ and $Q_2(t)$ being the two manipulated variables, and (b) with $Q_1(t)$ as the only manipulated variable and Q_2 constant.

13. Run the neural network FORTRAN code in

    `http://www.nd.edu/~msen/Teaching/IntSyst/Programs/ANN/`

    for 2 hidden layers with 5 nodes each and 20,000 epochs. Plot the results in the form of exact z vs. predicted z.

14. Consider the heat equation
$$\frac{\partial T}{\partial t} = \frac{\partial^2 T}{\partial x^2}$$
    with one boundary condition $T(0) = 0$. At the other end the temperature, $T(1) = u(t)$ is used as the manipulated variable. Divide the domain into 5 parts and use finite differences to write the equation as a matrix ODE. Find the controllability matrix and check for system controllability.

15. Determine the semi-derivative and semi-integral of (a) C (a constant), (b) x, and (c) x^μ where $\mu > -1$.

16. Find the time-dependent temperature field for flow in a duct wih constant T_∞ and T_{in}, but with variable flow rate $V(t) = V_0 + \Delta V \sin(\omega t)$ such that V is always positive. Write a computer program to solve the PDE, and compare numerical and analytical results.

17. Find the steady-state temperature distribution and velocity in a square-loop thermosyphon. The total length of the loop is L and the distribution of the heat rate per unit length is
$$q(x) = \begin{cases} Q & \text{for} \quad L/8 \le x \le L/4, \\ -Q & \text{for} \quad 5L/8 \le x \le 3L/4, \\ 0 & \text{otherwise.} \end{cases}$$

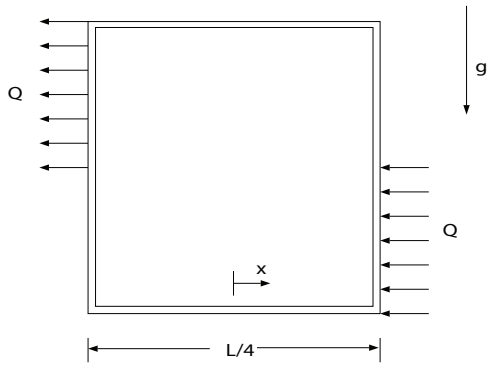

Figure E.5: Square naturcal circulation loop

18. Show that the dynamical system governing the toroidal thermosyphon with known wall temperature can be reduced to the Lorenz equations.

19. Draw the steady-state velocity vs. inclination angle diagram for the inclined toroidal thermosyphon with mixed heating. Do two cases: (a) without axial condution[1], and (b) with axial conduction.

20. Model natural convection in a long, vertical pipe that is being heated from the side at a constant rate. What is the steady-state fluid velocity in the pipe? Assume one-dimensionality and that the viscous force is proportional to the velocity.

21. The Brinkman model for the axial flow velocity, $u^*(r^*)$, in a porous cylinder of radius R is

$$\mu_{eff}\left[\frac{d^2u^*}{dr^{*2}}+\frac{1}{r^*}\frac{du^*}{dr^*}\right]-\frac{\mu}{K}u^*+G=0,$$

where $u^*=0$ at $r^*=R$ (no-slip at the wall), and $\partial u^*/\partial r^*=0$ at $r^*=0$ (symmetry at the centerline). μ_{eff} is the effective viscosity, μ is the fluid viscosity, K is the permeability, and G is the applied pressure gradient. Show that this can be reduced to the nondimensional form

$$\frac{d^2u}{dr^2}+\frac{1}{r}\frac{du}{dr}-s^2u+\frac{1}{M}=0,$$

where $M=\mu_{eff}/\mu$, $Da=K/R^2$, $s^2=(M\ Da)^{-1}$.

22. Using a regular perturbation expansion, show that for $s\ll 1$, the velocity profile from equation (E.3) is

$$u=\frac{1-r^2}{4M}\left[1-\frac{s^2}{16}\left(3-r^2\right)\right]+\ldots$$

[What is this?]

23. Using the WKB method, show that the solution of equation (1) for $s\gg 1$ is

$$u=Da\ \left[1-\frac{\exp\left\{-s(1-r)\right\}}{\sqrt{r}}\right]+\ldots$$

[1]M. Sen, E. Ramos and C. Treviño, On the steady-state velocity of the inclined toroidal thermosyphon, *ASME J. of Heat Transfer,* Vol. 107, pp. 974–977, 1985.

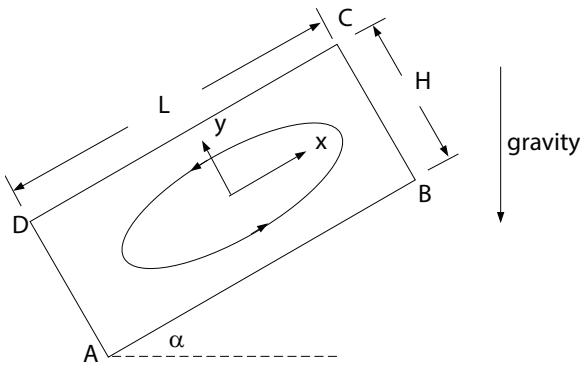

Figure E.6: Inclined natural cavity

[What is this?]

24. Consider steady state natural convection in a tilted cavity as shown. DA and BC are adiabatic while AB and CD have a constant heat flux per unit length. It can be shown that the governing equations in terms of the vorticity ω and the streamfunction ψ are

$$\begin{aligned} \frac{\partial^2\psi}{\partial x^2} + \frac{\partial^2\psi}{\partial x^2} + \omega &= 0 \\ \frac{\partial\psi}{\partial y}\frac{\partial\omega}{\partial x} - \frac{\partial\psi}{\partial x}\frac{\partial\omega}{\partial y} - Pr\ \left[\frac{\partial^2\omega}{\partial x^2} + \frac{\partial^2\omega}{\partial y^2}\right] - Ra\ Pr\left[\frac{\partial T}{\partial x}\cos\alpha - \frac{\partial T}{\partial y}\sin\alpha\right] &= 0 \\ \frac{\partial\psi}{\partial y}\frac{\partial T}{\partial x} - \frac{\partial\psi}{\partial x}\frac{\partial T}{\partial y} - \frac{\partial^2 T}{\partial x^2} - \frac{\partial^2 T}{\partial y^2} &= 0 \end{aligned}$$

where Pr and Ra are the Prandtl and Rayleigh numbers, respectively. The boundary conditions are:

$$\begin{aligned} \text{at } x = \pm\frac{A}{2}, \quad \psi = \frac{\partial\psi}{\partial x} = 0, \quad \frac{\partial T}{\partial x} = 0, \\ \text{at } y = \pm\frac{1}{2}, \quad \psi = \frac{\partial\psi}{\partial y} = 0, \quad \frac{\partial T}{\partial y} = 1. \end{aligned}$$

where $A = L/H$ is the aspect ratio. Find a parallel flow solution for ψ using

$$\begin{aligned} \psi &= \psi(y) \\ T(x,y) &= Cx + \theta(y) \end{aligned}$$

25. Obtain the response to on-off control of a lumped, convectively-cooled body with sinusoidal variation in the ambient temperature.

26. Determine the steady-state temperature field in a slab of constant thermal conductivity in which the heat generated is proportional to the exponential of the temperature such that

$$\frac{d^2T}{dx^2} = \exp(\epsilon T),$$

where $0 \le x \le 1$, with the boundary conditions $T(0) = T'(0) = 0$.

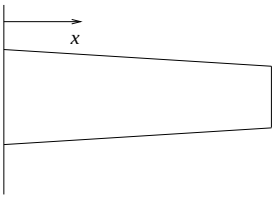

Figure E.7: Slightly tapered 2D fin.

27. In the previous problem, assume that ϵ is small. Find a perturbation solution and compare with the analytical. Do up to $O(\epsilon)$ by hand and write a Maple (or Mathematica) code to do up to $O(\epsilon^{10})$.

28. The temperature equation for a fin of constant area and convection to the surroundings at a constant heat transfer coefficient is

$$\left(\frac{d^2}{dx^2} - m^2\right)\theta = 0,$$

where $\theta = T - T_\infty$. Determine the eigenfunctions of the differential operator for each combination of Dirichlet and Neumann boundary conditions at the two ends $x = 0$ and $x = L$.

29. Add radiation to a convective fin with constant area and solve for small radiative effects with boundary conditions corresponding to a known base temperature and adiabatic tip.

30. Find the temperature distribution in a slightly tapered 2-dimensional convective fin with known base temperature and adiabatic tip.

31. Prove Hottel's crossed string method to find the view factor F_{AB} between two-dimensional surfaces A and B with some obstacles between them as shown. The dotted lines are tightly stretched strings. The steps are:

    (a) Assuming the strings to be imaginary surfaces, apply the summation rule to each one of the sides of figure *abc*.

    (b) Manipulating these equations and applying reciprocity, show that

$$F_{ab-ac} = \frac{A_{ab} + A_{ac} - A_{bc}}{2A_{ab}}.$$

    (c) For *abd* find F_{ab-bd} in a similar way.

    (d) Use the summation rule to show that

$$F_{ab-cd} = \frac{A_{bc} + A_{ad} - A_{ac} - A_{bd}}{2A_{ab}}$$

    (e) Show that $F_{ab-cd} = A_A F_{AB}/A_{ab}$.

    (f) Show the final result

$$F_{A-B} = \frac{A_{bc} + A_{ad} - A_{ac} - A_{bd}}{2A_A}$$

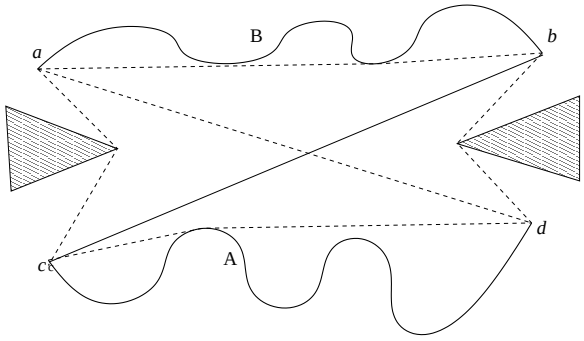

Figure E.8: Hottel's string method.

32. Complete the details to derive the Nusselt result for laminar film condensation on a vertical flat plate. Find from the literature if there is any experimental confirmation of the result.

33. Consider the hydrodynamic and thermal boundary layers in a flow over a flat plate at constant temperature. Use a similarity transformation on the boundary layer equations to get

$$2f''' + ff'' = 0, \tag{E.3}$$

$$\theta'' + \frac{Pr}{2} f\theta' = 0. \tag{E.4}$$

Using the shooting method and the appropriate boundary conditions, solve the equations for different Pr and compare with the results in the literature.

34. Solve the steady state conduction equation $\nabla^2 T = 0$ in the area in the figure between the square and the circle using the MATLAB Toolbox. Edges DA and BC have temperatures of 100 and 0 units, respectively, AB and CD are adiabatic and the circle is at a temperature of 200 units. Draw the isotherms.

35. (From Brauner and Shacham, 1995) Using Eq. 11, write a program to redraw Fig. 2 on a sunny day ($C_l = 0$) and a cloudy day ($C_l = 1$). Assume $T_a = 37°$C. Use Eq. 8 to calculate h_c. Note: since the physical properties are to be taken at the mean temperature between T_s and T_a, Eq. 11 must be solved numerically.

36. The steady-state temperature distribution in a plane wall of thermal conductivity k and thickness L is given by $T(x) = 4x^3 + 5x^2 + 2x + 3$, where T is in K, x in m, and the constants in appropriate units. (a) What is the heat generation rate per unit volume, $q(x)$, in the wall? (b) Determine the heat fluxes, q''_x, at the two faces $x = 0$ and $x = L$.

37. (From Incropera and DeWitt, 5th edition) Consider a square plate of side 1 m. Going around, the temperatures on the sides are (a) 50°C, (b) 100°C, (c) 200°C, and (d) 300°C. Find the steady-state temperature distribution analytically. Write a computer program to do the previous problem numerically using finite differences and compare with the analytical result. Choose different grid sizes and show convergence of the heat flux at any wall. Plot the 75, 150, and 250°C isotherms.

38. A plane wall of thickness 1 m is initially at a uniform temperature of 85°C. Suddenly one side of the wall is lowered to a temperature of 20°C, while the other side is perfectly insulated. Find

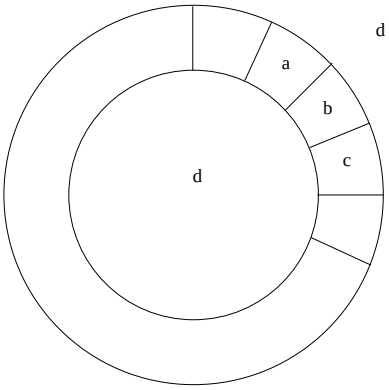

the time-dependent temperature profile $T(x,t)$. Assume the thermal diffusivity to be 1 m^2/s. Write a computer program to do the previous problem numerically using finite differences and compare with the analytical result.

39. At a corner of a square where the temperature is discontinuous, show how the finite difference solution of the steady-state temperature behaves ompared to the separation-of-variables solution.

40. Find the view factor of a semi-circular arc with respect to itself.

41. Derive the unsteady governing equation for a two-dimensional fin with convection and radiation.

42. Determine the steady temperature distribution in a two-dimensional convecting fin.

43. A number of identical rooms are arranged in a circle as shown, with each at a uniform temperature $T_i(t)$. Each room exchanges heat by convection with the outside which is at T_∞, and with its neighbors with a conductive thermal resistance R. To maintain temperatures, each room has a heater that is controlled by independent but identical proportional controllers. (a) Derive the governing equations for the system, and nondimensionalize. (b) Find the steady state temperatures. (c) Write the dynamical system in the form $\dot{\mathbf{x}} = \mathbf{A}\mathbf{x}$ and determine the condition for stability[2].

44. A sphere, initially at temperature T_i is being cooled by natural convection to fluid at T_∞. Churchill's correlation for natural convection from a sphere is

$$\overline{Nu} = 2 + \frac{0.589\ Ra_D^{1/4}}{\left[1 + (0.469/Pr)^{9/16}\right]^{4/9}},$$

[2]Eigenvalues of an $N \times N$, circulant, banded matrix of the form [3]

$$\begin{bmatrix} b & c & 0 & \dots & 0 & a \\ a & b & c & \dots & 0 & 0 \\ 0 & a & b & \dots & 0 & 0 \\ \vdots & \vdots & \vdots & \vdots & \vdots & \\ 0 & \dots & 0 & a & b & c \\ c & 0 & \dots & 0 & a & b \end{bmatrix}$$

are $\lambda_j = b + (a+c)\cos\{2\pi(j-1)/N\} - i(a-c)\sin\{2\pi(j-1)/N\}$, where $j = 1, 2, \dots, N$.

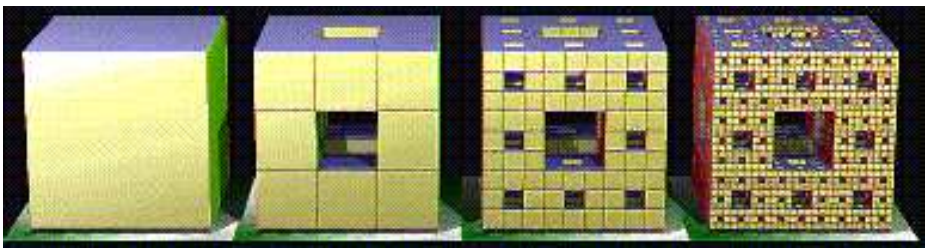

Figure E.9: Menger's Sponge

where

$$Ra_D = \frac{g\beta(T_s - T_\infty)D^3}{\nu\alpha}.$$

Assume that the temperature within the sphere $T(t)$ is uniform, and that the material properties are all constant. Derive the governing equation, and find a two-term perturbation solution.

45. (a) Show that the transient governing equation for a constant area fin with constant properties that is losing heat convectively with the surroundings can be written as

$$\frac{1}{\alpha}\frac{\partial\theta}{\partial t} = \frac{\partial^2\theta}{\partial x^2} - m^2\theta.$$

(b) With prescribed base and tip temperatures, use an eigenfunction expansion to reduce to an infinite set of ordinary differential equations. (c) Show that the steady state is attracting for all initial conditions.

46. Construct a fractal that is similar to the Cantor set, but instead remove the middle 1/2 from each line. Show that the fractal dimension is 1/2.

47. Shown below is Menger's Sponge. Calculate its Hausdorff dimension using each of the following methods: (a) $D_h = \log P/\log S$, (b) Box Counting (analytical), (c) Box Counting (graphical).

48. Shown below is a Peano curve, a single line that completely fills a unit square. Calculate its Hausdorff dimension and state if the Peano curve is indeed a fractal.

49. A duct carrying fluid has the cross-section of Koch's curve. Show that the perimeter of the cross-section is infinite while the flow area is finite.

50. Verify Cauchy's formula for repeated integration by (a) integrating $f(t)$ five times, (b) applying Cauchy's formula once with $n = 5$, (c) applying Cauchy's formula twice, once to $f(t)$ with $n = 2$ and then to the result with $n = 3$, showing that

$$\int\int\int\int\int_0^t f(\tau)d\tau = J^5 f(t) = J^3 J^2 f(t)$$

for $f(t) = 16t^3$.

51. Take $f(t) = 2t^5$ and using the Caputo Right Hand Derivative, (a) calculate $D^3 f(t)$ (take $m = 4$, $\alpha = 3$) and verify that you get the same result as traditional differentation by comparing to $d^3 f/dt^3$. (b) Calculate $D^{2.5} f(t)$ and plot the function.

(a) *Initator* (b) *Generator*

Figure E.10: Initiator and generator for a Peano (space filling) curve. The generator is recursively applied to generate the Peano curve.

52. Consider the heat flux in a blast furnace taht was calculated to be

$$q''(t) = \sqrt{cp\lambda}\ {}_0D_t^{1/2} g(t),$$

where

$$g(t) = T_{surf}(t) - T_0,$$

which is simply the derivative of order $\alpha = 1/2$ of the temperature difference at the surface. Assume that the function $g(t)$ is given as $g(t) = 14\sin(\pi t/60)$ where t is in minutes and the thermocouples sample once per minute, giving the discrete data set $g_i = 14\sin(\pi i/60)$. Calculate the fractional derivative numerically using the first 2 hours of data and plot both the heat flux at the surface and $g(t)$.

Hint: It is easiest to calculate the binomial coefficients recursively, according to the recursion formula:

$$\binom{\alpha}{0} = 1, \tag{E.5}$$

$$\binom{\alpha}{k+1} = \binom{\alpha}{k}\frac{\alpha - k + 1}{k}. \tag{E.6}$$

Note: In large time intervals (t very large), which would be of interest in this problem, the calculation we used would not be suitable because of the enormous number of summands in the calculation of the derivative and because of the accumulation of round off errors. In these situations, the principle of "short memory" is often applied in which the derivative only depends on the previous N points within the last L time units. The derivative with this "short memory" assumption is typically written as ${}_{(t-L)}D_t^{\alpha}$.

53. Consider the periodic heating and cooling of the surface of a smooth lake by radiation. The surface is subject to diurnal heating and nocturnal cooling such that the surface temperature can be described by $T_s(t) = T_o + T_a \sin\omega t$. Assume the heat diffusion to be one-dimensional and find the heat flux at the surface of the lake. The following steps might be useful:

(a) Assume transient one-dimensional heat conduction:

$$\frac{\partial T(x,t)}{\partial t} - \alpha\frac{\partial^2 T(x,t)}{\partial x^2} = 0,$$

with initial and boundary conditions $T(x,0) = T_o$ and $T(0,t) = T_s(t)$. Also assume the lake to be a semi-infinite planer medium (a lake of infinite depth) with $T(\infty,t) = 0$.

(b) Non-dimensionalize the problem with a change of variables $\xi = \alpha^{-1/2}x$ and $\theta(x,t) = T(x,t) - T_o$.

(c) Use the following Laplace transform properties to transform the problem into the Laplace domain:

$$\mathcal{L}\big[\frac{\partial^\alpha f(x,t)}{\partial t^\alpha}\big] = s^\alpha F(x,s) \qquad \text{(with 0 initial conditions)}$$

and

$$\mathcal{L}\big[\frac{\partial^\alpha f(x,t)}{\partial x^\alpha}\big] = \frac{\partial^\alpha}{\partial x^\alpha}F(x,s)$$

(d) Solve the resulting second order differential equation for $\Theta(\xi,s)$ by applying the transformed boundary conditions.

(e) Find $\partial\Theta/\partial\xi$ and then substitute $\Theta(\xi,s)$ into the result. Now take the inverse Laplace transform of $\partial\Theta/\partial\xi$ and convert back to the original variables. Be careful! The derivative of order 1/2 of a constant is not zero! (see simplifications in (g) to simplify)

(f) You should now have an expression for $\partial T(x,t)/\partial x$. Substitute this into Fourier's Law to calculate the heat flux, $q''(x,t) = -k\ \partial T(x,t)/\partial x$.

(g) Evaluate this expression at the surface ($x = 0$) to find the heat flux at the surface of the lake. The following simplifications might be helpful:

$$\frac{\partial^{1/2}C}{\partial t^{1/2}} = \frac{C}{\pi t^{1/2}}$$

$$\frac{\partial^\alpha [Cg(t)]}{\partial t^\alpha} = C\frac{\partial^\alpha g(t)}{\partial t^\alpha}$$

(h) The solution should look now look like

$$q_s''(t) = \frac{k}{\alpha^{1/2}}\frac{d^{1/2}(T_a \sin\omega t)}{dt^{1/2}}$$

54. Consider radiation between two long concentric cylinders of diameters D_1 (inner) and D_2 (outer). (a) What is the view factor F_{12}. (b) Find F_{22} and F_{21} in terms of the cylinder diameters.

55. Temperatures at the two sides of a plane wall shown in Fig. E.38 are T_L and T_R, respectively. For small ϵ, find a perturbation steady-state temperature distribution $T(x)$ if the dependence of thermal conductivity on the temperature has the form

$$k(T) = k_0\left(1 + \frac{T - T_L}{T_R - T_L}\,\epsilon\right).$$

56. One side of a plane wall shown in Fig. E.39 has a fixed temperature and the other is adiabatic. With an initial condition $T(x,0) = f(x)$, determine the temperature distribution in the wall $T(x,t)$ at any other time. Assume constant properties.

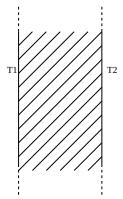

Figure E.11: Plane wall in steady state.

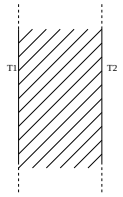

Figure E.12: Plane wall in unsteady state.

57. Using an eigenfunction expansion, reduce the governing PDE in Problem 56 to an infinite set of ODEs.

58. A room that loses heat to the outside by convection is heated by an electric heater controlled by a proportional controller. With a lumped capacitance approximation for the temperature, set up a mathematical model of the system. Determine the constraint on the controller gain for the system response to be stable. What is the temperature of the room after a long time?

59. A turbine blade internally cooled by natural convection is approximated by a rotating natural circulation loop of constant cross-section. The heat rate in and out at the top and bottom, respectively, is Q while the rest of the loop is insulated. Find the steady-state velocity in the loop. Consider rotational forces but not gravity. State your other assumptions.

60. An infinite number of conductive rods are set up between two blocks at temperatures T_a and T_b. The first rod has a cross-sectional area $A_1 = A$, the second $A_2 = A/\beta$, the third $A_3 = A/\beta^2$, and so on, where $\beta > 1$. What is the total steady-state heat transfer rate between the two blocks? Assume that the thermal conductivity k is a constant, and that there is no convection.

61. Show that the functions $\phi_1(x) = \sqrt{2}\ \sin \pi x$ and $\phi_2(x) = \sqrt{2}\ \sin 2\pi x$ are orthonormal in the interval $[0, 1]$ with respect to the L_2 norm. Using these as test functions, use the Galerkin

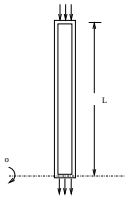

Figure E.13: Turbine blade.

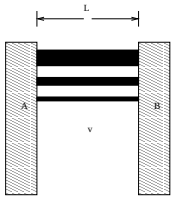

Figure E.14: Infinite number of rods.

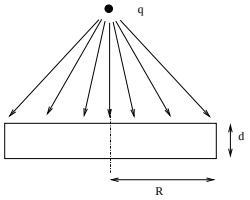

Figure E.15: Lamp and disk

method to find an approximate solution of the steady-state fin equation

$$T'' - T = 0,$$

with $T(0) = 0, T(1) = 1$.

62. A lamp of q W is radiating equally in all directions. Set up the governing equation for the temperature $T(r)$ in the disk.

63. Determine the steady-state temperature distribution in the triangle shown, if the hypotenuse is adiabatic, one of the sides is at one temperature and the other is at another.

64. A ball with coefficient of restitution r falls from height H and undergoes repeated bouncing. Determine the temperature of the ball as a function of time $T(t)$ if heat loss is by convection to the atmosphere. Assume that the energy loss at every bounce goes to heat the ball.

65. Heat at the rate of q per unit volume is generated in a spherical shell that lies between R and $R + \delta$. If heat loss is by convection on the external surface only, find the steady-state temperature distribution.

66. Two identical fins of square cross section exchange heat by radiation between them and with the surroundings. Set up the governing equations for the temperatures $T(x)$ in the fins and solve for weak radiation.

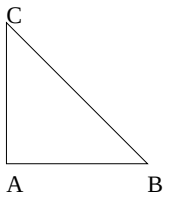

Figure E.16: Radiating triangle.

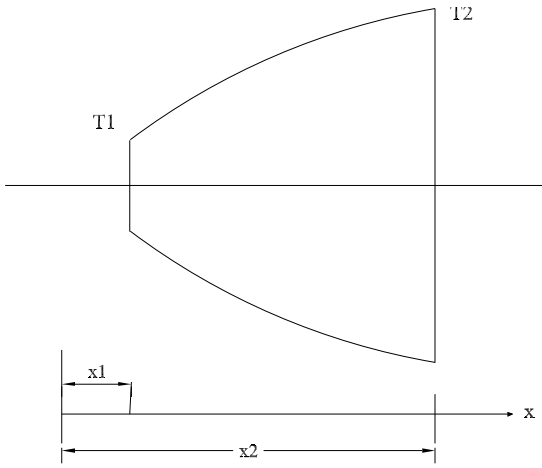

Figure E.17: Conical fin

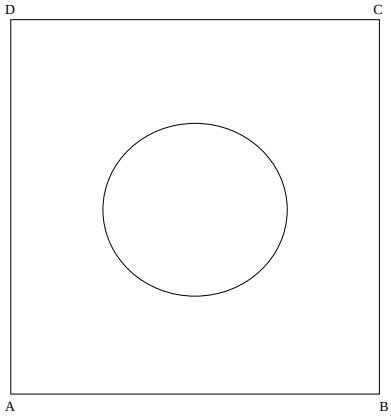

Figure E.18: Area between square and circle.

67. Determine the time-dependent temperature $T(t)$ of a block of weight Mg that is being slided at a constant velocity V across a horizontal surface. Assume that the frictional heat generated at the interface (with coefficient of friction μ) goes entirely to the block, that its temperature is uniform, and that heat loss from it is only by convection to the surroundings.

68. (From Incropera and DeWitt, 5th edition) The figure shows a conical section fabricated from pure aluminum. It is of circular cross section having diameter $D = ax^{1/2}$, where $a = 0.5\text{m}^{1/2}$. The small end is located at $x_1 = 25$ mm and the large end at $x_2 = 125$ mm. The end temperatures are $T_1 = 600$K and $T_2 = 400$K, while the lateral surface is well insulated. (a) Derive an expression for the temperature distribution $T(x)$ in symbolic form, assuming one-dimensional conditions. (b) Sketch the temperature distribution. (c) Calculate the heat rate q_x.

69. (From Incropera and DeWitt, 5th edition) Copper spheres of 20 mm diameter are quenched by dropping into a tank of water that is maintained at 280 K. The spheres may be assumed

to reach the terminal velocity on impact and to drop freely though the water. Estimate the terminal velocity by equating the drag and gravitational forces acting on the sphere. What is the approximate height of the water tank needed to cool the spheres from an initial temperature of 360 K to a center temperature of 320 K?

70. (From Incropera and DeWitt, 5th edition) Neglecting the longitudinal temperature gradient in laminar flow in a circular tube, the energy equation is

$$u\frac{\partial T}{\partial x} + v\frac{\partial T}{\partial r} = \frac{\alpha}{r}\frac{\partial}{\partial r}\left(r\frac{\partial T}{\partial r}\right).$$

The heat flux at the wall is $q_s'' = h(T_s - T_m)$, where T_m is the mean (or bulk) temperature of the fluid at a given cross section and T_s is the wall temperature. Slug flow is an idealized condition for which the velocity is assumed to be uniform over the entire tube cross section with $v = 0$, $u =$ constant, and $\partial T/\partial x = dT_m/dx =$ constant with respect to r. For uniform wall heat flux, determine $T(r)$ and the Nusselt number Nu_D.

71. (From Incropera and DeWitt, 5th edition) Consider natural convection within two long vertical plates maintained at uniform temperatures of $T_{s,1}$ and $T_{s,2}$, where $T_{s,1} > T_{s,2}$. The plates are open at their ends and are separated by the distance $2L$. (a) Sketch the velocity distribution in the space between the plates. (b)Write appropriate forms of the continuity, momentum, and energy equations for laminar flow between the plates. (c) Evaluate the temperature distribution, and express your result in terms of the mean temperature $T_m = (T_{s,1} + T_{s,2})/2$. (d) Estimate the vertical pressure gradient by assuming the density to be a constant ρ_m corresponding to T_m. Substituting from the Boussinesq approximation, obtain the resulting form of the momentum equation. (e) Determine the velocity distribution. (Hints: The net flow across any horizontal section should be zero. Assume that the flow is hydrodynamically and thermally fully developed. Here the Boussinesq approximation means use of the simplified density variation expression $\rho - \rho_m \approx -\beta\rho_m(T - T_m)$.)

72. (From Incropera and DeWitt, 5th edition) For forced convection boiling in smooth tubes, the heat flux can be estimated by combining the separate effects of boiling and forced convection. The Rohsenow and Dittus-Boelter correlations may be used to predict nucleate boiling and forced convection effects, with 0.019 replacing 0.023 in the latter expression. Consider water at 1 atm with a mean velocity of 1.5 m/s and a mean temperature of 95°C flowing through a 15-mm diameter brass tube whose surface is maintained at 110°C. Estimate the heat transfer rate per unit length of the tube.

73. (From Incropera and DeWitt, 5th edition) A single-pass, cross-flow heat exchanger uses hot exhaust gases (mixed) to heat water (unmixed) from 30 to 80°C at a rate of 3 kg/s. The exhaust gases, having thermophysical properties similar to air, enter and exit the exchanger at 225 and 100°C, respectively. If the overall heat transfer coefficient is 200 W/m^{2}K, estimate the required surface area using LMTD and ϵ-NTU method respectively.

74. (From Incropera and DeWitt, 5th edition) Saturated water vapor leaves a steam turbine at a flow rate of 1.5 kg/s and a pressure of 0.51 bar. The vapor is to be completely condensed to saturated liquid in a shell-and-tube heat exchanger that uses city water as the cold fluid. The water enters the thin-walled tubes at 17°C and is to leave at 57°C. Assuming an overall heat transfer coefficient of 2000 W/m^{2}K, determine the required heat exchanger surface area and the water flow rate. After extended operation, fouling causes the overall heat transfer

coefficient to decrease to 1000 W/m^{2}K, and to completely condense the vapor flow rate. For the same water inlet temperature and flow rate, what is the new vapor flow rate required for complete condensation?

75. (From Incropera and DeWitt, 5th edition) Advances in very large scale integration (VLSI) of electronic devices on a chip are often restricted by the ability to cool the chip. For mainframe computers, an array of several hundred chips, each of area 25 mm^2, may be mounted on a certain ceramic substrate (backside of substrate insulated). A method of cooling the array is by immersion in a low boiling point fluid such as refrigerant R-113. At 1 atm and 321 K, properties of the saturated liquid are $\mu = 5.147 \times 10^{-4}$ N $\cdot$ s/m^2, $c_p = 983.8$ J/kg·K, and $Pr = 7.183$. Assume values of $C_{s,f} = 0.004$ and $n = 1.7$. (a) Estimate the power dissipated by a single chip if it is operating at 50% of the critical heat flux. (b) What is the corresponding value of the chip temperature? (c) Compute and plot the chip temperature as a function of surface heat flux for $0.25 \leq q_s^{"}/q_{max}^{"} \leq 0.90$.

76. (From Incropera and DeWitt, 5th edition) A thermosyphon consists of a closed container that absorbs heat along its boiling section and rejects heat along its condensation section. Consider a thermosyphon made from a thin-walled mechanically polished stainless steel cylinder of diameter D. Heat supplied to the thermosyphon boils saturated water at atmospheric pressure on the surfaces of the lower boiling section of length L_b and is then rejected by condensing vapor into a thin film, which falls by gravity along the wall of the condensation section of length L_c back into the boiling section. The two sections are separated by an insulated section of length L_i.The top surface of the condensation section may be treated as being insulated. The thermosyphon dimensions are $D = 20$ mm, $L_b = 20$ mm, $L_b = 40$ mm, and $L_i = 40$ mm. (See figure in book) (a) Find the mean surface temperature, $T_{s,b}$, of the boiling surface if the nucleate boiling heat flux is to be maintained at 30% of the critical heat flux. (b) Find the mean surface temperature, $T_{s,c}$, of the condensation section assuming laminar film condensation. (c) Find the total condensation flow rate, $\dot{m}$, within the thermosyphon.

77. (From Incropera and DeWitt, 5th edition) A steam generator consists of a bank of stainless steel ($k = 15$W/mK) tubes having the core configuration of Fig. E.22 and an inner diameter of 13.8 mm. The tubes are installed in a plenum whose square cross section is 0.6 m on a side, thereby providing a frontal area of 0.36 m^2. Combustion gases, whose properties may be approximated as those of atmospheric air, enter the plenum at 900 K and pass in cross flow over the tubes at 3 kg/s. If saturated water enters the tubes at a pressure of 2.455 bars and a flow rate of 0.5 kg/s, how many tubes rows are required to provide saturated steam at the tube outlet? A convection coefficient of 10,000 W/m^2·K is associated with boiling in the tubes.

78. (From Incropera and DeWitt, 5th edition) The spectral, directional emissivity of a diffuse material at 2000 K has the distribution as in Fig. E.20. Determine the total, hemispherical emissivity at 2000 K. Determine the emissive power over the spectral range 0.8 to 2.5 μm and for the directions $0 \leq \theta \leq 30°$.

79. (From Incropera and DeWitt, 5th edition) Solar irradiation of 1100 W/m^2 is incident on a large, flat horizontal metal roof on a day when the wind blowing over the roof causes a convection heat transfer coefficient of 25 W/m^{2}K. The outside air temperature is 27°, the metal surface absortivity for incident solar radiation is 0.60, the metal surface emissivity is 0.20, and the roof is well insulated from below. Estimate the roof temperature under steady-state conditions.

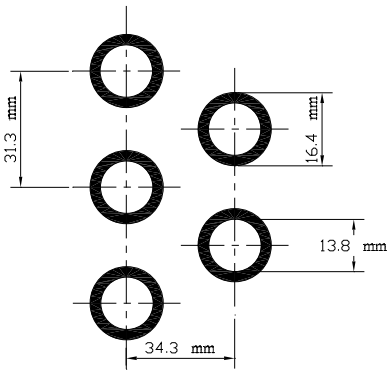

Figure E.19: Steam generator.

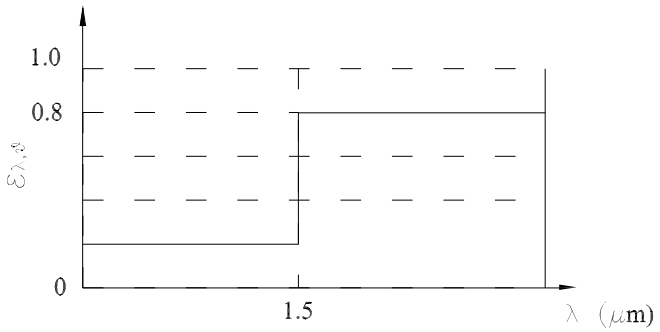

Figure E.20: Emissivity of material.

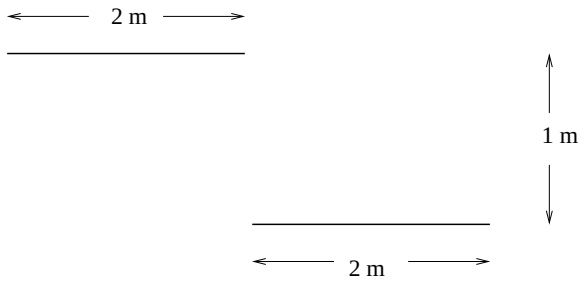

Figure E.21: Parallel plates.

80. Maxwell's equations of electromagnetic theory are

$$\nabla \times \mathbf{H} = \mathbf{J} + \frac{\partial \mathbf{D}}{\partial t} \tag{E.7}$$

$$\nabla \times \mathbf{E} = -\frac{\partial \mathbf{B}}{\partial t} \tag{E.8}$$

$$\nabla \cdot \mathbf{D} = \rho \tag{E.9}$$

$$\nabla \cdot \mathbf{B} = 0 \tag{E.10}$$

where $\mathbf{H}$, $\mathbf{B}$, $\mathbf{E}$, $\mathbf{D}$, $\mathbf{J}$, and ρ are the magnetic intensity, magnetic induction, electric field, electric displacement, current density, and charge density, respectively. For linear materials $\mathbf{D} = \epsilon\mathbf{E}$, $\mathbf{J} = g\mathbf{E}$ (Ohm's law), and $\mathbf{B} = \mu\mathbf{H}$, where ϵ is the permittivity, g is the electrical conductivity, and μ is the permeability. For $\rho = 0$ and constant ϵ, g and μ, show that

$$\nabla^2\mathbf{H} - \epsilon\mu\frac{\partial^2\mathbf{H}}{\partial t^2} - g\mu\frac{\partial \mathbf{H}}{\partial t} = 0 \tag{E.11}$$

$$\nabla^2\mathbf{E} - \epsilon\mu\frac{\partial^2\mathbf{E}}{\partial t^2} - g\mu\frac{\partial \mathbf{E}}{\partial t} = 0 \tag{E.12}$$

With $\epsilon = 8.8542 \times 10^{-12}$ $\mathrm{C^2N^{-1}m^{-2}}$, and $\mu = 1.2566 \times 10^{-6}$ $\mathrm{NC^{-2}s^2}$, find the speed of an electromagnetic wave is free space.

81. (From Incropera and DeWitt, 5th edition) Consider the parallel plates of infinite extent normal to the page having opposite edges aligned as shown in the sketch. (a) Using appropriate view factor relations and the results for opposing parallel planes, develop an expression for the view factor between the plates. (b) Write a numerical code based on the integral definition to compute the view factor and compare.

82. (From Incropera and DeWitt, 5th edition) A room is 6 m wide, 10 m long and 4 m high. The ceiling, floor and one long wall have emissivities of 0.8, 0.9 and 0.7 and are at temperatures of 40°C, 50°C and 15°C, respectively. The three other walls are insulated. Assuming that the surfaces are diffuse and gray, find the net radiation heat transfer from each surface.

83. (From Incropera and DeWitt, 5th edition) A radiant heater consists of a long cylindrical heating element of diameter $D_1 = 0.005$ m and emissivity $\epsilon_1 = 0.80$. The heater is partially enveloped by a long, thin parabolic reflector whose inner and outer surfaces emissivities are $\epsilon_{2i} = 0.10$ and $\epsilon_{2o} = 0.80$, respectively. Inner and outer surface areas per unit length of the reflector are each $A'_{2i} = A'_{2o} = 0.20$ m, and the average convection coefficient for the combined

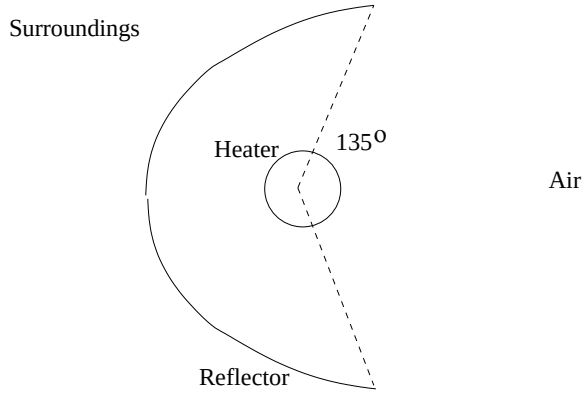

Figure E.22: Figure for problem 3.

inner and outer surfaces is $\overline{h}_{2(i,o)} = 2$ W/m^{2}K. The system may be assumed to be in an infinite, quiescent medium of atmospheric air at $T_\infty = 300$ K and to be exposed to large surroundings at $T_{sur} = 300$ K. (a) Sketch the appropriate radiation circuit, and write expressions for each of the network resistances. (b) If, under steady state conditions, electrical power is dissipated in the heater at $P_1' = 1500$ W/m and the heater surface temperature is $T_1 = 1200$ K, what is the *net* rate at which *radiant* energy is transferred from the heater? (c) What is the net rate at which radiant energy is transferred from the heater to the surroundings? (d) What is the temperature T_2 of the reflector?

84. Consider the convective fin equation

$$\frac{d^2T}{dx^2} - T = 0,$$

where $0 \leq x \leq 1$, with $x(0) = 1$, $x(1) = 0$. Solve using the following methods. You may have to transform the dependent or independent variable differently for each method. In each case show convergence.

(a) *Finite differences:* Divide into N parts, write derivatives in terms of finite differences, reduce to algebraic equations, apply boundary conditions, and solve.

(b) *Trigonometric Galerkin:* Expand in terms of N trigonometric functions, substitute in equation, take inner products, reduce to algebraic equations, and solve.

(c) *Chebyshev Galerkin:* Expand in terms of N Chebyshev polynomials, substitute in equation, take inner products, reduce to algebraic equations, and solve.

(d) *Trigonometric collocation:* Expand in terms of N trigonometric functions, substitute in equation, take inner products, apply collocation, and solve.

(e) *Galerkin finite elements:* Divide into N elements, assume linear functions, integrate by parts, assemble all equations, apply boundary conditions, and solve.

(f) *Polynomial moments:* Assume dependent variable to be a Nth-order polynomial that satisfies boundary conditions, obtain algebraic equations by taking moments, and solve.

85. If $e^{-E/T}$ is proportional to the heat generated within a tank by chemical reaction, and there is heat loss by convection from the tank, show that the temperature of the tank T is determined by

$$Mc\frac{dT}{dt} = ae^{-E/T} - hA(T - T_\infty)$$

where M is the mass, c is the specific heat, a is a proportionality constant, h is the convective heat transfer coefficient, A is the surface area of the tank, and T_∞ is the ambient temperature. Nondimensionalize the equation to

$$\frac{dT^*}{dt^*} = e^{-1/T^*} - H(T^* - T^*_\infty)$$

(a) For $T^*_\infty = 0.1$, draw the bifurcation diagram with H as the bifurcation parameter, and determine the bifurcation points.

(b) Determine the stability of the different branches of the bifurcation diagram.

86. The governing equations for the dynamic behavior of a toroidal convective loop with known heat flux has been shown to be

$$\frac{dx}{dt} = y - x \tag{E.13}$$

$$\frac{dy}{dt} = a - zx \tag{E.14}$$

$$\frac{dz}{dt} = xy - b \tag{E.15}$$

(a) Using the same approach and notation as far as possible, modify the dynamical system to include the effects of axial conduction.

(b) Determine the critical points of the conductive system and analyze their linear stability.

(c) Show that there is a conductive solution for heating that is symmetric about a vertical diameter, and analyze its nonlinear stability.

87. Consider a toroidal convective loop with known wall temperature. Show that the dynamical system for this problem can be reduced to the Lorenz equations. Determine the dimension of the strange attractor for these equations.

88. Graphically compare the numerical and approximate boundary layer solutions in the problem of one-dimensional flow in a pipe with advection, convection and axial conduction.

89. Consider the energy equation in the one-dimensional flow in a tube of finite wall thickness. Include convection between the fluid and the tube, between the tube and the environment, and axial conduction in the tube wall, but neglect axial conduction in the fluid. The inlet temperature of the in-tube fluid is known, and the tube wall is adiabatic at the two ends.

(a) Show that the governing equations can be reduced to a form

$$\frac{d\mathbf{y}}{d\xi} = \mathbf{A}\mathbf{y}.$$

ξ is the nondimensional axial coordinate,

$$\mathbf{y} = \begin{bmatrix} \theta_i \\ \theta_t \\ q_t \end{bmatrix},$$

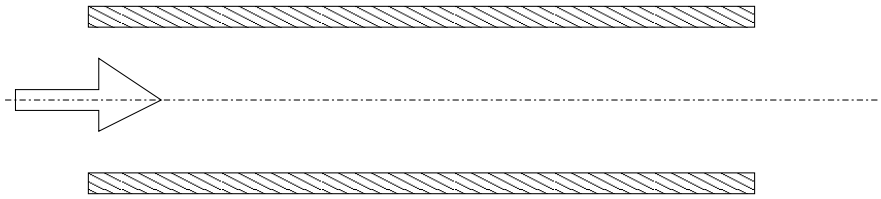

Figure E.23: CAPTION HERE.

and

$$\mathbf{A} = \begin{bmatrix} -a & a & 0 \\ 0 & 0 & 1 \\ -b & b+c & 0 \end{bmatrix}.$$

θ_i is the nondimensional temperature of the in-tube fluid, θ_t that of the tube, and q_t the heat flux.

(b) Show that this can also be written as a third-order differential equation.

(c) Solve as much as you can analytically, and then assume numerical values for the parameters (e.g. $a = 3, b = 10/3, c = 8/3$) and complete the solution.

(d) Which of the cases of the parameters a, b and c going to either zero or infinity are regular perturbations and which are singular?

90. Derive an expression for heat transfer in a fractal tree-like microchannel net[3].

91. A body is being cooled by natural convection and black-body radiation. Assume lumped parameters and derive an approximation for its temperature $T(t)$ based on neglecting one mode of heat transfer for small times and the other for long times. Compare with a numerical result.

92. Consider the two-dimensional steady-state temperature distribution $T(x, y)$ on the plate ABCDEFG where AB = BC = DE = FG = GA and CD = BE = EF. The line ABC is adiabatic, AG is at temperature T_1 and the others are at T_2. (a) Assume that the temperature distribution in the dashed (interior) line BE is $f(y)$ and solve the temperature distributions in the two rectangles separately. (b) Equate the normal heat flux on either side of BE to get an equation for $f(y)$. (c) Suggest a numerical solution.

93. Explore a perturbation solution of the previous problem for a geometry in which CD/AG is very small (instead of being 0.5 above).

94. Fluids A and B exchange heat in the concentric-tube counterflow heat exchanger shown. Analyze the dynamics of the temperature field for a step change in the inlet temperature of one of the fluids.

95. Derive the dynamical system for a convection loop with known heat flux that loops around in a circle twice in a vertical plane before merging with itself. Investigate its static and dynamic behavior.

[3]Y. Chen and P. Cheng, Heat transfer and pressure drop in fractal tree-like microchannel nets, *International Journal of Heat and Mass Transfer,* Vol. 45, pp. 2643–2648, 2002

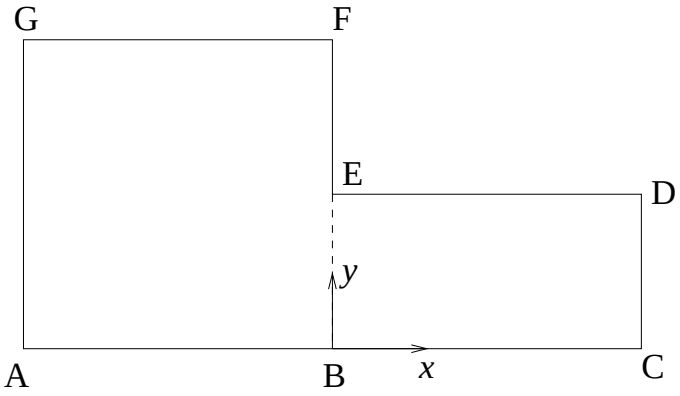

Figure E.24: CAPTION HERE

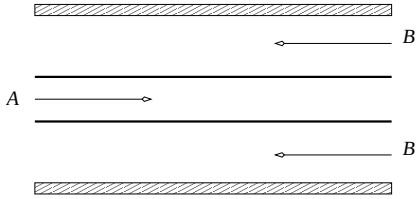

Figure E.25: CAPTION HERE

96. Show that a convectively cooled lumped mass that is heated with a time-varying source is governed by an equation of the type

$$\frac{dT}{dt} + T = Q(t).$$

If $Q = 1 + \sin \omega t$, find the amplitude of the temperature response as a function of ω.

97. Show that a radiative fin with heat generation is governed by an equation of the type

$$\epsilon \frac{d^2T}{dx^2} - T^4 + Q = 0.$$

for $0 \leq x \leq 1$. With $Q = 1$ and boundary conditions $T(0) = 0, T(1) = 2$, solve $T(x)$ numerically for different ϵ. From this see if and where boundary layers develop as $\epsilon \to 0$.

98. Consider steady-state conduction in a $L \times 2\epsilon L$ rectangular plate, with $\epsilon \ll 1$. If temperatures are prescribed on the short sides and the long sides are insulated, show that the governing equation in normalized spatial variables can be written as

$$\epsilon^2 \frac{\partial^2 T}{\partial x^2} + \frac{\partial^2 T}{\partial y^2} = 0$$

in $0 \leq x \leq 1, -1 \leq y \leq 1$ with boundary conditions $T(0, y) = f(y), T(1, y) = g(y), (\partial T/\partial y)_{y=-1} = (\partial T/\partial y)_{y=1} = 0$.

(a) Assume an outer expansion of the form

$$T(x,y) = T_0(x,y) + \epsilon^2 T_1(x,y) + \ldots$$

and show that

$$T_0 = a_0 x + b_0(1-x)$$

where a and b are undetermined constants.

(b) With boundary layers near $x = 0$ and $x = 1$, show that matching with the outer solution gives

$$a_0 = \frac{1}{2} \int_{-1}^{1} g(y)\ dy \tag{E.16}$$

$$b_0 = \frac{1}{2} \int_{-1}^{1} f(y)\ dy \tag{E.17}$$

99. Using multiple scales, solve the Fisher equation

$$\frac{\partial T}{\partial t} = \epsilon \frac{\partial^2 T}{\partial x^2} + T(1-T)$$

with $-\infty < x < \infty$, $t > 0$, $T(x,0) = 1/\{1 + \exp(\lambda x)\}$, and $\epsilon \ll 1$. Plot the analytical and numerical results for $\epsilon = 0.01, \lambda = 1$ and $t = 0$, $t = 5$, and $t = 10$.

100. Find an asymptotic approximation for

$$\frac{\partial T}{\partial t} + \frac{\partial T}{\partial x} = \epsilon f(T)$$

with $-\infty < x < \infty$, $t > 0$, $T(x,0) = g(x)$ and $\epsilon \ll 1$ that is valid for large t. Then reduce to the special case for $f(T) = T(1-T)$ and $g(x) = 1/\{1 + \exp(\lambda x)\}$.

101. Show that the temperature $T(t)$ of a lumped body that is subject to convection and radiation to a constant ambient temperature T_∞ is governed by an equation of the form

$$\frac{dT}{dt} + a(T - T_\infty) + b(T^4 - T_\infty^4) = 0,$$

and that two steady states are conditionally possible. Analyze the stability of each.

102. The temperature $T(t)$ of an object is controlled to a desired value T_s by blackbody radiation from a lamp at a temperature $T_\infty(t)$. T can be measured and on the basis of that T_∞ is varied by a PID controller. Model the system with control, and determine the condition for its stability.

103. A long tube held vertically is kept at a uniform temperature T_w that is higher than that of the surrounding fluid T_∞. There is an upward flow through the tube due to natural convection. What is the temperature of the fluid leaving the tube? Make suitable assumptions.

104. Consider transient thermal conduction in a convective fin with its two ends kept at fixed temperatures. Show that the steady-state temperature distribution is globally stable.

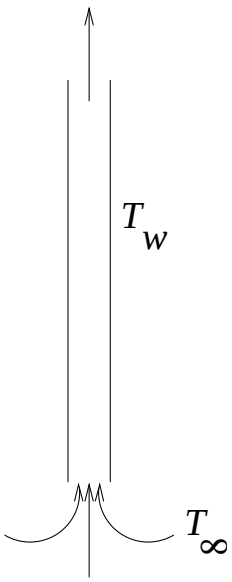

Figure E.26: CAPTION HERE

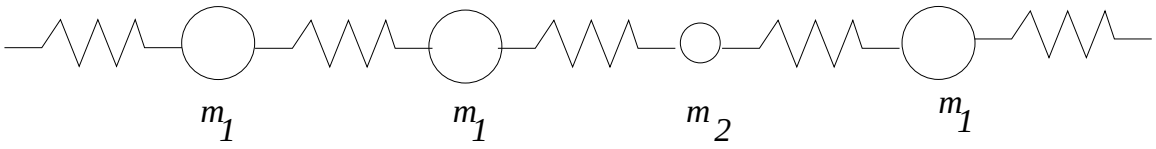

Figure E.27: CAPTION HERE

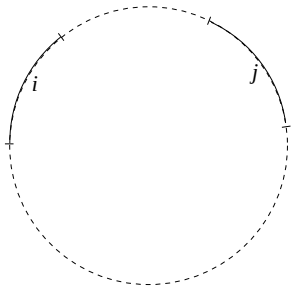

Figure E.28: CAPTION HERE

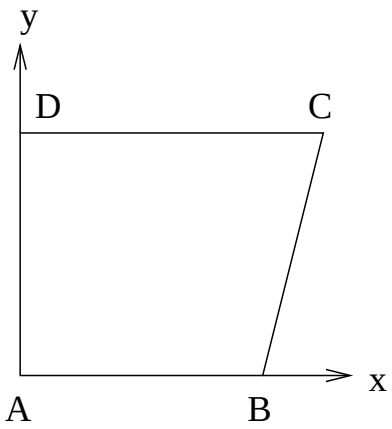

Figure E.29: CAPTION HERE.

105. An infinite one-dimensional lattice consists of repetitions of a unit consisting of two identical masses followed by a third mass that is different. The springs and distances between the masses are all identical. Find the small wave number phonon speed of the acoustic mode.

106. The surface of a sphere is divided into n unequal parts numbered $1, 2, \ldots, n$ with areas $A_1, A_2, \ldots, A_n$ respectively. Show that the view factor

$$F_{i-j} = \frac{A_j}{A_1 + A_2 + \ldots + A_n}.$$

107. There are at least *two* ways to obtain a regular perturbation solution for the steady-state temperature $T(x, y)$ due to conduction without heat generation for the plate shown in the figure, where $\epsilon \ll 1$, For each, *set up* two terms of the problem (i.e. provide the equations to be solved and the corresponding boundary conditions), but do not solve.

108. Find the maximum temperature on a thin rectangular plate with uniform temperature at the edges and constant heat generation per unit area by using a one-term method of moments approximation.

109. Determine the temperature distribution along a fin of constant area which has lateral convection and also a small amount of radiative cooling. The base temperature is known and the tip is adiabatic.

110. The governing equations for the dynamic behavior of a toroidal natural convection loop with axial conduction that is symmetrically heated with known heat flux is

$$\frac{dx}{dt} = y - x, \tag{E.18}$$

$$\frac{dy}{dt} = zx - cy, \tag{E.19}$$

$$\frac{dz}{dt} = xy - b - cz. \tag{E.20}$$

Draw the bifurcation diagram and determine the linear and nonlinear stability of the conductive solution.

111. Model and solve the dynamics of a counterflow heat exchanger.

112. Describe how you would solve this problem using more typical methods and what other information would be required.

113. (Chap. 1) A square silicon chip ($k = 150$ W/m K) is of width 5 mm on a side and of thickness 1 mm. The chip is mounted on a substrate such that its side and back surfaces are insulated, while the front surface is exposed to a coolant. If 4 W are being dissipated in circuits mounted to the back surface of the chip, what is the steady-state temperature difference between the back and front surfaces.

114. (Chap. 1) A square isothermal chip is of width 5 mm on a side and is mounted on a substrate such that its side and back surfaces are well insulated, while the front surface is exposed to the flow of a coolant at temperature 85°C. If the coolant is air and the corresponding convection coefficient is $h = 200$ W/m^{2}K, what is the maximum allowable chip power? If the coolant is a dielectric liquid for which $h = 3000$ W/m^{2}K, what is the maximum allowable power?

115. (Chap. 1) An overhead 25 m long, uninsulated industrial steam pipe of 100 mm diameter is routed through a building whose walls and air are at 25°C. Pressurized steam maintains a pipe surface temperature of 150°C, and the coefficient associated with natural convection is $h = 10$W/m^2 K. The surface emissivity is 0.8. (a) What is the rate of heat loss from the steam line? (b) If the steam is generated in a gas-fired boiler operating at an efficiency of 0.9 and natural gas is priced at \$0.01 per MJ, what is the annual cost of heat loss from the line?

116. (Chap. 1) Three electric resistance heaters of length 250 mm and diameter 25 mm are submerged in a 10 gallon tank of water, which is initially at 295 K. (a) If the heaters are activated, each dissipating 500 W, estimate the time required to bring the water to a temperature of 335 K. (b) If the natural convection coefficient is given by $h = 370(T_s - T)^{1/3}$, where h is in W/m^{2}K and T_s and T are temperatures of the heater surface and water in K, respectively, what is the temperature of each heater shortly after activation and just before deactivation? (c) If the heaters are inadvertently activated when the tank is empty, the natural convection coefficient associated with heat transfer to the ambient air at $T_\infty = 300$ K may be approximated as $h = 0.70(T_s - T_\infty)^{1/3}$. If the temperature of the tank walls is also 300 K and the emissivity of the heater surface is 0.85, what is the surface temperature of each heater under steady-state conditions?

117. (Chap. 2) Beginning with a differential control volume, derive the heat diffusion equation in cylindrical coordinates.

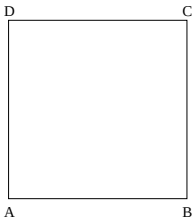

Figure E.30: CAPTION HERE.

118. (Chap. 3) A circular copper rod of 1 mm diameter and 25 mm length is used to enhance heat transfer from a surface that is maintained at 100°C. One end of the rod is attached to this surface, while the other end is attached to a second surface at 0°C. Air flowing between the surfaces and over the rods is at 0°C. The convective heat transfer coefficient at the surface of the rod is 100 W/m^{2}K. What is the rate of heat transfer by convection from the rod to the air?

119. (Chap. 4) Using the method of separation of variables, determine the steady-state temperature field $T(x, y)$ in the rectangle shown below. Make a three-dimensional plot. Also draw the isotherms on a two-dimensional plot.

    Lengths $AB = 3$, and $BC = 2$; temperatures at the boundaries at AB, CD and DA are zero, but at BC is

$$T(3, y) = \begin{cases} y, & 0 \leq y \leq 1 \\ 2 - y, & 1 < y \leq 2 \end{cases}$$

120. (Chap. 5) In a material processing experiment conducted aboard the space shuttle, a coated niobium sphere of 10 mm diameter is removed from a furnace at 900°C and cooled to a temperature of 300°C. Take $\rho = 8600$ kg/m^3, $c = 290$ J/kg K, and $k = 63$ W/m K. (a) If cooling is implemented in a large evacuated chamber whose walls are at 25°C, determine the time required to reach the final temperature if the emissivity is 0.1. How long would it take if the emissivity were 0.6? (b) To reduce the time required for cooling, consideration is given to immersion of the sphere in an inert gas stream at 25°C with $h = 200$ W/m^{2}K. Neglecting radiation, what is the time required for cooling?

121. (Chap. 5) The density and specific heat of a plastic material are known ($\rho = 950$ kg/m^3, $c_p = 1100$ J/kg K), but its thermal conductivity is unknown. An experiment is performed in which a thick sample is heated to a uniform temperature of 100° and then cooled by passing air at 25°C over one surface. A thermocouple embedded a distance of 10 mm below the surface records the thermal response of the plastic during cooling. If the convection coefficient associated with air flow is 200 W/m°, and a temperature of 60° is recorded 5 min after the onset of cooling, what is the thermal conductivity of the material?

122. (Chap. 6) A shaft with a diameter of 100 nm rotates at 9000 rpm in a journal bearing that is 70 mm long. A uniform lubricant gap of 1 mm separates the shaft and the bearing. The lubricant properties are $\mu = 0.03$ Ns/m^2, $k = 0.15$ W/m K, while the bearing material has a thermal conductivity of $k_b = 45$ W/m K. (a) Determine the viscous dissipation in W/m^3 in the lubricant. (b) Determine the rate of heat transfer in W from the lubricant, assuming that no heat is lost through the shaft. (c) If the bearing housing is water-cooled and the outer

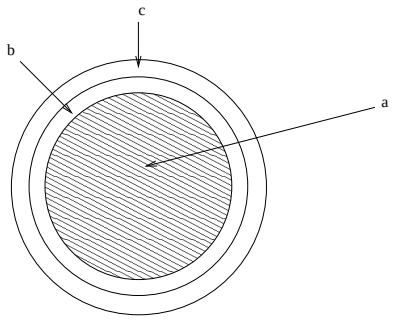

Figure E.31: CAPTION HERE.

surface of the housing is 30°C, determine the temperatures at the interface between lubricant and shaft and lubricant and bearing.

123. (Chap. 7) Consider the wing of an aircraft as a flat plate of length 2.5 m in the flow direction. The plane is moving at 100 m/s in air that is at a pressure of 0.7 bar and temperature −10°C. The top surface of the wing absorbs solar radiation at a rate of 800 W/m^2. Estimate the steady-state temperature of the wing, assuming it to be uniform.

124. (Chap. 8) The evaporator section of a heat pump is installed in a large tank of water, which is used as a heat source during the winter. As energy is extracted from the water, it begins to freeze, creating an ice/water bath at 0°, which may be used for air-conditioning during the summer. Consider summer cooling conditions for which air is passed through an array of copper tubes, each of inside diameter $D = 50$ mm, submerged in the bath. (a) If air enters each tube at a mean temperature of $T_{m,i} = 24$°C and a flow rate of $\dot{m} = 0.01$ kg/s, what tube length L is needed to provide an exit temperature of $T_{m,o} = 14$°C? With 10 tubes passing through a tank of total volume $V = 10$ m^3, which initially contains 80% ice by volume, how long would it take to completely melt the ice? The density and latent heat of fusion of ice are 920 kg/m^3 and 3.34×10^5 J/kg, respectively. (b) The air outlet temperature may be regulated by adjusting the tube mass flow rate. For the tube length determined in part (a), compute and plot $T_{m,o}$ as a function of $\dot{m}$ for $0.005 \leq \dot{m} \leq 0.05$ kg/s. If the dwelling cooled by this system requires approximately 0.05 kg/s of air at 16°C, what design and operating conditions should be prescribed for the system?

125. (Chap. 9) Beverage in cans 150 mm long and 60 mm in diameter is initially at 27°C and is to be cooled by placement in a refrigerator compartment at 4°C. In the interest of maximizing the cooling rate, should the cans be laid horizontally or vertically in the compartment? As a first approximation, neglect heat transfer from the ends.

126. (Chap. 9) A natural convection air heater consists of an array of N parallel, equally spaced vertical plates, which may be maintained at a fixed temperature T_s by embedded electric heaters. The plates are of length and width $L = W = 300$ mm and are in quiescent, atmospheric air at $T_\infty = 20$°C. The total width of the array cannot exceed a value of $W_{ar} = 150$ mm. For $T_s = 75$°C, what is the plate spacing (distance between plates) S that maximizes heat transfer from the array? For this spacing, how many plates comprise the array and what is the corresponding rate of heat transfer from the array?

127. (Chap. 10) Saturated steam at 1 atm condenses on the outer surface of a vertical 100 mm diameter pipe 1 m long, having a uniform surface temperature of 94°C. Estimate the total condensation rate and the heat transfer rate to the pipe.

128. (Chap. 11) A shell-and-tube heat exchanger consists of 135 thin-walled tubes in a double-pass arrangement, each of 12.5 mm diameter with a total surface area of 47.5 m^2. Water (the tube-side fluid) enters the heat exchanger at 15°C and 6.5 kg/s and is heated by exhaust gas entering at 200°C and 5 kg/s. The gas may be assumed to have the properties of atmospheric air, and the overall heat transfer coefficient is approximately 200 W/m^2K. (a) What are the gas and water outlet temperatures? (b) Assuming fully developed flow, what is the tube-side convection coefficient? (c) With all other conditions remaining the same, plot the effectiveness and fluid outlet temperature as a function of the water flow rate over the range from 6 to 12 kg/s. (d) What gas inlet temperature is required for the exchanger to supply 10 kg/s of hot water at an outlet temperature of 42°C, all other conditions remaining the same? What is the effectiveness for this operating condition?

129. (Chap. 11) A boiler used to generate saturated steam is in the form of an unfinned, cross-flow heat exchanger, with water flowing through the tubes and a high temperature gas in cross flow over the tubes. The gas, which has a specific heat of 1120 J/kg K and a mass flow rate of 10 kg/s, enters the heat exchanger at 1400 K. The water, which has a flow rate of 3 kg/s, enters as saturated liquid at 450 K and leaves as saturated vapor at the same temperature. If the overall heat transfer coefficient is 50 W/m^2K and there are 500 tubes, each of 0.025 m diameter, what is the required tube length?

130. (Chap. 12) The energy flux associated with solar radiation incident on the outer surface of the earth's atmosphere has been accurately measured and is known to be 1353 W/m^2. The diameters of the sun and earth are 1.39×10^9 and 1.29×10^7 m respectively, and the distance between the sun and the earth is 1.5×10^{11} m. (a) What is the emissive power of the sun? (b) Approximating the sun's surface as black, what is its temperature? (c) At what wavelength is the spectral emissive power of the sun a maximum? (d) Assuming the earth's surface to be black and the sun to be the only source of energy for the earth, estimate the earth's temperature.

131. (Chap. 12) The spectral reflectivity distribution for white paint can be approximated by the following stair-step function: $\alpha_\lambda = 0.75$ for $\lambda < 0.4$ μm, $\alpha_\lambda = 0.15$ for $0.4 < \lambda < 3$ μm, and $\alpha_\lambda = 0.96$ for $\lambda > 3$ μm. A small flat plate coated with this paint is suspended inside a large enclosure, and its temperature is maintained at 400 K. The surface of the enclosure is maintained at 3000 K, and the spectral distribution of its emissivity is $\varepsilon_\lambda = 0.2$ for $\lambda < 2.0$ μm, and $\varepsilon_\lambda = 0.9$ for $\lambda > 2.0$ μm. (a) Determine the total emissivity, ε, of the enclosure. (b) Determine the total emissivity, ε, and absorptivity, α, of the plate.

132. (Chap. 12) A thermocouple whose surface is diffuse and gray with an emissivity of 0.6 indicates a temperature of 180°C when used to measure the temperature of a gas flowing through a large duct whose walls have an emissivity of 0.85 and a uniform temperature of 450°C. (a) If the convection heat transfer coefficient between the thermocouple and the gas stream is $\bar{h} = 125$ $W/m^2 \cdot K$ and there are negligible conduction losses from the thermocouple, determine the temperature of the gas. (b) Consider a gas temperature of 125°C. Compute and plot the thermocouple measurement error as a function of the convection coefficient for $10 \leq \bar{h} \leq 1000$ $W/m^2 \cdot K$.

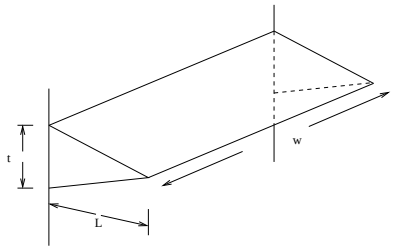

Figure E.32: Triangular fin [Same as Fig. 1.7 on p. 16].

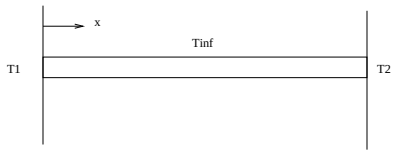

Figure E.33: Constant-area fin [Same as Fig. 1.8].

133. (Chap. 13) Consider two diffuse surfaces A_1 and A_2 on the inside of a spherical enclosure of radius R. Using the following methods, derive an expression for the viewfactor F_{12} in terms of A_2 and R. (a) Find F_{12} by beginning with the expression $F_{ij} = q_{i\to j}/A_i J_i$. (b) Find F_{12} using the view factor integral

$$F_{ij} = \frac{1}{A_i}\int_{A_i}\int_{A_j} \frac{\cos\theta_i \cos\theta_j}{\pi R^2}\, dA_i\, dA_j$$

134. (Chap. 13) Two parallel, aligned disks, 0.4 m in diameter and separated by 0.1 m, are located in a large room whose walls are maintained at 300 K. One of the disks is maintained at a uniform temperature of 500 K with an emissivity of 0.6, while the backside of he second disk is well insulated. If the disks are diffuse, gray surfaces, determine the temperature of the insulated disk.

135. (Chap. 13) A solar collector consists of a long duct through which air is blown; its cross section forms an equilateral triangle of side 1 m on a side. One side consists of a glass cover of emissivity $\varepsilon_1 = 0.9$, while the other two sides are absorber plates with $\varepsilon_2 = \varepsilon_3 = 1.0$. During operation the surface temperatures are known to be $T_1 = 25°\text{C}$, $T_2 = 60°\text{C}$, and $T_3 = 70°\text{C}$. What is the net rate at which radiation is transferred to the cover due to exchange with the absorber plates?

136. (Chap. 13) Consider a circular furnace that is 0.3 m long and 0.3 m in diameter. The two ends have diffuse, gray surfaces that are maintained at 400 and 500 K with emissivities of 0.4 and 0.5, respectively. The lateral surface is also diffuse and gray with an emissivity of 0.8 and a temperature of 800 K. Determine the net radiative heat transfer from each of the surfaces.

137. Show that no solution is possible in Problem 4 if the boundary layer is assumed to be on the wrong side.

138. Find the steady-state temperature distribution and velocity in a square-loop natural convection loop. The total length of the loop is L and the distribution of the heat rate per unit length is: Q between c and d, and $-Q$ between g and h. The rest of the loop is adiabatic.

Figure E.34: Flow in tube with non-negligible wall thickness.

Figure E.35: CAPTION HERE.

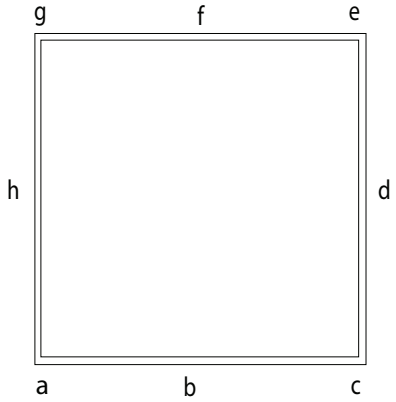

Figure E.36: CAPTION HERE.

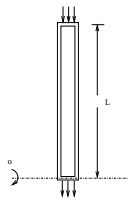

Figure E.37: CAPTION HERE.

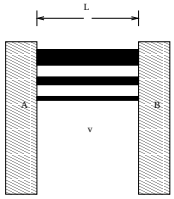

139. Consider a long, thin, vertical tube that is open at both ends. The air in the tube is heated with an electrical resistance running down the center of the tube. Find the flow rate of the air due to natural convection. Make any assumptions you need to.

140. Obtain the table below by solving the fin conduction equation for the different boundary conditions.

141. Derive the fin efficiency given below for a circular fin.

142. Read the section on the bioheat equation and solve the following.

143. Use separation of variables to find the steady-state temperature distribution $T(x, y)$ in the rectangle shown for the following boundary conditions. AB: $T = T_1$; BC: adiabatic; CD: $T = T_2$; DA: $T = T_2$. The dimensions are AB = 2 units, BC = 1 unit. Also write a finite-difference program to find a numerical solution to the problem, and compare with the analytical solution.

144. Use the finite-element based pde toolbox[4] in Matlab to solve the numerical example in the previous homework. Compare with the analytical result.

145. The exact solution of transient conduction in a plane wall with convection at the surfaces is given in the book. Derive it.

[4] Just type `pdetool` in Matlab.

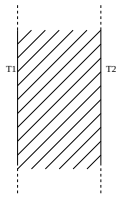

Figure E.38: Plane wall in steady state.

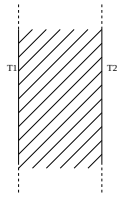

Figure E.39: Plane wall in unsteady state.

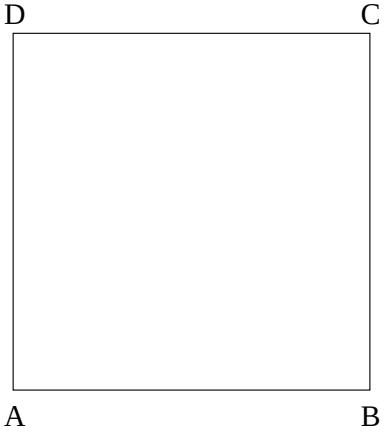

Figure E.40: CAPTION HERE.

146. Show, following the steps in the book, that the transient heat equation in a semi-infinite solid can be written as

$$\frac{d^2T}{d\eta^2} = -2\eta\frac{dT}{d\eta}.$$

Derive also the constant heat flux and surface convection solutions given.

147. The following problem is an example in the book. Write computer programs and find what is asked using more nodes and smaller time steps. Also integrate until steady state is reached, and plot the temperature at a few specific points.

148. Find the non-dimensional form of the energy equation for an incompressible fluid with constant properties

$$\frac{\partial T}{\partial t} + \mathbf{u}\cdot\nabla T = \alpha\nabla^2 T + \Phi/\rho c_p,$$

where the dissipation function is

$$\Phi = \mu\left[2\left(\frac{\partial u}{\partial x}\right)^2 + 2\left(\frac{\partial v}{\partial y}\right)^2 + 2\left(\frac{\partial w}{\partial z}\right)^2 + \left(\frac{\partial v}{\partial x} + \frac{\partial u}{\partial y}\right)^2 + \left(\frac{\partial w}{\partial y} + \frac{\partial v}{\partial z}\right)^2 + \left(\frac{\partial u}{\partial z} + \frac{\partial w}{\partial x}\right)^2\right]$$

in terms of the components of $\mathbf{u} = (u, v, w)$. Show that the Peclet and Eckert numbers arise naturally.

149. For the flat plate boundary layer in forced convection, solve the hydrodynamic and thermal equations

$$2\frac{d^3f}{d\eta^3} + f\frac{d^2f}{d\eta^2} = 0,$$
$$\frac{d^2T^*}{d\eta^2} + \frac{Pr}{2}f\frac{dT^*}{d\eta} = 0,$$

numerically, with the boundary conditions $f(0) = f'(0) = T^*(0) = 0$, and $f'(\infty) = T^*(\infty) = 1$. Compare $f(\eta)$ and $\frac{d^2f}{d\eta^2}(0)$ with values given in the book. Plot $\frac{dT^*}{d\eta}(0)$ as a function of Pr, and compare with the approximation for Pr larger than 0.6 given in the book.

150. For natural convection over a vertical flat plate, solve the boundary layer equations

$$\frac{d^3f}{d\eta^3} + 3f\frac{d^2f}{d\eta^2} - 2\left(\frac{df}{d\eta}\right)^2 + T^* = 0,$$
$$\frac{d^2T^*}{d\eta^2} + 3Prf\frac{dT^*}{d\eta} = 0,$$

numerically, with the boundary conditions $f(0) = f'(0) = 0$, $T^*(0) = 1$, and $f'(\infty) = T^*(\infty) = 0$. Plot graphs choosing values of Pr to compare with those in the book.

151. For a *counter-flow heat exchanger*, determine from first principles (a) the heat rate expression, (b) the log mean temperature difference, and (c) the ε-NTU relation.

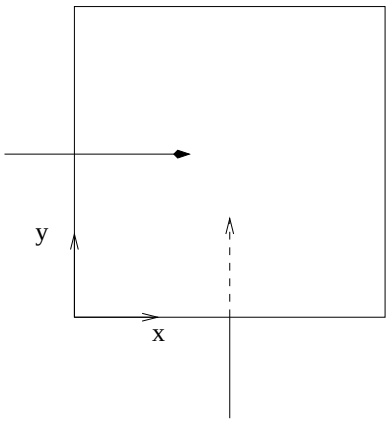

Figure E.41: CAPTION HERE.

152. There is flow on either side of a $L \times L$ metal plate as shown. Assume that the flow is laminar on both sides and that the local heat transfer coefficient is given by the boundary layer theory. Determine the local heat transfer coefficient $U(x, y)$ as a function of position. Neglect the conductive thermal resistance of the plate. If the incoming temperatures of the two fluids are $T_{h,i}$ and $T_{c,i}$, what are the temperature distributions at the outlets as functions of position.

153. Again consider a square plate as shown above, but with conduction important and the heat transfer coefficient independent of position. Neglecting the variation of temperature across the thickness of the plate, derive a steady state equation for the local temperature in the plate $T(x, y)$. With suitable boundary conditions, solve $T(x, y)$ analytically and compare with a numerical solution.

154. Show that Maxwell equations (Eqs. 1.53–1.56, p. 10 in the Notes) reduce to the wave equation in electric and magnetic fields for zero electrical conductivity.

155. For small electrical conductivity, show that the one-dimensional equation for the electric field

$$\frac{\partial^2 E}{\partial x^2} - \epsilon\mu \frac{\partial^2 E}{\partial t^2} - g\mu \frac{\partial E}{\partial t} = 0$$

has an approximate solution of the form

$$E = e^{-\beta x} f(x - at)$$

where $a = 1/\sqrt{\epsilon\mu}$, and β is small (so that β^2 can be neglected). What is β is terms of the parameters g, ϵ and μ?

156. Show, by integration, the expression in the book for the view factor between two aligned, parallel rectangles.

157. Find the steady-state temperature distribution $T(x)$ in a plate $x \in [0, L]$, with $T(0) = T_1$, and $T(L) = T_2$, and where the thermal conductivity varies linearly with temperature, i.e.

$$k = k_0 \left(1 + \epsilon \frac{T - T_1}{T_2 - T_1}\right),$$

with $\epsilon \ll 1$.

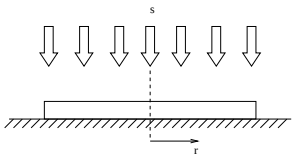

Figure E.42: CAPTION HERE

158. Consider a fin equation

$$\epsilon \frac{d^2\theta}{dx^2} - \theta = 0$$

with $\theta(0) = -1, \theta(1) = 1$. (a) Solve analytically. (b) Solve using perturbations for $\epsilon \ll 1$ with boundary layers on both sides. (c) Compare the two solutions graphically.

159. Determine the time-dependent temperature in the cooling of a lumped body with radiation and weak convection. For simplicity, take $T_\infty = 0$.

160. Two bodies are in thermal contact with each other (as in Section 2.6.1, p. 25 but without heating Q). Solve for initial conditions $T_1(0) = T_2(0) = T_0$. Solve the problem using perturbations if the contact thermal resistance k_s is small. Clearly specify the small parameter ϵ. Compare graphically with the analytical solution of the previous problem.

161. A circular disc of radius R lies on an adiabatic surface and is being heated by a radiative heater. The heat input per unit area from the radiator is q. The disc is thin enough for the transverse temperature variation to be neglected. If the temperature at the edge of the disc is $T(R) = T_0$, determine the steady-state temperature distribution, $T(r)$, in the disc, where r is the radial coordinate.

162. Consider a thin plate of thickness δ, and constant thermal conductivity k. Both sides of the plate are subjected to convective heat transfer with a constant heat transfer coefficient h. Show that the temperature field, $T(x, y)$, is governed by

$$\frac{\partial^2 T}{\partial x^2} + \frac{\partial^2 T}{\partial y^2} - m^2 \left(T - T_\infty\right) = 0,$$

where $m^2 = 2h/k\delta$, and T_∞ is the temperature of the fluid surrounding the plate.

163. The governing equation for the temperature distribution in a thermal boundary due to flow over a flat plate at constant temperature is

$$\frac{d^2 T^*}{d\eta^2} + \frac{Pr}{2}\ f\ \frac{dT^*}{d\eta} = 0,$$

where $f(\eta)$ is the known solution of the Blasius equation. The boundary conditions are $T^*(0) = 0$ and $T^*(\infty) = 1$. Show that the solution can be written as

$$T^*(\eta) = \frac{\displaystyle\int_0^\eta \exp\left(-\frac{Pr}{2}\int_0^r f(s)\ ds\right)\ dr}{\displaystyle\int_0^\infty \exp\left(-\frac{Pr}{2}\int_0^r f(s)\ ds\right)\ dr}.$$

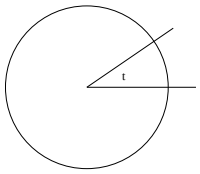

Figure E.43: CAPTION HERE

164. The inside wall of a long cylinder of radius R and length L has a temperature distribution of $T_w(\theta)$. Assuming that there is no participating medium inside the cylinder and that the inside surface acts a black-body, determine the heat flux distribution on the inside wall $q(\theta)$ due to internal radiation.

165. Show that the set of all continuous temperature distributions $T(x)$ in the interval $x \in [a, b]$ along a bar with $T(a) = 0$ and $T(b) = 1$ does not form a vector space.

166. In the above, show that $T(x)$ would be a vector space if the second condition were changed to $T(b) = 0$ (and T could assume any value). What is the dimension of that space?

167. $\mathcal{S}$ is a space of sufficiently smooth functions $f(x)$ with $x \in [0, 1]$ and $f(0) = f(1) = 0$ that is endowed with the L_2 inner product.

    (a) Show that
    $$\mathcal{L}_1 = \frac{d^2}{dx^2}$$
    that operates on members of $\mathcal{S}$ is self-adjoint. Show that
    $$\mathcal{L}_2 = \frac{d^2}{dx^2} - m^2$$
    where m is a constant, is also self-adjoint.

    (b) Find the eigenvalues, λ_n, and eigenfunctions of $\mathcal{L}_1$. Normalize each eigenfunction by dividing by its norm to obtain an orthonormal set, $\phi_n(x)$.

    (c) Solve the one-dimensional steady-state fin equation
    $$\mathcal{L}_2(T) = 0$$
    for the temperature distribution $T(x)$, with $T(0) = 0$, $T(1) = 1$, where $\mathcal{L}_2$ is defined as above.

    (d) Let $\theta(x) = T - x$. Write the differential equation that $\theta(x)$ satisfies in the form $\mathcal{L}(\theta) = g(x)$, and show that $\theta \in \mathcal{S}$. Expand $\theta(x)$ in terms of the eigenfunctions obtained above as
    $$\theta(x) = \sum_{i=0}^{\infty} a_i \phi_i(x).$$
    Substitute into $\mathcal{L}(\theta) = g(x)$, and take the inner product of the equation with ϕ_i to determine the coefficients a_i.

    (e) Graphically compare the exact and the eigenfunction expansion (using perhaps five terms) solutions of $T(x)$.

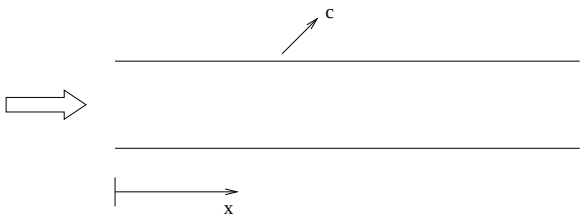

Figure E.44: CAPTION HERE

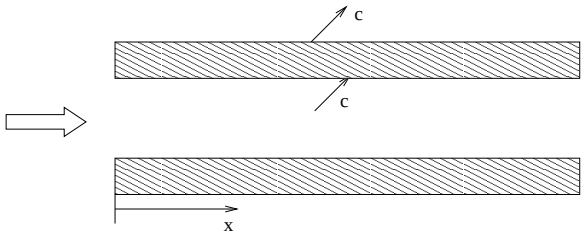

Figure E.45: CAPTION HERE

168. Consider one-dimensional flow in a pipe with lateral convection (with constant heat transfer coefficient h) as shown. The flow velocity is V and the temperature $T(x)$. Neglect the pipe wall.

    (a) Derive the governing energy balance differential equation and non-dimensionalize.

    (b) Solve with boundary conditions $T(0) = T_{in}$ and $T(L) = T_{out}$.

    (c) Using the boundary layer approximation for small axial conduction, find the inner and outer solutions as well as the composite solution.

    (d) Show that the adjoint differential equation represents a pipe with flow in the opposite direction.

169. Consider now the pipe with a thick wall which exchanges heat by convection with the fluid and with the surroundings (with constant but different heat transfer coefficients). Assume axial conduction in both wall and fluid.

    (a) Derive the two governing equations for the wall and fluid temperatures, $T_w(x)$ and $T_f(x)$, respectively.

    (b) Nondimensionalize using $\xi = x/L$, $\theta_w = (T_w - T_\infty)/\Delta T$, $\theta_f = (T_f - T_\infty)/\Delta T$, $\Delta T = T_f^{in} - T_\infty$, where L is the length of the pipe, T_∞ is the ambient temperature, and T_f^{in} is the inlet temperature of the fluid.

    (c) Writing $\mathbf{X} = \begin{bmatrix}\theta_w & \theta_f'\end{bmatrix}^T$ and $\mathbf{Y} = \begin{bmatrix}\theta_f & \theta_w'\end{bmatrix}^T$, show that the nondimensional equations can be written as

$$\frac{d}{d\xi}\mathbf{\Theta} = \mathbf{A}\mathbf{\Theta}, \tag{E.21}$$

    where $\mathbf{\Theta} = [\mathbf{X}\ \mathbf{Y}]^T$.

(d) Assume boundary conditions $T_f = T_{in},\ dT_w/dx = 0$ at $x = 0$, and $T_f = T_{out},\ dT_w/dx = 0$ at $x = L$. Show that Eq. (E.21) can be written as

$$\mathbf{X}(1) = \mathbf{D}_{11}\mathbf{X}(0) + \mathbf{D}_{12}\mathbf{Y}(0), \tag{E.22}$$

$$\mathbf{Y}(1) = \mathbf{D}_{21}\mathbf{X}(0) + \mathbf{D}_{22}\mathbf{Y}(0), \tag{E.23}$$

where $\mathbf{Y}(0)$ and $\mathbf{Y}(1)$ are known.

(e) Determine $\mathbf{X}(0)$ from Eq. (E.23), and use this to find $\mathbf{\Theta}(0)$.

(f) Solve Eq. (E.21).

(g) Find the total heat lost to the surroundings by convection in terms of $\theta_w(x)$.

170. Use the following numerical methods to solve the fin problem: $T'' - T = 0$ with $T(0) = 1$ and $T(1) = 0$.

(a) Finite differences with n divisions, where n is as large as necessary.

(b) Finite elements with n elements, where n is as large as necessary.

(c) Collocation method with Chebycheff polynomials. Use n polynomials, where n is as large as necessary. Remember to transform the equation first into one with homogeneous boundary conditions.

171. Consider the problem of pipe flow with a thick wall given in HW16, Prob. 2. Assume a vanishingly small axial conduction in both wall and fluid, and find the *outer* solution for the boundary layer approximation, and the corresponding heat loss to the surroundings.

172. Using a lumped approximation write the differential equation that governs the time dependence of the temperature of a body that is convecting and radiating to surroundings at T_∞. Find the steady state temperature and show that it is linearly stable.

173. Find the correlation dimension of the strange attractor for the Lorenz equations (that model flow in a thermosyphon under some conditions) [Probs 38, 53, 136]

$$\frac{dx}{dt} = \sigma(y - x), \tag{E.24}$$

$$\frac{dy}{dt} = \lambda x - y - xz, \tag{E.25}$$

$$\frac{dz}{dt} = -bz + xy. \tag{E.26}$$

from data obtained from numerical integration of the equation, where $\sigma = 10$, $\lambda = 28$ and $b = 8/3$. Use the following definition of the dimension D: vary r and count the number of points $N(r)$ within a sphere of radius r; the dimension is given by the slope $D = \ln N / \ln r$.

174. Find the linear stability of the critical points of the dynamical system (that also models flow in a thermosyphon under different conditions)

$$\frac{dx}{dt} = y - x, \tag{E.27}$$

$$\frac{dy}{dt} = a - zx, \tag{E.28}$$

$$\frac{dz}{dt} = xy - b. \tag{E.29}$$

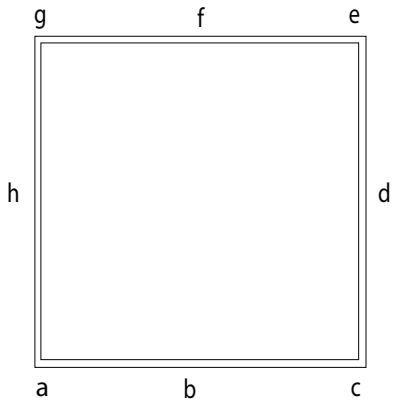

Figure E.46: CAPTION HERE

Plot (x, y, z) in three dimensional space for the initial condition (1,1,1) and (i) $a = 2, b = 1$, (ii) $a = 1, b = 1$, and (iii) $a = 0, b = 1$.

175. The dynamical system for an untilted, toroidal thermosyphon with axial conduction and known heat flux is

$$\frac{dx}{dt} = y - x, \tag{E.30}$$

$$\frac{dy}{dt} = -zx - cy, \tag{E.31}$$

$$\frac{dz}{dt} = -b + xy - cz. \tag{E.32}$$

Show that $(0, ?, ?)$ is a *globally* stable critical point for $b < c^2$.

176. Consider two thermosyphons that can exchange heat through a common wall[5], as shown in Fig. E.47. There is constant heating through wall ab and cooling through cd. Derive the time-dependent governing equations for this conjugate problem, and find the steady state solution(s).

177. A U-shaped open loop with constant heating from the side is rotated about its axis[6] as shown in Fig. E.48. Determine the steady-state flow rate.

178. Consider a PCR (polymerase chain reaction) thermocycler[7] as shown in Fig. E.49, that acts as a single-phase thermosyphon. The triangle is equilateral with a 2 cm base and 0.4 mm internal diameter. If water is the working fluid, estimate its cycle time (as a number). Assume a suitable heat transfer correlation.

[5]O. Salazar, M. Sen and E. Ramos, Flow in conjugate natural circulation loops, *AIAA Journal of Thermophysics and Heat Transfer,* Vol. 2, No. 2, pp. 180–183, 1988.

[6]M.A. Stremler, D.R. Sawyers, M. Sen, Analysis of natural convection in a rotating open loop, *AIAA Journal of Thermophysics and Heat Transfer,* Vol. 8, No. 1, pp. 100–106, 1994.

[7]N. Agrawal, Y.A. Hassan, V.M. Ugaz, A Pocket-Sized Convective PCR Thermocycler, *Angewandte Chemie International Edition,* Vol. 46, No. 23, pp. 4316–4319, 2007.

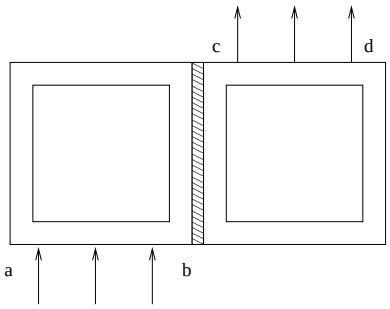

Figure E.47: CAPTION HERE.

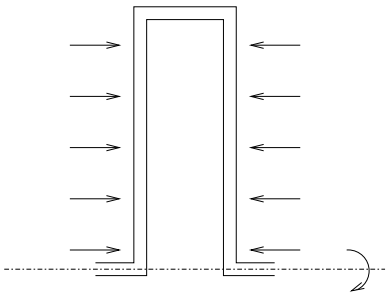

Figure E.48: CAPTION HERE.

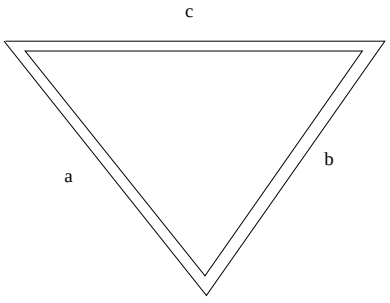

Figure E.49: CAPTION HERE.

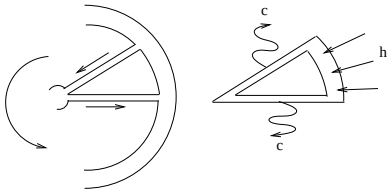

Figure E.50: CAPTION HERE

179. Consider a rotating torus (such as an automobile tire) that is being cooled by natural convection through hollow spokes as in Fig. E.50 (a single loop is also shown at the side). Estimate the heat rate that can be extracted by convection through the walls of the spoke.

180. A lumped mass with internal heat generation is radiating heat to its surroundings. Assume that the instantaneous temperature of the mass can be measured by a sensor, and the heat generation can be changed by an actuator. PI control is used to maintain the temperature of the mass at a constant value. Find the conditions on the PI constants for linear stability.

181. Consider a thermostatically-controlled heating model of a ring of n rooms

$$\frac{dT_i}{dt} + T_i + k\left(T_i - T_{i-1}\right) + k\left(T_i - T_{i+1}\right) = Q_i, \quad i = 1, \ldots, n$$

where T_i is the temperature of room i (with respect to the surroundings), and t is time. The third and fourth terms on the left are the heat transfer between room i and its neighbors $i-1$ and $i+1$, respectively. The parameter k represents the strength of this interaction. The heater Q_i goes on if the temperature T_i falls below T_{min}, and goes off if it rises above T_{max}, so that

$$Q_i = \begin{cases} 0 & \text{if heater is off,} \\ 1 & \text{if heater is on.} \end{cases}$$

Using $n = 3$, $T_{min} = 0.25$, $T_{max} = 0.75$, $T_1(0) = 0.10$, $T_2(0) = 0.50$, $T_3(0) = 0.85$, write a compute program to plot $T_1(t), T_2(t), T_3(t)$ on the same graph for $40 \leq t \leq 50$ with (a) $k = 0.28$, and (b) $k = 0.29$.

182. The following questions refer to the book S. Chandrasekhar, *Hydrodynamic and Hydromagnetic Stability,* Dover, 1961. Consider only the case of fluid between two rigid plates held at different temperatures. Show all the steps that are not given in the book.

(a) From the governing equations (2), (19) and (39), make suitable assumptions and get the steady state solutions for the fluid velocity, temperature, and pressure given in Section 9.

(b) From there, carry out the steps in the book to get to Eqs. (99) and (100). Set the eigenvalue $\sigma = 0$ to get Eqs. (126) and (127).

(c) Complete the solution in Section 15 (solve Eq. (216) numerically) to get the minimum Rayleigh number for an even mode to be 1707.762 as shown in Eq. (217).

183. The dispersion relation of gravity waves on the surface of water is

$$\omega = \sqrt{gk \tanh(kh)}\ ,$$

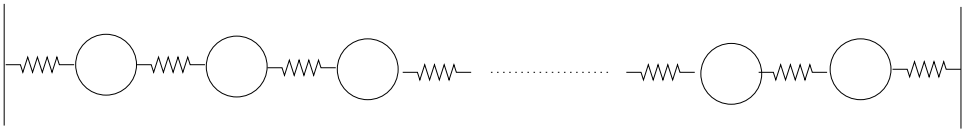

Figure E.51: CAPTION HERE

where h is the depth of water, and g is the acceleration due to gravity. (a) Find the two approximations for $kh \ll 1$ (shallow water), and $kh \gg 1$ (deep water) to leading order. (b) Determine the phase and group velocities in these two limits. (c) Calculate the speed of a tsunami (shallow-water wave) in km/hr for an average ocean depth of 3 km. (d) Show that the group velocity of a deep-water wave is one-half its phase velocity.

184. Analyze the wave motion in an infinite chain of masses connected by identical springs. The pattern of masses is m_1, m_1, m_2 repeating itself.

185. Consider the longitudinal motion of a string of ten identical masses connected to each other and to walls on either side by identical springs. Before starting, all masses are stationary and at equilibrium; then only the first mass is pulled a certain distance to one side and let go. Calculate numerically the resulting longitudinal motion of each mass as a function of time and plot the result.

186. Derive the Power Flow, Wave Energy and Power Flow, and Momentum and Mass Flow equations outlined in

    `http://www.silcom.com/~aludwig/Physics/QM/LatticeWaves.htm`

187. Using the one-dimensional formula as a guide, derive a formula for solving the steady-state diffusion equation in two dimensions using the random-walk method.

188. Assuming that the distribution function f depends on time alone, use the relaxation time approximation to solve the Boltzmann Transport Equation for $f(t)$.

More bibliography

[1] R. Acosta, M. Sen, and E. Ramos. Single-phase natural circulation in a tilted square loop. *Wärme- und Stoffübertragung*, 21(5):269–275, 1987.

[2] N.U. Ahmed. *Semigroup Theory with Applications to Systems and Control*. Longman, Harlow, U.K., 1991.

[3] R. Aldrovandi. *Special Matrices of Mathematical Physics: Stochastic, Circulant and Bell Metrices*. World Scientific, Singapore, 2001.

[4] S. Alotaibi. *Temperature Controllability in Cross-Flow Heat Exchangers and Long Ducts*. PhD thesis, Department of Aerospace and Mechanical Engineering, University of Notre Dame, Notre Dame, IN, 2003.

[5] S. Alotaibi, W.J. Goodwine M. Sen, and K.T. Yang. Controllability of cross-flow heat exchangers. *International Journal of Heat and Mass Transfer*, 47:913–924, 2004.

[6] S. Alotaibi, M. Sen, J.W. Goodwine, and K.T. Yang. Numerical simulation of the thermal control of heat exchangers. *Numerical Heat Transfer A*, 41:229–244, 2002.

[7] S. Alotaibi, M. Sen, W.J. Goodwine, and K.T. Yang. Flow-based control of temperature in long ducts. *International Journal of Heat and Mass Transfer*, 47:4995–5009, 2004.

[8] K.A. Antonopoulos and C. Tzivanidis. A correlation for the thermal delay of building. *Renewable Energy*, 6(7):687–699, 1995.

[9] P.J. Antsaklis and A.N. Michel. *Linear Systems*. McGraw-Hill, New York, 1997.

[10] R. Arena, R. Caponetto, L. Fortuna, and D. Porto. *Nonlinear Noninteger Order Circuits and Systems–An Introduction*. World Scientific, Singapore, 2000.

[11] Arpaci and Larson. *Convection Heat Transfer*. Prentice-Hall, 1984.

[12] V.S. Arpaci, S.-H. Kao, and A. Selamet. *Introduction to Heat Transfer*. Prentice-Hall, Upper Saddle River, NJ, 1999.

[13] A. Aziz and T.Y. Na. *Perturbation Methods in Heat Transfer*. Hemisphere Publ. Corp., Washington, DC, 1984.

[14] H.D. Baehr and K. Stephan. *Heat and Mass Transfer*. Springer, New York, 1998.

[15] A.-L. Barabási. *Linked: The New Science of Networks*. Perseus, Cambridge, MA, 2002.

[16] C Baruch and S. Darrell. On stability of systems of delay differential equations. *J. Comp. Appl. Math.*, 117:137–158, 2000.

[17] J.L. Battaglia, L. Le Lay, J.C. Batsale, A. Oustaloup, and O. Cois. Heat flux estimation through inverted non-integer identification models. *International Journal of Thermal Sciences*, 39(3):374–389, 2000.

[18] H.H. Bau. Control of Marangoni-Benard convection. *International Journal of Heat and Mass Transfer*, 42(7):1327–1341, 1999.

[19] Y. Bayazitoglu and M.N. Ozisik. *Elements of Heat Transfer*. McGraw-Hill, New York, 1988.

[20] M. Becker. *Heat Transfer, A Modern Approach*. Plenum Press, New York, 1986.

[21] A. Bejan. *Convection Heat Transfer*. John Wiley, New York, 1984.

[22] A. Bejan. *Heat Transfer*. John Wiley, New York, 1993.

[23] R. Bellman and K.L. Cooke. *Differential-Difference Equations*. Academic Press, New York, 1963.

[24] C.O. Bennett. *Momentum, Heat, and Mass Transfer*. McGraw-Hill, New York, 3rd edition, 1982.

[25] M.Q. Brewster. *Thermal Radiative Transfer and Properties*. John Wiley, New York, 3rd edition, 1992.

[26] L.C. Burmeister. *Heat Transfer*. Dover, New York, 1982.

[27] L.C. Burmeister. *Convection Heat Transfer*. John Wiley, New York, 2nd edition, 1993.

[28] E.F. Camacho and C. Bordons. *Model Predictive Control in the Process Industry*. Springer, London, 2001.

[29] V.P. Carey. *Liquid-Vapor Phase-Change Phenomena*. Hemisphere Publ. Corp., Washington, DC, 1992.

[30] J. Carr. *Applications of Centre Manifold Theory*. Springer-Verlag, New York, 1981.

[31] H.S. Carslaw and J.C. Jaeger. *Conduction of Heat in Solids*. Clarendon Press, Oxford, UK, 1959.

[32] O. Castillo and P. Melin. *Soft Computing for Control of Non-Linear Dynamical Systems*. Physica-Verlag, Heidelberg, 2001.

[33] Cebeci and Bradshaw. *Physical and Computational Aspects of Convective Heat Transfer*. Springer-Verlag, 1984.

[34] A.J. Chapman. *Fundamentals of Heat Transfer*. Macmillan, New York, 1987.

[35] C.K. Charny. Mathematical models of bioheat transfer. In Y.I. Cho, editor, *Advances in Heat Transfer*, volume 22, pages 19–155. Academic Press, New York, 1992.

[36] G. Chen. Heat transfer in micro- and nanoscale photonic devices. In C.-L. Tien, editor, *Annual Review of Heat Transfer*, volume 7, chapter 1. Begell House, New York, 1996.

[37] G. Chen and G. Chen. *Linear Stochastic Control Systems*. CRC Press, Boca Raton, 1995.

[38] P.D. Christofides. *Nonlinear and Robust Control of PDE Systems*. Birkhäuser, Boston, 2002.

[39] P.D. Christofides and Dautidis P. Feed-back control of hyperbolic PDE systems. *AIChE Journal*, 412:3063, 1978.

[40] J. Chu. Application of a discrete optimal tracking controller to an industrial electrical heater with pure delay. *J. Proc. Cont.*, 5(1):3–8, 1995.

[41] J. Chu, Su H., and x. Hu. A time-delay control algorithm for an industrial electrical heater. *J. Proc. Cont.*, 3(4):220–224, 1993.

[42] Collier. *Convective Boiling and Condensation*. McGraw-Hill, 1984.

[43] C. Comstock. On the delayed hot water problem. *Heat and Mass Transfer*, 96:166–171, 1974.

[44] J. Crank. *Free and Moving Boundary Problems*. Clarendon Press, Oxford, U.K., 1984.

[45] L. Dai. *Singular Control Systems*. Springer-Verlag, Berlin, 1989.

[46] A. Datta, M.-T. Ho, and S.P. Bhattacharyya. *Structure and Synthesis of PID Controllers*. Springer, London, 2000.

[47] D. Díaz, M. Sen, and K.T. Yang. Effect of delay in thermal systems with long ducts. To be published in *International Journal of Thermal Sciences*, 2004.

[48] G. Díaz. *Simulation and Control of Heat Exchangers using Artificial Neural Networks*. PhD thesis, Department of Aerospace and Mechanical Engineering, University of Notre Dame, Notre Dame, IN, 2000.

[49] G. Díaz, K.T. Yang M. Sen, and R.L. McClain. Simulation of heat exchanger performance by artificial neural networks. *International Journal of HVAC&R Research*, 5(3):195–208, 1999.

[50] G. Díaz, M. Sen, K.T. Yang, and R.L. McClain. Adaptive neurocontrol of heat exchangers. *ASME Journal of Heat Transfer*, 123(3):417–612, 2001.

[51] G. Díaz, M. Sen, K.T. Yang, and R.L. McClain. Dynamic prediction and control of heat exchangers using artificial neural networks. *International Journal of Heat and Mass Transfer*, 44(9):1671–1679, 2001.

[52] G. Díaz, M. Sen, K.T. Yang, and R.L. McClain. Stabilization of a neural network-based temperature controller for heat exchangers. *Proceedings of the 12th International Heat Transfer Conference*, 4:225–230, 2002.

[53] G. Díaz, M. Sen, K.T. Yang, and R.L. McClain. Stabilization of thermal neurocontrollers. To be published in *Applied Artificial Intelligence*, 2004.

[54] K.R. Diller. Models of bioheat transfer processes at high and low temperatures. In Y.I. Cho, editor, *Advances in Heat Transfer*, volume 22, pages 157–357. Academic Press, New York, 1992.

[55] C. Doumanidis and N. Fourligkas. Distributed-parameter control of the heat source trajectory in thermal materials processing. *ASME Journal of Manufacturing Science and Engineering*, 118(4):571–578, 1996.

[56] C. Doumanidis and N. Fourligkas. Distributed-parameter control of the heat source trajectory in thermal materials processing. *ASME Journal of Manufacturing Science and Engineering*, 118(4):571–578, 1996.

[57] P.G. Drazin. *Nonlinear Systems*. Cambridge University Press, Cambridge, U.K., 1992.

[58] R.D. Driver. *Ordinary and Delay Differential Equations*. Springer-Verlag, New York, 1977.

[59] D.K. Edwards. *Radiation Heat Transfer Notes*. Hemisphere Pub. Corp., Washington, DC, 3rd edition, 1981.

[60] P. Elgar. *Sensors for Measurement and Control*. Longman, Essex, U.K., 1998.

[61] A. Fakheri. *Intermediate Heat Transfer*. CRC Press, Boca Raton, FL, 2014.

[62] J. Feder. *Fractals*. Plenum, New York, 1988.

[63] W. Franco. *Hydrodynamics and Control in Thermal-Fluid Networks*. PhD thesis, Department of Aerospace and Mechanical Engineering, University of Notre Dame, Notre Dame, IN, 2003.

[64] W. Franco, M. Sen, K.T. Yang, and R.L. McClain. Comparison of thermal-hydraulic network control strategies. *Proceedings of the Institution of Mechanical Engineers, Part I: Journal of Systems and Control Engineering*, 217:35–47, 2003.

[65] W. Franco, M. Sen, K.T. Yang, and R.L. McClain. Dynamics of thermal-hydraulic network control strategies. *Experimental Heat Transfer*, 17(3):161–179, 2004.

[66] G.F. Franklin, J.D. Powell, and A. Emami-Naeini. *Feedback Control of Dynamic Systems, 3rd Ed.* Addison-Wesley, Reading, MA, 1994.

[67] M. Gad-el-Hak. *Flow Control: Passive, Active and Reactive Flow Management*. Cambridge University Press, Cambridge, U.K., 2000.

[68] V. Ganapathy. *Applied Heat Transfer*. PennWell Pub. Co., Tulsa, OK, 1982.

[69] B. Gebhart. *Heat Conduction and Mass Diffusion*. McGraw-Hill, New York, 1993.

[70] B. Gebhart, Y. Jaluria, R.L. Mahajan, and B. Sammakia. *Buoyancy-Induced Flows and Transport*. Hemisphere Publ. Corp., New York, 1988.

[71] U. Grigull. *Heat Conduction*. Hemisphere Pub. Corp., Washington, D.C., 1984.

[72] J. S. Guillermo, D. Aniruddha, and S.P. Bhattacharyya. PI stabilization of first-order systems with time delay. *Automatica*, 37:2020–2031, 2001.

[73] L. Hach and Y. Katoh. Thermal responses in control loop in indirect control of indoor environment of non-air-conditioned space with quasi-steady-state model. *JSME International Journal Series C-Mechanical Systems Machine Elements And Manufacturing*, 46(1):197–211, 2003.

[74] J.K. Hale and S.M. Lunel. *Introduction to Functional Differential Equations*. Springer-Verlag, New York, 1993.

[75] E.G. Hansen. *Hydronic System Design and Operation*. McGraw-Hill, New York, 1985.

[76] S. Haykin. *Neural Networks: A Comprehensive Foundation*. Macmillan, New York, 1999.

[77] G. Henryk, G. Piotr, and K. Adam. *Analysis and Synthesis of Time Delay Systems*. John Wiley Sons, Chichester, 1989.

[78] M.A. Henson and D.E. Seborg, editors. *Nonlinear Process Control*. Prentice Hall, Upper Saddle River, NJ, 1997.

[79] M.A. Henson and D.E. Seborg. *Nonlinear Process Control*. Prentice Hall, Upper Saddle River, NJ, 1997.

[80] G.F. Hewitt. *Process Heat Transfer*. CRC Press, Boca Raton, 1994.

[81] J.M. Hill and J.N. Dewynne. *Heat Conduction*. Blackwell Scientific Publications, Oxford, U.K., 1987.

[82] E.J. Hinch. *Perturbation Methods*. Cambridge University Press, Cambridge, U.K., 1991.

[83] K.-H. Hoffman and W. Krabs. *Optimal Control of Partial Differential Equations*. Springer-Verlag, Berlin, 1991.

[84] J.P. Holman. *Heat Transfer*. McGraw-Hill, New York, 7th edition, 1990.

[85] M.H. Holmes. *Laminar flow forced convection in ducts, a source book for compact heat exchanger analytical data*. Springer-Verlag, New York, 1995.

[86] M.F. Hordeski. *HVAC Control in the New Millennium*. Fairmont Press, Liburn, GA, 2001.

[87] L.E. Howle. Control of Rayleigh-Benard convection in a small aspect ratio container. *International Journal of Heat and Mass Transfer*, 40(4):817–822, 1997.

[88] C.J. Huang, C.C. Yu, and S.H. Shen. Selection of measurement locations for the control of rapid thermal processor. *Automatica*, 36(5):705–715, 2000.

[89] G. Huang, L. Nie, Y. Zhao, W. Yang, Q. Wu, and L. Liu. Temperature control system of heat exchangers, an application of DPS theory. *Lecture Notes in Control Information Sciences*, 159:68–76, 1991.

[90] H. Ibach and H. Lüth. *Solid-State Physics*. Springer, New York, 1990.

[91] D. Ibrahim. *Microcontroller-Based Temperature Monitoring and Control*. Newnes, Oxford, 2002.

[92] F.P. Incropera and D.P. DeWitt. *Fundamentals of Heat and Mass Transfer, 4th Ed.* Wiley, New York, 1996.

[93] F.P. Incropera and D.P. Dewitt. *Fundamentals of Heat and Mass Transfer*. John Wiley, New York, 5th edition, 2002.

[94] L. Irena and R. Triggiani. *Deterministic Control Theory for Infinite Dimensional Systems, Vols. I and II Encyclopedia of Mathematics*. Cambridge University Press, 1999.

[95] V.P. Isachenko, V.A. Osipova, and A.S. Sukomel. *Heat Transfer*. Mir, Moscow, 1977.

[96] A. Isidori. *Nonlinear Control Systems*. Springer, London, 1995.

[97] A. Ito, H. Kanoh, and M. Masubuchi. MWR approximation and modal control of parallel and counterflow heat exchangers. *Proc, 2nd IFAC Symposium on Distributed-Parameter Systems*, 41, 1978.

[98] O.L.R. Jacobs. *Introduction to Control Theory.* 2nd Ed., Oxford University Press, Oxford, 1993.

[99] O.L.R. Jacobs. *Introduction to Control Theory.* Oxford University Press, Oxford, U.K.,, 1993.

[100] M. Jakob. *Heat Transfer*, volume II. John Wiley, New York, 1957.

[101] Y. Jaluria. *Natural Convection Heat and Mass Transfer.* Pergamon Press, New York, 1980.

[102] Y. Jaluria. *Computational Heat Transfer.* Washington, DC, 1986.

[103] Y. Jaluria and K.E. Torrance. *Computational Heat Transfer.* Taylor and Francis, New York, 2nd edition, 2003.

[104] S. Kakac. *Convective Heat Transfer.* CRC Press, Boca Raton, 2nd edition, 1995.

[105] S. Kakac, R.K. Shah, and W. Aung, editors. *Handbook of Single-Phase Convective Heat Transfer.* John Wiley, New York, 1983.

[106] S. Kakac and Y. Yener. *Heat Conduction.* Taylor and Francis, Washington, DC, 3rd edition, 1993.

[107] R.D. Karam. *Satellite Thermal Control for Systems Engineers.* AIAA, Reston, VA, 1998.

[108] M. Kaviany. *Principles of Convective Heat Transfer.* Springer-Verlag, New York, 1994.

[109] M. Kaviany. *Principles of Heat transfer in Porous Media.* Springer-Verlag, New York, 2nd edition, 1995.

[110] M. Kaviany. *Heat Transfer Physics.* Cambridge University Press, New York, 2008.

[111] W.M. Kays and M.E. Crawford. *Convective Heat and Mass Transfer.* McGraw-Hill, New York, 3rd edition, 1993.

[112] W.M. Kays and A.L. London. *Compact Heat Exchangers.* McGraw-Hill, San Francisco, 3rd edition, 1984.

[113] D.Q. Kern. *Process Heat Transfer.* McGraw-Hill International, Auckland, 1950.

[114] J. Kevorkian and J.D. Cole. *Multiple Scale and Singular Perturbation Methods.* Springer, New York, 1996.

[115] M.-H. Kim, S.Y. Lee, S.S. Mehendale, and R.L. Webb. Microscale heat exchanger design for evaporator and condenser applications. In J.P. Hartnett, T.F. Irvine, Y.I. Cho, and G.A. Greene, editors, *Advances in Heat Transfer*, volume 37, pages 297–429. Academic Press, Amsterdam, 2003.

[116] C. Kittel and H. Kroemer. *Thermal Physics.* W.H. Freeman & Co., San Francisco, 2nd edition, 1980.

[117] J. Klamka. *Controllability of Dynamical Systems.* Kluwer, Dordrecht, Netherlands, 1991.

[118] F. Kreith and W.Z. Black. *Basic Heat Transfer*. Harper and Row, Cambridge, U.K., 1980.

[119] F. Kreith and M.S. Bohn. *Principles of Heat Transfer*. West Publ. Co., St. Paul, MN, 5th edition, 1993.

[120] A. Kumar and P. Daoutidis. *Control of Nonlinear Differential Algebraic Equation Systems*. Chapman and Hall/CRC, Boca Raton, FL, 1999.

[121] J.R. Leigh. *Temperature Measurement and Control*. Peregrinus, London, 1987.

[122] J.I. Levenhagen and D.H. Spethmann. *HVAC Controls and Systems*. Mc-Graw-Hill, New York, 1993.

[123] W.S. Levine, editor. *Control System Fundamentals*. CRC Press, Boca Raton, FL, 2000.

[124] F.L. Lewis. *Optimal Control*. Wiley, New York, 1986.

[125] J.H. Lienhard. *A Heat Transfer Textbook*. Prentice-Hall, Englewood Cliffs, NJ, 1981.

[126] J.L. Lions. On the controllability of distributed systems. *Natl. Acad. Sci. USA*, 94:4828–4835, 1997.

[127] W.W. Liou and Y. Fang. *Microfluid Mechanics: Principles and Modeling*. McGraw Hill, New York, 2006.

[128] B. Liu and T.R. Marchant. The occurrence of limit-cycles during feedback control of microwave heating. *Mathematical and Computer Modelling*, 35(9-10):1095–1118, 2002.

[129] L. Ljung. *System Identification: Theory for the User*. Prentice-Hall, Upper Saddle River, N.J., second edition, 1999.

[130] A. Luikov. *Heat and Mass Transfer*. Mir, Moscow, 1980.

[131] A. Majumdar. Microscale energy transport in solids. In C.-L. Tien, A. Majumdar, and F.M. Gerner, editors, *Microscale Energy Transport*, chapter 1. Taylor and Francis, Washington, DC, 1998.

[132] A. Majumdar. Microscale transport phenomena. In W.M. Rohsenow, J.P Hartnett, and Y.I. Cho, editors, *Handbook of Heat Transfer*, chapter 8. McGraw-Hill, New York, 1998.

[133] T. Marimbordes, A.O. El Moctar, and H. Peerhossaini. Active control of natural convection in a fluid layer with volume heat dissipation. *International Journal of Heat and Mass Transfer*, 45(3):667–678, 2002.

[134] W.J. Minkowycz, E.M. Sparrow, G.E. Schneider, and R.H. Pletcher, editors. *Handbook of Numerical Heat Transfer*. John Wiley, New York, 1988.

[135] M. Modest. *Radiative Heat Transfer*. Academic Press, Amsterdam, 2003.

[136] W. Munk. The delayed hot-water problem, brief notes. *ASME J. Applied Mechanics*, 21(10):?–?, 1954.

[137] O. Nelles. *Nonlinear System Identification*. Springer, Berlin, 2001.

[138] D.A. Nield and A. Bejan. *Convection in Porous Media*. Springer-Verlag, New York, 2nd edition, 1999.

[139] M. Nørgaard, O. Ravn, N.K. Poulsen, and L.K. Hansen. *Neural Networks for Modelling and Control of Dynamic Systems*. Springer, London, 2000.

[140] K. Ogata. *Modern Control Engineering*. Prentice-Hall, Englewood Cliffs, N.J., second edition, 1990.

[141] P.H. Oosthuizen and D. Naylor. *Introduction to Convective Heat Transfer Analysis*. McGraw-Hill, New York, 3rd edition, 1998.

[142] A. Oustaloup. *Systèmes Asservis Linéaires d'Ordre Fractionnaire: Théorie et Practique*. Masson, Paris, 1983.

[143] A. Oustaloup. *La Dérivation Non Entière*. Hermès, Paris, 1995.

[144] M.N. Ozisik. *Boundary Value Problems of Heat Conduction*. Dover Publications, New York, 1968.

[145] M.N. Ozisik. *Heat Conduction*. John Wiley, New York, 1980.

[146] M.N. Ozisik. *Heat Transfer, A Basic Approach*. McGraw-Hill, New York, 1985.

[147] A. Pacheco-Vega. *Simulation of Compact Heat Exchangers using Global Regression and Soft Computing*. PhD thesis, Department of Aerospace and Mechanical Engineering, University of Notre Dame, Notre Dame, IN, 2002.

[148] A. Pacheco-Vega, G. Díaz, M. Sen, K.T. Yang, and R.L. McClain. Heat rate predictions in humid air-water heat exchangers using correlations and neural networks. *ASME Journal of Heat Transfer*, 123(2):348–354, 2001.

[149] A. Pacheco-Vega, M. Sen, K.T. Yang, and R.L. McClain. Genetic-algorithm based prediction of a fin-tube heat exchanger performance. *Proceedings of the 11th International Heat Transfer Conference*, 6:137–142, 1998.

[150] A. Pacheco-Vega, M. Sen, K.T. Yang, and R.L. McClain. Neural network analysis of fin-tube refrigerating heat exchanger with limited experimental data. *International Journal of Heat and Mass Transfer*, 44:763–770, 2001.

[151] M.V. Papalexandris and M.H. Milman. Active control and parameter updating techniques for nonlinear thermal network models. *Computational Mechanics*, 27(1):11–22, 2001.

[152] P.N. Paraskevopoulos. *Modern Control Engineering*. Marcel Dekker, New York, 2002.

[153] H.M. Park and W.J. Lee. Feedback control of the Rayleigh-Benard convection by means of mode reduction. *International Journal for Numerical Methods in Fluids*, 40(7):927–949, 2002.

[154] S. Patankar. *Numerical Heat Transfer and Fluid Flow*. McGraw-Hill/Hemisphere, 3rd edition, 1980.

[155] M. Planck. *The Theory of Heat Radiation*. Dover Publications, New York, 1959.

[156] I. Podlubny. *Fractional Differential Equations*. Academic Press, San Diego, CA, 1999.

[157] D. Poulikakos. *Computational Heat Transfer*. Prentice-Hall, Englewood Cliffs, NJ, 1994.

[158] D.C. Price. A review of selected thermal management solutions for military electronic systems. *IEEE Transactions on Components and Packaging Technologies*, 26(1):26–39, 2003.

[159] P.A. Ramachandran. *Advanced Transport Phenomena: Analysis, Modeling, and Computations*. Cambridge University Press, 2014.

[160] W. H. Ray. *Advanced Process Control*. McGraw-Hill, New York, 1981.

[161] P. Riederer, D. Marchio, and J.C. Visier. Influence of sensor position in building thermal control: criteria for zone models. *Energy and Buildings*, 34(6):785–798, 2002.

[162] W. Roetzel and Y. Xuan. *Dynamic behaviour of Heat Exchangers*. WIT Press, Boston, 1999.

[163] Rohsenow, Hartnett, and Ganic, editors. *Heat Exchanger Design Handbook*. John Wiley, New York, 2nd edition, 1983.

[164] K.C. Rolle. *Heat and Mass Transfer*. Prentice-Hall, Upper Saddle River, NJ, 2000.

[165] H.H. Rosenbrock. *State-Space and Multivariable Theory*. John Wiley, New York, 1970.

[166] E.O. Roxin. *Control Theory and its Applications*. Gordon and Breach, Amsterdam, 1997.

[167] P.K. Roy, S.M. Merchant, and S. Kaushal. A review: thermal processing in fast ramp furnaces. *Journal of Electronic Materials*, 30(12):1578–1583, 2001.

[168] N. Saman and H. Mahdi. Analysis of the delay hot/cold water problem. *Energy*, 21(5):395–400, 1996.

[169] C.D. Schaper, M.M. Moslehi, K.C. Saraswat, and T. Kailath. Modeling, identification, and control of rapid thermal-processing systems. *Journal of the Electrochemical Society*, 141(11):3200–3209, 1994.

[170] L.J. Segerlind. *Applied Finite Element Analysis*. John Wiley, New York, 2nd edition, 1984.

[171] M. Sen. *Lecture Notes on Intelligent Systems*. Department of Aerospace and Mechanical Engineering, University of Notre Dame, Notre Dame, IN 46556, 2004.

[172] M. Sen and J.W. Goodwine. Soft computing in control. *The MEMS Handbook*, pages 1–37, Chapter 14, 2001.

[173] M. Sen, E. Ramos, and C. Treviño. On the steady-state velocity of the inclined toroidal thermosyphon. *ASME Journal of Heat Transfer*, 107(4):974–977, 1985.

[174] M. Sen, E. Ramos, and C. Treviño. The toroidal thermosyphon with known heat flux. *International Journal of Heat and Mass Transfer*, 28(1):219–233, 1985.

[175] M. Sen and P. Vasseur. Analysis of multiple solutions in plane poiseuille flow with viscous heating and temperature dependent viscosity. *Proceedings of the National Heat Transfer Conference, HTD-Vol. 107, Heat Transfer in Convective Flows*, pages 267–272, 1989.

[176] M. Sen, P. Vasseur, and L. Robillard. Multiple steady states for unicellular natural convection in an inclined porous layer. *International Journal of Heat and Mass Transfer*, 30(10):2097–2113, 1987.

[177] M. Sen and K.T. Yang. Applications of artificial neural networks and genetic algorithms in thermal engineering. *The CRC Handbook of Thermal Engineering*, 123(3):Section 4.24, 620–661, 2000.

[178] M. Sen and K.T. Yang. Laplace's equation for convective scalar transport in potential flow. *Proceedings of the Royal Society A: Mathematical, Physical and Engineering Sciences*, 455(2004):3041– 3045, 2000.

[179] R.K. Shah and A.L. London. *Laminar flow forced convection in ducts, a source book for compact heat exchanger analytical data*. Academic Press, New York, 1978.

[180] T.M. Shih. *Numerical Heat Transfer*. Hemisphere Pub. Corp., Washington, DC, 1984.

[181] K. Shimazaki, A. Ohnishi, and Y. Nagasaka. Development of spectral selective multilayer film for a variable emittance device and its radiation properties measurements. *International Journal of Thermophysics*, 24(3):757–769, 2003.

[182] R. Siegel and J.R. Howell. *Thermal Radiation Heat Transfer*. Hemisphere Publ. Corp., Washington, DC, 3rd edition, 1992.

[183] N. Silviu-lulian. *Delay Effects on Stability*. Lecture Notes in Control and Information Sciences, Springer, London,, 2001.

[184] J. Singer and H.H. Bau. Active control of convection. *Physics of Fluids A-Fluid Dynamics*, 3(12):2859–2865, 1991.

[185] J. Singer, Y.Z. Wang, and H.H. Bau. Controlling a chaotic system. *Physical Review Letters*, 66(9):1123–1125, 1991.

[186] L.E. Sissom and D.R. Pitts. *Elements of Transport Phenomena*. McGraw-Hill, New York, 1972.

[187] H. Smith and H.H. Jensen. *Transport Phenomena*. Clarendon Press, Oxford, U.K., 1989.

[188] E.D. Sontag. *Mathematical Control Theory*. Springer, New York, 1998.

[189] W.F. Stoecker and P.A. Stoecker. *Microcomputer Control of Mechanical and Thermal Systems*. Van Nostrand Reinhold, New York, 1989.

[190] B. Straughan. *The Energy Method, Stability, and Nonlinear Convection*. Springer-Verlag, New York, 1992.

[191] S.H. Strogatz. *Sync: The Emerging Science of Spontaneous Order*. Theia, New York, 2003.

[192] B. Sundén and M. Faghri. *Computer Simulations in Compact Heat Exchangers*. Computational Mechanics Publications, Southhampton, U.K., 1998.

[193] N.V. Suryanarayana. *Engineering Heat Transfer*. West Pub. Co., Minneapolis/St. Paul, 1995.

[194] T.D. Swanson and G.C. Birur. NASA thermal control technologies for robotic spacecraft. *Applied Thermal Engineering*, 23(9):1055–1065, 2003.

[195] M. Sweetland and J.H. Lienhard. Active thermal control of distributed parameter systems with application to testing of packaged IC devices. *ASME Journal of Heat Transfer*, 125(1):164–174, 2003.

[196] P. Tabeling. *Introduction to Microfluidics*. Oxford University Press, Oxford, UK, 2005.

[197] M. Tabib-Azar. *Microactuators: Electrical, Magnetic, Thermal, Optical, Mechanical, Chemical & Smart Structures*. Kluwer Academic, Boston, 1998.

[198] J. Taine. *Heat Transfer*. Prentice-Hall, Englewood Cliffs, N.J., 1993.

[199] J. Tang and H.H. Bau. Feedback-control stabilization of the no-motion state of a fluid confined in a horizontal porous layer heated from below. *Journal of Fluid Mechanics*, 257:485–505, 1993.

[200] J. Tang and H.H. Bau. Stabilization of the no-motion state in Rayleigh-Benard convection through the use of feedback-control. *Physical Review Letters*, 70(12):1795–1798, 1993.

[201] J. Tang and H.H. Bau. Stabilization of the no-motion state in the Rayleigh-Benard problem. *Proceedings of the Royal Society of London Series A-Mathematical and Physical Sciences*, 447(1931):587–607, 1994.

[202] J. Tang and H.H. Bau. Stabilization of the no-motion state of a horizontal fluid layer heated from below with Joule heating. *ASME Journal of Heat Transfer*, 117(2):329–333, 1995.

[203] J. Tang and H.H. Bau. Experiments on the stabilization of the no-motion state of a fluid layer heated from below and cooled from above. *Journal of Fluid Mechanics*, 363:153–171, 1998.

[204] J. Tang and H.H. Bau. Numerical investigation of the stabilization of the no-motion state of a fluid layer heated from below and cooled from above. *Physics of Fluids*, 10(7):1597–1610, 1998.

[205] J. Tang and H.H. Bau. Numerical investigation of the stabilization of the no-motion state of a fluid layer heated from below and cooled from above. *Physics of Fluids*, 10(7):1597–1610, 1998.

[206] J.C. Tannehill, D.A. Anderson, and R.H. Pletcher. *Computational Fluid Mechanics and Heat Transfer*. Taylor and Francis, Washington, DC, 2nd edition, 1997.

[207] C. Tin-Tai. Numerical modeling of thermal behavior of fluid conduit flow with transport delay. *ASHRAE Transactions*, 102(2):?–?, 1996.

[208] L.S. Tong and Y.S. Tang. *Boiling Heat Transfer and Two-Phase Flow*. Taylor and Francis, Washington, DC, 1997.

[209] C. Tricot. *Curves and Fractal Dimension*. Springer-Verlag, New York, 1995.

[210] V. Trivedi and S.J. Pearton. Evaluation of rapid thermal processing systems for use in CMOS fabrication. *Solid-State Electronics*, 46(5):777–783, 2002.

[211] J.W.C. Tseng. *Radiant Heat Transfer in Porous Media*. Springer-Verlag, 2nd edition, 1990.

[212] D.Y. Tzou. *Macro- to Microscale Heat Transfer: The Lagging Behavior*. Taylor and Francis, Washington, DC, 1997.

[213] E.I. Varga, K.M. Hangos, and F. Szigeti. Controllability of heat exchanger networks in the time-varying parameter case. *Control Engineering Practice*, 3(10):1409–1419, 1995.

[214] C.H. Wang, M. Sen, and P. Vasseur. Analytical investigation of bénard-marangoni convection heat transfer in a shallow cavity filled with two immiscible fluids. *Applied Scientific Research*, 48:35–53, 1991.

[215] Y.Z. Wang, J. Singer, and H.H. Bau. Controlling chaos in a thermal-convection loop. *Journal of Fluid Mechanics*, 237:479–498, 1992.

[216] B. Weigand. *Analytical Methods for Heat Transfer and Fluid Flow Problems*. Springer, Berlin, 2004.

[217] B. Weigand. *Analytical Methods for Heat Transfer and Fluid Flow Problems*. Springer, 2004.

[218] F.M. White. *Heat and Mass Transfer*. Addison-Wesley, Reading, MA, 1988.

[219] G.B. Whitham. *Linear and Nonlinear Waves*. John Wiley & Sons, New York, 1974.

[220] J.A. Wiebelt. *Engineering Radiation Heat Transfer*. Holt, Rinehart and Winston, New York, 1966.

[221] R.H.S. Winterton. *Heat Transfer*. Oxford University Press, New York, 1997.

[222] H. Wolf. *Heat Transfer*. Harper and Row, Cambridge, U.K., 1982.

[223] K.-F.V. Wong. *Intermediate Heat Transfer*. Marcel Dekker, New York, 2003.

[224] K.T. Yang and M. Sen. Agent networks for intelligent dynamic control of complex hydronic HVAC building systems–Part 1: Framework for agent network development. *International Journal on Architectural Science*, 3(1):43–50, 2002.

[225] C.-C. Yu. *Autotuning of PID Controllers*. Springer, London, 1999.

[226] P.K. Yuen and H.H. Bau. Rendering a subcritical Hopf bifurcation supercritical. *Journal of Fluid Mechanics*, 317:91–109, 1996.

[227] P.K. Yuen and H.H. Bau. Controlling chaotic convection using neural nets - theory and experiments. *Neural Networks*, 11(3):557–569, 1998.

[228] P.K. Yuen and H.H. Bau. Optimal and adaptive control of chaotic convection - theory and experiments. *Physics of Fluids*, 11(6):1435–1448, 1999.

[229] Z. Zhang and R. M. Nelson. Parametric analysis of a building space conditioned by a VAV system. *ASHRAE Transactions*, 98(1):43–48, 1992.

[230] Z.M. Zhang, C.J. Fu, and Q.Z. Zhu. Optical and thermal radiative properties of semiconductors related to micro/nanotechnology. In J.P. Hartnett, T.F. Irvine, Y.I. Cho, and G.A. Greene, editors, *Advances in Heat Transfer*, volume 37, pages 179–296. Academic Press, Amsterdam, 2003.

[231] A. Zilouchian and M. Jamshidi, editors. *Intelligent Control Systems Using Soft Computing Methodologies*. CRC Press, Boca Raton. FL, 2001.

[232] S. Zumbo, J. Leofanti, S. Corradi, G. Allegri, and M. Marchetti. Design of a small deployable satellite. *Acta Astronautica*, 53(4-10):533–540, 2003.

Index